Enzymatic synthesis of selected glycosides

A thesis submitted to the

University of Mysore

for the award of

Doctor of Philosophy

in

CHEMISTRY

By

G. R. Vijayakumar **M Sc.,**

cftri

Fermentation Technology and Bioengineering Department
Central Food Technological Research Institute
Mysore- 570020, INDIA

2006

G. R. VIJAYAKUMAR MSc
Senior Research Fellow
Fermentation Technology and Bioengineering
Central Food Technological Research Institute
Mysore – 570 020, India

Declaration

I hereby declare that the thesis entitled, **"Enzymatic synthesis of selected glycosides"** submitted for the degree of **Doctor of Philosophy** in **Chemistry** to the **University of Mysore** is the result of the work carried out by me under the guidance of **Dr. S. Divakar** in the Department of Fermentation Technology and Bioengineering, Central Food Technological Research Institute, Mysore, during the period 2003-2006.

I further declare that the results of this work have not been submitted for the award of any other degree or fellowship.

Date: 14th Aug 2006
Place: Mysore (G. R. Vijayakumar)

CENTRAL FOOD TECHNOLOGICAL RESEARCH INSTITUTE

(COUNCIL OF SCIENTIFIC & INDUSTRIAL RESEARCH)

MYSORE - 570 020. INDIA.

Dr. S. Divakar
Fermentation Technology and Bioengineering
E-mail: divakar643@gmail.com

Certificate

I hereby declare that the thesis entitled, **"Enzymatic synthesis of selected glycosides"** submitted by **Mr. G. R. Vijayakumar** for the degree of **Doctor of Philosophy** in **Chemistry** to the **University of Mysore** is the result of the work carried out by him under my guidance in the Department of Fermentation Technology and Bioengineering, Central Food Technological Research Institute, Mysore during the period 2003-2006.

Date: 14th Aug 2006
Place: Mysore

(S. Divakar)
Guide

..... To My Beloved Parents

Acknowledgements

I express my deep sense of gratitude to **Dr. S. Divakar**, Scientist, Central Food Technological Research Institute, Mysore for his guidance, invaluable suggestions and constant encouragement throughout the course of my Ph.D work.

I thank Director Dr. V. Prakash, for providing me an opportunity to carry out my research work at the Central Food Technological Research Institute, Mysore.

My gratitude to former Head Dr. N.G. Karanth, present Head Dr. M.C. Misra and all the scientific and non-scientific staff of Fermentation Technology and Bioengineering department for their support during the course of my research work.

I would like to acknowledge my gratitude to Mr. B. Manohar, Scientist, Food Engineering Department, CFTRI for his kind help in my work.

I express my sincere thanks to my colleagues Mr. K. Lohith, Mr. B.R. Somashekar, Mr. R. Sivakumar and Mr. Charles George for scientific inputs and being there for me whenever in need.

I express my sincere thanks to all the staff of Central Instrumentation Facilities and Service Departments for their technical help in analyzing my samples.

My sincere gratitude to NMR Research Centre, Indian Institute of Science, Bangalore for recording NMR spectra presented in this work.

I am thankful to all the students of FTBE and other departments of the Institute for their timely help during my course of work.

My special thanks to all the scientific and non-scientific staff of CFTRI, Mysore and those who have directly or indirectly helped me in carrying out this work.

My special gratitude to my parents, brother and relatives for their constant encouragement and support.

Last but not least, I am greatful to the Council of Scientific and Industrial Research, India for providing the Junior and Senior Research fellowships.

G. R. Vijayakumar

List of Patents and Publications

Patents

1 **Vijayakumar, G.R.,** Manohar, B., Divakar, S., 2003. An enzymatic process for the preparation of alkyl glycosides. NF-512/2003.

2 **Vijayakumar, G.R.,** Manohar, B., Divakar, S., 2004. An improved enzymatic method for the preparation of glycosides. Submitted to CSIR.

3 **Vijayakumar, G.R.,** Manohar, B., Divakar, S., 2004. An enzymatic method for the preparation of curcumin glycoside. 756/DEL/2005.

4 Sivakumar, R., **Vijayakumar, G. R.,** Manohar, B., Divakar, S., 2005. An enzymatic process for the preparation of vanillin glycosides. Submitted to CSIR.

Papers

1. **Vijayakumar, G.R.,** Manohar, B., Divakar, S., 2005. Amyloglucosidase catalyzed synthesis of n-octyl-D-glucoside-Analysis using Response Surface Methodology. **Eur. Food Res. Technol.** 220, 272-277.

2. **Vijayakumar, G.R.,** Divakar, S., 2005. Synthesis of guaiacol-α-D-glucoside and curcumin-bis-α-D-glucoside by an amyloglucosidase from *Rhizopus*. **Biotechnol. Lett.** 27, 1411-1415.

3. **Vijayakumar, G.R.,** Manohar, B., Divakar, S., 2005. Amyloglucosidase catalyzed synthesis of curcumin-bis-α-D-glucoside-A Response Surface Methodological study. **Eur. Food Res. Technol.** In Press.

4. Sivakumar, R., **Vijayakumar, G.R.,** Manohar, B., Divakar, S., 2006. Competitive substrate inhibition of amyloglucosidase from *Rhizopus* sp. by vanillin and curcumin. **Biocatal. Biotransform.** In Press.

5. K. Lohith, **Vijayakumar, G.R.,** Somashekar, B.R., Sivakumar, R., Divakar, S., 2006. Glycosides and amino acyl esters of carbohydrates as potent inhibitors of Angiotensin Converting Enzyme**. Eur. J. Med. Chem.** In Press.

6. **Vijayakumar, G.R.,** Charles G., Divakar, S., 2006. Synthesis of n-alkyl glucosides by amyloglucosidase. **Ind. J. Chem. Sec B.** In Press.

7. **Vijayakumar, G.R.,** Divakar, S., 2006. Amyloglucosidase catalyzed synthesis of phenyl propanoid glycosides. Submitted for publication.

List of abbreviations and symbols

A	Absorbance
ANOVA	Analysis of variance
ACE	Angiotensin Converting Enzyme
Å	Angstrom
bp	Boiling point
BSA	Bovine serum albumin
^{13}C	Carbon-13
cm	Centimeter
CCRD	Central Composite Rotatable Design
δ	Chemical shift value
J	Coupling constant
CMC	Critical Micellar Concentration
^{o}C	Degree centigrade
DMSO-d_6	Deuteriated Dimethyl sulfoxide
eV	Electronvolt
E/S	Enzyme by substrate ratio
EC	Enzyme commission
eq	Equivalents
g	Gram
Hz	Hertz
HSQCT	Heteronuclear Single Quantum Coherence Transfer
HPLC	High Performance Liquid Chromatography
h	Hour
IR	Infra red
K_i	Inhibitor constant
v	Initial velocity
IUPAC	International union of pure and applied chemistry
kDa	Kilo Dalton
kV	Kilovolts
MS	Mass spectroscopy
v_{max}	Maximum velocity
MHz	Mega hertz
mp	Melting point
K_M	Michelis Menton constant
µg	Microgram
µL	Microlitre
mg	Milligram
mL	Milliliter
mm	Millimeter
mmol	Millimole
min	Minute
ε	Molar extension coefficient
M	Molarity
mol	Mole

$[M]^+$	Molecular ion
nm	Nanometer
N	Normality
NMR	Nuclear Magnetic Resonance
$[\alpha]$	Optical rotation
ppm	Parts per million
%	Percentage
π	Pi
PAGE	Polyacrylamide gel electrophoresis
KBr	Potassium bromide
^1H	Proton
RSM	Response Surface Methodology
RT	Retention time
rpm	Round per minute
sec	Seconds
σ	Sigma
SDS	Sodium dodecyl sulfphate
$SCCO_2$	Super critical carbon dioxide
SCF	Super critical fluid
TMS	Tetra methyl silane
TLC	Thin layer chromatography
2D	Two-Dimensional
UV	Ultra violet
v/v	Volume by volume
v/w	Volume by weight
a_w	Water activity
cm^{-1}	Wave per centimeter
w/w	Weight by weight
w/v	Weight by volume

List of Tables

List of Figures

List of Schemes

Chapter 1

Introduction

1.1 Enzymatic transformations

Enzymes are specific, catalytically active proteins, simple or conjugated capable of catalyzing biochemical reactions. An enzyme in a reaction lowers the amount of activation energy required by the reaction. Enzymes are thermolabile, inactivated at certain temperatures in a manner characteristic for protein denaturation. Substrates are substances on which enzymes act specifically. Substrate specificity places a role in enzyme classification.

From the past two decades, the application of enzymes in organic synthesis has emerged as an extremely important field, with a wide variety of enzymes in enzymatic, chemo enzymatic synthesis have been described (Schulze and Wubbolts 1999; Ward and Singh 2000; Davis and Boyer 2001). Most of the organic chemists use biocatalysts because these save additional reaction steps compared to chemical synthesis. Highly chemo, regio and stereo specific reactions are safer and eco friendly and can be used for the preparation of wide range of organic compounds, especially in food and pharmaceutical preparations. Oxido-reductases, hydralases (lipases, esterases, glycosidases, transglycosidases, peptidases, acylases, amidases, epoxide hydralases, nitrilases and hydantoinases), lyases and isomerases have been used in the organic synthesis. (Drauz and Waldmann 2002; Faber 2004; Buchholz *et al.* 2005).

1.2 Glycosidases

Among the enzymes, glycosidases and transglycosidases play an important role in organic synthesis of glycosides. They belong to the group of carbohydrate processing enzymes, widely employed in the regio and stereoselective glycosylation reactions. Glycosidases (also termed carbohydrases) are enzymes that catalyze the hydrolysis of glycosidic bonds in simple glycosides, oligosaccharides and polysaccharides, as well as in complex carbohydrates such as glycoproteins and glycolipids, with the liberation of

monosaccharides and oligosaccharides of lower molecular weight than the native substrate. These enzymes are very widely distributed in nature, being found in all organisms. These large and important groups of enzymes were investigated long back. Payen and Persoz were probably the first to recognize this enzyme in 1833 and they named it as “diastase” (now known as amylase). The phenomenon of hydrolysis was investigated by Liebig and Wohler in 1837 and Robiquet in 1838 on amygdalin (an aromatic glycoside) by bitter almonds and named the active principle as “emulsions”. Subsequently, a detailed study on glycosidases was carried out by many eminent chemists and biochemists (Fischer 1894).

1.2.1 Amylolytic enzymes

Starch degrading enzymes have been broadly classified into two groups - endo acting enzymes or endohydralases and exo-acting enzymes or exohydralases (Berfoldo and Antranikian 2001). α-Amylase (α-1,4-glucan-4-glucanohydralse; EC 3.2.1.1) is an endo acting enzyme which hydrolyzes linkages in the interior of the starch polymer in a random fashion, leading to the formation of linear and branched oligosaccharides. Most starch hydrolyzing enzymes belong to the α-amylase family and they contain a characteristic catalytic $(\beta/\alpha)_8$ barrel domain. Exo acting starch hydrolases include β-amylase, glucoamylase, α-glucosidase and isoamylase. These enzymes attack the substrate from the nonreducing end, producing oligosaccharides. β-Amylase (EC 3.2.1.2) also referred to as α-1,4-D-glucan maltohydrolase or saccharogen amylase, hydrolyzes α-1,4-glucosidic linkages to remove successive maltose units from the nonreducing ends of the starch chains, producing β-maltose units by an inversion of configuration of the maltose. α-Glucosidase (EC 3.2.1.20) attacks α-1,4 linkages of oligosaccharides and liberates glucose with α-anomeric configuration. Isoamylase or glycogen 6-

glucoanohydrolase, is a debranching enzyme specific for α-1,6 linkages in polysaccharides, such as amylopectin, glycogen, and β-limit dextrin.

1.2.1.1 Glucoamylase

Glucoamylase (E.C 3.2.1.3), is a fungal enzyme called by several names as amyloglucosidase, 1,4-α-D-glucan hydrolase and γ-amylase. EC 3.2.1.3 is the enzyme code assigned by the Enzyme Commission (IUBM 1992). Number 3 denotes hydrolases, which catalyze the hydrolytic cleavage of large molecules with the addition of water. Number 2 indicates glucosidases, which catalyze the cleavage of a glycosidic bond. Number 1 refers to hydrolysis of O-glycosyl compounds. Under the group 3.2.1, there are several enzymes, of which glucoamylase is number 3 (fourth number in the nomenclature) which mainly hydrolyzes terminal α-1,4-linked-D-glucose residues successively from nonreducing ends of the carbohydrate chains (starch and malto oligosaccharides) releasing β-D-glucose (Fogarty 1983). Most forms of the enzyme can hydrolyze α-1,6-D-glucosidic bonds also when the next bond sequence is α-1,4. However, in *vitro* this enzyme hydrolyzes α-1,6- and α-1,3-D-glucosidic bonds in other polysaccharides with high molecular weights. Since this enzyme is able to completely hydrolyze starch if incubated for extended periods of time, it is called the saccharifying enzyme. Glucoamylases have the capacity to degrade large oligosaccharides up to about 90% α-1,6 linkages. However, the size of the substrate and the position of the α-1,6 linkages play a significant role in the hydrolytic process. Reverse reactions involving resynthesis of saccharides and glycosides from D-glucose occur with a very high glucoamylase concentration for prolonged incubation periods and high concentrations of substrates.

1.2.1.2 Sources of glucoamylases

Glucoamylases are derived from a wide variety of plants, animals and microorganisms, though most glucoamylases occur in fungi. Commercial enzymes originate from strains of either *Aspergillus niger* or *Rhizopus* sp. where they are used for the conversion of malto-oligosaccharides into glucose (Fogarty 1983). Since the discovery of two forms of glucoamylase from black koji mold in the 1950's, many reports have appeared on the multiplicity of glucoamylases. Various forms of glucoamylases are thought to be the result of several mechanisms: mRNA modifications, limited proteolysis, variation in carbohydrate content or presence of several structural genes (Pretorius *et al.* 1991).

Fungal glucoamylases are usually glycoproteins, which consist of one to five forms. *Aspergillus niger* has been used widely in the commercial production of an extracellular glucoamylase. Two forms of glucoamylase were isolated from *A. niger* (Pazur *et al.* 1971), glucoamylase I (99 kDa) and glucoamylase II (112 kDa). AG-I and AG-II forms of glucoamylase isolated from *A. niger,* differed in their carbohydrate content, as well as the pH and temperature stabilities and optima for activity (Ramasesh *et al.* 1982). There were several reports on purification and characterization of glucoamylase from *A. niger* strains (Williamson *et al.* 1992; Stoffer *et al.* 1993).

Gucoamylase from *Aspergillus terreus* strains were also examined to make it suitable for production of D-glucose and corn syrups (Ghosh *et al.* 1990; Ali and Hossain 1991). *Rhizopus* sp. produced a glucoamylase capable of releasing glucose from starch with 100% efficiency (Yu and Hang 1991). Three forms of glucoamylase were isolated (Takahashi *et al.* 1985) from *Rhizopus* sp., GA-I (74 kDa), GA-II (58.6 kDa) and GA-III (61.4 kDa). Glucoamylases from other mold strains are *Humicola lanuginosa* (Taylor *et al.* 1978), *Thermomyces lanuginosa* (Haasum *et al.* 1991) and *Myrothecium* sp. M1

(Malek and Hossain 1994). A phyto pathogenic fungus *Colletotrichum gloeosporiodes* also produces a glucoamylase (Krause *et al.* 1991).

There are several well reviewed reports on the production of yeast glucoamylases (Saha and Zeikus 1989; Pretorius *et al.* 1991). Glucoamylase has been identified in *Saccharomyces cerevisiae* (Pugh *et al.* 1989), *Saccharomyces cerevisiae* var. *diastaicus* (Kleinman *et al.* 1988; Pretorius *et al.* 1991), *Saccharomycopsis fibuligera* (Itoh *et al.* 1989), *Schwanniomyces castellii* (Sills *et al.* 1984), *Schwanniomyces occidentalis* (Gellissen *et al.* 1991), *Pichia burlonii* and *Talaromyces* sp. Glucoamylase from a diastatic strain of *S. cerevisiae* was purified chromatographically and characterized (Kleinman *et al.* 1988).

Bacterial glucoamylases have also been identified from including aerobic strains such as *B. stearothermophilius* (Srivastava 1984), *Flavobacterium* sp. (Bender 1981), *Halobacterium sodamense* (Chaga *et al.* 1993) and *Arthrobacter globiformis* I42 (Okada and Unno 1989). Anaerobic strains include *Clostridium thermohydrosulfuricum* (Hyun and Zeikus 1985), *Clostridium* sp. G0005 (Ohinishi *et al.* 1991), *Clostridium acetobutylicum* (Chojecki and Blaschek, 1986; Soni *et al.* 1992), *Clostridium thermosaccharolyticum* (Specka *et al.* 1991) and the microaerophile, *Lactobacillus amylovorus* (James and Lee 1995).

1.2.1.3 Sources of other glycosidases

A number of thermostable glycosidases have been identified and characterized in recent years, which have already been used in the synthesis of glycosides. The most remarkable one among these newcomers is the β-glucosidase from the hyperthermophillic archeon *Pyrococcus furiosus* (Kengen *et al.* 1993). The organism is relatively easy to grow and the β-glucosidase it produces is stable for an unprecedented 85 h at 100 ^{o}C. The enzyme has been cloned and over expressed in *Escheria Coli*

(Voorhorst *et al.* 1995). β-Galactosidase from *Aspergillus oryzae* was the more efficient enzymes towards alkylation (Stevenson *et al.* 1996). The enzyme β-galactosidase from *Streptococcus thermophilus* (Stevenson and Furneaux 1996) was employed for the synthesis of ethyl glycoside. The enzyme β-galactosidase from *Bacillus circullans* had been exploited by number of workers for synthetic purposes (Kojima *et al.* 1996). Enzymatic synthesis of butylglycoside via a transglycosylation reaction of lactose was carried out using β-galactosidase from *A. oryzae* (Ismail *et al.* 1999). β-Xylosidase from *A. niger* is a remarkably efficient glycosyl transfer catalyst that gave high (> 80%) yields of alkyl xylosides (Shinoyama *et al.* 1988) with primary as well as secondary alcohols from methanol up to butanol. Almond glucosidase has been widely employed for the synthesis of alkyl and phenolic glycosides (Ljunger *et al.* 1994; Vic and Crout 1995; Vic *et al.* 1995; Ducret *et al.* 2002).

1.2.2 Structural features of glucoamylase

A subsite theory for analyzing the substrate affinities of glucoamylases was developed (Hiromi 1970; Hiromi *et al.* 1973). The structure of different glucoamylases showed a common subsite arrangement with seven in total and the catalytic site was located between subsite 1 and 2 (Ohinishi 1990; Fagerstrom 1991; Ermer *et al.* 1993). Subsite 2 has the highest affinity for oligomeric substrates and glucose, followed by decreasing affinity towards subsites 3 to 7 (Frgerstrom 1991). The catalytic domain of glucoamylase from *A. niger* was purified and characterized from glucoamylases G1 and G2 using subtilisin with the aim of preparing a fragment for crystallization studies (Stoffer *et al.* 1993). The glucoamylase G1 of *A. niger* consists of three parts such as (1) Ala-1-Thr-440 - that contains the catalytic site, (2) Ser-441-Thr-551 - a highly O-glycosylated linker segment, and (3) Pro-512-Arg-616 - a C-terminal domain responsible for substrate (starch) binding (Svensson *et al.* 1983). Functionally important carboxyl

groups in glucoamylase G2 from *A. niger* were identified using a differential labeling approach and it was concluded that the three groups Asp176, Glu179 and Glu180 were active in the catalytic site (Svensson *et al.* 1990). Based on chemical modification studies on *A. niger* glucoamylase, tryptophan residues have been proposed to be essential for enzymatic activity (Rao *et al.* 1981). Tryptophan120 is responsible for binding of substrate and might maintain a structural integrity necessary for catalysis (Clarks and Svensson 1984).

Aspergillus awamori GA-I, has three catalytic domains (Svensson *et al.* 1983), a catalytic domain (residues 1-440), an O-glycosylated domain (residues 441-512) and a starch binding domain (residues 513-616). Aleshin *et al* (1992) produced a structural model for the catalytic domain of glucoamylase from *A. awamori* who reported a 2.2 Å crystal structure of a proteolized form of GA-I *A. awamori* var *X100,* which contains the complete catalytic domain plus the N-terminal half of the O-glycosylated domain (residue 1-471) the latter being referred as GA-II. Amino acid sequence of three glucoamylases from *Rhizopus, Aspergillus* and *Saccharomyces* were compared (Tanaka *et al.* 1986). The glucoamylases from *Rhizopus* and *Aspergillus* are highly homologous in the nucleotide sequence as well as the amino acid sequence suggesting that these two glucoamylases are the most closely related among the three. The catalytic site in glucoamylase is believed to consist of two carboxyl groups (Hiromi *et al.* 1966a; 1966b). In accordance with a commonly accepted mechanism for carbohydrases (Braun *et al.* 1977; Masumura *et al.* 1984; Post and Karplus 1986) one of these acts as a general acid protonating the glucosidic oxygen, while the other is present in the ionized carboxylate form and stabilizes the substrate intermediary oxonium ion (Rantwijk *et al.* 1999).

From the Itoh *et al* (1989), study of *S. fibuligera* glucoamylase, it was revealed that Ala-81, Asp-89, Trp-94, Arg-96, Arg-97 and Trp-166 were required for wild type

levels of activity and Ala-81 and Asp-89 were not essential for catalytic activity which however played a role in thermal stability.

Complexes of glucoamylase from *A. awamori* with acarbose and D-gluco-dihydroacarbose indicate hydrogen bonds between sugar OH groups and Arg54, Asp55, Leu177, Try178, Glu180 and Arg305 involved in binding at subsites 1 and 2, an array of outer subsites leading into these inner ones (Aleshin *et al.* 1994; Stoffer *et al.* 1995). The geometry of the general acid and base catalysis, Glu179 (Sierks *et al.* 1990; Aleshin *et al.* 1992) and Glu400, is excellent for the glucoside bond cleavage and assistance in the nucleophilic attack of water at the anomeric center of the carbohydrate (Harris *et al.* 1993; Frandsen *et al.* 1994). The active site of *A. niger* glucoamylase is very much identical to that of the *Rhizopus oryzae* (Stoffer *et al.* 1995). In the active site of *R. oryzae,* the aminoacid residues Arg191, Asp192, Leu312, Trp313, glu314, Glu315 and Arg443 are responsible for substrate binding through hydrogen bonds where as Glu314 and Glu544 is for glucosidic bond cleavage (Ashikari *et al.* 1986; Sierks *et al.* 1990; Aleshin *et al.* 1992).

1.2.3 Structural features of β-glucosidase

Since long time sweet almond β-glucosidase has been known to hydrolyze glycosides resulting in the net retention of anomeric configuration (Eveleigh and Perlin 1969). It has followed the standard mechanism of such retaining glycosidases, in which the substrates binds to an active site containing a pair of carboxylic acids (McCarter and Withers 1994; Sinnott 1990). Assignment of sweet almond β-glucosidase as a Family 1 glycosidase and identification of its active site nucleophiles was done by He and Withers (1997). On the basis of the sequence of the peptide derived from a trapped glycosyl-enzyme intermediate, the sweet almond β-glucosidase has been assigned to glycosidase

Family 1, with its active site nucleophile contained within the sequence Ile-Thr-Glu-Asn-Gly (He and Withers 1997).

The maize and sorghum β-glucosidases primary structures possess highly conserved peptide motifs TENEP and ITENG, which contains the two glutamic acids (Glu191 and Glu406) involved in catalysis as the general acid/base catalyst and the nucleophiles, respectively in all Family 1 β-glucosidases (San-Aparicio *et al.* 1998). The part of a slot like active site (Davies and Henrissat 1995) was formed by these residues necessary for the substrate hydrolysis (Withers *et al.* 1990). In the glycosylation step, the nucleophile Glu406 attacks the anomeric carbon (C-1) of the substrate and forms a covalent glycosyl-enzyme intermediate with concomitant release of the aglycon after protonation of the glucosidic oxygen by the acid catalyst Glu191 (Withers *et al.* 1990). In the next step (deglycosylation), Glu191 acts as a base and a water molecule performs as the nucleophile and attack the covalent glycosyl-enzyme, releasing the glucose and regenerating the nuclephilic Glu406. In maize β-glucosidase isozyme Glu1, these two catalytic glutamic acids are positioned within the active site at expected distances (~5.5 Å) for this mechanism (Czjzek *et al.* 2001). Verdoucq *et al.* (2003) studied the structural data from cocrystlas of enzyme substrate and enzyme aglycon complexes of maize β-glucosidase isozyme Glu1 (ZmGlu1) and has shown that five amino acid residues (Phe198, Phe205, Try378, Phe466 and Ala467) are located in the aglycon-binding site of ZmGlu1 and form the basis of aglycon reconition and binding and hence the substrate specificity. Kaper *et al.* (2000) have studied the substrate specificity of the β-glucosidase (CelB) from the hyperthermophilic archean *Pyrococcus furiosus,*a Family 1 glycosyl hydrolase at a molecular level. β-Glucosidase CelB shows a homo-tetramer configuration, with subunits having a typical $(\beta\alpha)_8$-barrel fold. The 3D model of the *Pyrococcus furiosus* β-glucosidase was compared with the previousely determined 6-

phospho-β-glycosidase (LacG) from the mesophillic bacterium *Lactococcus lactis* (Kaper *et al.* 2000). The positions of the active site residues in LacG and CelB are very well conserved and the conserved residues involved in substrate binding are Asn17, Arg77, His150, Asn206, Tyr307 and Trp410 (Wiesmann *et al.* 1997). Glu207 and Glu372 in CelB are the equivalents of the catalytic glutamate residues in LacG. The average distance between the oxygen atoms of these glutamate carboxylic acids is 4.3 Å (±1 Å) in CelB, which is in the range of the general observed distance in retaining glycosyl hydrolases (~5 Å) (McCarter and Withers 1994).

Hays *et al.* (1998) investigated the catalytic mechanism, substrate specificity and transglycosylation acceptor specificity of guinea pig liver Cytosalic β-glucosidase by several methods. Results indicated that CBG employs a two-step catalytic mechanism with the formation of a covalent enzyme-sugar intermediate and that CBG will transfer sugar residues to primary hydroxyls and equatorial but not axial C-4 hydroxyls of aldopyranosyl sugars (Hays *et al.* 1998). Also results have shown that the specificity of CBG for transglycosylation reactions is different from its specificity for hydrolytic reactions (Hays *et al.* 1998). From the inhibitor stoichiometry and reactivation studies, it was shown that the catalytic mechanism of CBG involves a covalent enzyme-sugar intermediate. From its aminoacid sequence, CBG is predicted to have a single active site nucleophile, specifically the glutamate residue in the sequence TITENG (Hays *et al.* 1996).

1.3 Glycosylation

While hydrolysis is the natural reaction for glucosidases and glucoamylases, glycosylation is a forced, reversed reaction. Glycosides are asymmetric mixed acetals formed by the reaction of the anomeric carbon atom of the intermolecular hemiacetal or pyranose/furanoses form of the aldohexoses or aldoketoses with a hydroxyl group

furnished by an alcohol. The bond formed is called glycosidic bond and the reaction is called glycosylation (Lehinger 1975; Ernst *et al.* 2000). Because of multiple hydroxyl groups of similar reactivity, controlled glycosylation remains a challenge to organic chemists. Well elaborated and still widely employed classical chemical approaches inevitably require quite a number of protection, activation, coupling and deprotection steps (Igarashi 1977; Konstantinovic *et al.* 2001). In contrast, enzymes (glycosidases and transglycosidases) offer the opportunity of one step synthesis under mild conditions in a regio and stereoselective manner (Vic and Thomas 1992). Enzyme-catalyzed glycoside and oligosaccharides synthesis involves two approaches, one is glycosidase and the other one is glycosyl transferase catalyzed glycoside bond formation. A sugar nucleotide donor and acceptor are incubated with the appropriate glycosidase or glycosyl transferase that catalyzes the efficient and selective transfer of the glycosyl residue to the acceptor. A great number of reports using glycosyltransferases are now available but these enzymes are often difficult to obtain (Auge *et al.* 1990). In contrast, the glycosidase approach uses simpler glycosyl donors, which can be the free monosaccharide itself. This method has the advantage of using relatively simple glycosyl donors and readily available commercial enzymes. Its main disadvantage is that regioselectivity may not be observed in all the cases (Trincone *et al.* 2003).

There are three types of reactions catalyzed by glycosidases such as hydrolysis, reverse hydrolysis and transglycosylation **(Scheme 1.1)**. In aqueous media, when there is large excess of water, glycoside or oligosaccharide or polysaccharide hydrolysis is the dominant reaction **(Scheme 1.1A)**. Other two reactions namely reverse hydrolysis and transglycosylation were employed for the synthesis of glycosides using glycosidases or transglycosidase enzymes. The difference between the two methods of synthesis depends on the nature of the glycosyl donor.

The reverse hydrolysis approach is an equilibrium controlled synthesis where the equilibrium is shifted towards synthesis (Panintrarux *et al.* 1995; Vic *et al.* 1997; Rantwijk *et al.* 1999) involving a carbohydrate and an alcohol **(Scheme 1.1B)**. This can be achieved by reducing the water activity and by increasing the substrate concentrations so that the substrate itself acts as a solvent media (Vic and Crout 1995). This method is widely employed for the enzymatic synthesis of alkyl glycosides and phenolic glycosides in an organic co solvent (Vic and Crout 1995; Vic *et al.* 1997; Ducret *et al.* 2002).

The transglycosylation method is a kinetically controlled synthesis where the enzyme catalyzes the transfer of a glycosyl residue from a glycosyl donor to the glycosyl acceptor (**Scheme 1.1C**). The reaction yield depends on the rate of product synthesis relative to the rate of hydrolysis. An efficient acceptor used in a high concentration should favor the synthesis (Ismail *et al.* 1999; Rantwijk *et al.* 1999; Stevensson *et al.* 1993; Vulfson *et al.* 1990).

1.1A Glycosyl-OR + H_2O ⟶ Glycosyl-OH + ROH

1.1B Glycosyl-OH + ROH ⇌ Glycosyl-OR + H_2O

1.1C Glycosyl-OR + R^1OH ⟶ Glycosyl-OR^1 + ROH

(Glycosyl = glycopyranosyl moiety, ROH & R^1OH = alcohol)

Scheme 1.1 Reactions catalyze by glycosidases

1.3.1 Glycosylation mechanism

In general, every hydrolysis of a glycosidic linkage by glycosidase is a reaction in which the product retains ($\alpha\rightarrow\alpha$ or $\beta\rightarrow\beta$) or inverts ($\alpha\rightarrow\beta$ or $\beta\rightarrow\alpha$) the anomeric configuration of the substrate (Chiba 1997). In the normal, hydrolytic reaction the leaving group is an (oligo)saccharide and the nucleophile (glycosyl acceptor) is water (**Scheme 1.1A**). However, an alcohol or a monosaccharide can also acts as glycosyl acceptor (glycosylation). Reversed hydrolysis, the condensation of a monosaccharide and an alcohol in which water is the leaving group (**Scheme 1.1B**), was first reported in 1913 (Rantwijk *et al.* 1999). A recent review by Zechel and Withers (2001) focuses on the recent developments in the understanding of nucleophilic and general acid-base catalysis in glycosidase–catalyzed reactions. Various models have been proposed for the catalytic reaction mechanisms of carbohydrate hydrolase in the transition state, but an unequivocal model remains to be established. Two significant models, such as nucleophilic displacement mechanism (**Scheme 1.2A**) and an oxo-carbenium ion intermediate mechanism (**Scheme 1.2B**) were suggested for the hydrolytic reaction where glycosyl acceptor is water (Chiba 1997).

The double displacement mechanism was found to be applicable to the enzymes, which retain the anomeric configuration of the substrate. The two catalytic ionisable groups, a carboxyl –COOH, and a carboxylate, -COO^-, cleave the glucosidic linkage cooperatively by direct electrophilic and nucleophilic attacks against the glycosyl oxygen and anomeric carbon atoms respectively, resulting in a covalent glucosyl-enzyme complex by a single displacement. Subsequently glucosyl-acetal bond is attacked with the hydroxyl group of the water (alcohol hydroxyl group in glycosylation) by retaining the anomeric configuration of the product by the double displacement. The double

displacement mechanism is adequate for explaining the reaction, where the anomeric configuration of the substrates is retained (Chiba 1997).

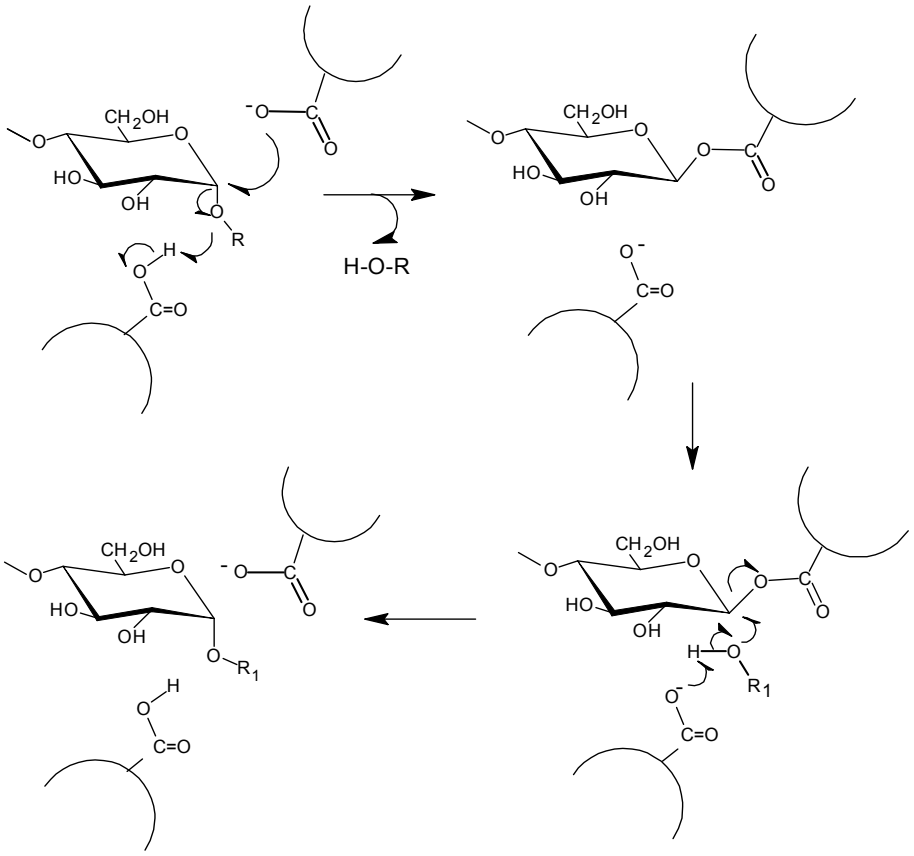

Scheme 1.2A Nucleophilic double displacement mechanism

In the oxo-carbenium intermediate mechanism, the two catalytic groups of the carboxyl and carboxylate ion participate cooperatively in the departure of the leaving group by a proton transfer to the anomeric oxygen atom (**Scheme 1.2B**). An enzyme bound oxonium ion intermediate has been detected by NMR (Withers and Street 1988). The second carboxylate, which is deprotonated in the resting state, stabilizes the oxonium ion intermediate. In the next step, a nucleophile adds to the same face of the glycosyl-enzyme intermediate from which the leaving group was expelled, resulting in the net retention of the anomeric configuration at the anomeric center. The addition of

the nucleophile is assisted by the first carboxylate which in this step reverts to carboxylic acid. The oxo-carbenium intermediate mechanism has been applied to interpret the catalytic mechanism of many carbohydrate degrading enzymes. This mechanism is applicable to both 'retaining' and 'inverting enzymes' (Chiba 1995). Mutagenesis and X-ray structural studies have confirmed that the mechanism of retaining glycosidases is similar (Sinnot 1990; Jacobson *et al.* 1994; Jacobson *et al.* 1995).

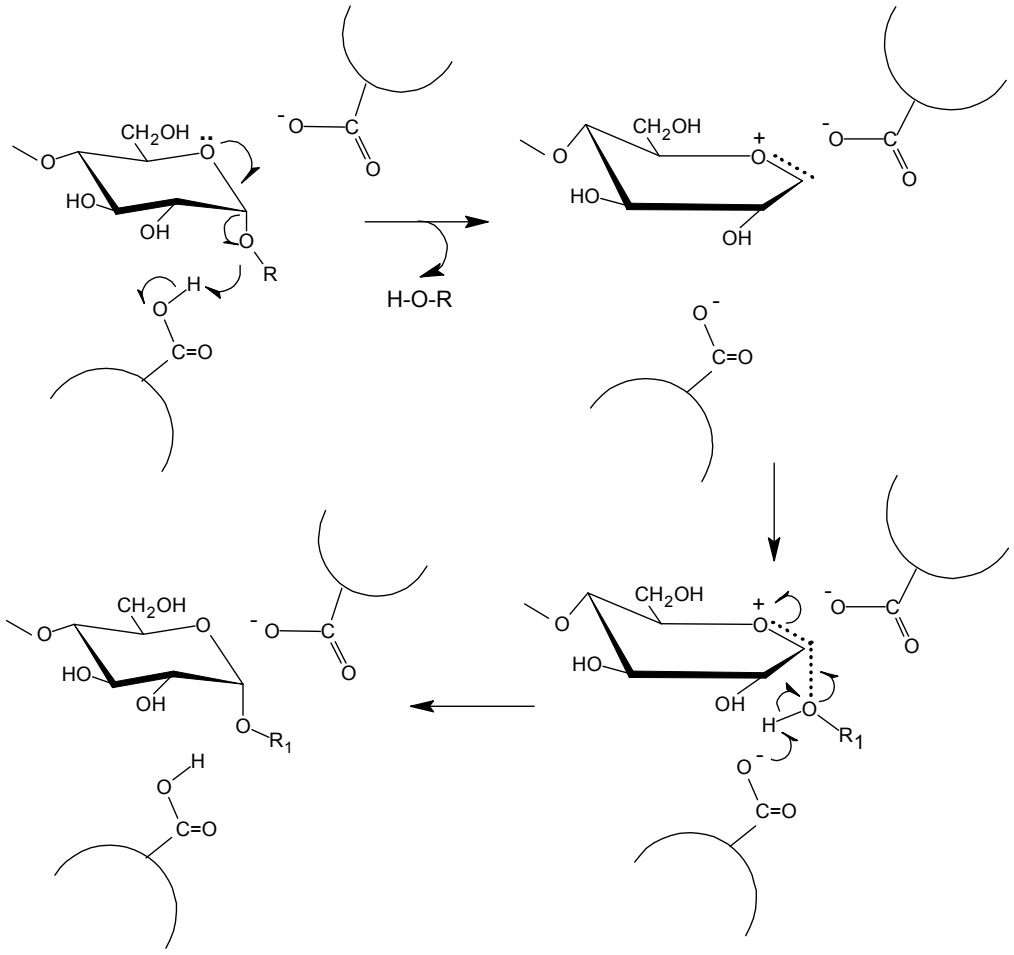

Scheme 1.2B: Oxocarbenium ion intermediate mechanism

1.3.2 Advantages of enzymatic glycosylation over chemical methods

There are many advantages of using glycosidases

1. Exploitation of regio and stereo specificity and selectivity
2. Milder reaction conditions
3. Non-generation of by-products associated with the use of several chemical procedures
4. Improved product-yield and better product quality
5. Use of non-polar solvents which impart stability to glycosidases, renders insolubility of the enzyme, solubility of alcohols and products in organic solvents and easy product workout procedures
6. No protection activation and deprotection required
7. Less environmental pollution

Table 1.1 lists some of the important surfactants, phenolic, flavonoid, terpinyl, sweetner and medicinal glycosides, which have been prepared by the use of glycosidases, glucoamylases and glycosyl transferases.

Table 1.1 Glycosides from enzymatic glycosylations

Name of the compound	Source of enzyme	Applications	References
A. Surfactant glycosides			
i) β-D-Glycopyranosides of n-heptanol, n-octanol, 2-phenyl hexanol, 3-phenyl propanol, 4-phenyl butanol, 5-phenyl petanol, 6-phenyl hexanol, 2-pyridine methanol, isobutanol, isopentanol, p-methoxy cinamyl alcohol, isopropanol, cyclohexanol, 1-phenyl ethanol, 1,5-pentanediol, 1,6-hexanediol, 1,7-heptanediol, 1,8-octanediol, 1,9-nonanediol, salicyl alcohol and 4-nitrophenol.	β-Glucosidase from almonds	As non ionic surfactants, in detergents and cosmetics	Katusumi *et al.* 2004
ii) β-D-Glucopyranosides of propanol, hexanol and octanol.	Raw almond meal	In detergents and cosmetics	Chahid *et al.* 1992
iii) α/β-Glucopyranosides of ethanol, 1-propanol, 2-propanol, 2-methyl 2-propanol, 1-butanol, 2-butanol, 1-	Glucoamylase and β-glucosidase	In detergents and cosmetics	Laroute and Willemot 1992a

pentanol, 1-hexanol, 1,3-butanediol, 1,4-butanediol, 2,3-butanediol, 1,2-pentanediol, 1,5-pentanediol.			
iv) Allyl and benzyl β-D-glucopyranoside, allyl-β-D-galactopyranoside.	Almond β-D-glucosidase	Used in the synthesis of glycopolymers, as temporary anomeric protected derivatives in carbohydrate chemistry	Vic and Crout 1995
v) n-Octyl glucoside, n-octyl galactoside	β-Galactosidase from *A. oryzae*, almond meal	In detergents and cosmetics	Chahid *et al.* 1994
vi) n-Octyl -β-D-glucoside, 2-hydroxy benzyl glucopyranoside.	Almond β-glucosidase	In detergents and cosmetics	Vic *et al.* 1997
vii) n-Octyl-β-D-glucoside, n-octyl-β-D-xylobioside, n-octyl-β-D-xyloside		As biological detergents and as emulsifying agents in cosmetics	Nakamura *et al.* 2000
B. Phenolic glycosides			
i) Eugenol-α-glucoside	α-Glucosyl transfer enzyme of *Xanthomonas campestris* WU-9701	As a prodrug of a hair restorer, as a derivative of spices	Sato *et al.* 2003
ii) Eugenol-β-glucoside	Biotransformation by cultured cells of *Eucalyptus perriniana*	As a prodrug of a hair restorer	Orihara *et al.* 1992

iii) Vanillin-β-D-monoglucopyranoside	By suspension cultured cells of *Coffea arabica*	As a food additive flavor	Kometani *et al.* 1993b
iv) Capsaicin-β-D-glucopyranoside	By suspension cultured cells of *Coffea arabica*	Food ingradient, and pharmacological applications	Kometani *et al.* 1993a
	By cultured cells of *Phytolacca americana*		Hamada *et al.* 2003
v) α-Salicin, α-isosalcin, β-salicin	*Bacillus macerans* cyclodextrin glucanyl transferase and *Leuconostoc mesenteroides* B-742CB dextransucrase	Anti-inflammatory, analgesic antipyretic prodrug	Yoon *et al.* 2004
vi) Curcumin glycosides	By cell suspension cultures of *Catharanthus roseus*	Food colorant, as antioxidant	Kaminaga *et al.* 2003
C. Flavonoid glycosides i) Quercetin-3-O-β-D-xylopyranosyl (1→2)-β-D-galactopyranoside, ii) Kaempferol-3-O-β-D-xylopyranosyl (1→2)-β-D-galactopyranoside	Isolated from *Trifolium repens L*	UV-B radiation protection	Hofman *et al.* 2000

D. Sweetener glycosides			
i) Stevioside, steviobioside, rebaudioside A, rebaudioside B	Isolated from the leaves of *Stevia rebaudiana*	As a natural sweeteners, utilized in beverages	Kohda *et al.* 1976
ii) Steviol-13-O-glucopyranoside, steviobioside, stevioside and rebaudioside	Enzyme fractions prepared from the soluble extracts of stevia	As a natural food sweeteners	Shibata *et al.* 1991
E. Terpineyl glycosides			
i) Gereniol β-glucoside, nerol β-glucoside, citroniol β-glucoside	β-Glucosidase from *A. niger, Trichoderma reesei, Candida molischiana* and almond	Good bioavailibilty, antifungal and antimicrobial activity	Gunata *et al.* 1994
ii) Gereniol β-galactoside, nerol β-galctoside, citroniol β-galactoside	β-Galactosidase from *A. oryzae*	Good bioavailibilty, antifungal and antimicrobial activity	Donho *et al.* 1996
F. Glycosides in medicine			
i)Enedyne antibiotics-calicheamycin	Isolated from the cultivation broth of *Micromonospora echinospora*	Antitumor agents	Lee *et al.* 1987; Golik *et al.* 1987
ii) Esperamycins	Isolated from *Actinomadura verrucosospora*	Antitumor activity	Long *et al.* 1989

iii) Vitamin glycosides- 5′-O-(β-D-galactopyranosyl)-thiamin 5′-O-(β-D-glucopyranosyl)-thiamin 4-α-D-glucopyranosyl rutin 2-O-α-glucopyranosyl-L-ascorbic acid	A. oryzae β-galactosidase Cyclomaltodextrin glucanotransferase from *Bacillus stearothermophilus* Cyclomaltodextrin glucanotransferase from *Bacillus stearothermophilus*	Excellent nutritional efficiencies, more stable against UV and light, Pleasant taste and odor, good bioavailability. More stable towards oxidative stress and UV irradiation	Suzuki and Uchida 1994 Uchida and Suzuki 1998 Suzuki and Suzuki 1991 Aga *et al.* 1990
iv) Alkaloid glycosides-elymoclavine-O-β-D-fructofuranoside	Isolated from a saprophytic culture of *Claviceps* sp.	In the treatment orthostatic circulary disturbances, hypertension, hyperprolactinemia, antibacterial and cytostatic effects and hypolipemic activty	Ken and Cvak 1999
v) Steroidal glycosides-glycosides of diosgenin, solasodine, solasonine	Isolated from *Solanum* sp.	Anticarcinogenic activity	Nakamura *et al.* 1996

1.4 Important factors influencing glycosylation in organic solvents

A few important factors that govern the glycosidase-catalysed reactions in organic solvents like nature of substrate, solvent, thermal stability, role of water, kinetics and immobilization are discussed below.

1.4.1 Nature of substrate

Glycoside synthesis and affinity of the enzyme towards substrate depends upon the nature of substrate as well as substrate concentration. The effect of initial D-glucose concentration on the glucoside yield in the glycosylation of alkanols was evaluated using glucoamylase from *Rhizopus oryzae* and β-glucosidase from almonds (Laroute and Willemot 1992a). A difference in behaviour existed between these two enzymes. By increasing the D-glucose concentration, the glucoside yields with glucoamylase decreased very rapidly whereas with β-glucosidase the yields were constant and finally fell low drastically. The formation of oligosaccharides (side products) depends upon the substrate concentration employed (Laroute and Willemot 1992a). Substrate study provides useful information on optimum substrates concentrations for carbohydrates and aglycons to be employed. Glycoside yield can be increased by increasing the concentration of the acceptor alcohol, provided that concentration is not sufficient enough to reduce the enzyme stability or sugar solubility (Stevensson *et al.* 1993). Effect of lactose and substrate alcohols were varied to investigate the effects on the galactoside yields (Stevensson *et al.* 1993). Galactoside yields distinctly increased with the increase in concentrations of both the substrates.

In some of the glycosylation reactions, acceptor alcohols employed acts as both substrate and reaction media (Laroute and Willemot 1992a; Ljunger *et al.* 1994; Vic and Crout 1995; Vic *et al.* 1997; Crout and Vic 1998). The effect of D-glucose concentration on the synthesis of allyl β-glucopyranoside catalyzed by β-D-glucosidase showed that

higher concentrations of D-glucose gave lower yields (Vic and Crout 1995). Glycosidases like α-glucoamylase, β-glucosidase and galctosidases accept broad range of alcohols and very hydrophobic compounds as their substrates for glycosylation (Vic *et al.* 1997; Kosary *et al.* 1998; Kurashima *et al.* 2004).

The high specificity of enzymes, that is to say the strict limitation of the action of each enzyme to one substrate or to a very small number of closely related substances, is one of their most striking characteristics. In case of glycosidases, the interchange of hydrogen and hydroxyl on any single carbon atom of a glycoside substrate is sufficient to prevent the action of the corresponding enzyme. For example, β-glucosidase does not act on β-mannosides, and probably not on β-galactosides, nor does it act on α-D-glucosides (Dixon and Webb 1958). In the case of the epimers involving carbon atoms 1, 2 and 4 of the aldohexoses ring, separate enzymes exist for each structure and the corresponding specific enzymes are α and β-glucosidases α and β-mannosidases and α and β-galacosidases (Brown *et al.* 1997; Fujimoto *et al.* 1997; Woudenberg-van *et al.* 1998; Kim *et al.* 2003). Substrate specificity of a *Spodoptera frugiperda* β-glycosidase (Sfbetagly50) using site directed mutagenesis and bioenergetics analysis was investigated (Marana *et al.* 2004). It showed that replacement of E451 with glutamine increased the preference of Sfbetagly50 for glucosides in comparison to galactosides, whereas replacing E451 with serine had the opposite effect (Marana *et al.* 2004). In contrast, the replacement of E451 with aspartate did not change Sfbetagly50 specificity. The groups involved in catalysis of this enzyme were E187 (proton donor) and E399 (nucleophile) (Marana *et al.* 2001). A subsite model proposed by Hiromi (1970) was applied to various hydrolases including glucoamylase (Natarajan and Sierks 1997). The substrate specificity of pig intestinal glucoamylase-maltase was investigated (Gunther and Heymann 1998). Various substrates with α-1,4-glycosidic bonds (maltose,

oligosaccharides) were hydrolyzed with high maximal reaction velocities, whereas α-1, β-2 glycosidic bond of the disaccharide sucrose was not hydrolyzed (Gunther and Heymann 1998). The β-glucosidase fixes one molecule of D-glucose on 1,2 pentanediol at position 1 or 2 with glucoamylase, two glucosides were formed with alcohol 1, 3 butanediol (Laroute and Willemot 1992a). Thus the authors demonstrated that the behaviour of these two enzymes were different so for as affinity and substrate specificity were concerned. Cytosolic β-glucosidase from mammalian liver is known for its broad specificity, which hydrolyses β-D-galactopyranosides, β-D-fucopyranosides, β-D-xylopyranosides and α-L-arabinosides in addition to β-glucopyranosides (Glew *et al.* 1993).

1.4.2 Nature of solvent

Since the beginning of 1980s, it has been clearly shown that enzymes can be used in organic solvents with great efficiency. For most of the organic compounds soluble in nonaqueous solvents and in such media, biotransformations can be performed on a preparative scale (Vic and Crout 1995; Vic *et al.* 1997). In the case of hydrolases, organic solvents shift the equilibrium towards synthesis (Vulfson *et al.* 1990; Vic *et al.* 1997; Crout and Vic 1998). In organic media, enzymatic thermostability may be increased (Zaks and Klibanov 1984) and enzyme specificity may be changed (Rubio *et al.* 1991). Moreover, since enzymes are not soluble in organic solvents, they can be easily removed and reused. Organic solvents also affect the binding of substrates to the active site by altering the apparent K_m values and controlling the enantio selectivity of the enzymatic synthesis (Margolin *et al.* 1987; Sakurai *et al.* 1988). Also, organic solvents employed influence reaction rate, maximum velocity (V_{max}) or specific activity (K_{cat}), substrate affinity (K_M) and specificity (K_{cat}/K_M) constants (Zaks and Klibanov 1986).

Two classes of water-organic solvent systems can be roughly distinguished, first one is water-water organic solvent homogeneous liquid system and the second one is water-water-immiscible organic solvent two-liquid system (Antonini *et al.* 1981; Butler 1979). In the latter case, the free or immobilized biocatalysts are present in the aqueous phase, whereas the main part of the substrates and products are contained in the organic phase (Vulfson *et al.* 1990). High concentrations of poorly water-soluble substrates and/or products are possible in organic solvent containing media. The chance of microbial contamination is reduced. Further more, reaction equilibria may be shifted favorably, and substrate and/or product hydrolysis can be largely prevented. In case of two-liquid-phase systems extra advantages could occur. Substrate or product inhibition may be reduced as a consequence of a lower inhibitor concentration in the aqueous environment of the enzyme and recovery of product and biocatalyst is facilitated (Vic *et al.* 1997).

For some years, models have been proposed to establish a correlation between the nature of solvent and the observed enzyme behaviour (stability or initial reaction rate). The most commonly used parameters are dielectric constant (ε), dipole moment (μ), Hildebrand solubility parameter (δ) and the logarithm of the partition coefficient in a standard octanol-water two-phase system (log P). For most of the solvents, these values were found in the literature (Weast 1983) or could be calculated. Investigations on quantification of solvent effects on enzyme catalysis were carried out (Brink and Tramper 1985; Laane *et al.* 1987). Brink and Tramper (1985) tried to explain the influence of many water immiscible solvents on biocatalysis by employing the Hildebrand parameter, δ, as a measure of solvent polarity. They concluded that enhanced reaction rates could be expected when the polarity of the organic solvents was low ($\delta \approx 8$) and its molecular weight > 150. But later, it was demonstrated that δ was a poor

measure of solvent polarity. Laane *et al.* (1987) quantified solvent polarity on the basis of log P values. Generally, biocatalysis is low in solvents of log P< 2, is moderate in solvents with a log P value between 2 and 4 and high in non-polar solvents of log P>4.

Laroute and Willemot (1992b) tested the harmfulness of 66 solvents for two glycosidases (glucoamylase from *Rhizopus oryzae* and β-glucosidase from *Aspergillus flavus*) to allow for a first choice before considering the feasibility of reversing hydrolytic reactions. The biocatalysts were placed in the anhydrous organic solvents at 24 ^{o}C and residual activities were checked. They found that most of the ethers, alcohols and esters are not harmful and enzymes retain 65 to 100% of their initial activity after 24h of incubation. Physicochemical properties of solvent and enzyme stability was also studied for the synthesis of 2-hydroxybenzyl-β-D-glucopyranoside (Vic *et al.* 1997), who used the Hidebrand solubility parameter which gives a measure of the overall cohesive energy density of a solution and Hansen parameters that distinguish between the different types of interactions in a solution. However, still no correlation was found between enzymatic stability and hydrophobicity of the organic medium whatever the selected parameters (δ, logP) may be.

1.4.3 Thermal Stability

The factors which affect the thermal stability and catalytic activity of glycosidases in the glycosylation reactions are pH, solvent, water activity (a_w) and reaction temperature. Of them, the two major ones are the nature of the organic solvent employed and water content in the reaction medium. There are few reports on the thermal stability of glycosidases in organic-aqueous media at low water activity. Almond β-D-glucosidase stability was carried out (Vic *et al.* 1997) by suspending a known amount of enzyme in 9:1 (v/v) and 3:7 (v/v) solvent-water mixture (acetone, acetonitrile, tert-butanol, DMF and DMSO). The suspension was incubated at 40 ^{o}C for

24h and the enzyme was employed for the hydrolytic activity against salicin. Enzyme incubated in 9:1 (v/v) acetone, acetonitrile and tert-butanol mixture showed 75 to 90% of the hydrolytic activity, whereas the enzyme in 9:1 (v/v) DMF and DMSO lost almost completely its hydrolytic activity. For a 30% (v/v) of solvent, the effect on enzyme stability is exactly reversed. In acetone, acetonitrile and tert-butanol, the enzyme was rapidly inactivated. However, 66% and 97% of the initial activity was still present after 24 h of incubation in DMF and DMSO respectively. From this study, authors concluded that stability of the enzyme depends on the concentration of the solvent in the medium but the effect may be reversed depending on the nature of the solvent. For the glucoamylase from *Rhizopus oryzae* and β-glucosidase from *Asperzillus flavus*, thermal stability in a low water environment and at a high temperature of 60 ^{o}C was observed (Laroute and Willemot 1992b). Half-life times for the two enzymes have been found to be in the range of several hours, whereas in water, they lost their activity in a few minutes. There were 66 solvents employed for studying the residual activity at 24 ^{o}C. It was found that some solvents in which the enzymes retained 57 to 95% of their residual activity at 24 ^{o}C did not stabilize against thermal denaturation. When the carbon chain length increase, the solvents prevented thermal denaturation effectively (Laroute and Willemot 1992b). Stability of β-glucosidase from *Caldocellum Saccharolyticum* was studied in comparison to commercially available β-galactosidase *A. oryzae* (Stevenson *et al.* 1996). The enzyme was incubated in 0, 2, 4, 5 and 6 M ethanol solutions at 65 ^{o}C and assayed for activity at hourly intervals. No reduction in activity was observed over a period of 6 h except with 6 M ethanol present. Where as *A. oryzae* enzyme was denatured in 4 M ethanol at 45 ^{o}C and the enzyme form *Kluyveromyces fragilis* and *Kluyveromyces lactis,* where inactivated in 3M ethanol at 40 ^{o}C (Stevenson *et al.* 1993). The stability of the immobilized β-glucosidase preparation was investigated by

measuring the residual activity after incubation in octanol at 50 ^{o}C and a_w =1.0 (Ljunger *et al.* 1994). The remaining enzyme activity was determined after 6, 13 and 27 days and compared with the original activity at time zero. Due to stability of this enzyme, the conditions were employed for the repeated synthesis of octyl-β-glucoside. Stability of glycosidases also enhanced due to substrates (Svendsen 2003). Thermal stability of glucoamylase was enhanced 2 fold in the presence of 0.5% starch (Gill and Kour 2004). *Talaromyces emersonii* glucoamylase showed significantly improved thermal stability with a half life of 48 h at 65 ^{o}C in 30% (w/v) D-glucose, compared to 10 h for *A. niger* glucoamylase (Nielsen *et al.* 2002). Another factor, which enhanced the thermal stability of the enzymes, was immobilization. The relationship between the activity of immobilized enzyme and the properties of the porous polymer supports were investigated (Huo *et al.* 2004). Compared to the native enzyme, temperature profile of immobilized glucoamylase was widened and the optimum pH also changed. Thermal stability of the enzyme can be modified by means of cloning and mutation (Nielsen *et al.* 2002; Allen *et al.* 2003). Mutation provides increased thermal stability, reduced isomaltose formation and increased pH optimum to the enzyme (Allen *et al.* 2003). Based on the results of molecular dynamics simulations, twelve mutations were constructed to improve the thermal stability of glucoamylase from *A. awamori* (Liu and Wang, 2003). Glycation of the enzyme also results in increase in thermal stability (Pornpong *et al.* 2005). The stability and kinetic parameters of glycated and the intact enzyme were compared. The glycated enzyme was more resistant to heat, but glycation did not affect the pH stability and the isoelectric value significantly (Pornpong *et al.* 2005).

1.4.4 Role of water

For enzymatic conversions in organic media, the water content is most often a critical parameter influencing not only the equilibrium but also enzyme stability (Halling 1992). It is well known that completely dry enzymes do not function as catalysts. The enzyme molecules have some bound water to gain flexibility. As the hydration level increases, the enzyme becomes more flexible and the activity increases. Different enzymes have different demands of hydration level. Some require rather high water to be active, whereas others can be active at very dry conditions (Valivety *et al.* 1992). In order to achieve glycosylation using glycosidases instead of hydrolysis, the equilibrium position should be shifted (kinetically controlled reaction). This can be achieved by using predominantly organic media at low water activity. One approach to shift the equilibrium position is to add a water-miscible solvent, which decreases the thermodynamic water activity and thereby favors synthesis. An alternative approach is to add a water immiscible solvent. In this case, a hydrophobic product is extracted to the organic phase, so that its concentration in the aqueous phase is kept low and more product synthesized. This approach has been applied successfully in the synthesis of alkyl glycoside in the two-phase system using the hydrophobic alcohol as both substrate and organic phase. (Vulfson *et al.* 1990; Ljunger *et al.* 1994).

Almond β-glucosidase catalyzed synthesis of octyl-β-glucoside showed that a water activity of at atleast 0.67 was required for the synthesis and the rate increased with increasing a_w (Ljunger *et al.* 1994). But the final yield decreased with increasing water activity. The best results were obtained using a high initial water activity which decreased during the course of the reaction. The condensation of glucose and allyl alcohol showed that the water concentration should be adjusted carefully to balance the enzyme activity against equilibrium yield to optimize the productivity (Vic and Crout

1995). Comparable minimum water procedures have been adopted in the glycosylation of butanol (Ismail and Ghoul 1996), 1,6-hexanediol as well as medium chain alcohols (Vic *et al.* 1996; Chahid *et al.* 1992) by many researchers in this field.

By analogy with the lipase-catalysed esterification of carbohydrates (Oosterom *et al.* 1996), it would seem advantageous to use an inert polar solvent to increase the solubility of the sugar. Acetonitrile, acetone and tert-butyl alcohol (Vic and Crout 1994; Vic *et al.* 1995; Vic *et al.* 1997) containing 10% water (a_w~ 0.8) have been used for this purpose, but the reaction rates and the yields were generally lower than when the acceptor alcohol was used as the solvent. As an alternative to the minimum water procedures, reactions have also been performed with aqueous glucose at a_w~1. Such an approach has the advantage of optimum enzyme activity (Ljunger *et al.* 1994) but its efficiency in terms of equilibrium yield depends upon the extraction of the product into the organic phase. Compared to lipases, glucosidases require higher water activity for glycosylation reaction. However, unlike in case of lipases, a systematic study on water activity on glycosidase action is yet to be done.

1.4.5 Kinetic studies of glycosidase catalyzed reactions

Kinetics of enzyme catalyzed reactions help in not only quantifying a reaction but also bring out some intricate details of enzyme inhibition and mechanism which have quite a lot of bearing on the industrial application of glycosidases. The kinetics of the maltose hydrolysis by free and immobilized (in polyacrylamide gel) glucoamylase was investigated by constructing a mathematical model (Yankov *et al.* 1997). Kinetic parameters determined by Michaelis-Menten equation for both free and immobilized enzyme resulted in a good correlation between calculated and experimental data. Statistical analysis for the kinetic model developed for the saccharification of potato starch with glucoamylase showed that the Michaelis-Menten equation could be used as a

simulation model, the Line weaver-Burk and Wilkinson methods could be used for mathematical regression and the final proposed kinetic model explained the enzyme behaviour clearly (Zhang *et al.* 1998). In the kinetics of almond β-glucosidase catalyzed hexyl-glycoside synthesis, the kinetic constants V_{max}, K_m (glycosyl donor) and V_{max} / K_m were all influenced by the water activity and they all increased in value with increasing water activity (Andersson and Adlercreutz 2001). Alcoholysis and reverse hydrolysis reactions performed enzymatically with a hyperthermophilic β-glucosidase and lactose or glucose used as substrate to produce heptyl-β-galactoside and/or heptyl-β-glucoside in one phase water saturated 1-heptanol system followed Michaelis-Menten kinetics behavior and conversions were limited by a strong product inhibition and the formation of oligosaccharides (Mariano *et al.* 2000). In the kinetic study of a thermostable β-glycosidase of *Thermus thermophillus,* addition of D-glucose to reaction mixtures of enzyme and glycosyl donors (β-D-glucoside, β-D-galactoside and β-D-fucosides), resulted in an inhibition or activation depending upon both the substrate concentration and temperature. Enzyme displayed non-Michaelian kinetic behavior within the range of 25-80 ^{o}C, except around 60 ^{o}C, might be due to inactivation (below 60 ^{o}C) and activation (above 60 ^{o}C) in presence of high substrate concentrations (Fourage *et al.* 2000).

1.4.6 Immobilization

The use of enzymes for analytical purposes or any synthetic purposes has been limited because of certain disadvantages, such as their instability, and lack of availability. Moreover, aqueous solutions of enzymes often lose their catalytic ability fairly rapidly and the enzymes can be neither recovered from such solutions nor their activities regenerated (Taki *et al.* 1997; Barolini *et al.* 2004). These difficulties have been overcome by the development of enzymes in immobilized forms (Jianping *et al.* 2003; Roig *et al.* 1995). The free enzyme is immobilized (insolubilized) by trapping it in an

inert matrix such that the immobilized enzyme retains its catalytic properties for a much longer time than the free enzyme and can be used continuously for many more synthesis (Huo *et al.* 2004). When enzymes are immobilized they are held in an environment more like that in which they are found naturally and are generally more stable. Many types of immobilization impart greater stability to the enzyme making them more useful over wider pH ranges and at higher temperatures (Chang and Juang 2005). The immobilized enzyme appears to be less susceptible to the normal activators and inhibitors that affect the soluble enzyme (Taki *et al.* 1997; Barolini *et al.* 2004). Only the strongest inhibitors will decrease its activity and only the strongest activators will boost its catalytic power.

The immobilized glucoamylase possess excellent storage and working stability. Immobilization of glucoamylase can be performed on to the polyvinyl alcohol complex gel (Jianping *et al.* 2003), chitosan-clay composite (Chang and Juang 2005) and plastic material (Roig *et al.* 1995). Thermal and pH stabilities of free and immobilized α-amylase, β-amylase, and glucoamylases were compared, in which immobilization support was prepared by equal weights of chitosan and activated clay and were cross-linked with glutaraldehyde. It was shown that the relative activities of immobilized enzymes are higher than free enzymes over broader pH and temperature ranges for starch hydrolytic reaction (Chang and Juang 2005). Glucoamylase from *A. niger* was immobilized through ionic adsorption onto DEAE-agarose, Q1A-Sepabeads, and Sepabeads EC-EP3 supports (Torres *et al.* 2004) coated with polyethyleneimine (PEI). Thermal stability and optimal temperature was marginally improved by this immobilization. Huo *et al.* (2004) reported, glucoamylase immobilization onto novel porous polymer supports. Compared with the native enzyme, the temperature profile of immobilized glucoamylase was widened, and the optimum pH was also changed. The optimum substrate concentration of the immobilized glucoamylase was higher than that

of the native enzyme. After storage for 23 days, the immobilized glucoamylase still maintained about 84% of its initial activity, whereas the native enzyme only maintained about 58% of the initial activity. Moreover, after using repeatedly seven times, the immobilized enzyme maintained about 85% of its initial activity (Huo *et al.* 2004). Kosary *et al.* (1998) studied α- and β-glucosidases catalyzed O-glycosylation activity with D-glucose as substrate and with different alcohols both as reaction partners and solvents in reverse hydrolytic processes. With native glucosidases, upscaling resulted in low yields due to heterogeneity of the reaction mixtures and the aggregation of undissolved enzymes in organic media. Immobilization of the enzymes on a modified polyacrylamide-type bead support (Acrylex C-100) increased enzyme stability resulting in higher yields necessary to perform glucosylations on a larger scale (Kosary *et al.* 1998). In this report, immobilized glucosidases retained 55–80% of their original activity depending on the water content and the type of alcohol after 72 h incubation. The enzymatic synthesis of alkyl-β-glucosides by water-immiscible alcohols studied using immobilized β-glycosidase gave a higher conversion yield and a final product concentration than that using the enzyme in its free state (Papanikolaou 2001).

There have been reports that reaction could not take place after immobilization. Gargouri *et al.* (2004) reported the production of β-xylosidase and β-glucosidase by the fungus *Sclerotinia sclerotiorum* and immobilization supports with different physico-chemical characteristics were evaluated for use in continuous reactors. Synthesis of glycosides by *trans*-glycosylation of sugars and long-chain alcohols, with primary and secondary alcohols as substrates, in the presence of free or immobilized enzyme was investigated (Gargouri *et al.* 2004). The majority of the immobilized preparations were unable to catalyze the synthesis of alkyl-glycosides. The immobilized β-glycosidase systems using ion exchange resins were found to increase the enzyme stabilities when

tested for hydrolysis but did not increase the synthetic efficiency. This may be due to the unfavorable conformation of the immobilized enzyme for synthetic reaction (Gargouri *et al.* 2004). Glucoamylase (1,4-α-D-glucan glucohydrolase, EC 3.2.1.3) from *A. niger* was immobilized on cationic nonporous glass beads by electrostatic adsorption followed by cross linking with glutaraldehyde (Wasserman *et al.* 1982). Immobilized glucoamylase showed decreased stability upon heating, compared to the soluble enzyme.

1.5 Strategies employed in glycosylation

The advantages of carrying out glycosylation using reverse micelles, super critical carbon di-oxide, microwave and response surface methodology are discussed below with few examples.

1.5.1 Glycosylation in reverse micelles

Water in oil microemulsions with reverse micelles provides an interesting alternative to normal organic solvents in enzyme catalysis with hydrophobic substrates. Reverse micelles are useful microreactors because they can host proteins like enzymes (Luisi *et al.* 1998). Catalytic reactions with water–oil substrates can occur at the large internal water-oil interface inside the microemulsion (Eriksson *et al.* 2004). A salient feature in all the enzymes in which thermostability has been documented is that thermostability decreases as the water content in the system increases. In this media, both the activity and stability of biomolecules can be controlled by the concentration of water (Srivastava and Strasser 2001; Orlich and Schomacker 2002). In the reverse micelles, it has been possible to probe the relation between the solvent and enzyme kinetics, as well as some of the factors that affect enzyme thermostability and catalysis (Srivastava and Strasser 2001). The overall activity of amyloglucosidase entrapped into reverse micelles of Triton-X-100-xylene-hexanol was lower, than in aqueous systems, but showed higher stability upto 50 ^{o}C (Shah *et al.* 2000). Synthetic applications of enzymes entrapped in

reverse micelles and organo-gels were discussed elaborately by Fadnavis and Deshpande (2002). Study of β-1,4-glucosidase in water/Phosphatidylcholine/heptane-butanol reverse micelles was reported (Miao and Yao 1999). The activity and kinetics of β-1,4-glucosidase in hydrolysis of salicin showed that Michaelis-Menton kinetics was followed, V_{max} was found to be 11.8 times larger than that in aqueous media and K_m was only 1/25 of that in aqueous media. There are reports on the synthesis of alkyl glycosides, oligosaccharides (galacto-oligosaccharides) in reverse micelles by using glycosidases and higher yields were reported compared to aqueous media (Chen *et al.* 2001; 2003; Kouptsova *et al.* 2001). Transgalactosylation reaction of the enzyme β-galactosidase was strongly dependent on the molar ratio of water to surfactant (Wo) of Aerosol-OT (AOT)/isooctane reverse micelles (Chen *et al.* 2001). Synthesis of alkyl glycosides in AOT reverse micelles system was studied (Kouptsova *et al.* 2001) and the direction of the reaction was shown to depend on the pH of the aqueous solution solubilized in reverse micelles.

1.5.2 Glycosylation in supercritical carbon dioxide

Use of super critical carbon dioxide ($SCCO_2$) as a solvent and reaction medium is growing rapidly in recent years. Super critical carbon dioxide has several advantages over organic solvents. Carbon dioxide was chosen as the super critic fluid (SCF) for the following reasons: (1) CO_2 becomes a SCF above 31 °C and 73.8 atm, conditions which are easily accomplished with gentle heating from ambient temperature and a commercial liquid chromatography pump, (2) the solvent properties of $SCCO_2$ can be continuously varied by changing the pressure or temperature and (3) CO_2 is nontoxic and the medium is easily removed by decompression to atmospheric pressure (Mori and Okahata 1998; 2000). Several reviews describe the variety of organic reactions including chemical (hydrogenations, hydroformylations, photorections, halogenations, Diels Alder

cycloadditions, oxidations, coupling reactions, Pauson-Khand reactions, olefin methatheses, Friedel-Crafts alkylations, asymmetric reactions) and enzymatic reactions carried out in supercritical fluids (Mori and Okahata 2000; Oakes *et al.* 2001; Mori and Okahata 2002; Matsuda *et al.* 2002). Enzyme stability can be improved by $SCCO_2$ pretreatment. The application of supercritical fluids in the control of enzyme reactions, with emphasis on the use of supercritical fluroform in the regulation of β-D-galactosidase mediated transglycosylation and oxidation has been discussed (Mori and Okahata 2003). The $SCCO_2$ pretrated α-amylase retained 41% activity based on the original activity, whereas the non-treated α-amylase completely lost its activity in an hour in water (Liu and Chang 2000). n-Octyl-β-D-xylotrioside and xylobioside synthesis were significantly increased in supercritical CO_2 and fluroform (CHF_3) fluids mediated one-step reaction of xylan and n-octanol using the acetone powder (acetone-dried cells) of *Aureobasidium pullulants* as the enzyme source of xylanase (Nakamura *et al.* 2000; Matsumura *et al.* 1999). A lipid-coated β-galactosidase catalyzed trans galactosylation reactions carried out in $SCCO_2$ resulted in good conversion yields up to 72% whereas native β-galactosidase hardly catalyzed the transgalactosylation in $SCCO_2$ due to its insolubility and instability in $SCCO_2$ (Mori and Okahata 1998). Apart from the enzymatic transformations, super critical CO_2 can be useful for the extraction of glycosides from the natural sources (Zeng and Huang 2000; Palma *et al.* 2000).

1.5.3 Microwave-assisted glycosylation reactions

Ultrasonification and microwave assistance are two emerging approaches for enhancing reaction rates in low water media. Microwave irradiation is becoming an increasingly popular method of heating which replaces the classical one because it proves to be a clean, cheap, and convenient method. Often, it affords higher yields and results in shorter reaction times (De Oliveira *et al.* 2002). A new trend in organic

synthesis by utilizing microwave irradiation and enzyme catalysis has evolved (Cai *et al.* 2003), is called Microwave Irradiation Enzyme Coupling Catalysis (MIECC). This technique can be divided into two categories, such as enzyme synthesis under microwave irradiation in non/micro-aqueous media (wet method) and without media (dry method). Microwave irradiation of a mixture of tri-O-acetyl-D-glucal and an appropriate alcohol in the presence of Montmorillonite K-10 as a catalyst, provided unsaturated glycosides in much shorter time and in yields comparable to conventional heating (De Oliveira *et al.* 2002). Glucose and dodecanol were reacted in the presence of dodecyl-benzenesulfonic acid under microwave irradiation to yield dodecanol glucoside with a degree of oligomerization of 1.43 (Rhode *et al.* 1999). A three step microwave assisted solvent-free synthesis of decyl D-glucopyranoside with 1-decanol was established for D-glucose and extended to D-galactose, D-mannose and N-(2,2,2 trichloroethoxy-carbonylamino)-D-glucosamine with 70% avarage overall yield for the three steps such as peracetylation, glycosylation and saponification (Limousin *et al.* 1997). In the synthesis of alkyl glycosides under microwave assistance using catalytic amount of acid, the ratio of the α/β-anomers was influenced by the reaction conditions (Nuchter *et al.* 2001). The effect of microwave irradiation on a thermostable β-galactosidase from *Bacillus acidocaldarius* enzyme was experimentally tested, showing that residual activity depends on enzyme concentration, microwave power level and exposure time (La Cara *et al.* 1999). The selectivity for galacto-oligosaccharides synthesis can be increased by 217-fold under microwave irradiation using immobilized β-glucosidase from *Kluyveromyces lactis* with added co-solvents such as hexanol (Maugard *et al.* 2003). Reduced hydrolysis product and increased rates of conversion have been reported in tranasglycosylation reactions to simple alcohols catalyzed by other thermophilic β-galactosidases in microwave irradiated, dry media (Gelo-Pujic *et al.* 1997).

1.5.4 Response Surface Methodology (RSM) in glycosylation

Response surface methodology (RSM) is a technique used in the experimental study of relationship between response variables and many input variables. The techniques have been used to answer the key question of what values of the input variables will yield a maximum for the response variables. RSM has been widely used in various disciplines such as foods, chemicals and in the biological processes (Linder *et al.* 1995; Shieh *et al.* 1995; Chen *et al.* 1997).

In recent years, this methodology has been applied to some glycosylation reactions as well. The objective of these studies is to evaluate the optimum conditions within the parameters employed to achieve a maximum conversion yield. Enzymatic synthesis of butyl glucoside by β-glucosidase from sweet almonds was optimized by response surface methodology (Ismail *et al.* 1998). The empirical models were developed to describe relationship between the operating variables - temperature, water/butanol volume ratio, glucose concentration and enzyme concentration and responses - butyl glucoside concentration and conversion yield. The statistical analysis indicated that the four factors have significant effects on the butyl glucoside synthesis. Ismail *et al.* (1998) found good agreement between predicted and experimental data. Optimization was also carried out for the synthesis of butyl galactoside by β-galactosidase from *A. oryzae* by using RSM (Ismail *et al.* 1999). In this work, they performed a transglycosylation reaction using lactose as a glycosyl donor. n-Octyl glucoside was produced and optimized by using this method by employing Doehlert's matrix design (Chahid *et al.* 1994). The three parameters employed were amount of acetate buffer, octanol and lactose and the products obtained were octyl glycosides (octyl galactoside and octyl glucoside).

Usefulness of several statistical designs in experimental optimization including Box-Behnken, Central Composite Rotatable and Plackett-Burman designs in lipase catalysed esterification reactions have been carried out (Kiran *et al.* 1999; 2000; Manohar and Divakar 2002). Analyses of several response surface plots obtained by employing statistical designs in glycosidase catalysed reactions have indicated that such plots could explain the glycosylation behaviour in the presence of different kinds of substrates and reaction conditions. The statistical design employed in the glycosylation reactions were Central composite rotatable design (Ismail *et al.* 1998) and Doehlert uniform shell design for four parameters (Ismail *et al.* 1999). A Doehlert experimental matrix displays a uniform distribution of the points within the experimental domain. A feature of Doehlert design is that the number of levels of each experimental factor is not the same. One should use the design so that the parameter with most-complex relationship is modeled with the largest number of levels. Similarly CCRD design can be employed for four level and five level parameter experiments and significance of the parameters employed can be found out by this design in the glycosylation reactions (Ismail *et al.* 1998).

1.6 Scope of the present work

In the last two decades, a large number of publications on biotransformation involving enzymes are available. Structurally diverse substrates have been employed emphasizing the broad specificity of such enzyme catalyzed transformation. Glucosidases and glucoamylases are not also exceptions to the broad specificity observed. Such broad specificity could be largely due to large amounts of enzymes being employed to turn the equilibrium to the reverse direction. Another reason to the broad specificity may be the smaller molecular weights of acceptor and donors employed compared to the natural substrates. Still feasibility of transformation especially in

glycosylation involving certain selected acceptor and donors have to be investigated. The present investigation attempts to explore the potentiality of amyloglucosidase and β-glucosidase in effecting glycosylation of a wide variety of glycosyl acceptors from straight chain alcohols to few selected substituted phenols like guaiacol, eugenol, curcumin and α-tocopherol.

Many glycosides are used in broad range of applications as surfactants (Busch *et al.* 1994), as food colorants and flavoring agents (Sakata *et al.* 1998), sweeteners (Shibata *et al.* 1991), antioxidants, anti-inflammatory (Gomes *et al.* 2002), antitumor (Kaljuzhin and Shkalev 2000), antibiotics (Ikeda and Umezawa 1999), antifungal (Tapavicza *et al.* 2000), antimicrobial (Zhou 2000) and cardiac related drugs (Ooi *et al.* 1985). Glycosylation renders lipophilic compounds more water soluble and thereby increase bioavailability of biologically active compounds besides imparting stability to the aglycon (Kren and Martinkova 2001). Thus enzymatic synthesis of alkyl glycosides used as surfactants in food, glycosides of guaiacol, eugenol, curcumin and α-tocopherol which exhibit antioxidant activity have been investigated in detail in the present work. Of these glycosides of selected phenols can be also made water-soluble, and stable necessary to enhance the bioavailability of the compounds in food and pharmaceutical applications. Besides, curcumin glycosides can also be used as a water-soluble food colorant.

Amyloglucosidase from *Rhizopus* sp. and β-glucosidase from sweet almonds catalyzed synthesis of above mentioned alcohols and phenols were carried out in di-isopropyl ether solvent in an experimental setup where larger concentration of substrates can be employed with lesser concentration of enzyme to get better conversion. The carbohydrate molecules employed for the glycoside preparations were D-glucose, D-galactose, D-mannose, D-fructose, D-arabinose, D-ribose, maltose, sucrose, lactose, D-

mannitol and D-sorbitol. The reactions were investigated in detail in terms of incubation period, pH and buffer concentration, enzyme concentration, substrate concentration, regio and stereo selectivity and kinetics. The glycosides prepared were isolated and characterized and few of them showed angiotensin-converting enzyme inhibition activities. The salient features of these investigations are described in detail with ensuring chapters.

Chapter 2

Materials and Methods

2.1 Materials

2.1.1 Glycosidases

Two glycosidases, amyloglucosidase from *Rhizopus* sp. and β-glucosidase isolated from sweet almonds were employed for the present work.

Amyloglucosidase

Amyloglucosidase (3.2.1.3), from *Rhizopus* sp., a fungal source, with an activity of 22,570 units / g of solid purchased from Sigma Chemical Co., St. Louis, MO, USA was employed for most of the glycosylation work. One unit liberates 1.0 mg of glucose from starch, in 3 min at pH 4.5 at 55 ^{o}C. This enzyme was used for the synthesis of glycosides of alcohols of carbon chain length C1 to C18, guaiacol, eugenol, curcumin and α-tocopherol.

β-Glucosidase

β-Glucosidase was isolated from sweet almonds and the crude enzyme was employed for the synthesis of glucosides of n-octanol, guaiacol, eugenol, curcumin and α-tocopherol.

2.1.2 Alcohols/Phenols

Methanol, ethanol, n-propanol, n-butanol, n-heptanol, n-stearyl alcohol and guaiacol from SD fine chemicals (Ind.) Ltd. and n-hexanol, n-octanol, n-nonyl alcohol, n-decyl alcohol n-lauryl alcohol from Sisco Research Laboratories Pvt. Ltd. India were employed. Cetyl alcohol and eugenol were procured from Loba Chemie Pvt. Ltd. India and α-tocopherol was from Hi-Media Ind. Ltd. Curcumin (>95% purity) was from Flavors and Essences Pvt. Ltd. India.

2.1.3 Carbohydrates

D-Glucose and sucrose purchased from SD fine chemicals (Ind.) Ltd., D-galactose and D-fructose from Hi-Media Ind. Ltd.; D-mannose, D-arabinose, D-ribose, D-sorbitol

and D-mannitol, from Loba Chemie Pvt. India Ltd., maltose from Sigma Chemical Co., St. Louis, MO, USA and lactose from Sisco Research Laboratories Pvt. Ltd. India, were employed in the glycosylation reactions.

2.1.4 Solvents

Chloroform, di-isopropyl ether, diethyl ether, dimethyl sulphoxide (DMSO), ethyl acetate, petroleum ether (60-80 ^{o}C) were purchased from SD fine Chemicals (Ind.) Ltd. All the solvents employed were distilled once before use. HPLC grade acetonitrile was purchased from Qualigens Fine Chemicals Ltd., and was used as such.

2.1.5 Other chemicals

The following chemicals and their sources are shown in Table 2.1

Table 2.1 Chemicals and their companies of procurement.

Chemicals	Company
Sodium acetate (CH_3COONa), di-sodium hydrogen phosphate (Na_2HPO_4)	Ranboxy Laboratories Ltd. India.
Di-sodium tetra borate ($Na_2B_4O_7$ 10 H_2O), sodium choride (NaCl), sodium hydroxide (NaOH), sodium sulphite (Na_2SO_3), sodium sulphate anhydrous (Na_2SO_4), hydrochloric acid (HCl), sulphuric acid (H_2SO_4), iodine resublimed (I_2), sodium potasium tartarate (Rochelle salt), di-nitrosalicylic acid and silica gel, ammonium per sulphate.	SD fine Chemicals (Ind.) Ltd.
1-Naphthol, hippurric acid and triton X-100, coomassie brilliant blue R 250, β-mercaptoethanol, bromophenol, trichloro acetic acid	Loba Chemie Pvt. Ltd. India.
Hippuryl-L-histidyl-L-leucine acetate, 2,2-diphenyl-1-picrylhydrazyl (DPPH), butylated hydroxyanisole (BHA), bovine serum albumin (BSA), Sephadex G-10 and Sephadex G-15, acrylamide, bis-acrylamide, sodium dodecyl sulphate (SDS)	Sigma Chemical Co., St. Louis, MO, USA.

Potassium bromide (KBr), Folin-Cicolteau reagent and HEPES buffer (N-[2-hydroxyethyl] piperazine-N'-[2-ethanesulphonic acid])	Sisco Research Laboratories Pvt. Ltd. India.

2.2 Methods

2.2.1 Enzyme activity assay for amyloglucosidase, α-glucosidase and β-amylase

Enzyme activities for amyloglucosidase, α-glucosidase, β-amylase were determined using Sumner and Sisler (1944) method. Activity was expressed in terms of micromoles (μmol) of glucose released per min per mg of enzyme employed. Specific activity was expressed as μmol of glucose released per min per mg of protein present in the enzyme (Table 2.2).

2.2.1.1 Calibration of glucose

A stock solution was prepared by dissolving 10 mg of D-glucose in 10 mL of distilled water. A series of aliquots of 0.1 to 1.5 mL were pipetted out into appropriate volumes of 0.2 M sodium acetate buffer pH 4.2 such that, the final volume was 3.0 mL. To this 3.0 mL of di-nitro salicylic acid (DNS) reagent (Sumner and Sisler 1944) containing 1% di-nitro salicylic acid, 0.2% phenol, 0.05% sodium sulphite and 1% NaOH was added and the reaction mixture was incubated on a boiling water bath for 5 min with shaking. Then the reaction mixture was cooled under running tap water. Absorbance of each solution was determined on a Shimadzu UV-1601 Spectrophotometer at 575 nm. A calibration plot was constructed for the concentration of glucose in the range 0.1 mg to 1.5 mg (Fig. 2.1).

2.2.1.2 Activity assay

A stock solution of 4% starch was prepared by dissolving 4 g of potato starch in 100 mL 0.2 M acetate buffer pH 4.2. Enzyme amyloglucosidase (1 mg), α-glucosidase (1

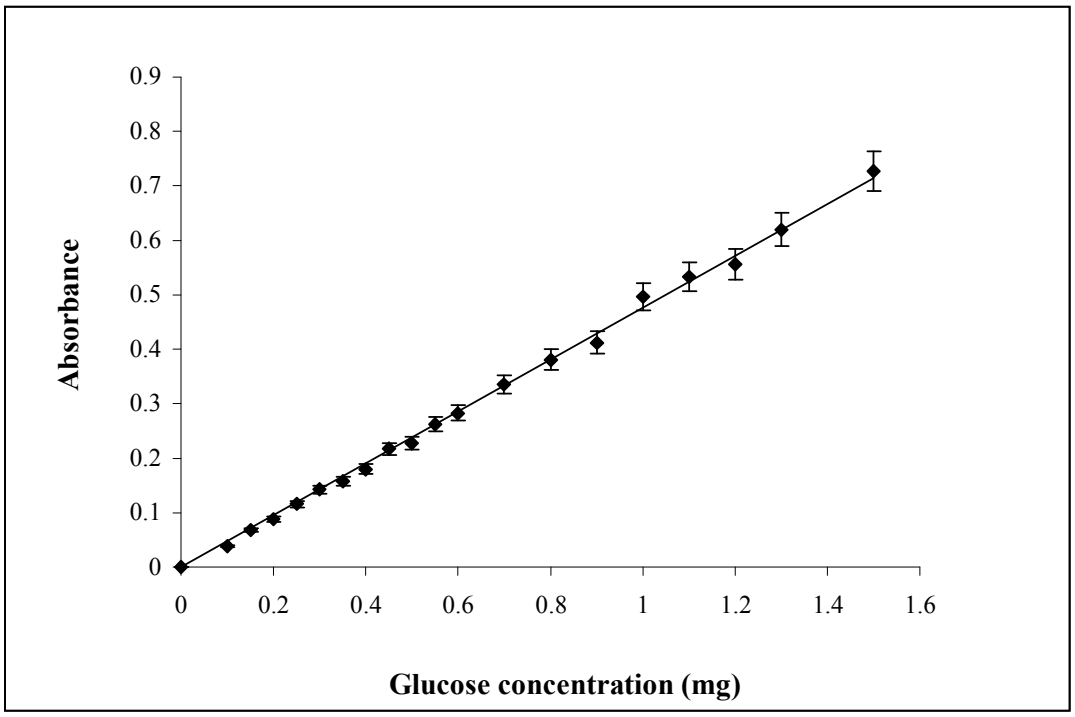

Fig. 2.1 Calibration plot for D-glucose concentration. A stock solution of 10 mg/ 10 mL D-glucose solution was used for taking 0.1 to 1.5 mL aliquots. Absorbance was measured at 575 nm.

mg) and β-amylase (1 μL) were added separately into 5.0 mL of stock solution and incubated at 60 °C on a Heto-Holten shaking water bath for 60 min at 200 rpm. The reaction was arrested by adding 0.8 mL 4 N NaOH. A duplicate was also performed. Pipetted out 0.3 mL of this solution and the same was made up to 3.0 mL using 0.2 M acetate buffer pH 4.2. Then 3 mL of DNS reagent was added and incubated for 5 min on a boiling water bath with shaking and then cooled. Absorbance values were measured at 575 nm using a Shimadzu UV-1601 Spectrophotometer and the amount of glucose present was determined from the calibration plot. The activity of each enzyme was evaluated and shown in Table 2.2.

Table 2.2 Activity assay for amyloglucosidase, α-glucosidase, β-amylase and β-glucosidase

Enzyme	[a] Protein content (%)	[b] Unit activity μmol/min/mg	Specific activity μmol/min/mg of protein
Amyloglucosidase	60.5	2.83	4.67
α-Glucosidase	43.9	2.27	5.16
β-Amylase[c]	2.69	2.20	81.8
β-Glucosidase[d]	49.2	2.93	5.92

[a] Protein estimation by Lowry's method. [b] Activity assay by Sumner and Sisler method. [C]Unit activity for β-amylase is μmol/min/μL of enzyme. [d]Activity assay by Colowick and Kaplan (1976).

2.2.2 Protein estimation

Protein content of amyloglucosidase, α-glucosidase, β-amylase and the isolated β-glucosidase (from sweet almonds) were determined by using Lowry's method (Lowry *et al.* 1951). In order to leach out the protein from the immobilized matrix or carrier, 25 mg of enzyme (amyloglucosidase, α-glucosidase and β-glucosidase) in 50 mL, 0.5 M NaCl and 200 μl of β-amylase in 20 mL of 0.5 M NaCl were stirred at 4 °C for 12 h and from this, known volumes of the samples were taken for protein estimation.

Solution A – 1% of copper sulphate in water, solution B – 1% of sodium potassium tartarate in water and solution C – 2% of sodium carbonate solution in 0.1 N NaOH were prepared. Working solution I was prepared by mixing one part each of solution A and B and 98 parts of C. A 1:1 diluted solution of commercially available Folin-Cicolteau reagent with distilled water served as working solution II. To the protein sample in 1 mL water, 5 mL of working solution I was added and incubated for 10 min at room temperature. A 0.5 mL of working solution II was then added followed by incubation at room temperature for 30 min and the absorbance was measured at 660 nm using a Shimadzu UV – 1601 spectrophotometer. Calibration plot for protein concentration was prepared by employing bovine serum albumin (BSA) in the concentration range 0-100 μg in 6.5 mL of the sample (Fig. 2.2). Using this calibration plot, protein content of the glycosidases was determined and the values are shown in Table 2.2.

2.2.3 Preparation of buffers

A buffer concentration of 10 mM CH_3COONa for pH 4.0 and 5.0, Na_2HPO_4 for pH 6.0 and 7.0 and $Na_2B_4O_7$ $10H_2O$ for pH 8.0 buffers were prepared by dissolving appropriate quantities of the respective buffer salts in distilled water. The pH of the solutions was adjusted by adding 0.1 M of HCl or NaOH using Control Dynamics pH meter model APX175E/C, India.

2.2.4 Glycosylation procedure

2.2.4.1 Shake flask method

Shake flask method was employed only for the preparation of alkyl glucosides. In this method, reactions were carried out in a 25 mL stoppered conical flasks wherein D-glucose and alcohols were taken in a molar ratio of 1:50. Known quantities of amyloglucosidase (10-75 % w/w D-glucose) was added along with 0.1 to 1.0 mL of 0.01

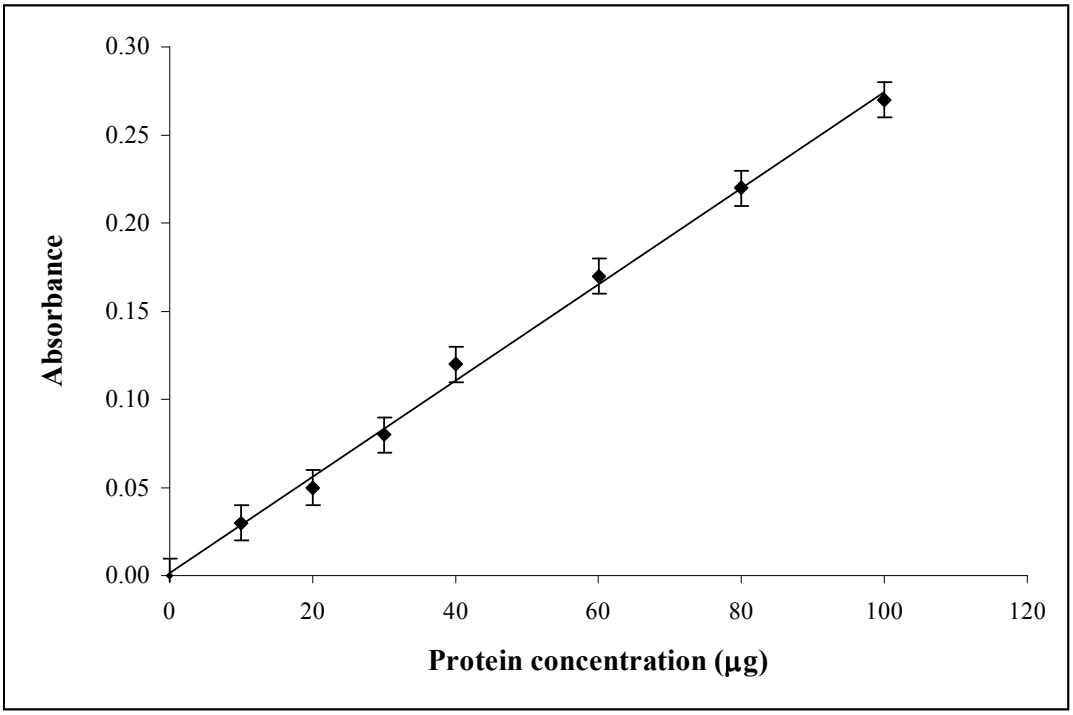

Fig. 2.2 Calibration curve for the estimation of protein by Lowry's method. A stock solution of 500 µg/ 5mL BSA solution was prepared. From the stock solution 0.1 - 1.0 mL solutions were pipetted out and the total volume was made upto 1.0 mL with distilled water. Absorbance was measured at 660 nm.

M buffer of appropriate pH (pH 4.0-8.0) and incubated at 60 °C in a temperature control shaker at 150 rpm for 72 hours.

After the reaction, the reaction mixture was held in a boiling water bath for 5-10 min to denature the enzyme in order to prevent the hydrolytic reaction. Then 15-20 mL of water was added to dissolve the unreacted glucose and the product glycoside. The unreacted alcohol was separated in a separating funnel with petroleum ether or n-hexane. The bottom water layer was evaporated to get the unreacted glucose and the product glycoside.

2.2.4.2 Reflux method

Reflux method was employed for the preparation of all the glycosides described in the present work. In the reflux method, the carbohydrate and alcohol/phenol of known concentrations were taken along with appropriate quantities of amyloglucosidase (% w/w carbohydrate) in a 150 mL two-necked flat-bottomed flask. A known concentration of buffer of 0.01M (pH 4.0 to 8.0) was added and then refluxed in 100 mL di-isopropyl ether with stirring for a specified period of incubation, usually 72 h unless otherwise specified. The products were worked up as mentioned in shake flask method experiments for all the glycosides except those of curcumin. In case of curcumin glycosides, the unreacted D-glucose and the glycosides were extracted using 20-30 mL of water and further filtered to remove the unreacted curcumin and the filtrate was evaporated to dryness to get the unreacted D-glucose and the product curcumin glycoside. The reaction mixtures containing unreacted D-glucose and the product glycosides were analyzed by HPLC.

2.2.5 Isolation of glycosides

The synthesized glycosides were isolated from the reaction mixture by column chromatography. Sephadex G25 and Sephadex G15 as column material was employed. A

sample concentration of 100 to 200 mg was loaded on to the column (100x 1cm) and eluted with water at a flow rate of 2 mL/h. Various fractions were collected and the separation was monitored by thin layer chromatography (TLC). A chloroform:methanol:water:pyridine (65:30:4:1v/v) solvent system was used as a mobile phase for TLC. The spots were detected by spraying solution containing 1.59 g of α-naphthol dissolved in 50 mL of ethanol, 5 mL of water and 6.5 mL of 18 M of sulfuric acid and heating at 100 °C in an oven for 5 min (Ismail *et al.* 1998). The product glycoside fractions pooled were evaporated on a water bath and subjected to characterization. Although the chromatography separation resulted in separating glycosides from the unreacted carbohydrate molecules, further separation of the individual glycosides was not possible with Sephadex G15 or any other column materials employed because of similar polarity of the molecules.

2.2.6 HPLC

The reaction mixtures were analyzed by high performance liquid chromatography (HPLC) in a Shimadzu LC 8A instrument using a μ-Bondapak amino-propyl column (10 μm particle size, 3.9 x 300 mm length) and acetonitrile: water in 80:20 (v/v) as the mobile phase at a flow rate of 1mL/min using refractive index detector. The retention time for carbohydrates were found to be 4.8 to 6.8 min and for the glycosides it was in the 7.0 to 10.0 min range. Conversion yields were determined from the HPLC peak areas of the glucoside and the free carbohydrates with respect to the carbohydrate concentration employed. Error measurements in HPLC yields will be ± 5-10%.

2.2.7 UV-Visible spectroscopy

Ultra Violet-Visible spectra were recorded on a Shimadzu UV-1601 spectrophotometer. Known concentrations of the samples dissolved in the indicated solvents were used for recording the spectra.

2.2.8 Infrared spectroscopy

Infrared spectra were recorded on a Nicolet-FTIR spectrophotometer. Isolated solid glycoside samples (5-8 mg) were prepared as KBr pellet and employed for spectral recording. Liquid alcohol standards were employed as such between salt plates to obtain the IR spectra.

2.2.9 NMR

2.2.9.1 ^{1}H NMR

^{1}H spectra were recorded on a Brüker DRX 500 MHz NMR spectrometer (500.13MHz). Proton pulse width was 12.25 μs. Sample concentration of about 40 mg of the sample dissolved in DMSO-d_6 was used for recording the spectra at 35 ^{o}C. About 100-200 scans were accumulated to get a good spectrum. The region between 0-10 ppm was recorded for all the samples. Chemical shift values were expressed in ppm relative to internal tetra-methyl silane (TMS) as the standard.

2.2.9.2 ^{13}C NMR

^{13}C NMR spectra were recorded on a Brüker DRX 500 MHz NMR spectrometer (125MHz). Carbon 90° pulse widths was 10.5 μs. Sample concentration of about 40 mg dissolved in DMSO-d_6 was used for recording the spectra at 35 ^{o}C. About 500 to 2000 scans were accumulated for each spectrum in the 0-200 ppm region. Chemical shift values were expressed in ppm relative to internal tetramethyl silane (TMS) as the standard.

2.2.9.3 2D-HSQCT

Two-dimensional Heteronuclear Single Quantum Coherence Transfer Spectra (2-D HSQCT) were recorded on a Brüker DRX 500 MHz NMR spectrometer. A sample concentration of about 40 mg in DMSO-d_6 was used for recording the spectrum. Spectra were recorded in magnitude mode with the sinusoidal shaped Z gradients of strength

25.7, 15.42 and 20.56 G/cm in the ratio of 5:3:4 applied for a duration of 1 ms each with a gradient recovery delay of 100 μs to defocus unwanted coherences. Then it was incremented in 256 steps. The size of the computer memory used to accumulate the 2D data was 4K. The spectra were processed using unshifted and π/4 shifted sine bell window function in F_1 and F_2 dimensions respectively.

2.2.10 Mass spectroscopy

Mass spectra were obtained using a Q-TOF Waters Ultima instrument (Q-Tof GAA 082, Waters corporation, Manchester, UK) fitted with an electron spray ionization (ESI) source. A software version 4.0 was used for the data acquisition. The positive ion mode using a spray voltage at 3.5 kV and a source temperature of 80 °C was employed for recording the spectra. Mass spectra were recorded under electron impact ionization at 70 eV electron energy. Samples were prepared in the concentration range of 0.5-1.0 mg/mL in distilled water and injected by flow injection analysis at a flow rate of 10 μL/ min. The recorded mass of the sample were in the range of 100-1500.

2.2.11 Polarimetry

Optical rotations of the isolated glycosides were recorded on Perkin-Elmner 243 Polarimeter. Sodium lamp at 599 nm was used as the light source. Sample concentration of 0.5 to 1% in H_2O were used for the rotation measurements and specific rotations were calculated using the equation.

$$[\alpha]_D^{25^\circ C} = \frac{[\alpha]_{obs} \times 100}{C \times l}$$

where, $[\alpha]_D$ is the specific rotation in degrees at 25 ^oC, $[\alpha]_{obs}$ is the observed rotation, C is the concentration of the samples in percentage and l is the path length in dm.

2.2.12 Critical micellar concentration (CMC)

Critical micellar concentration for the non-ionic surfactant octyl-D-glucoside, was determined by using Comassive brilliant blue-G250 (Rosenthal and Koussale 1983). A series of aliquots of sample in the concentration range 0 - 20 mM were prepared and made up to 1 mL by adding comassive brilliant blue-G250 reagent. The reaction mixtures were shaken well and the absorption was measured at 620 nm. A plot of concentrations of the sample versus absorption was constructed, from which CMC was determined as the concentration of the glycoside corresponding to a change in the slope of the absorption versus concentration plot.

2.2.13 Extraction of Angiotensin Converting Enzyme (ACE) from pig lung

ACE was extracted from pig lung by the method on Sanchez *et al.* (2003). A 100 g of pig lung was minced and homogenized using a blender with 10 mM pH 7.0 HEPES buffer containing 0.4 M NaCl at a volume ratio of 5:1 (v/w of pig lung). The temperature was maintained at 4 °C throughout the procedure. The homogenate was centrifuged at 9000 g for 60 min. The supernatant was discarded and the precipitate was washed twice with 200 mL of 10 mM pH 7.0 HEPES buffer containing 0.4 M NaCl. The final precipitate was resuspended in 200 mL of pH 7.0, 10 mM HEPES buffer containing, 0.4 M NaCl, 10 μM $ZnCl_2$, 0.5%(w/v) triton X 100 and stirred over night. The solution was centrifuged to remove the pellets. The supernatant was dialyzed against water using a dialysis bag of molecular weight cut off 10 kDa and later lyophilized.

2.2.14. Angiotensin Converting Enzyme (ACE) inhibition assay

ACE inhibition assay for the glycosides prepared were performed by the Cushman and Cheung (1971) method. Aliquots of glycoside solutions in the concentration range 0.13 to 1.06 mM (0.1 mL to 0.8 mL of 2.0 mM stock solution) were taken and to this 0.1 mL of ACE solution (0.1% in 0.1 M phosphate buffer, pH 8.3

containing 300 mM NaCl) was added. To this solution further 0.1 mL of 5.0 mM hippuryl-L-histidyl-L-leucine (HHL) was also added and the total volume made upto 1.25 mL with phosphate buffer (0.95 mL to 0.25 mL of 0.1 M pH 8.3 containing 300 mM NaCl). The solution was incubated on a Heto-Holten shaking water bath for 30 min at 37 °C. Blanks were performed without the enzyme by taking only the glycoside solution (0.1 to 0.8 mL) along with 0.1 mL of 5.0 mM HHL. The total volume was made upto to 1.25 mL with the same buffer (1.05 mL to 0.35 mL). The reaction was terminated by adding 0.25 mL of 1 M HCl. Hippuric acid formed in the reaction was extracted with 1.5 mL of ethyl acetate. One mL of ethyl acetate layer was evaporated to dryness and treated with equal amount of distilled water and the absorbance was measured at 228 nm for hippuric acid. The hippuric acid formed in 1.5 mL of ethyl acetate was determined from a calibration curve prepared using a standard 0-400 nmol hippuric acid solution in 1 mL of distilled water (Fig. 2.3). Specific activity was expressed as μmol of hippuric acid formed per min per mg of enzyme protein.

$$\text{Specific activity} = \frac{A_{ts} - A_{blank}}{T \times S \times E}$$

A_{ts} = absorbance of test solution, A_{blank} = absorbance of blank solution, T = incubation period in min, S = slope value of the calibration plot, E = amount of the enzyme in mg protein.

Percentage inhibition was expressed as the ratio of the specific activity of ACE in the presence of the inhibitor to that in the absence of the inhibitor, the latter being considered as 100%. IC_{50} value was expressed as the concentration of the inhibitor required for 50% reduction in ACE specific activity. Molecular weights of the glycosides employed in the calculations are weighted averages of molecular weights of glycosides detected by NMR spectroscopy.

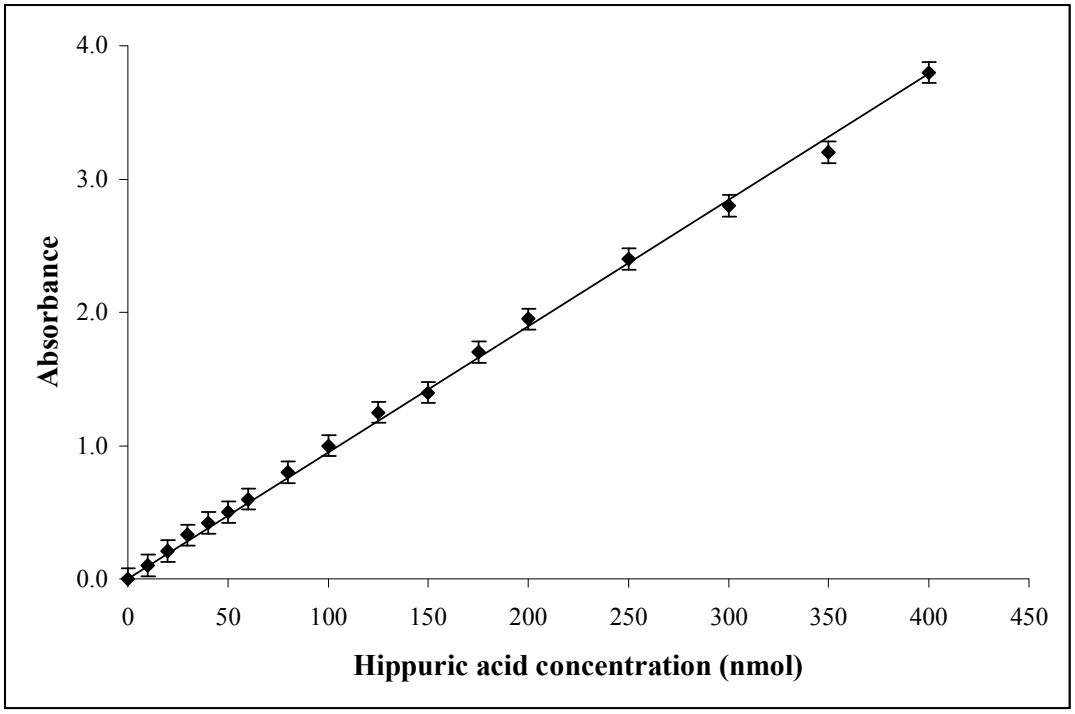

Fig. 2.3 Calibration plot for hippuric acid estimation by the spectrophotometric method. A stock solution of 10 mM hippuric acid in water was prepared, from which different aliquots of concentrations 0 to 400 nmol were pipetted out and made up to 1.0 mL. Absorbance was measured at 228 nm.

2.2.15 Protease activity

The hydrolyzing activity of the protease (in ACE) was carried out using bovine hemoglobin as substrate (Dubey and Jagannadham 2003). To the 0.5 mL of enzyme solution, 0.5 mL of 0.6% (w/v) substrate was added and the reaction was allowed to proceed for 30 min at 37 °C. The reaction was terminated by an addition of 0.5 mL of 10% trichloro acetic acid and allowed to stand for 10 min. The resulted precipitate was removed by centrifugation at 20000 g for 15 min. A 0.5 mL of supernatant was taken and mixed with equal volume of 0.5 M NaOH and the color developed was measured by absorbance at 440 nm. A control assay without enzyme was carried out and used as reference (blank). Inhibitory activity was carried out by adding 0.5 mL of inhibitor solution to 0.5 mL of enzyme solution. To this was added 0.5 mL of hemoglobin solution and incubated at 37 °C for 30 min.

One unit of enzyme activity was expressed as the amount of enzyme under given assay conditions that give rise to an increase of one unit absorbance at 440 nm per min digestion. Number of units of activity per milligram of protein taken as the specific activity of the enzyme.

$$\text{Activity} = \frac{A_{\text{sample}} - A_{\text{blank}}}{T \times E}$$

A_{sample} = Sample absorbance at 440 nm
A_{blank}= Blank absorbance at 440 nm
T = Time in min
E = mg enzyme protein

2.2.16 Lipase activity

Lipase activity was determined by the tributyrin method (Vorderwulbecke *et al.* 1992). A stock solution containing 10 mL of tributyrin, 90 mL of 0.01 M pH 7.0 sodium

phosphate buffer, 0.2 g sodium benzoate, 0.5 g of gum acacia and 50 µL 10% SDS was prepared. It was emulsified by stirring and the pH was adjusted to 7.0 with concentrated NaOH. From this stock solution, 4 mL was pipetted out into stoppered conical flasks (S), containing 8 mL, 0.01 M pH 7.0 sodium phosphate buffer to obtain a solution with a final concentration of 0.113 M tributyrin. Known quantities of enzyme (5 –15 mg) were added to this solution and incubated at 37 ^{o}C in a Heto-Holten shaker water bath for different intervals of time. After incubation, the pH of the reaction mixture in the flask was adjusted to 9.5 with standard 0.04 N NaOH. A blank (B) was also performed without adding enzyme. The hydrolytic activity was evaluated by using the following equation.

$$\text{Hydrolytic activity} = \frac{(S\text{-}B) \times N}{1000 \times E \times T} \quad \mu\text{mol/min.mg of enzyme preparation or protein}$$

Where, (S-B) = difference in volume of NaOH in mL between sample (S) and blank (B), N= normality of NaOH, E = amount of enzyme preparation or protein taken in mg and T= incubation period in min.

2.2.17 Extraction of β-glucosidase

About 250 g of finely powdered defatted sweet almond powder was dispersed in a solution of 12.5 g of $ZnSO_4$ $7H_2O$ in 1 L of water and left standing at 0 °C for 4 to 5 h (Hestrin *et al.* 1955). The cold solution was then filtered through cloth and well pressed on the filter. To the filtrate was cautiously added, a solution of 350 mg tannin in 125 mL water. A precipitate consisting mostly of impurities was removed by centrifugation and discarded. The bulk of the enzyme was then precipitated slowly by adding 125 mL of 3% tannin solution (3.75 g/125 mL) in water. The precipitate was isolated by centrifugation, freed from tannin by repeatedly dispersing it in acetone, and centrifuging it to get crude

powder. The crude powder was dialyzed using 3.5 kDa membrane and finally lyophilized to get a dry powder. The procedure was repeated for 1 Kg of sweet almond powder also.

β-Glucosidase, 10.3 g was obtained from 1 Kg of almond powder. Protein content determined by Lowry's method was found to be 49.2% and activity determined by Colowick and Kaplan (1976) method was found to be 2.93 μmol/min/mg.

2.2.17.1 Activity assay

β-Glucosidase (EC 3.2.1.21) was assayed by the method of Colowick and Kaplan (1976). A volume of 10 mL, 25 mM p-nitrophenyl-β-D-glucopyranoside was prepared in 50 mM sodium acetate buffer (pH 5.5). A known amount of the enzyme was added into 0.25 mL of the freshly prepared p-nitrophenyl-β-D-glucopyranoside solution and incubated at 30 ^{o}C for a definite intervals. To follow the course of the reaction, aliquots of the reaction mixture were treated with 0.7 mL of sodium carbonate (200 mM), and the p-nitrophenol concentration was determined from a calibration plot from the absorbance measured using a Shimadzu UV – 1601 spectrophotometer at 420 nm. A calibration plot was constructed by employing p-nitrophenol in the 0 to 0.4 μmol concentration range (Fig. 2.4).

2.2.18 Antioxidant activity by DPPH method

Antioxidant activity of guaiacol, guaiacyl-α-D-glucoside, curcumin and curcuminyl-bis-α-D-glucoside by DPPH (2,2-Diphenyl-1-picrylhydrazyl) radical scavenging method (Moon & Terao 1998), was evaluated. Absorbance of a solution in duplicate, containing 0.1 mL of test sample (8.6 mM guaiacol and guaiacyl-α-D-glucoside and 5.3 mM curcumin and curcuminyl-bis-α-D-glucoside in DMSO) with 0.9 mL of Tris-HCl buffer (pH 7.4) and 1mL DPPH (500 μM in ethanol) was measured at 517 nm in a UV-Visible spectrophotometer (Shimadzu, UV 1601). Decrease in

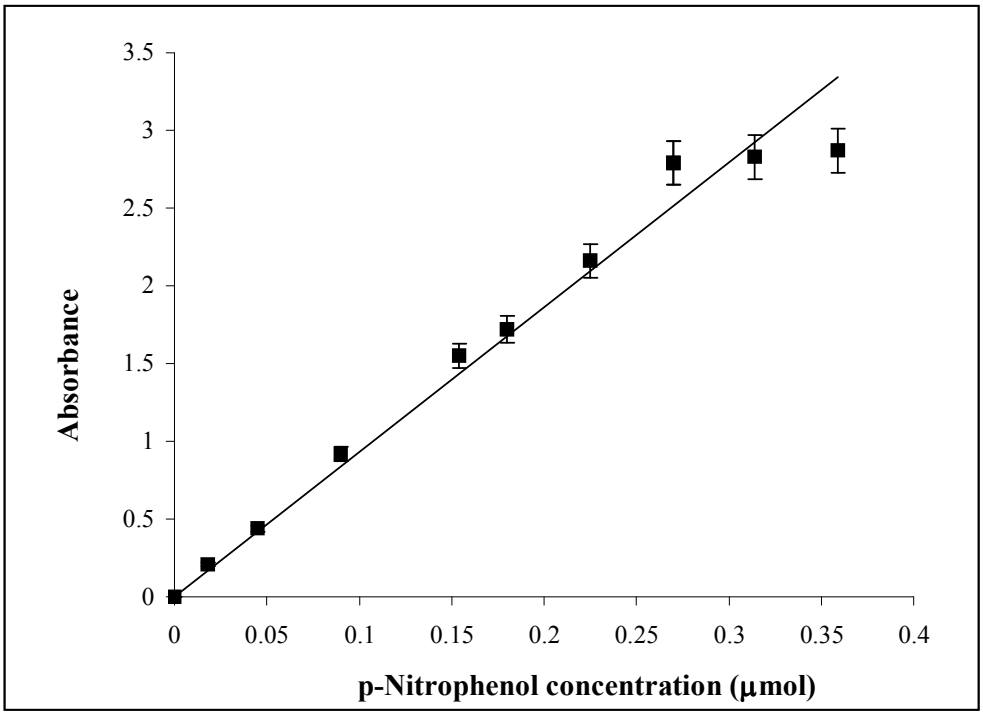

Fig. 2.4 Calibration plot for the determination of p-nitrophenol concentration by β-glucosidase activity. p-Nitrophenol concentration - 0 to 0.4 µmol. Absorbance was measured at 420 nm.

absorbance compare to DPPH itself was a measure of the radical scavenging ability of the test samples. Butylated hydroxyanisole (BHA, 5.55 mM) was used as a positive control. Error in the measurements will be $\pm$ 10%.

2.2.19 Gel electrophoresis of glycosidases and ACE

Sodium dodecyl sulphate-polyacrylamide gel electrophoresis (SDS-PAGE) was carried out to check the purity of glycosidases and ACE employed in the present work. SDS-PAGE was carried out according to the method described by Lamelli (1970) in a discontinuous buffer system.

The following reagents were prepared.

A. Acrylamide (29.2 g) and bis-acrylamide (0.8 g) were dissolved in 100 mL water filtered and stored in a dark brown bottle at 4 ^{o}C (amounting to 30% acrylamide solution).
B. Separating gel buffer (18.1 g) was dissolved in water and the pH of the solution was adjusted to 8.8 with HCl. Then the solution was made upto 100 mL and stored at 4 ^{o}C.
C. Stocking gel buffer – Tris-HCl (3.0 g) was dissolved in water, pH of the solution was adjusted to 6.8 with HCl (6.0 N) and made upto 100 mL in water.
D. Sodium dodecyl sulphate (SDS), 10 g was dissolved in 100 mL water
E. Ammonium persulphate was freshly prepared by dissolving 50 mg in 0.5 mL of distilled water.
F. Tank buffer – Tris-HCl (0.3 g), glycine (1.44 g) and SDS (0.15 g) were dissolved in 150 mL of water.
G. Staining solution – A 0.2 g of Coomassie brilliant blue R 250 was dissolved in a mixture of methanol: acetic acid : water (25: 15: 60 v/v/v). The reagent was filtered and stored in room temperature.

H. Destaining solution – methanol: acetic acid: water (25: 15: 60 v/v/v).

I. Sample buffer was prepared in solution C diluted to 1:4 containing SDS (4% w/v), β-mercaptoethanol (10% v/v), glycerol (20% v/v) and bromophenol blue (0.1%).

Preparation of separating gel (10% T, 2.7%C) – A 2.6 mL of A, 2.0 mL of B, 3.31 mL of distilled water, 0.05 mL of D and 0.03 mL of solution E were mixed and then degassed which was then poured between the assembled glass plates sealed with agar (2% w/v). The gels were layered with 0.5 mL of distilled water and allowed to polymerize at room temperature for 30 min.

Stocking solution (5% T, 2.7% C) was prepared by mixing the solutions of 0.83 mL of A, 1.25 mL of C, 3.0 mL of distilled water, 0.05 mL of solution D, 0.01 mL of TEMED and 0.03 mL of E and poured above the polymerized gel. The gel thus prepared were of the size 10.5 x 9.0 cm and thickness 0.8 mm.

Glycosidase and ACE samples were prepared by dissolving 25 mg of protein in solution 'I' (50 μL). The samples were heated in a boiling water bath for 10 min, then the samples were loaded onto the wells immersed in solution F (tank buffer) and were run at a constant voltage of 40 Volts until the tracking dye, bromophenol blue was just (0.5 cm) above the lower end of the gel. Medium range protein markers phosphorylase (97.4 kDa), bovine serum albumin (66.3 kDa), ovalbumin (43.0 kDa) and carbonic anhydrase (29.0 kDa) were used. The markers were supplied as a solution having each protein at a concentration of 0.5 to 0.8 mg/mL. The markers were diluted 1:1 with solution I and boiled prior to use. Later the gel was stained for protein with reagent 'G' for 6 h at room temperature followed by destaining in reagent H.

A graph was plotted by taking R_f values of molecular marker on X-axis and log M_r values of each molecular marker on Y-axis (Fig 2.5). From this graph molecular

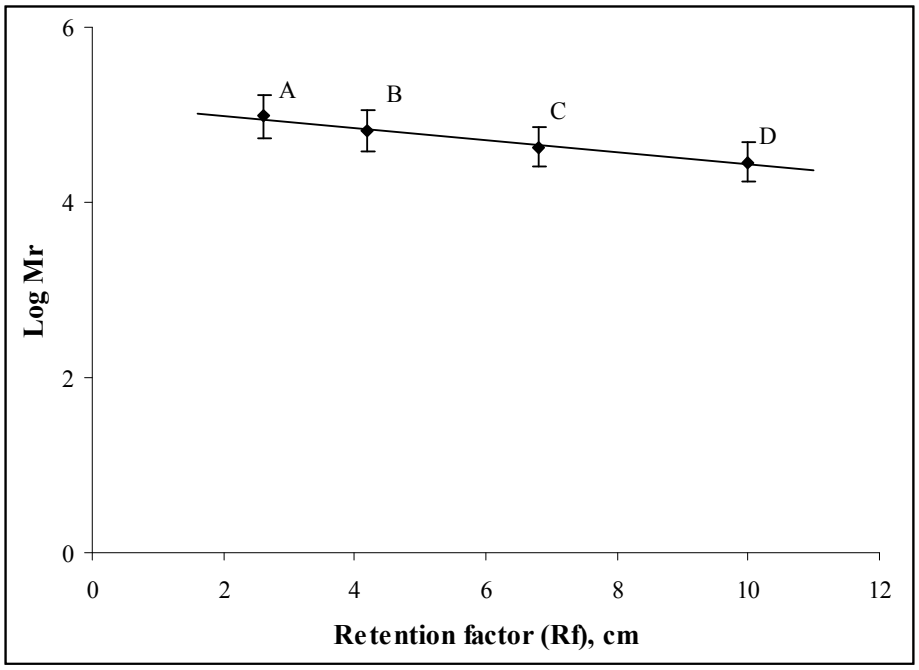

Fig. 2.5 Log M_r versus R_f plot . (A) Phosphorylase (97.4 kDa), (B) BSA (66.3 kDa), (C) Ovalbumin (43.0 kDa), (D) Carbonic anhydrase (29.0 kDa).

weight of unknown protein was determined. Enzyme amyloglucosidase from *Rhizopus* sp. (obtained from Sigma), β-glucosidase, isolated from sweet almonds and molecular weight markers were subjected to SDS-PAGE and stained with Coomassie brilliant blue R 250 (Fig. 2.6A). Lane 1 contained amyloglucosidase, showing molecular masses 72.4 kDa, 60.3 kDa, 58.6 kDa along with other protein contaminants having molecular masses 43.6 kDa, 39.8 kDa and 31.6 kDa. Molecular masses 72.4 kDa, 60.3 kDa and 58.6 kDa showed good correspondence to the GA-I (74.2 kDa), GA-II (58.6 kDa) and GA-III (61.4 kDa) reported by Takahashi *et al.* (1985).

Lane 2 contained β-glucosidase isolated from sweet almonds showing single band of molecular mass 64.6 kDa, which is having good correspondence with the one active component of molecular mass 66.5 kDa reported by Helferich and Kleinschmidt (1965).

ACE showed a molecular mass 152 kDa corresponding to 150 kDa reported by Lee *et al.* (1971) along with the other protein contaminations (Fig. 2.6 B, Lane 1).

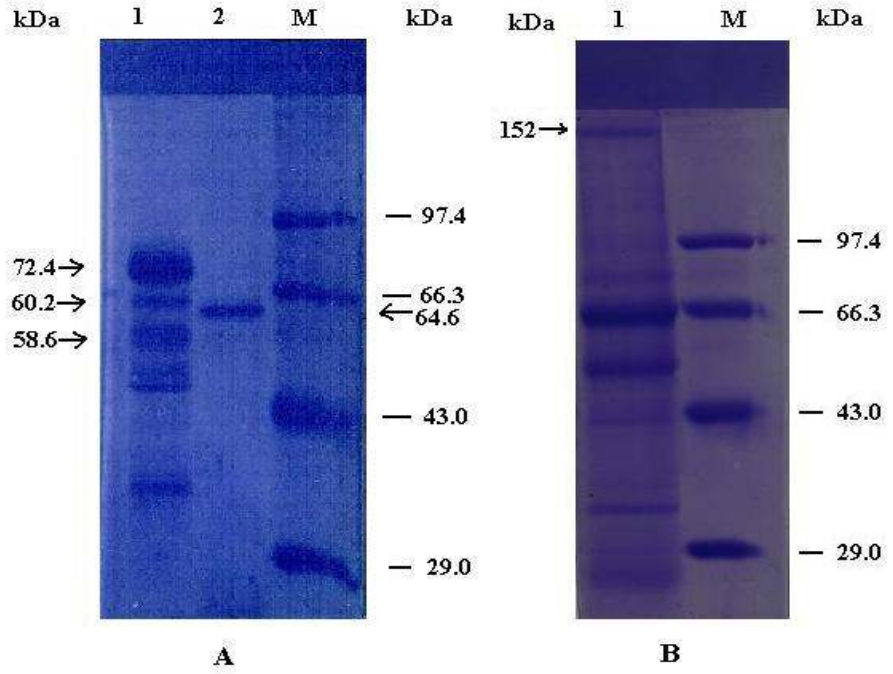

Fig. 2.6 SDS-PAGE (A) Lane 1 for amyloglucosidase from *Rhizopus* sp. (from Sigma); Lane 2 for β-glucosidase isolated from sweet almond; Lane M for M_r standard proteins: Phosphorylase (97.4 kDa), BSA (66.3 kDa), Ovalbumin (43.0 kDa) and Carbonic anhydrase (29.0 kDa). (B) Lane 1 for ACE isolated from pig lung; Lane M for M_r standard proteins.

Chapter 3

Enzymatic Synthesis of Alkyl Glycosides

3.1 Introduction

Regioselective glycosylation involving carbohydrates is a quite challenging synthetic objective because of several hydroxyl groups in these molecules (Haines 1976). Many regio and stereo selective transformations of carbohydrate have been carried out recently using enzymes (Klibanov 1986). Chemical methods of glycosylation involve protection and deprotection (Konstantinovic *et al.* 2001). The use of enzymatic method for glycoside synthesis in principle avoids selective protection – deprotection and control of configuration (Chahid *et al.* 1992; Theim 1995; Vic *et al.* 1997; Kosary *et al.* 1998). Glycosyl transfer reactions for the synthesis of glycosides can be carried out under thermodynamically or kinetically controlled conditions (Ichikawa *et al.* 1992; Rantwijk *et al.* 1999). Reverse hydrolyic method is a thermodynamically controlled method employed for the synthesis of alkyl glycosides (Chahid *et al.* 1992; Ismail and Ghoul 1996; Vic *et al.* 1996; Ljunger *et al.* 1994). The reaction comprises a monosaccharide with a nucleophile such as an alcohol to give the corresponding glycoside and water. Transglycosylation is kinetically controlled reaction wherein glycoside (for example disaccharide) is used as a glycosyl donor (Stevenson *et al.* 1993; Ismail *et al.* 1999).

The use of organic solvent in enzyme catalysis has been stimulated by several factors such as solubilities of the organic compounds, shifting equilibrium towards the synthesis, increasing the enzyme stability and recovery of the enzyme (Rubio *et al.* 1991). One critical limitation in these systems is the poor solubility of the carbohydrate substrate in the organic phase especially when hydrophobic alcohol (glycosyl acceptor) itself is used as a substrate and in some cases as a solvent media to obtain surfactant with a long hydrocarbon chain (Laroute and Willemot 1992a; Vic and Crout 1995; Crout and Vic 1998). There are reports, where glycosylations were carried out either in biphasic systems of a water-immiscible alcohol and water (that maintains sugar substrate and

enzyme) or water and water-miscible monophasic system (Mitsuo *et al.* 1984; Monsan *et al.* 1996). The process of glycosylation can be effected under non-aqueous, solvent free conditions, high substrate, high temperature and moderate to high water activity to yield glycosides (Nilsson 1987; Roitsch and Lehle 1989; Gygax *et al.* 1991; Laroute and Willemot 1992a; Vic and Thomas 1992; Shin *et al.* 2000).

Recently, synthesis of glycosides has generated much interest because of their broad range of applications in various fields. This class of compounds is mainly used as nonionic surfactants in food and pharmaceuticals. These types of nonionic surfactants exhibit several interesting properties in detergency, foaming, wetting, emulsification and antimicrobial effect (Matsumura *et al.* 1990; Balzar 1991). Alkyl glycosides are non-toxic, non skin-irritating and biodegradable (Matsumura *et al.* 1990; Busch *et al.* 1994; Madsen *et al.* 1996)**.** Further alkyl glycosides are used as raw materials for sugar fatty acid ester synthesis (Mutua and Akoh 1993). Because of these properties, alkyl glycosides find great potential application in many diversified areas such as pharmaceutical, chemical, cosmetic and detergent industries.

The present study describes synthesis of n-alkyl glucosides of alcohols of carbon chain lengths C1 – C18 using amyloglucosidase enzyme by both shake flask and reflux methods besides investigating the synthesis of n-octyl-D-glucoside in detail.

3.1.1 Present work

Enzymatic glycosylation in this work was carried out using amyloglucosidase from *Rhizopus* sp., a commercially available enzyme known to cleave $\alpha(1\rightarrow4)$ glycosidic linkage of starch to give glucose. Comparative studies of the preparation in shake flasks under non-solvent conditions (employed alcohol itself acts as solvent) or in presence of solvents and by reflux method involving refluxing and stirring the reaction mixture using di-isopropyl ether as solvent were carried out. In the present work,

glucosylation occurred with amyloglucosidase only in the presence of water, which is added in the form of buffer of certain pH, volume of water and salt concentration. A general scheme for the glycosylation reaction involving synthesis of n-alkyl glucosides is shown in **Scheme 3.1.**

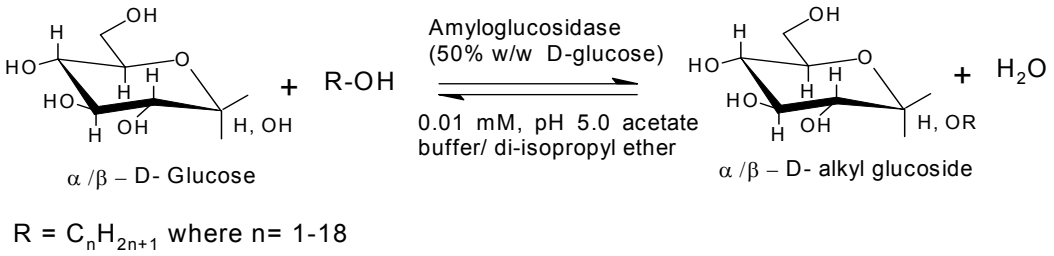

Scheme 3.1 Synthesis of n-alkyl glucosides

3.2 n-Octyl-D-glucoside

Synthesis of n-octyl-D-glucoside was studied in detail. Effects of incubation period, pH, buffer concentration and enzyme concentration were studied by both shake flask and reflux methods. The reaction mixture was analyzed by high performance liquid chromatography (HPLC). The retention time for free D-glucose was found to be 5.2 min and 7.2 min for n-octyl-D-glucoside (Fig. 3.1). The glucoside was isolated by column chromatography by passing through Sephadex G-15 using water as the eluent. Spectral characterization by UV, IR, Mass and 2-D NMR spectroscopy was carried out for the isolated glucoside. Conversion yields were determined from the HPLC peak areas of the free D-glucose and glycoside and expressed as percentage of the product formed with respect to the D-glucose employed.

3.2.1 Effect of incubation period on n-octyl-D-glucoside synthesis

At shake flask level, the effect of incubation period studied from 72 h to 168 h for 50% enzyme concentration and 60 °C, showed that an yield of 15% (83 μmol) observed after 72 h decreased to 2% (9 μmol) after 120 h and thereafter no conversion took place for incubation up to 168 h. However, the reflux method gave the maximum conversion to

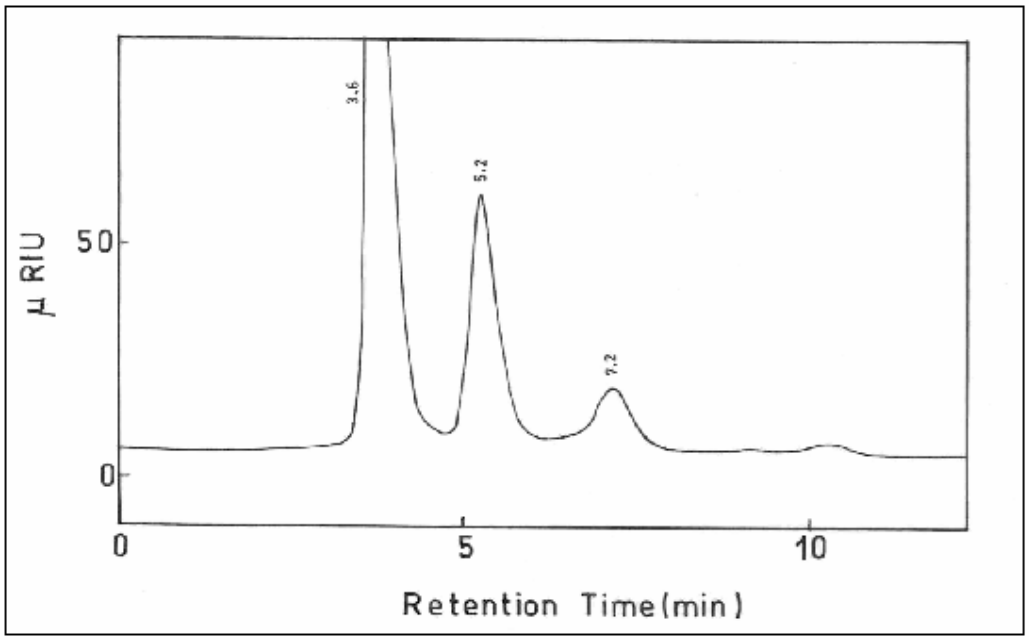

Fig. 3.1 Typical HPLC chromatogram for the reaction mixture of D-glucose and n-octyl-D-glucoside. HPLC conditions: Aminopropyl column (10 μm particle size, 3.9x300 mm length), solvent-CH_3CN: H_2O (80:20 v/v), Flow rate-1 mL/min, RI detector. Retention times: solvent peak-3.6 min, D-glucose-5.2 min and n-octyl-D-glucoside-7.2 min.

41% (225 μmol) just after 48 h and thereafter it decreased to 13% (70 μmol) after 120 h probably due to hydrolysis of the glucoside formed or due to decrease in the thermal stability of the enzyme after a long incubation time. From the reflux method, the rate of glucosylation was found to be 4.74 μmol/h (Fig. 3.2).

3.2.2 Effect of amyloglucosidase on n-octyl-D-glucoside synthesis

Effect of amyloglucosidase concentration was studied in presence of 0.4 mL of 10 mM, pH 6.0 buffer at both shake flask and reflux conditions (Table 3.1). At shake flask level, the yields increased with increase in enzyme concentration up to 30% and decreased at higher enzyme concentrations. However, the yields between 20-40% enzyme concentrations were quite similar. By reflux method, the highest yield of 46% (255 μmol) was obtained for 30% enzyme concentration.

Table 3.1 Effect of amyloglucosidase concentration on the synthesis of n-octyl-D-glucoside[a].

Enzyme % (w/w D-glucose)	Shake flask method Yield - % (μmol)	Enzyme % (w/w D-glucose)	Reflux method Yield - % (μmol)
10	26 (143)	10	11 (58)
20	28 (153)	20	8 (42)
30	28 (155)	30	46 (255)
40	28 (154)	40	26 (142)
50	17 (96)	50	40 (223)
80	19 (106)	75	27 (147)
100	10 (55)	100	20 (113)

[a] Conversion yields were from HPLC with respect to 0.555 mmol of D-glucose. D-Glucose-0.555 mmol, n-octanol – 50 eq (0.027 mol), temperature – 60 ^{o}C for shake flask and 68 ^{o}C for reflux method. pH – 6.0, 0.01 M, buffer volume-0.4 mL (0.04 mM for reflux method and 0.8 mM for shake flask method). Error in yield measurements will be ± 5-10%. This applies to all the yields given in the subsequent tables also.

3.2.3 Effect of pH on n-octyl-D-glucoside synthesis

Effect of pH was studied at 50% amyloglucosidase (Fig 3.3) with a buffer concentration 0.8 mM (0.4 mL of 10 mM buffer added in 4.8 mL of reaction mixture) at shake flask and 0.04 mM (0.4 mL of 10 mM buffer added in 100 mL of the reaction

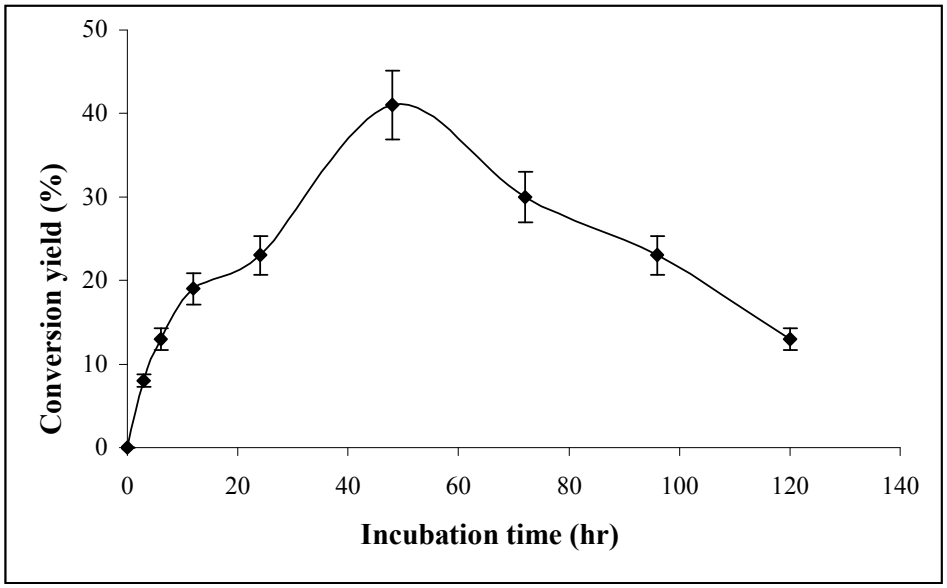

Fig. 3.2 A typical reaction profile for n-octyl-D-glucoside synthesis by the reflux method. Conversion yields were from HPLC with respect to 0.555 mmol of D-glucose. Reaction conditions: D-glucose-0.555 mmol, n-octanol-0.027 mol, amyloglucosidase-50% (w/w D-glucose), 0.04 mM (0.4 mL of 10 mM buffer), pH 5.0 acetate buffer, solvent-di-isopropyl ether and temperature-68 °C.

mixture) at reflux level. The highest yield at shake flask level was 20% (109 μmol) at pH 4.0. However, slightly lesser yields were obtained at pH 6.0 (17%, 96 μmol) and 8.0 (15%, 86 μmol). At reflux level, the yields were generally higher between pH 4.0 and 8.0. However, maximum yield was observed at pH 8.0 (43%, 238 μmol) although the yields were generally higher above pH 6.0.

3.2.4 Effect of buffer concentration on n-octyl-D-glucoside synthesis

Effect of buffer concentration was studied with 50% amyloglucosidase concentration at both shake flask as well as reflux levels (Table 3.2). Shake flask experiments carried out at pH 4.0 in the buffer concentration range 0.2 to 1.6 mM (0.1 mL – 0.8 mL) showed the highest yield of 109 μmol (20%) at 0.8 mM (0.4 mL) of buffer.

Table 3.2 Effect of buffer concentration on the synthesis of n-octyl-D-glucoside[a].

Buffer concentration (mM)	Shake flask method Yield - % (μmol)	Buffer concentration (mM)	Reflux method Yield - % (μmol)
0.2	15 (86)	0.01	5 (29)
0.4	17 (94)	0.02	8 (44)
0.8	20 (109)	0.04	40 (223)
1.2	4 (24)	0.06	31 (173)
1.6	4 (24)	0.08	No yield
-	-	0.1	No yield

[a] Conversion yields were from HPLC with respect to 0.555 mmol of D-glucose. D-Glucose-0.555 mmol, n-octanol – 50 eq (0.027 mol), temperature – 60 ^{o}C for shake flask and 68 ^{o}C for reflux method. Enzyme – 50% w/w D-glucose, pH-4.0 (0.2 – 1.6 mM), for shake flask and pH-6.0 (0.01 - 0.1 mM) for reflux method.

The experiments carried out by the reflux method at pH 6.0 in the buffer concentration range 0.01 to 0.1 mM (0.1 mL - 1.0 mL) showed that the highest yield was 40% (223 μmol) at 0.04 mM (0.4 mL) buffer. There was practically no conversion above 1.6 mM (0.8 mL) of buffer concentration in shake flask and 0.08 mM (0.8 mL) buffer

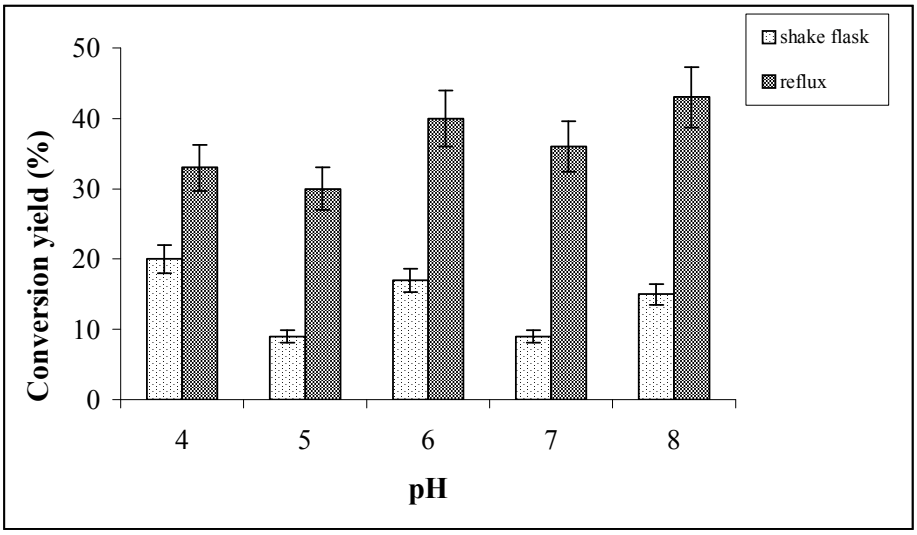

Fig. 3.3 Effect of pH on n-octyl-D-glucoside synthesis. Conversion yields were from HPLC with respect to 0.555 mmol of D-glucose. Reaction conditions: D-glucose – 0.555 mmol, n-octanol-0.027 mol, buffer concentration-0.04 mM (0.4 mL of 10 mM buffer) for reflux method and 0.8 mM (0.4 mL of 10 mM buffer) for shake flask method and incubation-72 h. Reflux method: solvent–di-isopropyl ether and temperature-68 °C. Shake flask method: temperature – 60 °C.

concentration in the reflux method. Higher volumes of buffer although contribute to higher water activity could also results in hydrolysis. Amyloglucosidase could also denature due to excess amount of water especially in shake flask experiments.

3.2.5 Effect of D-glucose concentration on n-octyl-D-glucoside synthesis

Effect of D-glucose concentration on the synthesis of n-octyl-D-glucoside was studied by the reflux method in presence of 0.4 mL (0.04 mM) pH 6.0 buffer and 30% (w/w D-glucose) enzyme concentration. D-Glucose concentration was varied from 0.5 mmol to 3.0 mmol and the glucoside conversion decreased (Fig. 3.4) with the increase in D-glucose concentration and the highest yield of 47% was obtained for 0.5 mmol of D-glucose. Higher D-glucose concentrations at a fixed lower enzyme concentrations could result to predominant binding of D-glucose to the active site and reducing the facile transfer of D-glucose to n-octanol.

At shake flask level, the optimum conditions were found to be 30% (w/w D-glucose) amyloglucosidase (Table 3.1) concentration and 0.8 mM (0.4 mL) pH 6.0 phosphate buffer at an incubation period of 72 h. Similarly, the optimum conditions for the reflux method was found to be 30% (w/w D-glucose) amyloglucosidase (Table 3.1) concentration and 0.04 mM (0.4 mL), pH 6.0 phosphate buffer at an incubation period of 72 h.

3.2.6 Synthesis of n-octyl-D-glucoside using β-glucosidase

n-Octyl-D-glucoside was synthesized by the reflux method using β-glucosidase isolated from sweet almond. D-Glucose and n-octanol were taken in the 1:50 molar ratio along with 30% (w/w D-glucose) β-glucosidase and 0.4 mL (0.04 mM) pH 6.0 phosphate buffer in a di-isopropyl ether solvent and incubated for 72 h. The reaction mixture analyzed by HPLC showed 23% (230 μmol) conversion with respect to the D-glucose employed. The glucoside was isolated by column chromatography by using Sephadex

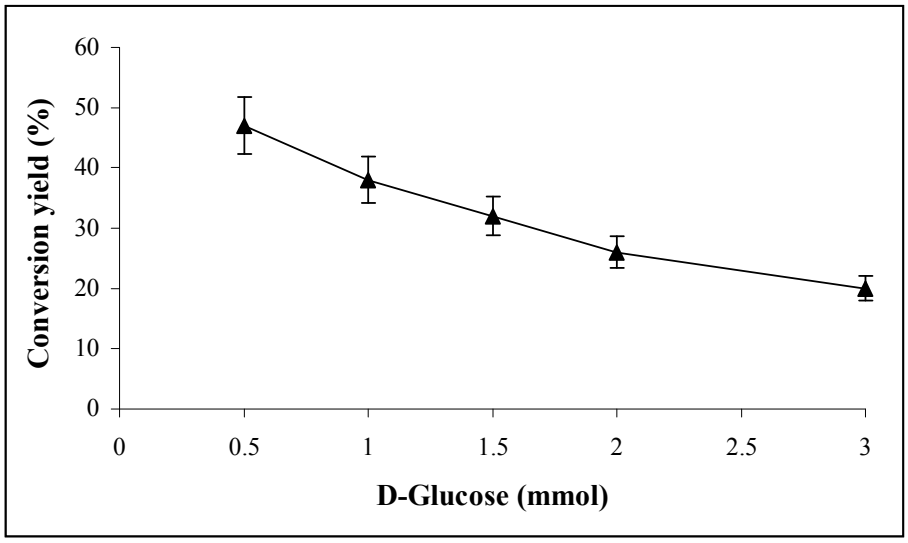

Fig. 3.4 Effect of D-glucose concentration on n-octyl-D-glucoside synthesis. Reaction conditions: D-glucose-0.5 to 3.0 mmol, n-octanol-0.05 mol, amyloglucosidase - 54 mg (10-60% w/w D-glucose), 0.04 mM (0.4 mL of 10 mM buffer) pH 6.0 phosphate buffer, solvent-di-isopropyl ether, temperature-68 °C and incubation-72 h.

G15 as column material and water as the eluent. Spectral characterization (UV, IR, 2D NMR and MS) was carried out for the isolated glucoside. Two dimensional NMR (HSQCT) confirmed formation of n-octyl-β-D-glucoside.

3.2.7 Determination of Critical Micellar Concentration (CMC)

Since glycosides of long chain alcohols serve as non ionic surfactants, Critical Micellar Concentration (CMC) of n-octyl-D-glucoside was determined (Rosenthal and Koussale 1983)**.** A series of aliquots having sample concentration in the range 0 - 20 mM were prepared and made up to 1.0 mL by adding Comassive brilliant blue-G250 reagent. The reaction mixtures were shaken well and the absorbance was measured at 620 nm. The concentration at which an abrupt change in the linearity of the concentration versus absorbance plot obtained was considered as the critical micellar concentration. Critical micellar concentration of n-octyl-D-glucoside was found to be 16.1 mM (0.47%).

3.3 Synthesis of n-octyl glycosides

The optimum conditions worked out for the synthesis of n-octyl-D-glucoside by the reflux method were employed for the synthesis of n-octanol **1**, glycosides of various carbohydrates. The various carbohydrates employed were D-glucose **2**, D-galactose **3**, D-mannose **4**, D-fructose **5**, D-arabinose **6**, D-ribose **7**, maltose **8**, sucrose **9**, lactose **10**, D-mannitol **11** and D-sorbitol **12**. Carbohydrates and n-octanol were taken in 1:50 molar ratio along with 30% of amyloglucosidase and 0.04 mM (0.4 mL) pH 6.0 buffer and refluxed for 72 h in di-isopropyl ether. n-Octyl maltoside (conversion yield 15%, 150 μmol) and n-octyl sucrose (conversion yield 13%, 130 μmol) were obtained by this procedure **(Scheme 3.2)**.

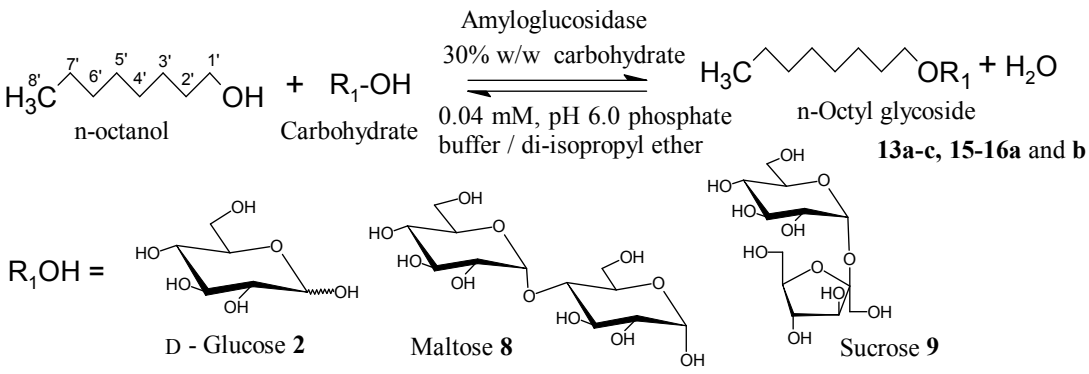

Scheme 3.2 Synthesis of n-octyl glycosides

The extent of glycosylation was analyzed by HPLC. The retention times for free carbohydrate and n-octyl glycosides were D-glucose-5.2 min, n-octyl-D-glucoside-7.2 min, maltose-7.4 min, n-octyl maltoside-10.5 min, sucrose-6.4 min and n-octyl sucrose-9.1 min. The glycosides were isolated by subjecting the reaction mixture to column chromatography on Sephadex G-15 and the isolated glycosides were characterized by various spectroscopic techniques as mentioned before. NMR data of the carbohydrates employed are shown in Table 3.3. The structures of the glycosides formed, HPLC yield and product proportions are presented in Table 3.4. Other carbohydrates such as D-fructose **5**, D-arabinose **6**, D-ribose **7**, lactose **10** and D-sorbitol **12** did not form any glycoside with n-octanol **1**. However HPLC indicated glycosylation of D-galactose **3**, D-mannose **4** and D-mannitol **11** with conversion yields less than 5%.

3.3.1 Spectral characterization

The glycosides were characterized by UV, IR, 2-D NMR (HSQCT) and optical rotation. Two dimensional HSQCT NMR gave information on the nature and proportions of the products formed (Table 3.4). n-Octanol signals are primed; non reducing end sugar unit is double primed. Only resolvable signals are shown. Some assignments are interchangeable. Since n-octyl glycosides are surfactant molecules, the proton signals are

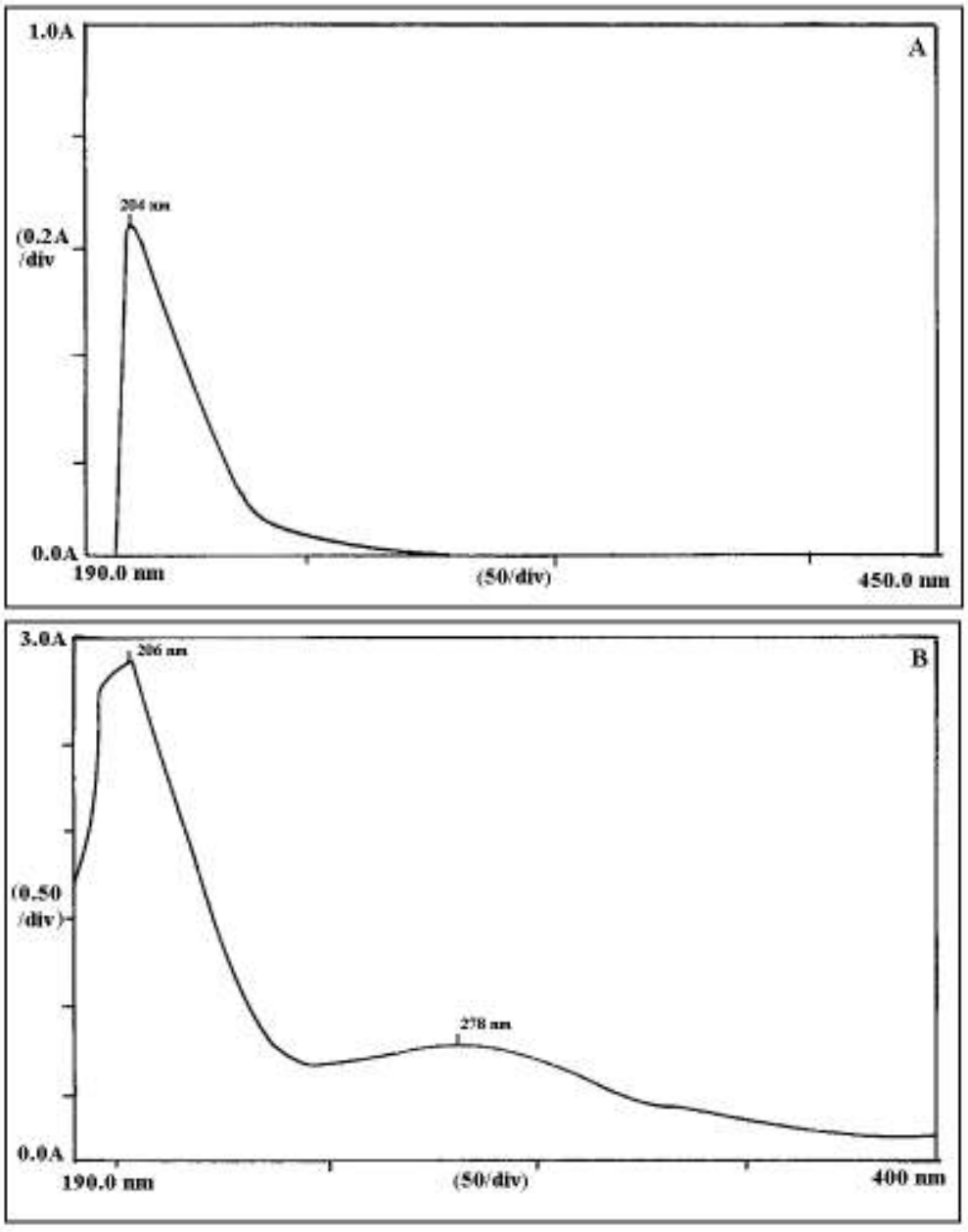

Fig. 3.5 Typical UV spectrum: **(A)** n-Octanol **(B)** n-Octyl-D-glucoside.

broad due to aggregation at concentration above CMC employed and hence coupling constant values could not be determine satisfactorily for these compounds.

n-Octanol, 1: Liquid; bp 194.4 °C; UV (Ethanol, λmax): 204 nm ($\sigma \rightarrow \sigma^*$, ε_{204}-5.0 M^{-1}); IR : 3276 cm^{-1} (OH), 2965 cm^{-1} (alkyl CH); ^1H NMR δ_{ppm}: (500.13 MHz) 1.39 (CH_2-1′), 1.24 (CH_2-3′-7′), 0.84 (CH_2-8′); ^{13}C NMR δ_{ppm} (125 MHz): 62.0 (C1′), 32.7 (C2′), 26.2 (C3′), 28.1 (C4′), 29.6 (C5′), 32.1 (C6′), 22.5 (C7′), 14.1 (C8′). The assignments were based on Pouchert 1983.

3.3.1.1 n-Octyl-D-glucoside, 13a-c: Solid; UV (H_2O, λ_{max}): 206 nm ($\sigma \rightarrow \sigma^*$, $\log\varepsilon_{206}$ - 1230 M^{-1}), 278 nm ($n \rightarrow \pi^*$, ε_{278} – 72 M^{-1}); IR (KBr): 1053 cm^{-1} (glycosidic C-O-C symmetrical), 3605 cm^{-1} (OH); $[\alpha]\ ^{25}_D$ = +45.8 ^{o} (*c* 1, H_2O); CMC = 16.1 mM; MS (*m/z*) - 294 $[M+2]^+$; 2D-HSQCT (DMSO-d_6) **n-octyl-α-D-glucoside, 13a:** ^1H NMR δ_{ppm}: (500.13 MHz) 4.62 (H-1α), 3.18 (H-2α), 3.42 (H-3α), 3.74 (H-4α), 3.18 (H-5α), 3.42 (H-6a), 3.1 (CH_2-1′), 1.51 (CH_2-2′), 1.23 (CH_2-3′-7′), 0.85 (CH_2-8′); ^{13}C NMR δ_{ppm} :(125 MHz) 98.5 (C1α), 72.0 (C2α), 72.4 (C3α), 70.2 (C4α), 72.1 (C5α), 60.8 (C6 α), 14.0 (C8′), 23.0 (C7′), 31.2 (C6′), 29.8 (C3′), 30.0 (C5′), 70.2 (C1′). **n-octyl-β-D-glucoside, 13b:** ^1H NMR δ_{ppm}: 4.17 (H-1β), 2.88 (H-2β), 3.12 (H-5β), 3.60 (H-6a), 3.1 (CH_2-1′), 1.51 (CH_2-2′), 1.23 (CH_2-3′-7′), 0.85 (CH_2-8′); ^{13}C NMR δ_{ppm} : 103.2 (C1β), 74.7 (C2β), 77.1 (C3β), 71.0 (C4β), 77.1 (C5β), 61.5 (C6 β), 14.0 (C8′), 23.0 (C7′), 31.2 (C6′), 30.0 (C5′), 70.5 (C1′). **C6-O-octyl-D-glucose, 13c:** ^1H NMR δ_{ppm}: 4.90 (H-1α), 3.20 (H-2α), 3.10 (H-5α), 3.64 (H-6a), 3.1 (CH_2-1′), 1.51 (CH_2-2′), 1.21 (CH_2-3′-7′), 0.85 (CH_2-8′); ^{13}C NMR δ_{ppm} : 92.2 (C1α), 72.5 (C2α), 72.1 (C5α), 67.2 (C6 α), 14.0 (C8′), 29.5 (C3′), 30.0 (C5′), 70.5 (C1′).

Table 3.3 NMR data of free carbohydrates [a]

Carbohydrate	Chemical shift values in ppm (J Hz)											
	^{1}H ^{13}C	^{1}H ^{13}C	^{1}H ^{13}C	^{1}H ^{13}C	^{1}H ^{13}C	^{1}H ^{13}C	^{1}H ^{13}C	^{1}H ^{13}C	^{1}H ^{13}C	^{1}H ^{13}C	^{1}H ^{13}C	^{1}H ^{13}C
	H-1 C1	H-2 C2	H-3 C3	H-4 C4	H-5 C5	H-6 C6	H-1″ C1″	H-2″ C2″	H-3″ C3″	H-4″ C4″	H-5″ C5″	H-6″ C6″
D-Glucose α	4.95 92.3	3.14 72.5 (6.2)	3.44 3.2 (5.01)	3.07 70.7 (5.01)	3.58 72.0 (6.49)	3.53 61.4 (11.3, 6.5)						
β	4.30 97.0 (6.2)	2.92 75.0 (6.2)	3.06 76.9 (5.01)	- -	3.45 76.9 (4.14, 1.3)	3.62 61.6 11.3, 6.5)						
D-Galactose α	4.14 92.7	3.50 68.4 (6.2)	3.59 69.0 (5.01)	3.70 70.0 (5.0, 4.14)	3.35 70.5 (4.14, 1.3)	3.31 60.7 (1.3, 11.3)						
β	4.83 97.6 (6.2)	--	3.15 73.7 (5.01)	3.10 72.3 (5.0, 4.14)	3.25 74.8 (4.14, 1.3)	3.32 60.8 (1.3, 11.3)						
D-Mannose α	4.89 94.0	3.54 71.3 (6.2)	3.55 70.0 (6.2, 5.0)	3.36 67.4 (5.0, 4.14)	3.50 73.0 (4.14, 1.3)	3.63 61.5 (1.3, 11.3)						
β	4.54 93.9 (6.2)	3.32 71.5	3.26 73.7 (6.2, 5.0)	3.37 67.0 (5.0, 4.14)	3.02 77.0 (4.14, 1.3)	3.46 61.4 (1.3, 11.3)						
D-Fructose β	3.80 63.9 (12.23)	- 97.5	3.56 67.9 (5.8)	3.64 69.9 (5.8, 4.07)	3.57 68.7 (4.07, 2.4)	3.50 62.6 (2.4, 12.0)						
D-Ribose α	4.75 93.2 (5.1)	3.23 70.6 (5.1, 5.0)	3.33 68.8 (5.0, 4.97)	3.71 66.7 (4.97, 2.4)	3.51 62.8 (2.4, 12.0)							
β	4.31 94.0 (2.6)	3.31 71.5 (2.6, 4.7)	3.38 68.0 (4.7, 4.97)	3.54 67.5 (4.97, 2.4)	3.29 62.8 (2.4, 12.0)							
D-Arabinose α	4.92 92.3 (1.7)	4.32 - (1.7, 5.8)	4.6 - (5.8, 4.07)	4.08 - (4.07, 2.4)	3.73 60.4 (2.4, 12.0)							
β	4.33 96.2 (4.5)	3.65 69.1 (4.5, 7.2)	4.02 68.9 (7.2, 4.07)	3.37 67.1 (4.07, 2.4)	3.64 60.7 (2.4, 12.0)							
Lactose α	4.90 91.9 (6.2)	3.70 69.8 (6.2)	3.54 71.4 (6.2, 5.0)	3.27 80.8 (5.0, 4.14)	3.55 72.1 (4.14, 1.3)	3.64 60.5 (1.3, 11.3)	4.19 103.7 (6.2)	3.30 70.7 (6.2)	3.18 73.2 (6.2, 5.0)	3.62 68.2 (5.0, 4.14)	2.93 75.4 (4.14, 1.3)	3.52 60.9 (1.3, 11.3)
β	4.34 96.3	3.31 74.2 (6.2)	3.53 74.7 (6.2, 5.0)	3.28 81.1 (5.0, 4.14)	3.44 74.9 (4.14, 1.3)	3.72 60.6 (1.3, 11.3)						
Maltose α	4.80 92.0 (6.2)	2.85 73.9 (6.2)	3.29 76.4 (6.2, 5.0)	3.15 69.7 (5.0, 4.14)	3.30 73.3 (4.14, 1.3)	3.50 60.8 (1.3, 11.3)	4.90 100.3 (6.2)	2.94 72.0 (6.2)	3.10 73.0 (6.2, 5.0)	3.51 69.5 (5.0, 4.14)	3.62 72.7 (4.14, 1.3)	3.60 60.2 (1.3, 11.3)
β	4.20 96.9	3.10 74.3 (6.2)	3.31 76.0 (6.2, 5.0)	3.19 79.4 (5.0, 4.14)	3.38 76.4 (4.14, 1.3)	3.34 60.9 (1.3, 11.3)						
Sucrose Glc α Fru β							5.18 91.7 (6.2)	3.65 72.7 (6.2)	3.20 71.5 (6.2, 5.0)	3.11 69.8 (5.0, 4.14)	3.47 72.8 (4.14, 1.3)	3.54 60.5 (1.3, 11.3)
	3.41 62.0 (12.23)	- 103.9	3.78 77.1 (5.8)	3.88 74.1 (5.8, 4.07)	3.41 82.4 (4.07, 2.4)	3.55 62.0 (2.4, 12.0)						
D-Sorbitol	3.41 62.5 (12.0, 7.3)	3.54 73.6 (7.3, 4.3)	3.68 68.9 (4.3)	3.39 72.2 (4.3)	3.48 71.4 (4.3, 7.3)	3.56 63.3 (7.3, 12.0)						
D-mannitol	3.40 63.7 (12.0, 7.3)	3.47 71.2 (7.3, 4.3)	3.54 69.6 (4.3)	3.54 69.6 (4.3)	3.47 71.2 (4.3, 7.3)	3.61 63.7 (7.3, 12.0)						

[a] Assignments were based on Book and Pedersen 1983; Book *et al.* 1983.

Table 3.4 n-Octyl glycosides with conversion yields and product proportions [a].

Glycosides and product proportions [b]	Glycosylation yield (%)[c]
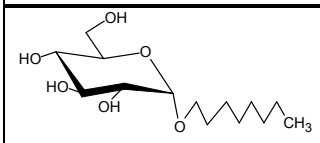 **13a**, n-octyl-α-D-glucoside (63) 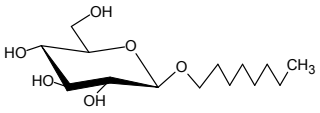 **13b**, n-octyl-β-D-glucoside (25) 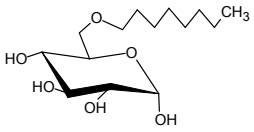 **13c**, C6-O-octyl-D-glucose (12)	46
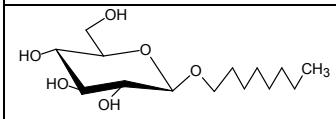 **14**, n-octyl-β-D-glucoside [d]	23
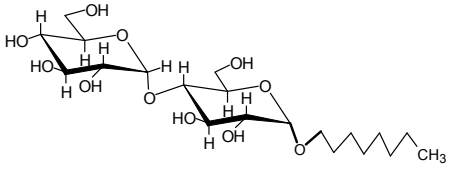 **15**, n-octyl maltoside	15
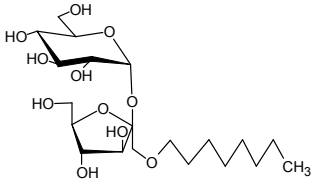 **16a**, C1-O-octyl sucrose (44) 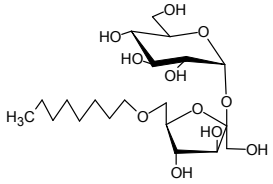 **16b**, C6-O-octyl sucrose (56)	13

[a] Carbohydrate and n-octanol - 1:50 equivalents, amyloglucosidase - 30% (w/w carbohydrate), solvent-di-isopropyl ether, temperature - 68 °C and incubation-72 h. [b] The Product proportions determined from 2D-HSQCT NMR C1/C6 cross peak areas are shown in brackets. [c] Conversion yields were from HPLC with respect to free carbohydrate. [d] The compound was synthesized by using β-glucosidase from sweet almonds.

UV spectrum showed $\sigma \rightarrow \sigma^*$ band at 206 nm and $n \rightarrow \pi^*$ band at 278 nm (Fig. 3.5B). The IR spectral band at 1053 cm^{-1} corresponded to the glycosidic C-O-C symmetrical stretching. From the area of the C1 anomeric cross peaks, it was confirmed that α: β anomeric composition was 63 : 25 (Fig 3.6A) obtained. A small amount of C6-

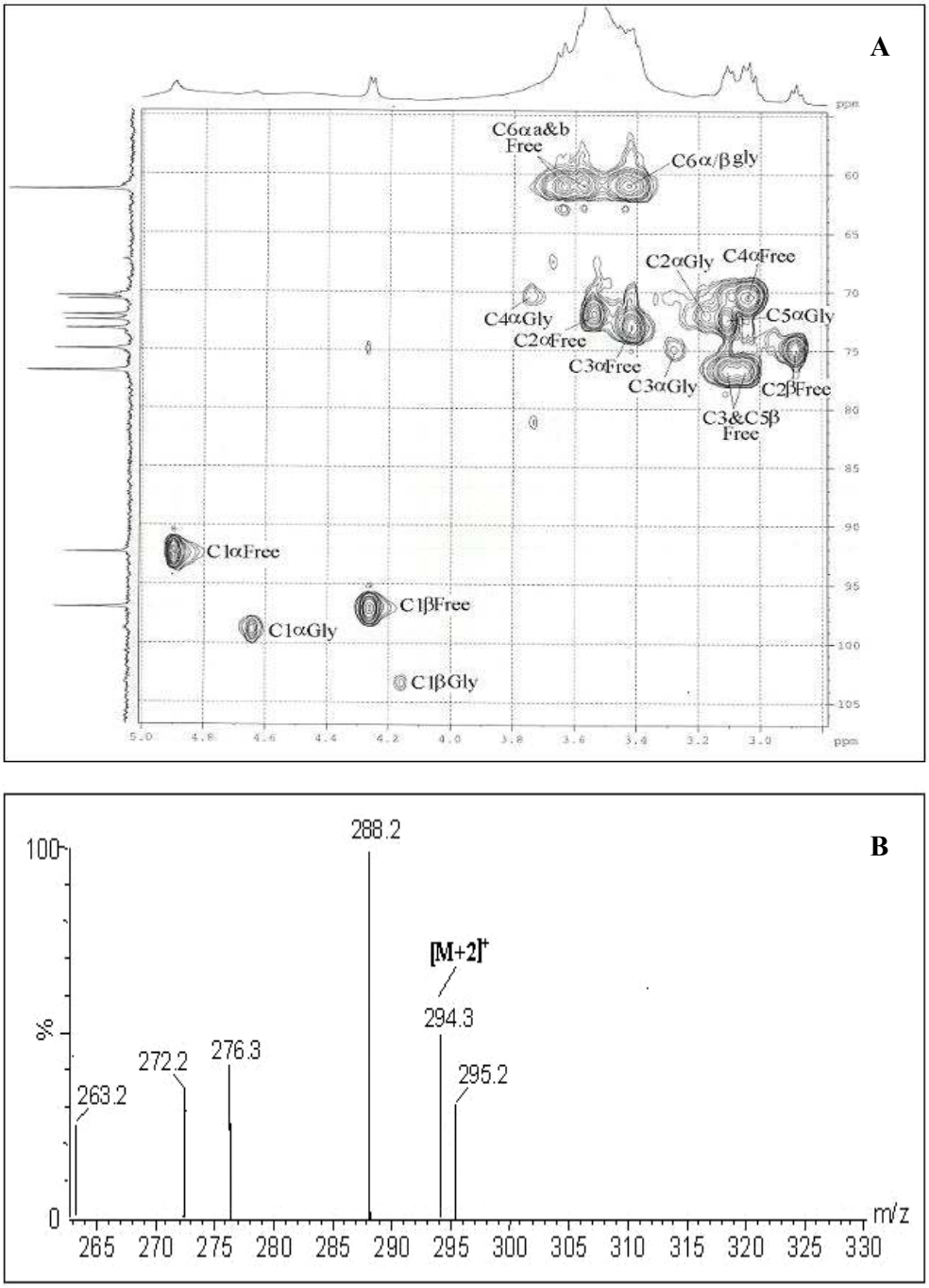

Fig. 3.6 (A) 2D-HSQCT spectrum of n-octyl-D-glucoside **13a-c** reaction mixture using amyloglucosidase. A 40 mg of the sample was taken in DMSO-d_6. Some assignments are interchangeable. This applies to subsequent 2D NMR spectrum also. NMR assignments are based on Vic *et al.* (1997). **(B)** Mass spectrum of n-octyl-D-glucoside **13a-c**.

O-alkylated product **13c** was detected. Apart from the free C1α and C1β signals, the cross peaks in the anomeric region with ^{13}C chemical shift values at 98.5 ppm and 103.2 ppm with the corresponding ^{1}H values at 4.62 ppm and 4.17 ppm clearly indicated C1α of the glucoside **13a** and C1 β glucoside **13b** formation. The cross peak in the C6 region (^{13}C at 67.2 ppm and ^{1}H at 3.64 ppm) indicated C6-O-alkylated product **13c**. Chromatographic separation did not aid in isolation of the individual glycosides, as the polarity between these compounds are similar. Mass value 294 [M+2] obtained from mass spectrum, further confirmed the product formation (Fig. 3.6B).

3.3.1.2 n-octyl-β-D-glucoside, 14: Solid; mp 107 °C; UV (H_2O, λmax): 201 nm ($\sigma\rightarrow\sigma^*$, $\log\varepsilon_{201}$ - 1584 M^{-1}), 275 nm ($n\rightarrow\pi^*$, ε_{275} – 208 M^{-1}); IR (KBr): 1027 cm^{-1} (glycosidic C-O-C symmetrical), 1225 cm^{-1} (glycosidic C-O-C asymmetrical), 3315 cm^{-1} (OH); $[\alpha]_D^{25}$ = -31.8 ^{o} (*c* 1, H_2O); MS (*m/z*) - 294 $[M+2]^+$; 2D-HSQCT (DMSO-d_6) ^{1}H NMR δ_{ppm}: 4.18 (H-1β), 3.15 (H-3β), 3.10 (H-4β), 3.18 (H-5β), 3.37 (H-6a), 3.47 (H-6b), 3.1 (CH_2-1′), 1.41 (CH_2-2′), 1.22-1.37 (CH_2-3′-7′), 0.83 (CH_2-8′); ^{13}C NMR δ_{ppm} : 103.2 (C1β), 77.2 (C3β), 71.0 (C4β), 61.0 (C6 β), 14.0 (C8′), 23.0 (C7′), 31.2 (C6′), 30.0 (C5′), 26.0 (C3′), 70.5 (C1′).

UV spectrum of n-octyl-β-D-glucoside **14** synthesized by β-glucosidase showed $\sigma \rightarrow \sigma^*$ band at 201 nm and $n\rightarrow\pi^*$ band at 275 nm. The IR spectral band at 1027 cm^{-1} corresponded to the glycosidic C-O-C symmetrical stretching and 1225 cm^{-1} for the glycosidic C-O-C asymmetrical stretching frequencies (Fig. 3.7B). Two dimensional HSQCT showed the down field chemical shift for C1β at 103.2 ppm and the corresponding ^{1}H value at 4.18 ppm, indicating the formation of only C1β glucoside (Fig. 3.7A). No other product formation (C1α glucoside or C6-O-alkylated) was detected unlike the amyloglucosidase catalyzed reaction.

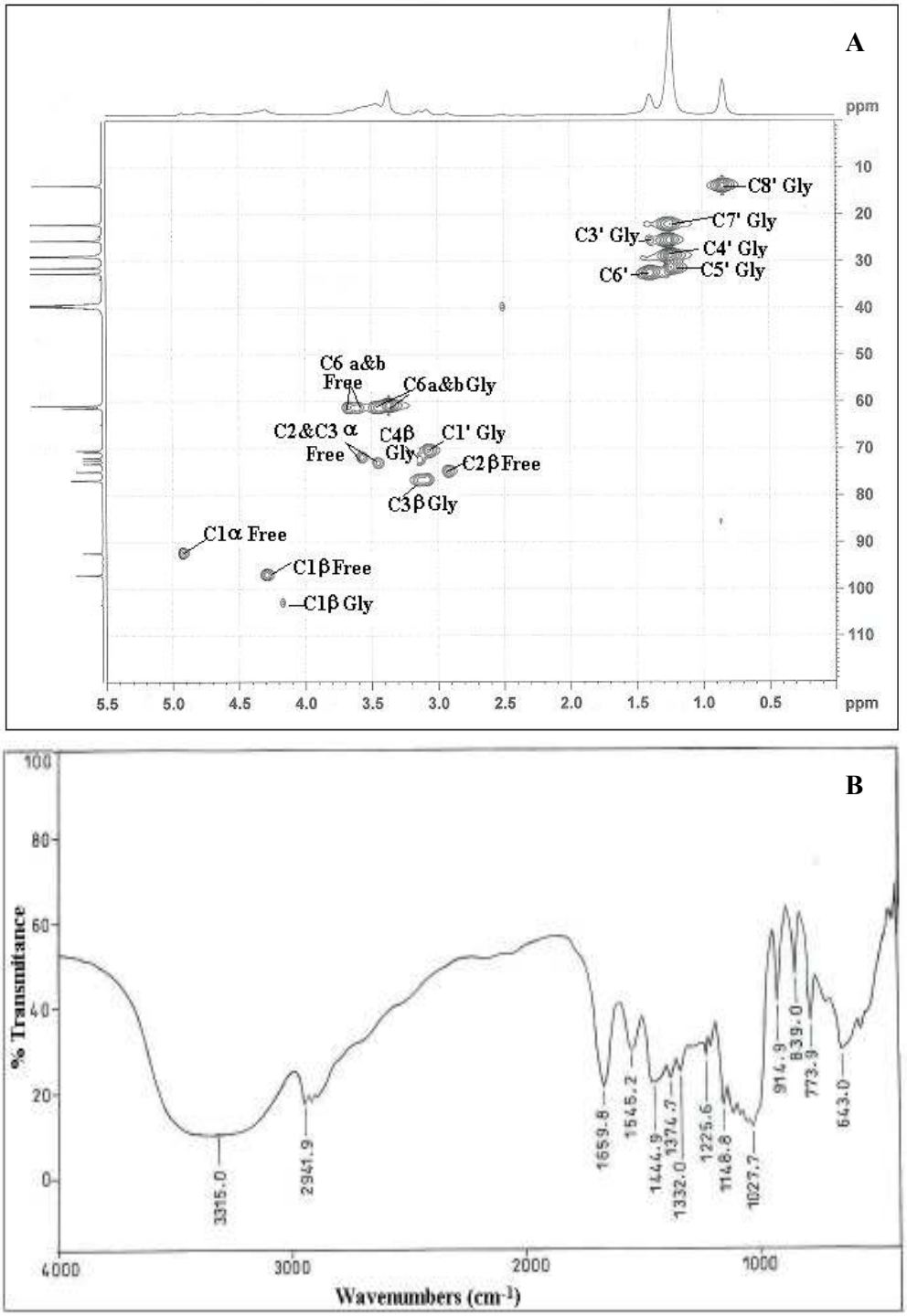

Fig. 3.7 (A) 2D-HSQCT spectrum of n-octyl-β-D-glucoside **14** reaction mixture using β-glucosidase from sweet almonds. A 40 mg of the sample was taken in DMSO-d_6. NMR assignments are based on Vic *et al.* (1997). **(B)** IR spectrum of n-octyl-β-D-glucoside **14**.

3.3.1.3 n-Octyl maltoside, 15: Solid; mp105 ^{o}C; UV (H_2O, λ_{max}): 194 nm ($\sigma\rightarrow\sigma^*$, ε_{194} – 1479 M^{-1}), 278.5 nm ($n\rightarrow\pi^*$, $\varepsilon_{278.5}$ – 95.5 M^{-1}); IR (KBr): 1033 cm^{-1} (glycosidic C-O-C symmetrical), 1255 cm^{-1} (glycosidic C-O-C asymmetrical), 3415 cm^{-1} (OH); $[\alpha]^{25}_{D}$ = +91.1^{o} (*c* 1, H_2O); MS (*m/z*) - 455 $[M+1]^+$; 2D-HSQCT (DMSO-d_6) ^{1}H NMR δ_{ppm} : (500.13 MHz) 4.63 (H-1α), 3.30 (H-5α), 3.66 (H-6a), 4.99 (H-1″α), 3.46 (H-2″), 3.20 (H-3″, 3.08 (H-4″), 3.44 (H-6a″), 2.9 (CH_2-1′), 1.11-1.25 (CH_2-2′-7′), 0.85 (CH_2-8′); ^{13}C NMR δ_{ppm} : (125 MHz) 98.8 (C1α), 75.0 (C5α), 60.5 (C6α), 100.8 (C1″α), 71.8 (C2″), 72.1 (C3″), 70.2 (C4″), 61.0 (C6″), 14.1 (C8′), 23.0 (C7′), 31.5 (C6′), 29.8 (C3′), 29.0 (C2′), 70.3 (C1′).

UV spectrum showed $\sigma \rightarrow \sigma^*$ band at 194 nm and $n\rightarrow\pi^*$ band at 278.5 nm. The IR spectral band at 1033 cm^{-1} corresponded to the glycosidic C-O-C symmetrical stretching and 1255 cm^{-1} for the C-O-C asymmetrical stretching frequencies (Fig. 3.9A). From 2D HSQCT, the down field chemical shift for C1α at 98.8 ppm and the corresponding ^{1}H value at 4.63 ppm indicated formation of only C1α maltoside and no C-6-O-alkylated products (Fig. 3.8 A and B). A mass value 455 was obtained for [M+1] peak (Fig. 3.9B).

3.3.1.4 n-Octyl sucrose, 16 a and **b:** Solid; UV (H_2O, λ_{max}): 205 nm ($\sigma\rightarrow\sigma^*$, ε_{205} - 2570 M^{-1}), 276 nm ($n\rightarrow\pi^*$, ε_{276} – 257 M^{-1}); IR (KBr): 1054 cm^{-1} (glycosidic C-O-C symmetrical), 1259 cm^{-1} (glycosidic C-O-C asymmetrical), 3357 cm^{-1} (OH); $[\alpha]^{25}_{D}$ = +13.3 ^{o} (*c* 1, H_2O); MS (*m/z*) - 455 $[M+1]^+$; 2D-HSQCT (DMSO-d_6) **C1-O-octyl sucrose, 16a:** ^{1}H NMR δ_{ppm} (500.13 MHz) 3.76 (H-1α), 3.81 (H-4α), 3.79 (H-5α), 3.40 (H-6a), 5.18 (H-1″α), 3.10 (H-3″), 3.03 (H-4″), 3.54 (H-5″), 3.62 (H-6″), 3.01 (H-1′), 1.01-1.23 (H-2-7′), 0.84 (H-8′); ^{13}C NMR δ_{ppm} : (125 MHz) 62.8 (C1α), 104.0 (C2α), 75.4 (C4α), 83.0 (C5α), 62.0 (C6α), 91.5 (C1″α), 72.2 (C3″), 70.5 (C4″), 72.0 (C5″),

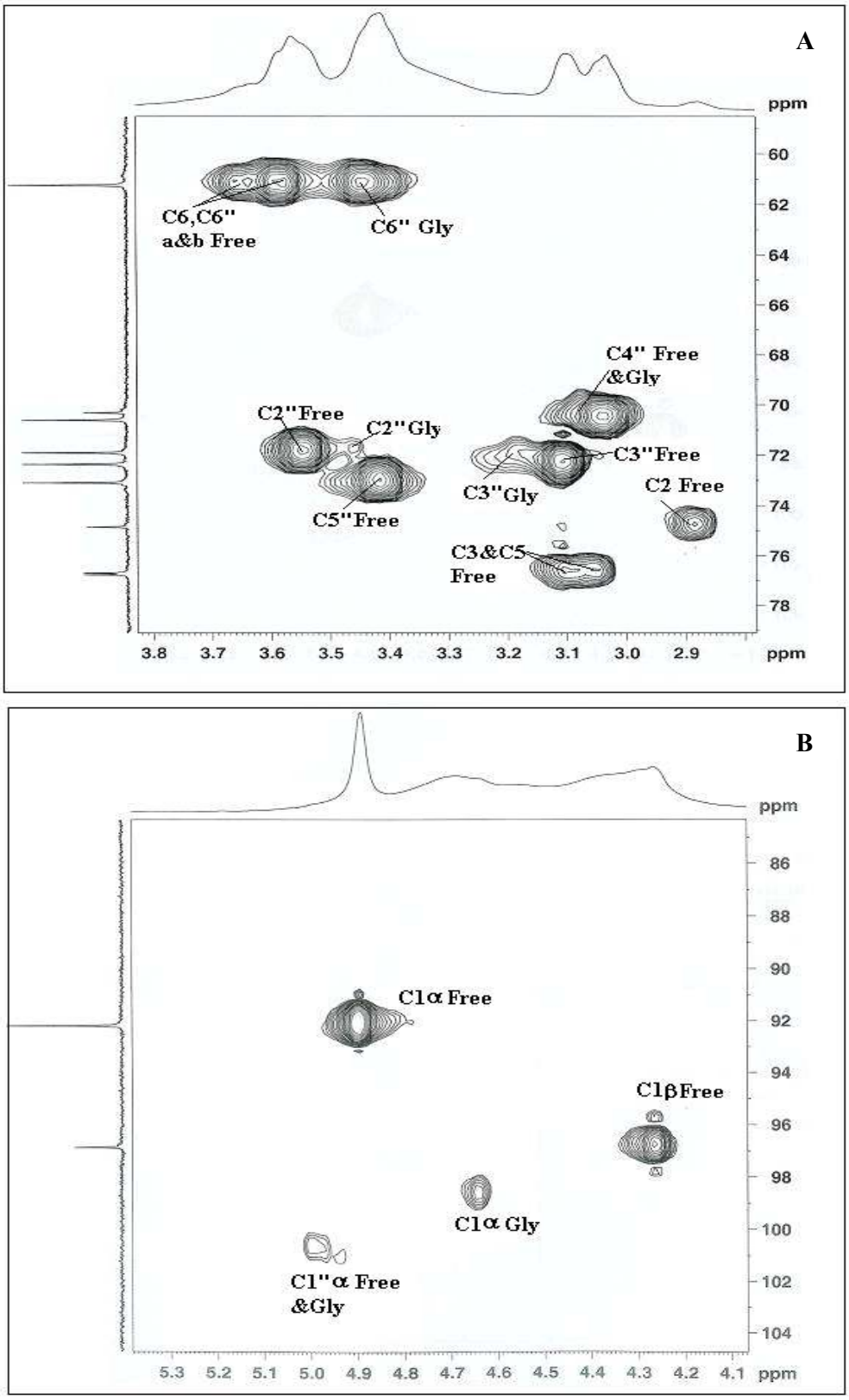

Fig. 3.8 2D HSQCT spectrum of n-octyl maltoside **15 (A)** C2-C6 region **(B)** C1 region.

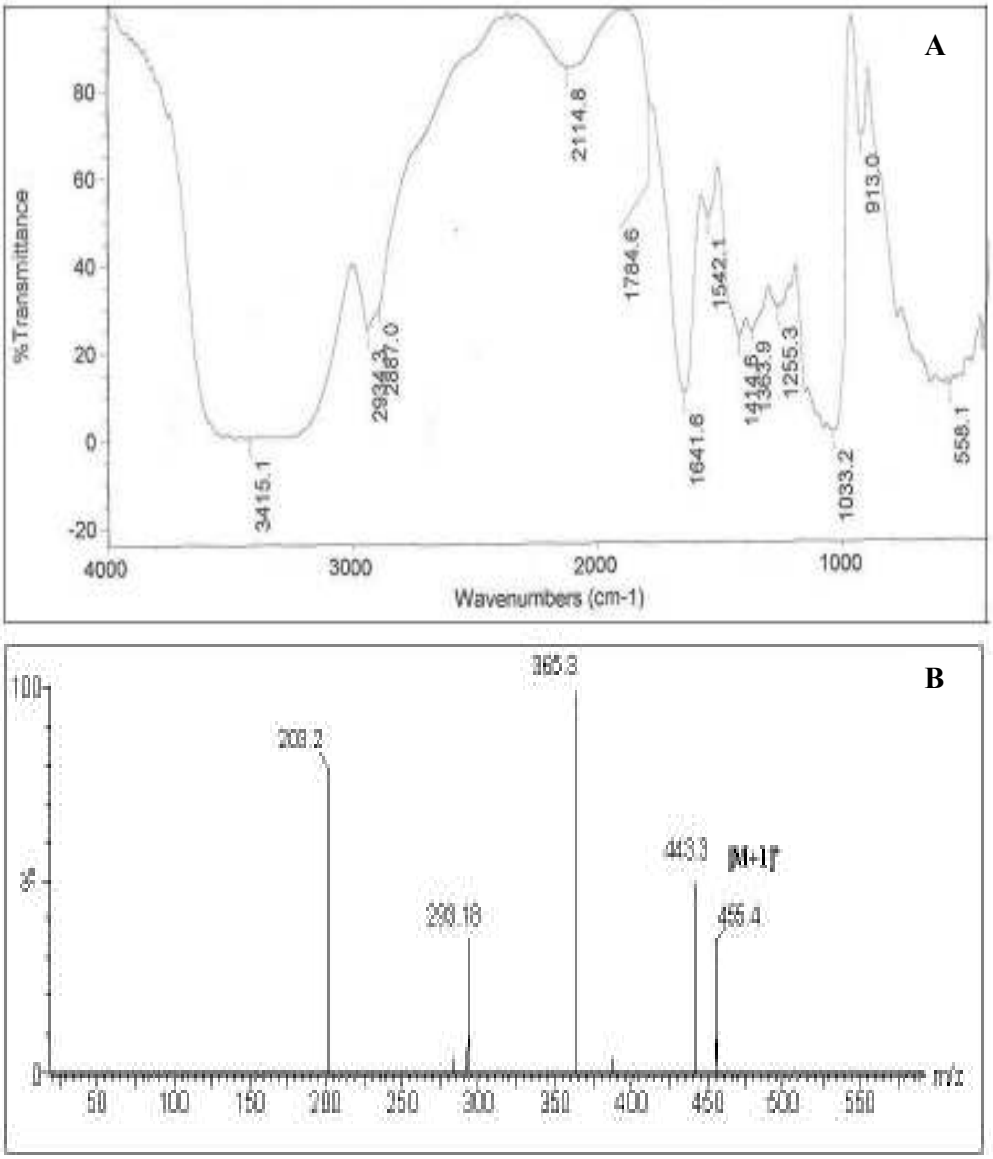

Fig. 3.9 n-Octyl maltoside **15 (A)** IR spectrum **(B)** Mass spectrum.

61.0 (C6″), 14.4 (C8′), 23.2 (C7′), 31.5 (C6′), 29.2 (C5′), 29.6 (C2′), 70.2 (C1′). **C6-O-octyl sucrose, 16b:** ^{1}H NMR δ_{ppm} : 3.54 (H-1α), 3.87 (H-3α), 3.72 (H-4α), 3.72 (H-5α), 3.25 (H-6a), 4.90 (H-1″α), 3.17 (H-3″), 3.11 (H-4″), 3.44 (H-5″), 3.48 (H-6″), 3.01 (H-1′), 1.0-1.25 (H-2-7′), 0.85 (H-8′); ^{13}C NMR δ_{ppm} : 61.8 (C1α), 104.04 (C2α), 77.4 (C3α), 76.0 (C4α), 82.0 (C5α), 63.0 (C6α), 92.1 (C1″α), 72.2 (C3″), 70.2 (C4″), 72.0 (C5″), 61.2 (C6″), 14.6 (C8′), 23.3 (C7′), 31.3 (C6′), 29.6 (C4′), 29.7 (C2′), 70.0 (C1′).

UV spectrum showed $\sigma \rightarrow \sigma^*$ band at 205 nm and $n \rightarrow \pi^*$ band at 276 nm. The IR spectral band at 1053 cm^{-1} corresponded to the anomeric C-O-C symmetrical stretching and 1259 cm^{-1} for the C-O-C asymmetrical stretching frequencies (Fig. 3.11A). Two-dimensional HSQCT confirmed the formation of C1-O- and C6-O- of alkylated products. The chemical shift values for C1 at 62.8 ppm (^{1}H at 3.76 ppm) and C6 at 63.0 ppm (^{1}H at 3.25 ppm) indicated the formation C1 alkylated **16a** and C6 alkylated **16b** products respectively (Fig. 3.10). Also NMR data clearly showed that hydrolysis of sucrose has taken place and the hydrolyzed D-glucose is glycosylated at C1α (^{13}C at 98.7 ppm and ^{1}H at 4.64 ppm) and alkylated at the C6-O- position (^{13}C at 67.5 ppm and ^{1}H at 3.54 ppm). The mass value 455 for [M+1] peak confirmed the product formation (Fig. 3.11B).

3.4 Synthesis of n-alkyl glucosides using amyloglucosidase

n-Alkyl glucosides using alcohols of carbon chain length C1 - C18, were synthesized with the following specific alcohols, viz. methyl alcohol, ethyl alcohol, n-propyl alcohol, n-butyl alcohol, n-amyl alcohol, n-hexyl alcohol, n-heptyl alcohol, n-octyl alcohol, n-nonyl alcohol, n-decyl alcohol, lauryl alcohol, cetyl alcohol and stearyl alcohol **(Scheme 3.1)**. The reaction mixtures were analyzed by HPLC. Retention times are: D-glucose - 5.2 min, n-methyl-D-glucoside-7.0 min, n-ethyl-D-glucoside-7.1 min, n-

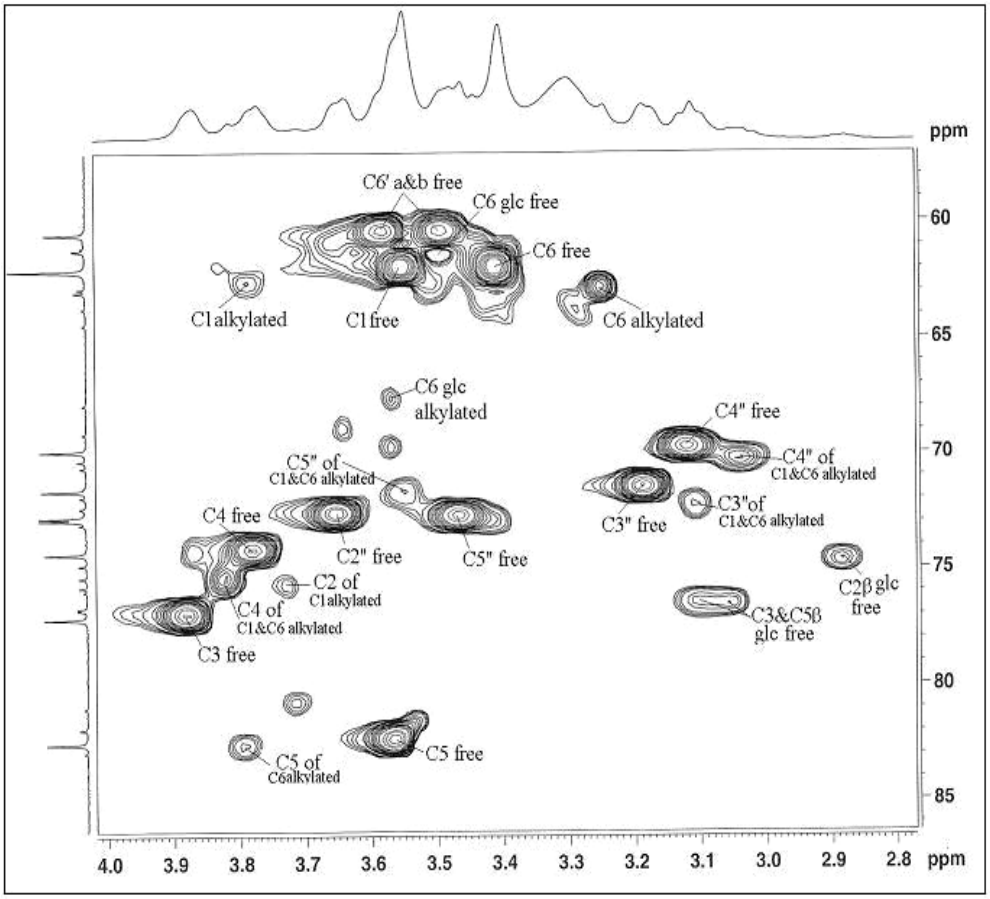

Fig. 3.10 2D-HSQCT spectrum of n-octyl sucrose **16a** and **b**.

propyl-D-glucoside-7.1 min, n-butyl-D-glucoside-7.1 min, n-amyl-D-glucoside-7.1 min, n-hexyl-D-glucoside-7.2 min, n-heptyl-D-glucoside-7.2 min, n-nonyl-D-glucoside-7.5 min, n-decyl-D-glucoside-7.6 min, laryl-D-glucoside-7.6 min, cetyl-D-glucoside-7.7 min and stearyl-D-glucoside-7.7 min. Conversion yields were determined from HPLC peak areas of the glucoside and free D-glucose with respect to a D-glucose concentration of 0.555 mmol. Error measurements in HPLC yields will be ± 5-10%.

3.4.1 Shake flask method

Alcohols of carbon chain lengths C2 - C18 were employed for the synthesis of glucosides by shake flask method in presence of 0.8 mM (0.4 mL in reaction mixture) of 0.01M, pH 4.0 acetate buffer (Fig. 3.12). The yields obtained (with respect to D-glucose) were found to be in the range 3% to 28% (16 μmol - 156 μmol). The results showed that the yields are higher for ethanol (10%, 57 μmol), n-propyl alcohol (13%, 73 μmol) and n-butanol (9%, 52 μmol). For other medium chain length alcohols like n-amyl alcohol (3%, 16 μmol), n-hexyl alcohol (9%, 47 μmol) and n-heptyl alcohol (5%, 26 μmol), the yields were much lower. However, from n-octyl alcohol to n-decyl alcohol, the yields were the highest (20%, 109 μmol to 23%, 127 μmol) with n-nonyl alcohol giving the highest yield (28%, 155 μmol). The yields decreased slightly with further increase in alcohol chain lengths up to stearyl alcohol. The shake flask method gave lesser yields at pH 4.0 in general for the carbon chain lengths up to C7. From n-octyl alcohol onwards, the yields increased with increase in chain lengths upto C10.

3.4.2 Reflux method

Alkyl glucosides were also synthesized with various alcohols by the reflux method in presence of 0.04 mM (0.4 mL), pH 4.0 and 5.0 acetate buffer (Table 3.5). At pH 4.0 the yields were lower for methyl (13%, 71 μmol), ethyl (5%, 27 μmol) and n-propyl alcohols (7%, 39 μmol). However, the yields were higher for the remaining

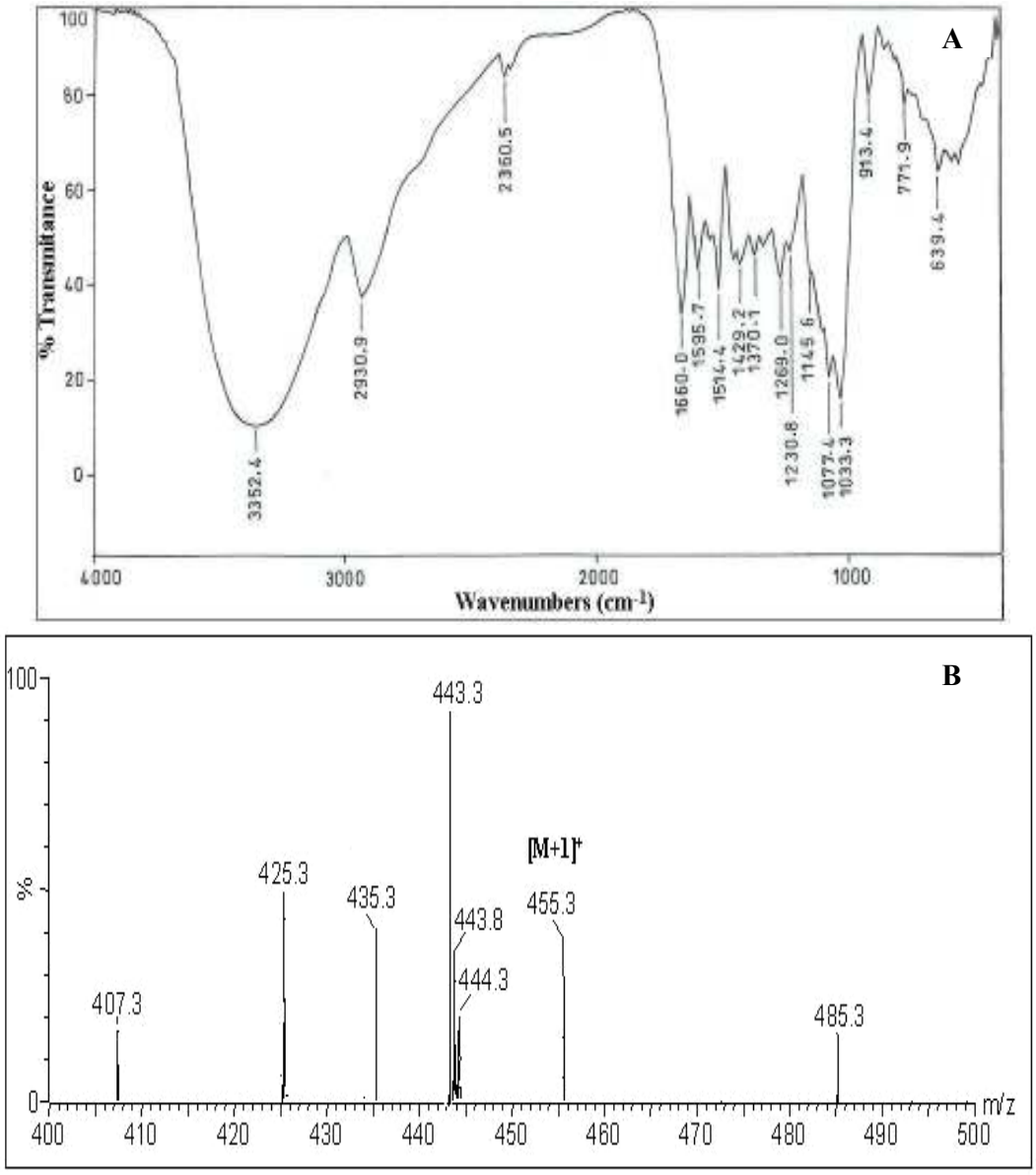

Fig. 3.11 n-Octyl sucrose **16a** and **b (A)** IR spectrum **(B)** Mass spectrum.

alcohols. The highest yield was observed for n-amyl alcohol (44%, 245 μmol). In general, except lauryl alcohol (10%, 55 μmol), the yields were higher for n-octyl alcohol (24%, 134 μmol) onwards towards higher chain length alcohols.

At pH 5.0, the yields obtained were found to be in the range 12% (65 μmol) - 44% (242 μ mol). Higher yields were observed for ethyl alcohol (44%, 242 μ mol) and lauryl alcohol (36%, 200 μ mol).

Table 3.5 Synthesis of n-alkyl-D-glucosides by the reflux method[a].

Name of the glycoside	Yield - % (μmol) pH 4.0 (0.04 mM)	Yield - % (μmol) pH 5.0 (0.04 mM)
Methyl-D-glucoside	13 (71)	25 (141)
Ethyl-D-glucoside	5 (27)	44 (242)
n-Propyl-D-glucoside	7 (39)	35 (197)
n-Butyl-D-glucoside	28 (156)	16 (89)
n-Amyl-D-glucoside	44 (245)	36 (199)
n-Hexyl-D-glucoside	19 (107)	36 (198)
n-Heptyl-D-glucoside	19 (105)	16 (87)
n-Octyl-D-glucoside	24 (134)	30 (164)
n-Nonyl-D-glucoside	22 (123)	22 (120)
n-Decyl-D-glucoside	29 (160)	12 (65)
Lauryl-D-glucoside	10 (55)	36 (200)
Cetyl-D-glucoside	20 (111)	30 (128)
Stearyl-D-glucoside	41 (230)	19 (96)

[a] Conversion yields were determined from HPLC peak areas of glucoside and free D-glucose with respect to D-glucose concentration of 0.555 mmol. All the experiments have been carried out in duplicate and the values are an average of the two experiments. Alcohol – 50 eq, enzyme – 50% w/w glucose, buffer concentration-0.04 mM (0.4mL of 0.01M buffer in 100 mL reaction mixture), temperature– 68 ^{o}C.

3.4.3 Cetyl and Stearyl glucosides

The effect of increasing enzyme concentration on the synthesis of cetyl and stearyl glucosides was investigated at enzyme concentrations ranging from 10% to 50% w/w D-glucose in presence of 0.8 mM (0.4 mL in reaction mixture) and pH 4.0 acetate

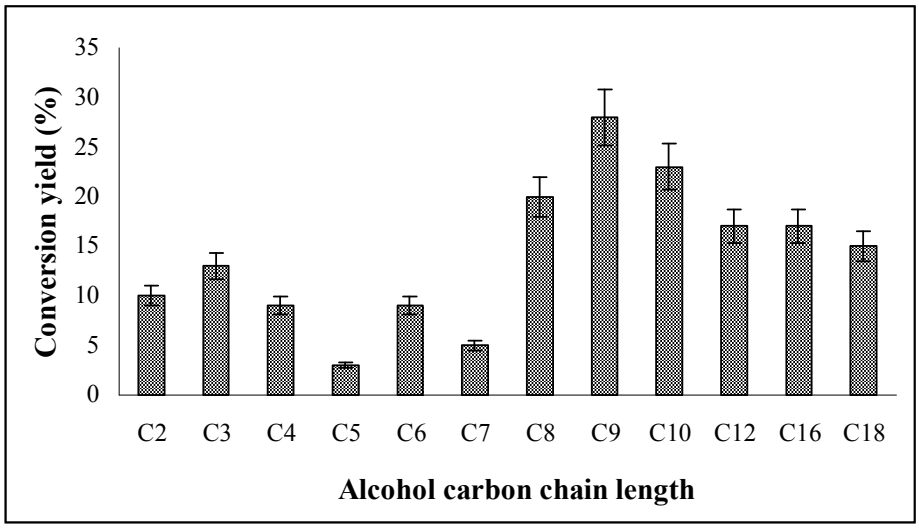

Fig. 3.12 Synthesis of n-alkyl-D-glucosides by the shake flask method. Conversion yields were from HPLC with respect to 0.555 mmol of D-glucose. Reaction conditions: D-glucose-0.555 mmol, alcohol–0.027 mol, 0.4 mL of 10 mM pH 4.0 acetate buffer, enzyme – 50% w/w D-glucose.

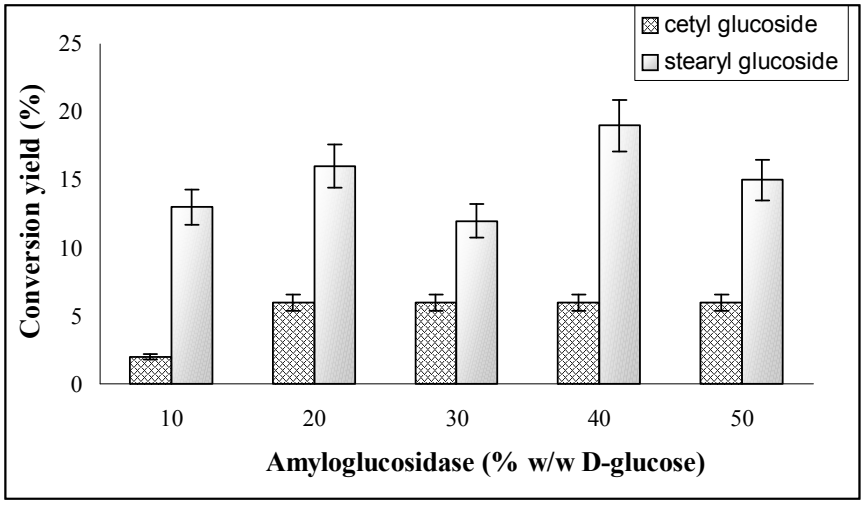

Fig. 3.13 Effect of amyloglucosidase on cetyl and stearyl glucosides. Conversion yields were from HPLC with respect to 0.555 mmol of D-glucose. Reaction conditions: D-glucose-0.555 mmol, alcohol–0.027 mol, pH – 4.0 acetate buffer, buffer concentration 0.8 mM (0.4 mL of 10 mM buffer), enzyme – 50% w/w D-glucose.

buffer (Fig. 3.13). In order to ensure proper mixing of the components, 5 mL of n-heptane was added to solublise the alcohols. The yields obtained at 40% enzyme concentration was higher in case of both cetyl (6%, 34 μmol) and stearyl glucosides (19%, 105 μmol) compared to the other enzyme concentrations. The yields generally were higher at all the enzyme concentrations for stearyl alcohol compared to cetyl alcohol. This could be because the longer chain length alcohol functioned as a better nucleophile for accepting a D-glucose molecule than the shorter chain length alcohol.

3.5 Optimization of n-octyl-D-glucoside synthesis using Response Surface Methodology

Response Surface Methodology (RSM) is a useful statistical technique widely employed in the preparation of food additives which involve complex processes (Shieh *et al.*, 1995; Huang and Akoh, 1996; Manohar and Divakar, 2002). Ismail *et al.* (1998) have reported the synthesis of butyl glucoside by RSM. Using β–galactosidase, Chahid *et al.*, (1994) have reported the synthesis of a mixture of octylglucoside and octylgalactoside through a transglycosylation reaction involving lactose and n-octanol.

The present work deals with a detailed RSM analysis of the synthesis of n-octyl-D-glucoside using amyloglucosidase from *Rhizopus* sp. by the shake flask method. A central composite rotatable design (CCRD) was employed with five parameters, namely, n-octanol concentration, enzyme concentration, pH, buffer concentration (buffer volume) and temperature to arrive at optimum glucosylation conditions.

A five variable parametric study was employed for the central composite rotatable design (CCRD) analysis (Montgomery 1991). The five variables employed were n-octanol concentration, amyloglucosidase concentration, pH, buffer concentration (buffer volume) and temperature. Extent of glucosylation was the output analyzed. The experimental design included 32 experiments of five variables at five levels (-2,-

1,0,+1,+2). Table 3.6 shows the coded and actual levels of the variables employed in the design matrix. Actual set of experiments undertaken as per the CCRD with coded values and the glucosylation yields obtained is given in Table 3.7. A second order polynomial equation was developed to study the effects of the variables on the glycoside yields. The equation indicates the effect of variables in terms of linear, quadratic and cross product terms. The equation is of the general form

$$Y = A_0 + \sum_{i=1}^{N} A_i X_i + \sum_{i=1}^{N} A_{ii} X_i^2 + \sum_{i=1}^{N-1} \sum_{j=i+1}^{N} A_{ij} X_i X_j \qquad (3.1)$$

Where Y is the glucosylation yield (%), X_i is the variable, A_o = constant term, A_i is the coefficient of the linear terms, A_{ii} is the coefficient of the quadratic terms, A_{ij} is the coefficient of the cross product terms and N is the number of variables.

Table 3.6 Coded values of the variables and their corresponding actual values used in the design of experiments.

Variables	-2	-1	0	1	2
n-Octanol (eq)	15	30	45	60	75
Amyloglucosidase (mg)	20	40	60	80	100
pH	4.0	5.0	6.0	7.0	8.0
Buffer volume (mL)	0.2	0.4	0.6	0.8	1.0
Temperature (^oC)	30	40	50	60	70

The coefficients of the equation were determined by employing Microsoft Excel software, version 5.0. The analysis of variance (ANOVA) for the final predictive equation was also done using Microsoft Excel software. ANOVA is required to test the significance and adequacy of the model (Table 3.7). The response surface equation was optimized for maximum yield in the range of process variables employed using Microsoft Excel Solver function.

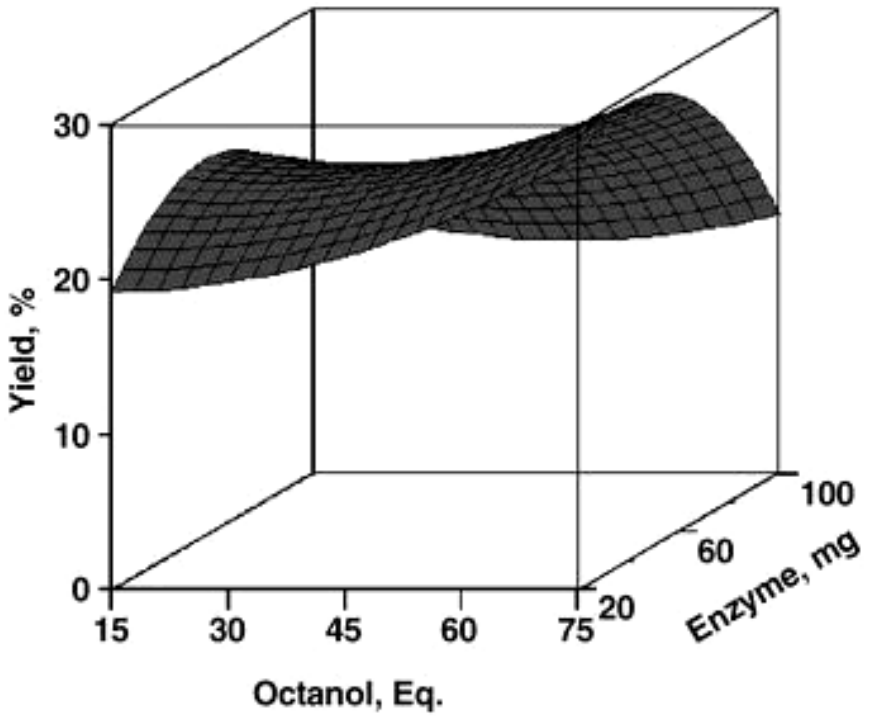

Fig. 3.14 Three – dimensional surface plot showing the effect of n-octanol concentration and enzyme concentration on the extent of glucosylation (pH-6.0, 0.6 mL of 10 mM buffer, temperature – 50 ^{o}C).

Table 3.7 Experimental design with experimental and predicted yields of n-octyl-D-glucoside.

Expt No	n-Octanol	Amylo glucosidase	pH	Buffer volume	Temperature	Yield[a] Experimental	Yield Predicted
1	-1	-1	-1	-1	1	20.0	22.4
2	-1	-1	-1	1	-1	10.7	12.3
3	-1	-1	1	-1	-1	29.2	30.3
4	-1	-1	1	1	1	0.9	5.8
5	-1	1	-1	-1	-1	39.5	35.6
6	-1	1	-1	1	1	1.8	1.8
7	-1	1	1	-1	1	14.4	13.8
8	-1	1	1	1	-1	13.1	11.6
9	1	-1	-1	-1	-1	31.6	30.8
10	1	-1	-1	1	1	1.2	4.2
11	1	-1	1	-1	1	26.6	29.1
12	1	-1	1	1	-1	17.8	19.4
13	1	1	-1	-1	1	18.1	15.6
14	1	1	-1	1	-1	17.9	14.5
15	1	1	1	-1	-1	37.2	33.3
16	1	1	1	1	1	2.5	2.4
17	0	0	0	-2	0	40.9	43.8
18	0	0	0	2	0	12.1	9.1
19	0	0	-2	0	0	14.1	15.9
20	0	0	2	0	0	20.0	18.1
21	0	-2	0	0	0	29.6	21.5
22	0	2	0	0	0	7.1	15.1
23	-2	0	0	0	0	26.3	24.3
24	2	0	0	0	0	26.2	28.1
25	0	0	0	0	-2	13.8	18.4
26	0	0	0	0	2	0	0
27	0	0	0	0	0	29.6	24.1
28	0	0	0	0	0	21.4	24.1
29	0	0	0	0	0	21.1	24.1
30	0	0	0	0	0	30.1	24.1
31	0	0	0	0	0	23.4	24.1
32	0	0	0	0	0	19.1	24.1

[a] Conversion yields were from HPLC with respect to 0.555 mmol of D-glucose. The experimental yields were an average from two experiments.

The experimental yields data fitted the 2nd order polynomial equation well as indicated by a R^2 value of 0.895 (Table 3.8). The ANOVA shows the model is significant at $P<0.01$. The final predictive equation is given by

$$Y=-98.557-0.780X_1+1.280X_2+17.752X_3-82.346X_4+4.005X_5+0.002X_1X_1-0.004\ X_2X_2-1.783\ X_3X_3+14.526X_4X_4-0.043X_5X_5-0.002X_1X_2+0.124X_1X_3+0.051X_1X_4+0.0003\ X_1X_5-0.066X_2X_3+0.049\ X_2X_4-0.009\ X_2X_5+1.341\ X_3X_4+0.035\ X_3X_5+0.166\ X_4X_5 \quad (3.2)$$

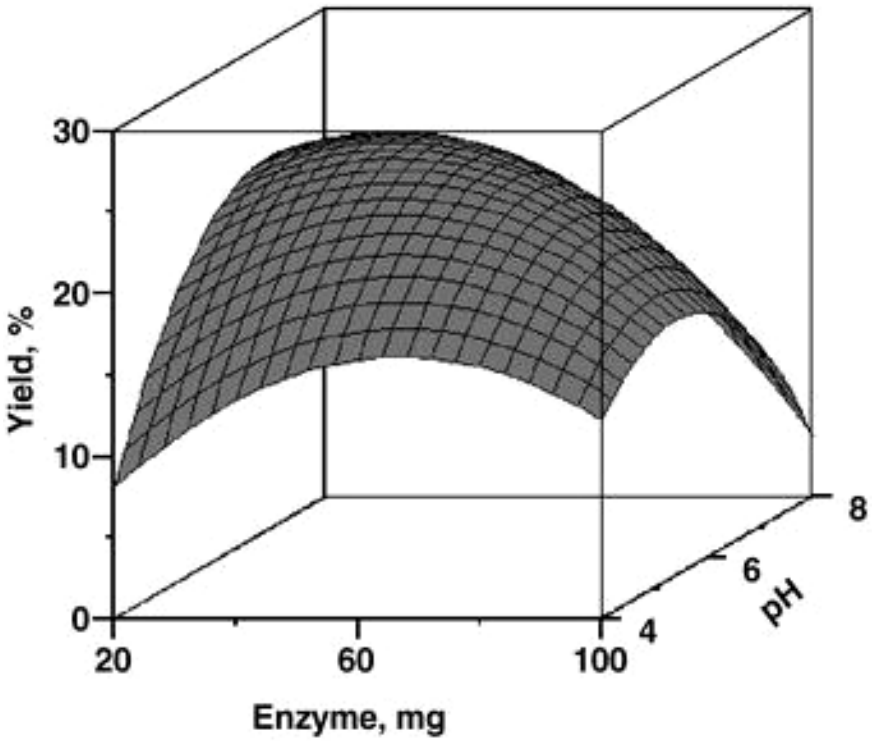

Fig. 3.15 Three – dimensional surface plot showing the effect of enzyme concentration and pH on the extent of glucosylation (n-Octanol concentration – 45 eq, 0.6 mL of 10 mM buffer, temperature – 50 ^{o}C).

Where X_1 - n-octanol concentration; X_2 – amyloglucosidase concentration; X_3 - pH; X_4 – buffer volume; X_5 – temperature.

The maximum yield predicted based on the response model 53.5% is obtained at an n-octanol concentration of 75 eq., 20 mg amyloglucosidase concentration, 0.30 mM (0.2 mL of 10 mM buffer) pH 7.8, buffer and 50 °C. The experiments conducted at the above optimum conditions resulted in 53.8% yield. Apart from the above experiment, validation of the response model was carried out at selected random process conditions. These validation experiments closely agreed with the predicted yields (Table 3.9).

The effect of n-octanol and enzyme concentration on the glucosylation of n-octanol to n-octyl-D-glucoside at 0.6 mL of 10 mM, pH 6.0 at 50 ^{o}C is shown in Figure 3.14. The extent of conversion increased with the increase in n-octanol equivalents at lower enzyme concentrations. With increase in enzyme concentration from 20-60 mg (20-60% with respect to w/w D-glucose), the extent of glucosylation reached a maximum of 29.0 % at 60 mg (60% w/w D-glucose) enzyme concentration. With further increase in enzyme concentration to 100 mg (100% w/w D-glucose), the yield decreased. This was the behavior at all equivalents of n-octanol. Around an enzyme concentration of 60 mg (60% w/w D-glucose), increase in n-octanol equivalents exhibited a trough with a slight dip around an n-octanol concentration of 45 eq. The surface plot illustrates that at lower enzyme concentrations, sufficient amount of free n-octanol is available for transfer of D-glucose to n-octanol resulting in increase in glucosylation. At higher enzyme concentrations, a complete binding of n-octanol to the enzyme would effectively reduce the concentration of free n-octanol, thereby causing a reduction in the transfer of D-glucose molecule to n-octanol leading to reduced glucosylation.

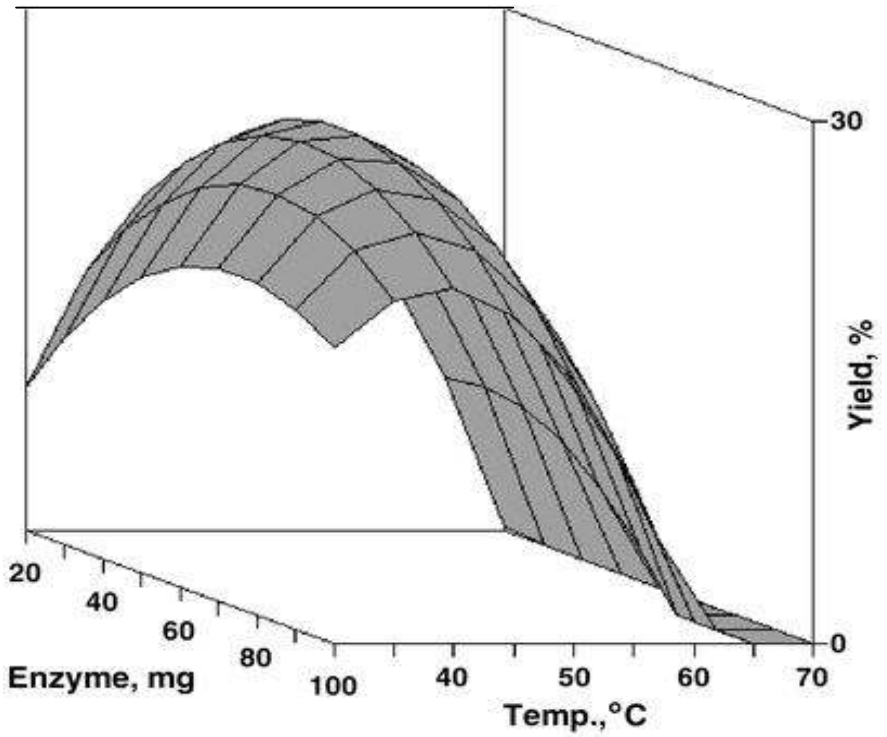

Fig. 3.16 Three – dimensional surface plot showing the effect of enzyme concentration and temperature on the extent of glucosylation (n-Octanol – 45 eq, pH – 6.0, 0.6 mL of 10 mM buffer.

Table 3.8 Analysis of variance of the response surface model along with coefficients of the response equation.

Regression Statistics*:*

Multiple R	0.946
R Square	0.895
Standard Error	6.157
Observations	32

ANOVA:

	degrees of freedom	**sum of squares**	**mean sum of squares**	**F ratio**	**Significance F**
Regression	20	3556.1	177.8	4.69	P<0.01**
Residual	11	417.0	37.9		
Total	31	3973.1			

Coefficients	**Values of Coefficients**	**Standard Error**	**t-Stat**
Ao	-98.55	99.628	-0.989
A_1	-0.780	1.022	-0.762
A_2	1.280	0.766	1.668
A_3	17.752	17.632	1.006
A_4	-82.346	76.695	-1.073
A_5	4.005	1.673	2.393
A_{11}	0.002	0.005	0.457
A_{22}	-0.004	0.002	-1.271
A_{33}	-1.783	1.136	-1.568
A_{44}	14.526	28.420	0.511
A_{55}	-0.043	0.011	-3.799
A_{12}	-0.002	0.005	-0.390
A_{13}	0.124	0.102	1.203
A_{14}	0.051	0.513	0.098
A_{15}	0.0003	0.010	-0.029
A_{23}	-0.066	0.076	-0.085
A_{24}	0.049	0.384	0.126
A_{25}	-0.009	0.007	-1.220
A_{34}	1.341	7.696	0.174
A_{35}	0.035	0.153	0.229
A_{45}	0.166	0.769	0.215

The effect of increasing enzyme concentration and pH on the extent of glucosylation at an n-octanol concentration of 45 eq, 1.3 mM (0.6 mL of 10 mM buffer) buffer concentration and 50 ^{o}C is shown in Figure 3.15. At lower enzyme concentrations

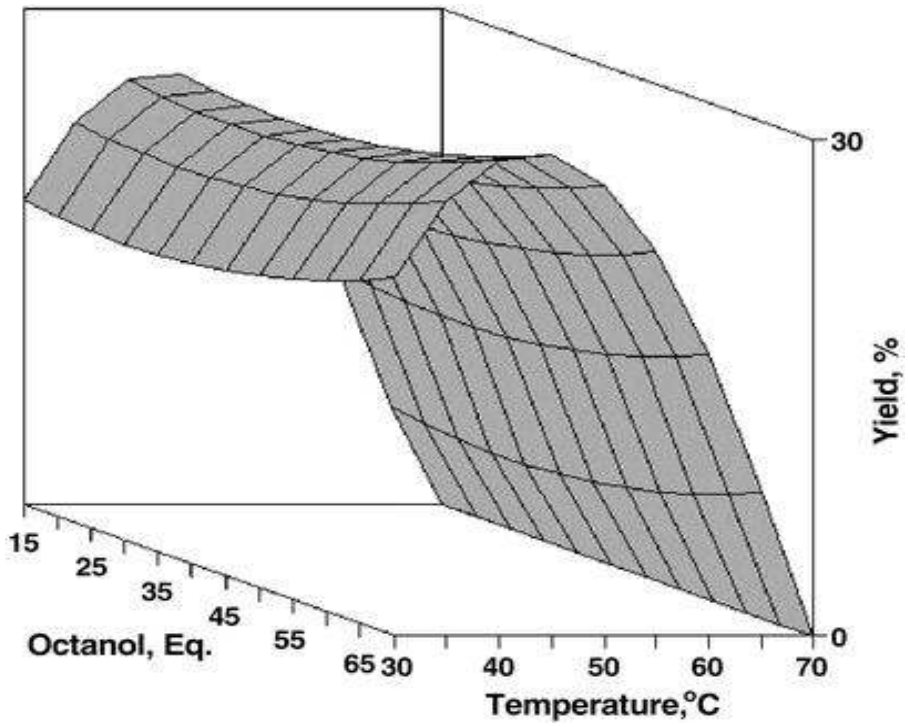

Fig. 3.17 Three – dimensional surface plot depicting the effect of n-octanol equivalents and temperature on the extent of glucosylation (amyloglucosidase – 60 mg, pH – 6.0, 0.6 mL of 10 mM buffer).

of 20 mg, increase in pH from 4.0 to 8.0 resulted in increase extent of glucosylation. At higher concentrations of enzyme and higher pH, the extent of glucosylation decreased. At all pH values, there is increase in glucosylation with the increase in the enzyme concentration up to 60 mg, which decreased thereafter at higher enzyme concentrations. This shows that at lower enzyme concentrations, the catalytic efficiency of the enzyme increased with increase in pH from pH 4.0 to 8.0. However, at higher enzyme concentrations, the catalytic efficiency increased up to a pH of 6.0 and decreased thereafter up to a pH of 8.0. Since the experiments were performed at a constant buffer concentration of 1.4 mM (0.6 mL buffer volume) an effective 'pH memory' is rendered for catalytic glucosylation at lower concentrations of enzyme. At higher enzyme concentrations, the buffer salt concentration could be insufficient to impart an effective 'pH memory' to the enzyme to enhance its catalytic efficiency.

Table 3.9 Validation of experimental data.

n-Octanol (eq)	Amylo glucosidase (mg)	pH	Buffer volume (mL)	Temperature (^{o}C)	Yield Predicted	Yield[a] Experimental
50	50	4.5	0.3	55	29.3	23.8
40	30	6.5	0.5	65	13.6	6.09
65	50	7.5	0.3	65	25.2	25.3
55	45	4.5	0.3	45	34.2	30.1
55	45	4.5	0.3	35	31.0	20.9
10	65	5.5	0.7	65	2.8	4.2
50	55	4.5	0.9	65	0	5.0
75	20	7.8	0.2	50	53.5	53.8

[a] Conversion yields were from HPLC with respect to 0.555 mmol of D-glucose. The experimental yields were an average from two experiments.

The catalytic efficiency of the enzyme was found to be the highest at 50 ^{o}C and it decreased to very low values at 70 ^{o}C at all enzyme concentrations (Fig. 3.16). Other conditions kept constant were n-octanol – 45 eq, pH – 6.0 and buffer concentration 1.3 mM (0.6 mL of 10 mM buffer). At 30 ^{o}C, glucosylation occurred at all enzyme

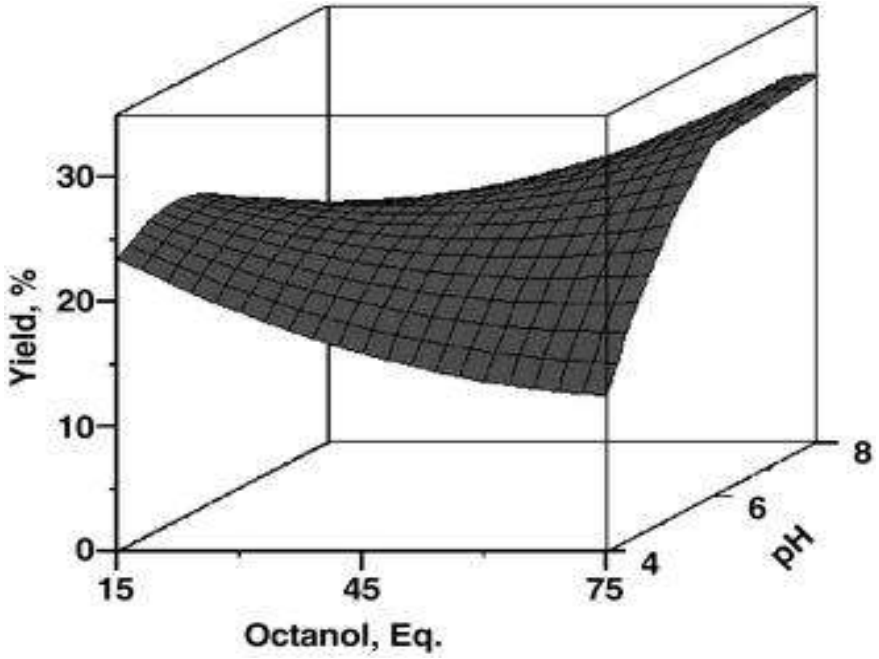

Fig. 3.18 Three – dimensional surface plot showing the effect of n-octanol concentration and pH on the extent of glucosylation (amyloglucosidase – 60 mg, 0.6 mL of 10 mM buffer, temperature 50 ^{o}C).

concentrations. The highest conversion was with 60 mg (60% w/w D-glucose) of enzyme. At lower enzyme concentrations, the conversions were lower. However, they increased with increase in temperature up to 50 ^{o}C indicating that the optimum temperature required for glucosylation is 50 ^{o}C. At a higher temperature of 70 ^{o}C, the enzyme most probably underwent denaturation leading to a loss in catalytic activity.

The effect of various equivalents of n-octanol was studied along with increase in temperature, on the extent of glucosylation (Fig. 3.17) at an enzyme concentration of 60 mg (60% w/w D-glucose), pH 6.0 and 0.6 mL of 10 mM buffer. Here also as in the previous figure (Fig. 3.16) the optimum temperature of 50 ^{o}C was detected. At the highest temperature of 70 ^{o}C, the extent of glucosylation was the lowest, indicating that the enzyme was not able to effectively convert n-octanol to its glycoside. Temperature was found to be a significant parameter in deciding the extent of conversion. The effect of various equivalents of n-octanol had a very slight effect on the extent of glucosylation at all the temperatures studied.

Besides the effect of enzyme concentration and temperature, another variable that affected the conversion efficiency was the pH of the buffer employed (Fig. 3.18). The effect of increase in n-octanol equivalents and increase in pH was studied at an enzyme concentration of 60 mg (60% w/w D-glucose), 0.6 mL of 10 mM buffer and 50 ^{o}C. For all the equivalents of n-octanol, increase in pH increased the extent of conversion. However, at a higher pH of 8.0, increase in n-octanol decreased the extent of conversion. The role of the nucleophile, n-octanol, was found to be almost opposite to that of the enzyme at all the pH values employed. Hence, it is quite essential that the n-octanol concentration to be kept at a minimum.

Figure 3.19 shows the effect of buffer volume and pH on the extent of glucosylation at an n-octanol concentration of 45 eq, 60 mg enzyme and 50 ^{o}C. These

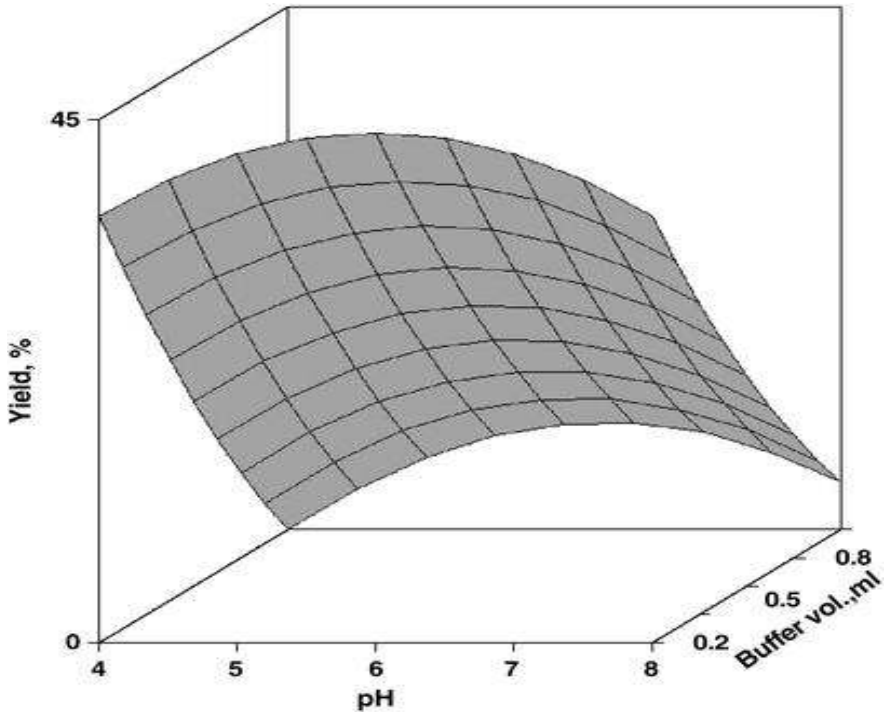

Fig. 3.19 Three – dimensional surface plot showing the effect of pH and buffer volume on the extent of glucosylation (amyloglucosidase – 60 mg, n-octanol – 45 eq, temperature - 50 ^{o}C).

two parameters (pH and buffer volume) effectively indicated the concentration of buffer salts and their effect on importing 'pH memory' to amyloglucosidase. With increase in pH, glucosylation decreased at all buffer volumes. An optimum buffer volume 0.6 mL buffer was found to be the best for this reaction.

Thus, this study showed that this model is very good in predicting the glucosylation of n-octanol by the amyloglucosidase enzyme.

3.6 Discussion

Amyloglucosidase is a starch-degrading enzyme, which catalyzed the synthesis of n-octyl glycosides of D-glucose, maltose and sucrose in di-isopropyl ether solvent and in the presence of water, added in the form of buffer (10 mM). The other carbohydrates employed showed less than 5% glycosylation for D-galactose, D-mannose, D-fructose and D-mannitol. D-Arabinose D-ribose, lactose and D-sorbitol did not undergo glycosylation. D-Glucose showed a maximum conversion yield (46%, 255 μmol) at optimized conditions.

In general, the yields obtained by the reflux method were much higher than those by the shake flask method for all the alcohols studied. Further in the reflux method, the yields obtained at pH 5.0 were better compared to those observed at pH 4.0.

Vic and Thomas (1992) reported a glucoside yield (with respect to glucose concentration) of 13.1% for methanol, 9.8% for ethyl alcohol, 6.6% for n-butanol, 4.9% for n-hexanol and 3.6% for n-octanol in the reactions carried out with almond β-glucosidase. The present work, especially the reflux method with amyloglucosidase showed that the glucoside yields were much higher (methanol - 25%, ethyl alcohol - 44%, n - butanol -28%, n-hexanol - 36% and n-octanol - 46% with respect to D-glucose concentration employed) than those reported.

Besides C1 glycosylation, C6-O-alkylation also occurred although the latter products are formed to a very small extent. Since large concentration of amyloglucosidase is employed in the present work, compared to hydrolysis, the specificity is lost. However, only certain carbohydrates like D-glucose, maltose and sucrose underwent reaction. Other carbohydrates showed either very less yields or did not undergo either glycosylation nor alkylation under the reaction conditions employed. Among the nucleophilic straight chain alcohols employed, while shake flask favored medium chain length alcohols, the reflux method at pH 4.0 favored shorter chain length alcohols and pH 5.0 more or less favored almost all the chain length. This clearly shows that since pH affects the ionization states of the surface amino acid residues in amyloglucosidase between pH 4.0 and pH 5.0 the enzyme should be favoring a more open active site at pH 5.0, accomodating alcohols of different chain length favorably for glycosylation. However, no such generalization is possible to explain the difference in glycosylation behavior where aldohexoses, aldopentoses, ketohexose, carbohydrate alcohols and disaccharides were employed.

There are not many reports on the glycosylating potential of amyloglucosidase in the literature. The results from this investigation have shown conclusively that amyloglucosidase is an excellent enzyme for carrying out effective glucosylation of straight chain alcohols.

3.7 Experimental section

3.7.1 Synthetic procedures

3.7.1.1 Shake flask method

Reactions were carried out in 25 mL stoppered conical flasks wherein D-glucose, 0.1g (0.555 mmol) and alcohol were taken in a molar ratio of 1:50. Appropriate quantities of amyloglucosidase (10-50 % w/w D-glucose) was added along with 0.1-0.8

mL of 0.01 M buffer of appropriate pH (corresponding to 0.2-1.6 mM) and incubated at 60 ^{o}C in a temperature control shaker at 150 rpm for 72 h. The reaction mixture was held in a boiling water bath for 5-10 minutes to denature the enzyme in order to avoid the hydrolytic reaction. Then 15-20 mL of water was added to dissolve the unreacted glucose and the product glucoside. The unreacted alcohol was separated in a separating funnel with petroleum ether or n-hexane. The bottom water layer was evaporated to get the unreacted glucose and the product glucoside.

3.7.1.2 Reflux method

In the reflux method, the reactions were carried out in a 150 mL two-necked flat-bottomed flask. Carbohydrate, 0.1g (0.555 mmol) and alcohol were taken in 1: 50 molar ratio. An appropriate quantity of amyloglucosidase (10-75% w/w D-glucose) was added along with 0.1-1.0 mL of 0.01 M buffer of appropriate pH (corresponding to 0.01-0.1 mM concentration in 100 mL reaction mixture). The reaction mixture was refluxed with 100 mL of di-isopropyl ether with stirring for 72 h. The product work out was as described above. The product glycoside was isolated by column chromatography by passing through Sephadex G15 using water as the eluent. Although the glycoside compounds were separated from unreacted carbohydrates, further separation of glycosides into individual one was not possible because of similar polarity of the molecules.

3.7.1.3 Experimental procedure for the response surface methodology

D-Glucose, 0.1g (0.555 mmol) and n-octanol (15 to 75 equivalents) were taken in a 25 mL stoppered conical flasks in presence of 0.01 M, pH 4.0 to 8.0 buffer (volume 0.2 to 1.0 mL). The enzyme amyloglucosidase (20 to 100 mg, 20-100% w/w D-glucose) was added and incubated in a temperature control shaker in the temperature range 30 ^{o}C to

70 ^{o} C at 150 rpm for 72 h. Buffer salts used were, CH_3COONa for pH 4.0 and pH 5.0, Na_2HPO_4 for pH 6.0 and pH 7.0 and $Na_2 B_4O_7$ 10 H_2O for pH 8.0.

The reaction mixture was kept in a boiling water bath for 5-10 min to denature the enzyme in order to avoid hydrolysis. Then 15-20 mL of water was added to dissolve the unreacted D-glucose and the product glucoside. The unreacted alcohol was separated in a separating funnel using petroleum ether. The bottom aqueous layer was evaporated to get the unreacted D-glucose and the product glucoside, which was further subjected to analytical HPLC.

3.7.2 HPLC

The reaction mixtures were analyzed by HPLC using an amino-propyl column (3. 9 x 300 mm length) and acetonitrile: water in 80:20 ratio (v/v) as the mobile phase at a flow rate of 1mL/min with refractive index detector.

3.7.3 Spectral characterization

Ultra Violet-Visible spectra were recorded on a Shimadzu UV-1601 spectrophotometer. Known concentrations of the glycoside samples dissolved in the water were used for recording the spectra. Infrared spectra were recorded on a Nicolet-FTIR spectrophotometer. Isolated solid glycoside samples (5-8 mg) were prepared as KBr pellets and employed for recording the IR spectra. n-Octanol standard was employed as such between salt plates to obtain IR spectra. Mass spectra were obtained using a Q-TOF Waters Ultima instrument (Q-Tof GAA 082, Waters corporation, Manchester, UK) fitted with an electron spray ionization (ESI) source.

3.7.4 NMR

3.7.4.1 ^{1}H NMR

^{1}H spectra were recorded on a Brüker DRX 500 MHz NMR spectrometer (500.13MHz). Proton pulse width was 12.25 μs. Sample concentration of about 40 mg of

the sample dissolved in DMSO-d_6 was used for recording the spectra at 35 ^{o}C. About 100-200 scans were accumulated to get a good spectrum. The region between 0-10 ppm was recorded for all the samples. Chemical shift values were expressed in ppm relative to internal tetra-methyl silane (TMS) as the standard.

3.7.4.2 ^{13}C NMR

^{13}C NMR spectra were recorded on a Brüker DRX 500 MHz NMR spectrometer (125MHz). Carbon 90° pulse width was 10.5 μs. About 40 mg of sample was dissolved in DMSO-d_6 was used for recording the spectra at 35 ^{o}C. About 500 to 2000 scans were accumulated for each proton-proton decoupled spectrum for the 0-200 ppm scanning region. Chemical shift values were expressed in ppm relative to TMS as the standard.

3.7.4.3 2D-HSQCT

Two-dimensional Heteronuclear Single Quantum Coherence Transfer Spectra (2-D HSQCT) were recorded on a Brüker DRX 500 MHz NMR spectrometer (500.13 MHz for ^{1}H and 125 MHz for ^{13}C). A sample concentration of about 40 mg in DMSO-d_6 was used for recording the spectra.

3.7.5 Critical micellar concentration (CMC)

Critical micellar concentration for the non-ionic surfactant octyl-D-glucoside was determined by using Comassive brilliant blue-G250 method (Rosenthal and Koussale 1983). A sample concentration of 0.1 M solution was prepared in water and from this, a series of aliquots of sample concentration in the range of 5 - 20 mM (5-200 μL) were prepared and made up to 1.0 mL by adding corresponding volume of Comassive brilliant blue-G250 reagent. The reaction mixtures were shaken well and the absorbance was measured at 620 nm. A plot of concentrations of the sample verses absorbance was constructed. From this the concentration at which an abrupt change in the linearity of the plot obtained was considered as the critical micellar concentration.

Chapter 4

Enzymatic Synthesis of Phenolic Glycosides

4.1 Introduction

Biological activities of a naturally occurring glycoside (Robyt 1998; Schmid *et al.* 2001; Akao *et al.* 2002) are primarily due to an aglycon moiety of that molecule. It is generally accepted that glycosides are more water-soluble than most of the respective aglycons. Attaching a glycosidic moiety into the molecule increases its hydrophilicity and thereby influences physicochemical and pharmacokinetic properties of the respective compound like circulation, elimination and concentrations in the body fluids (Kren 2001). Glycosides with unsaturated alkyl chains like terpenes are claimed to possess antifungal and antimicrobial activity (Tapavicza *et al.* 2000, Zhou 2000) although it is unclear why the activity of these aglycons is improved by glycosylation. Glycosides of peptides and steroids are used in antitumor formulations (Kaljuzhin and Shkalev 2000) and in cardiac related drugs (Ooi *et al.* 1985) respectively. Curcumin [1E,6E-1,7-di(4-hydroxy-3-methoxy-phenyl)-1,6-heptadiene-3,5-dione] a yellow pigment of turmeric (the dried rhizome of curcuma longa belonging to Zingiberaceae) is used primarily as a food colorant but it is also a pharmacologically-active principle of turmeric with potent anti-oxidative, anti-inflammatory and anti-leishmanial (Gomes *et al.* 2002) activities. Eugenol, main part of the clove oil (more than 90%), is used as a precursor of vanillin. It was found that eugenol possess pharmacological activity and modification is needed in its application (Hamada and Ikemoto 2001). Guaiacol, eugenol, curcumin and α-tocopherol are lipophilic and insoluble in water, which limits their further pharmacological exploitation and practical applications. Currently, very few reports are available on the synthesis of curcuminyl glycosides (Hergenhahn *et al.* 2002; Kaminaga *et al.* 2003; Mohri *et al.* 2003) and eugenol glycosides (Orihara *et al.* 1992; Sato *et al.* 2003) and that too by cell suspension and chemical methods.

Chemical preparation of glycosides cannot meet EC food regulations and therefore chemical preparation of glycosides is not applicable in the food industry. Further, regio and sterioselctivity are two main criteria which are difficult to achieve by chemical methods due to multiple hydroxyl groups in sugar molecule which require protection and deprotection (Mohri *et al.* 2003). Hence, enzyme catalyzed reactions appear to be good alternatives.

4.1.1 Present work

The present chapter describes synthesis and optimization of phenolic glycosides-guaiacyl-α-D-glucoside, eugenyl maltoside, curcuminyl-bis-α-D-glucoside and α-tocopheryl-α-D-glucoside by reflux method using amyloglucosidase from *Rhizopus* mold as a catalyst. Optimization conditions obtained were also employed for the synthesis of guaiacol **17**, eugenol **18**, curcumin **19** and α-tocopherol **20** glycosides of other carbohydrates: D-glucose **2**, D-galactose **3**, D-mannose **4**, D-fructose **5**, D-arabinose **6**, D-ribose **7**, maltose **8**, sucrose **9**, lactose **10**, D-mannitol **11** and D-sorbitol **12**. Attempts were also made to synthesize the glucosides of guaiacol, eugenol, curcumin and α-tocopherol using β-glucosidase isolated from sweet almonds. Optimization study was carried out for the amyloglucosidase-catalyzed synthesis of curcuminyl-bis-α-D-glucoside using response surface methodology (RSM). Reaction kinetics was studied for the amyloglucosidase catalyzed curcuminyl-bis-α-D-glucoside synthesis. Antioxidant activities for guaiacyl-α-D-glucoside and curcuminyl-bis-α-D-glucoside were also evaluated.

4.2 Guaiacyl glycosides

Attempts were made to synthesize guaiacol glycosides using amyloglucosidase. Synthesis of guaiacyl-α-D-glucoside was studied in detail to understand phenolic

glycosylation of such molecules. Guaiacyl-α-D-glucoside synthesis in di-isopropyl ether using amyloglucosidase was optimized in terms of incubation period, pH, buffer concentration, enzyme concentration and D-glucose concentration. The reaction conditions employed were 0.09 - 0.54 g D-glucose (0.5-3.0 mmol), 0.027 mol of guaiacol (50 equivalents with respect to 0.5 mmol D-glucose), 10-75% (w/w D-glucose) amyloglucosidase, 0.1-0.01 mM pH 4.0-8.0 buffer (0.1-1.0 mL of 10 mM buffer in 100 mL of reaction mixture), 100 mL di-isopropyl ether solvent and 3 to 96 h incubation period **(Scheme 4.1)**. The reaction mixture was monitored by high performance liquid chromatography. HPLC retention times are 5.2 min for D-glucose and 6.83 min for guaiacyl-D-glucoside. Conversion yields were determined from the HPLC peak areas of the glycoside and unreacted D-glucose and expressed as percentage with respect to the free D-glucose concentration employed. Errors in the HPLC measurements were in the order of ± 5-10%. The glucoside was isolated by column chromatography by passing through Sephadex G-15 using water as eluent. Spectral characterization was carried out by UV, IR, MS and 2-D NMR spectroscopy for the glucoside and also isolated glycosides. Although glycosides were separated from the unreacted carbohydrate by column chromatography on Sephadex G15, individual glycosides could not be isolated due to the similar polarity of these molecules.

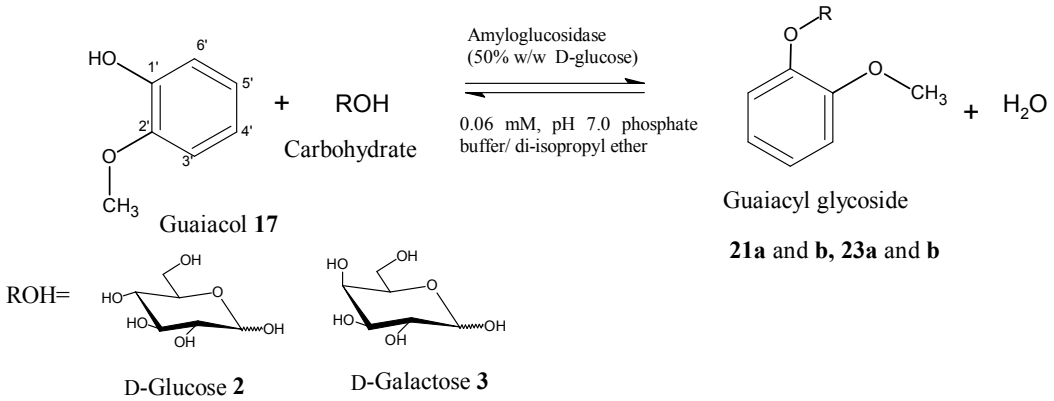

Scheme 4.1 Amyloglucosidase catalyzed synthesis of guaiacyl glycosides

4.2.1 Effect of incubation period on guaiacyl-α-D-glucoside synthesis

The effect of incubation period studied from 3 h to 96 h at 0.555 mmol D-glucose, 0.027 mol guaiacol, 50% (w/w D-glucose) amyloglucosidase and 0.06 mM (0.6 mL) buffer concentration showed that the highest glycosylation yield of 52% (w/w D-glucose) was obtained at 72 h (Fig. 4.1). At the initial stage the conversion yield increased with the increase in the incubation period up to 72h and almost remained constant at 96 h (50% yield) of incubation period. The reaction rate determined from the initial slope was found to be 14.8 μmol/h.

4.2.2 Effect of buffer pH and concentration on guaiacyl-α-D-glucoside synthesis

Different buffers of pH 4.0 to 8.0 at 0.04 mM (0.4 mL of 10 mM buffer employed in 100 mL of the reaction mixture) gave the highest yield of 51 % at pH 7.0 (Table 4.1). At pH 7.0, buffer concentration in the range 0.01-0.1 mM (0.1-1.0 mL), gave the highest conversion yield of 52% at 0.06 mM (0.6 mL) buffer (Table 4.1). With increase in buffer volume water activity also increased. Product hydrolysis appeared to be evident at higher water activity.

Table 4.1 Effect of buffer pH and buffer concentration on guaiacyl-α-D-glucoside synthesis[a].

pH[b]	Yield, %	Buffer concentration[c] (mM) at pH 7.0	Yield, %
4.0	30	0.01	3
5.0	43	0.02	11
6.0	31	0.04	51
7.0	51	0.06	52
8.0	32	0.08	39
		0.1	11

[a]Conversion yields from HPLC with respect to 0.55 mmol of D-glucose. Error in yield measurements ± 5-10%. Guaiacol-0.027 mol, enzyme – 50% (w/w D-glucose), incubation – 72 h, temperature – 68 °C. [b]0.04 mM (0.4 mL of 10 mM buffers added in 100 mL reaction mixture). [c]0.1-1.0 mL of pH 7.0 phosphate buffer.

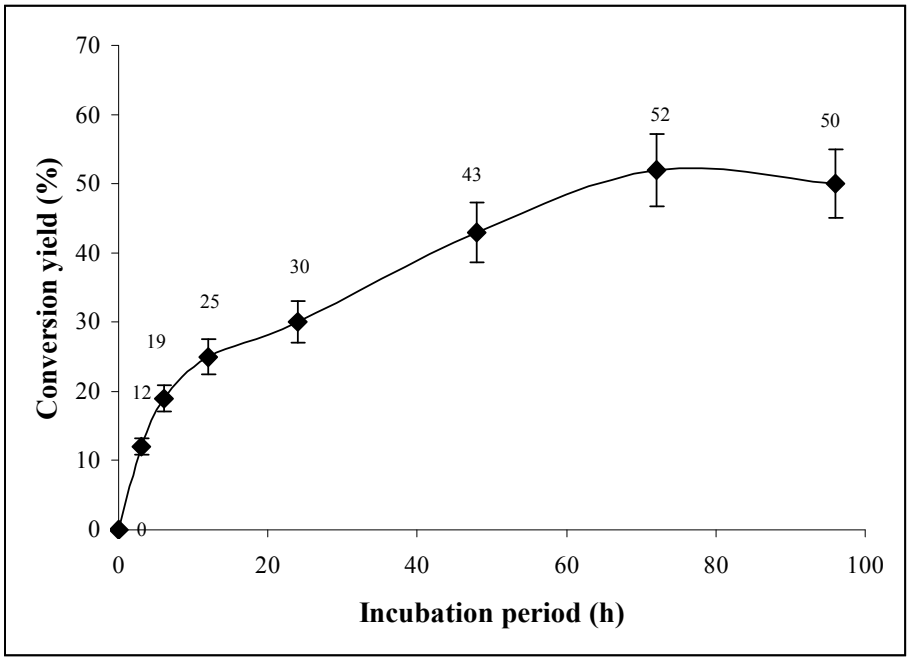

Fig. 4.1 Reaction profile for guaiacyl-α-D-glucoside synthesis. Conversion yields were from HPLC with respect to 0.555 mmol of D-glucose. Reaction conditions: D-glucose – 0.555 mmol, guaiacol - 0.027 mol, 50% (w/w D-glucose), 0.06 mM (0.6 mL of 10 mM buffer in 100 mL reaction mixture) pH 7.0 phosphate buffer, solvent-di-isopropyl ether, temperature - 68 °C.

4.2.3 Effect of amyloglucosidase on guaiacyl-α-D-glucoside synthesis

In the enzyme concentration range 10-75% (w/w D-glucose) and 0.05 mM (0.5 mL) pH 7.0 buffer, the conversion yield was almost constant (40-44%) between 20 and 50% enzyme concentration (Fig. 4.2).

4.2.4 Effect of D-glucose on guaiacyl-α-D-glucoside synthesis

D-Glucose concentration was varied from 0.5-3.0 mmol. Conversion yields were almost constant (26 to 28% w/w D-glucose) between 1.0 to 2.0 mmol of D-glucose and the highest yield of 28% was obtained at 1.0 mmol of D-glucose (Table 4.2). Thereafter at 3.0 mmol of D-glucose (yield 9 %), the conversion yield decreased. Higher concentrations of D-glucose (3.0 mmol, yield 9%) might bind to the entire enzyme molecules preventing transfer to the nucleophilic guaiacol, thereby decreasing the conversion yield. Since very high concentration (50 equivalents to D-glucose) of guaiacol was employed in the reaction, its increasing effect on the glycosylation behavior of the enzyme was not studied.

Table 4.2 Effect of D-glucose concentration on the synthesis of guaiacyl-α-D-glucoside[a].

D-glucose (mmol)	% Yield
0.5	16
1.0	28
1.5	26
2.0	27
3.0	9

[a]Conversion yields from HPLC with respect to D-glucose concentration employed. Error in yield measurements ±5-10%. Guaiacol-0.027 mol, enzyme – 90 mg (16-100% w/w D-glucose), incubation period – 72 h, solvent-di-isopropyl ether, temperature – 68 °C. 0.06 mM (0.6 mL of 10 mM buffers added in 100 mL of solvent) of pH 7.0 phosphate buffer.

Thus the optimum condition for guaiacyl-α-D-glucoside synthesis was found to be 1: 50 equivalents of D-glucose and guaiacol, 50% (w/w D-glucose) of

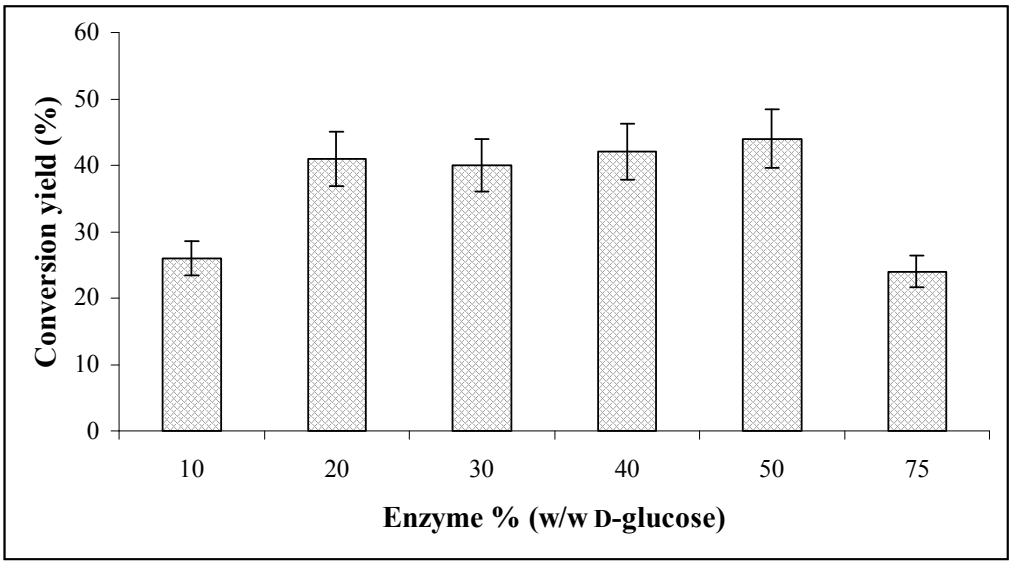

Fig. 4.2 Effect of amyloglucosidase concentration on guaiacyl-α-D-glucoside synthesis. Conversion yields were from HPLC with respect to 0.555 mmol of D-glucose. Reaction conditions: D-glucose – 0.555 mmol, guaiacol - 0.027 mol, 0.05 mM (0.5 mL of 10 mM buffer in 100 mL reaction mixture) pH 7.0 phosphate buffer, solvent-di-isopropyl ether, incubation-72 h, temperature - 68 °C.

amyloglucosidase, 0.06 mM (0.6 mL) pH 7.0 phosphate buffer and 72 h incubation period.

4.2.5 Synthesis of guaiacyl glucoside using β-glucosidase

Guaiacyl-D-glucoside was also synthesized by the reflux method using β-glucosidase isolated from sweet almonds. D-Glucose and guaiacol were taken in 1:50 molar ratio along with 50% (w/w D-glucose) enzyme and 0.06 mM (0.6 mL) pH 7.0 buffer in di-isopropyl ether solvent and refluxed for 72 h. The reaction mixture analyzed by HPLC showed 22% conversion with respect to the D-glucose concentration employed. The product guaiacol glucoside was isolated by column chromatography by using Sephadex G15 as column material and water as the eluent and subjected to spectral characterization by UV, IR, MS and 2D NMR (HSQCT). Two-dimensional NMR confirmed formation of guaiacyl-β-D-glucoside **22**.

4.2.6 Antioxidant activity

Antioxidant activity of guaiacol and guaiacyl-α-D-glucoside were tested to show that glucosylation of the phenolic OH did not affect the biological activities of these molecules. Antioxidant activity was evaluated by DPPH (2,2-diphenyl-1-picrylhydrazyl) radical scavenging method (Moon and Terao 1998). An antioxidant activity of 62% for guaiacyl-α-D-glucoside (89% for free guaiacol) was determined. Standard BHA activity was found to be 82%. Glucosylation thus lowered the antioxidant activity of guaiacol.

4.2.7 Synthesis of guaiacyl glycosides

Aldohexoses (D-galactose **3** and D-mannose **4**), ketohexose (D-fructose **5**), aldopentoses (D-arabinose **6** and D-ribose **7**), disaccharides (maltose **8**, sucrose **9** and lactose **10**) and carbohydrate alcohols (D-mannitol **11** and D-sorbitol **12**) were employed for the synthesis of guaiacyl glycosides under the optimum conditions obtained for guaiacyl-α-D-glucoside synthesis **(Scheme 4.1)**. The optimized reaction conditions

employed for the synthesis were carbohydrate and guaiacol in the 1:50 molar equivalent ratio, 50% (w/w carbohydrate) of amyloglucosidase, 0.06 mM (0.6 mL of 10 mM buffer in 100 mL solvent) pH 7.0 phosphate buffer and 72 h incubation period. The reaction mixtures were analyzed by HPLC D-Galactose reacted with guaiacol and gave the conversion yield of 17%. The retention times for D-galactose and guaiacyl-D-glalactoside were 5.2 min and 8.1 min respectively. Other carbohydrates did not undergo any glycosylation with guaiacol. Guaiacyl-D-glucoside and guaiacyl-D-glalactoside were isolated from the free sugars by passing through Sephadex G-15 column (100x1 cm) eluting with water at a flow rate of 2 mL/h.

Table 4.3 Guaiacyl glycosides with conversion yields and product proportions.

Glycosides and product proportions (%)[a]	**Glycosylation yield**[b] **%**
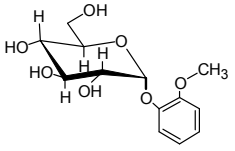 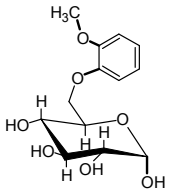 **21a**, guaiacyl-α-D-glucoside (52) **21b**, C6-O-guaiacyl D-glucose (48)	52
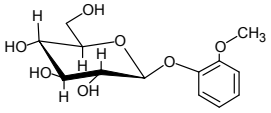 **22**, guaiacyl-β-D-glucoside [c]	22
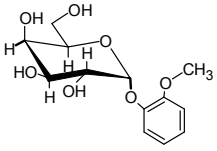 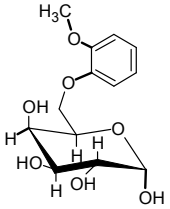 **23a**, guaiacyl-α-D-galactoside (95) **23b**, C6-O-guaiacyl D-galactose (5)	17

[a] Product proportions shown in brackets were determined from 2D-HSQCT NMR C1/C6 cross peak areas. [b] Conversion yields were from HPLC with errors in yield measurements ± 5-10%. [c]The compound was synthesized by using β-glucosidase from sweet almonds.

4.2.8 Spectral characterization

The glycosides were characterized by UV, IR, 2-D NMR (HSQCT) and optical rotation, which provided good information on the nature and proportions of the products

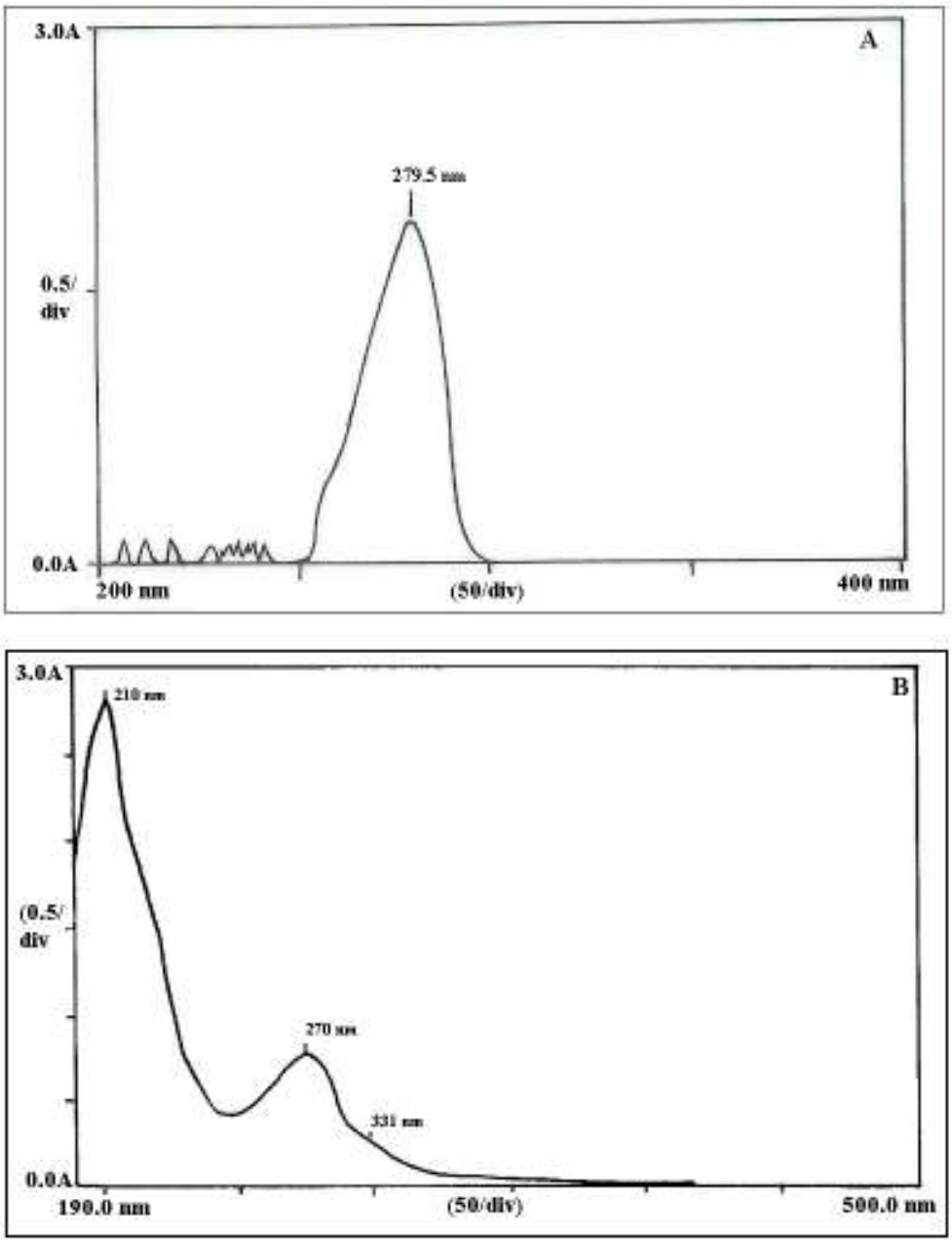

Fig. 4.3 Typical UV spectrum: **(A)** Guaiacol **17 (B)** Guaiacyl-α−D-glucoside **21a** and **b**.

formed. The structures of the glycosides synthesized, HPLC yield and product proportion are presented in Table 4.3. Only resolvable signals are shown. Some assignments are interchangeable. Guaiacol signals are primed. Since the synthesized glycosides are surfactants, they tend to aggregate in solution giving rise to broad signals. Hence coupling constant values could not be resolved satisfactorily.

Guaiacol, 17: Liquid; bp 205 °C; UV (DMSO, λ_{max}): 279.5 nm ($n\rightarrow\pi^*$, $\varepsilon_{279.5}$ - 2525 M^{-1}) Fig. 4.3A; IR: 3507 cm^{-1} (OH), 1597 cm^{-1} (aromatic C=C), 2959 cm^{-1} (alkyl CH), 3006 cm^{-1} (alkene CH) Fig 4.4A. ^{13}C NMR δ_{ppm} (125 MHz): 147.7 (C1′), 146.7 (C2′), 112.5 (C3′), 121.0 (C4′), 119.3 (C5′), 115.7 (C6′), 55.6 (OCH_3).

4.2.8.1 Guaiacyl-α-D-glucoside, 21a and **b:** Solid; UV (H_2O, λ_{max}): 210 nm ($\sigma\rightarrow\sigma^*$, ε_{210} - 398 M^{-1}), 270 nm ($n\rightarrow\pi^*$, ε_{270} – 69 M^{-1}), 331 nm ($n\rightarrow\pi^*$, ε_{331} - 178); IR (KBr): 1030 cm^{-1} (glycosidic aryl alkyl C-O-C symmetrical), 1236 cm^{-1} (glycosidic aryl alkyl C-O-C asymmetrical); $[\alpha]^{25}_D$ = +92.3° (*c* 1, H_2O); MS (*m/z*) - 286 $[M]^+$; 2D-HSQCT (DMSO-d_6) **guaiacyl-α-D-glucoside, 21a**: ^1H NMR δ_{ppm} (500.13 MHz): 4.65 (H-1α), 3.3 (H-2α), 3.72 (H-3α), 3.75 (H-4α), 3.10 (H-5α), 3.43 (H-6a), 7.08 (H-6′), 6.98 (H-5′), 6.94 (H-4′), 7.09 (H-3′); ^{13}C NMR δ_{ppm} (125 MHz): 98.7 (C1α), 74.9 (C2α), 72.0(C3α), 70.1 (C4α), 74.9 (C5α), 60.9 (C6α), 113.4 (C6′), 118.5 (C5′), 121.9 (C4′), 110.5 (C3′). **C6-O-guaiacyl-D-glucose, 21b**: ^1H NMR δ_{ppm}: 4.97 (H-1α), 3.06 (H-2α), 3.16 (H-3α), 3.63 (H-4α), 3.14 (H-5α), 3.60 (H-6a), 6.80 (H-5′), 6.84 (H-4′), 6.88 (H-3′); ^{13}C NMR δ_{ppm} 100.0 (C1α), 74.9 (C2α), 74.0(C3α), 70.2 (C4α), 74.0 (C5α), 67.0 (C6α), 119.0(C5′), 121.7 (C4′), 110.0 (C3′).

4.2.8.2 Guaiacyl-β-D-glucoside, 22: Solid; mp 121 °C; UV (H_2O, λ_{max}): 206 nm ($\sigma\rightarrow\sigma^*$, ε_{206} - 1628 M^{-1}), 274 nm ($n\rightarrow\pi^*$, ε_{274} – 409 M^{-1}). IR (KBr): 1031 cm^{-1} (glycosidic aryl alkyl C-O-C symmetrical), 1250 cm^{-1} (glycosidic aryl alkyl C-O-C

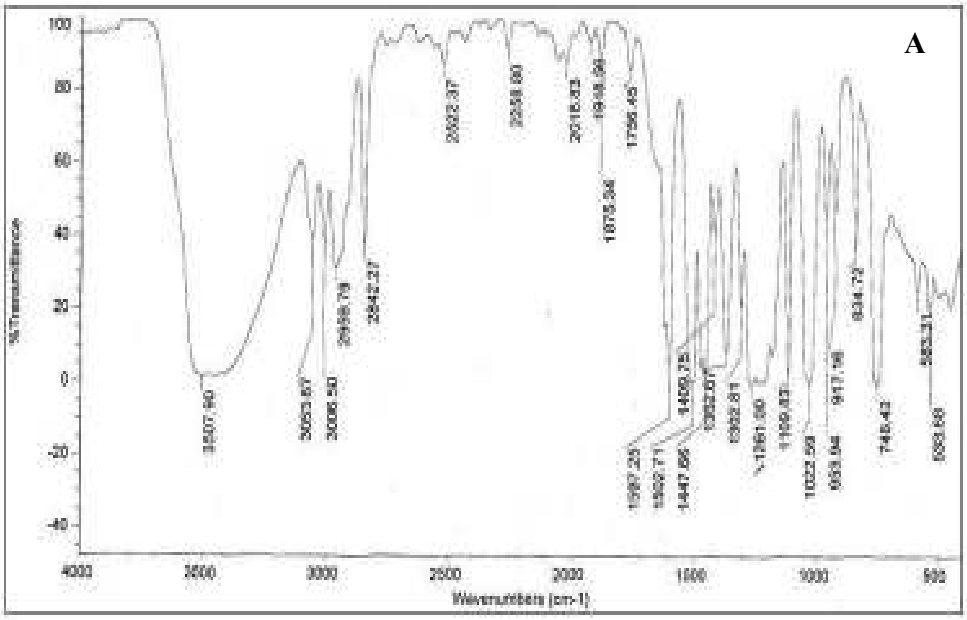

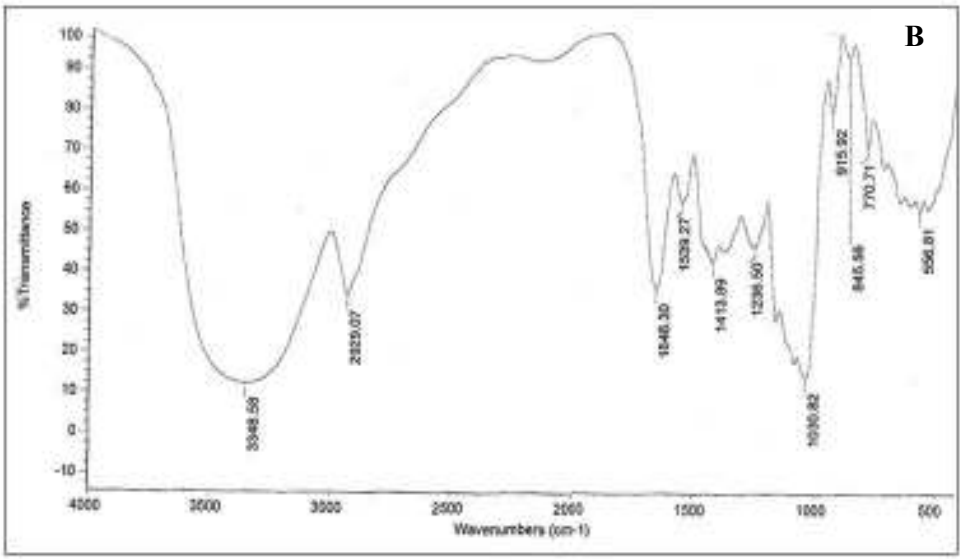

Fig. 4.4 Typical IR spectrum: **(A)** Guaiacol **17** **(B)** Guaiacyl-α-D-glucoside **21a** and **b**.

asymmetrical), 2935 cm^{-1} (alkene CH), 3324 cm^{-1}(OH); $[\alpha]^{25}_D$ = -12.1° (*c* 1, H_2O); MS (*m/z*) - 286 $[M]^+$; 2D-HSQCT (DMSO-d_6) ^1H NMR δ_{ppm} (500.13 MHz): 4.18 (H-1β), 2.97 (H-2β), 3.28 (H-3β), 3.73 (H-4β), 3.45 (H-6a), 3.82 (OCH_3), 7.09 (H-6′), 7.0 (H-5′), 6.96 (H-4′), 7.10 (H-3′); ^{13}C NMR δ_{ppm} (125 MHz): 103.3 (C1β), 73.5 (C2β), 76.0 (C3β), 70.5 (C4β), 61.0 (C6β), 56.0 (OCH_3), 113.5 (C6′), 118.5 (C5′), 121.3 (C4′), 110.0 (C3′).

4.2.8.3 Guaiacyl-α-D-galactoside, 23a and **b**: Solid; UV (H_2O, λ_{max}): 201 nm (σ→σ*, ε_{201} - 1360 M^{-1}), 282 nm (n→π*, ε_{282} – 297 M^{-1}), 331 nm (n→π*, ε_{331} - 184), IR (KBr): 1043 cm^{-1} (glycosidic aryl alkyl C-O-C symmetrical), 1599 cm^{-1} (C=C), 3290 cm^{-1} (OH); $[\alpha]^{25}_D$ = +22.1°(*c* 1, H_2O); MS (*m/z*) - 286 $[M]^+$; 2D-HSQCT (DMSO-d_6) **guaiacyl-α-D-galactoside, 23a:** ^1H NMR δ_{ppm}: (500.13 MHz): 4.97 (H-1α), 3.52 (H-2α), 3.92 (H-4α), 3.46 (H-5α), 3.36 (H-6a). 3.73 (OCH_3), 6.78 (H-6′), 6.74 (H-5′), 6.76 (H-4′), 6.91 (H-3′); ^{13}C NMR δ_{ppm} (125 MHz): 95.2 (C1α), 69.9 (C2α), 74.0 (C4α), 71.0 (C5α), 63.0 (C6α), 55.8 (OCH_3) 115.0 (C6′), 118.8 (C5′), 121.0 (C4′), 112.5 (C3′). **C6-O-guaiacyl-D-galactose, 23b:** ^1H NMR δ_{ppm}: 4.91 (H-1α), 3.70 (H-6a), 3.81 (OCH_3), 6.99 (H-5′), 6.95 (H-4′), 7.12 (H-3′); ^{13}C NMR δ_{ppm}: 92.5 (C1α), 67.0 (C6α), 56.0 (OCH_3), 119.0(C5′), 121.2 (C4′), 111.0 (C3′).

UV spectrum of guaiacyl-α-D-glucoside (Fig. 4.3B) showed σ→σ* band at 210 nm and n→π* band at 270 nm (free guaiacol 279.5 nm). The hypsochromic shift observed for the glycoside indicated that guaiacol had undergone glycosylation. IR spectral band at 1030 cm^{-1} corresponded to glycosidic aryl alkyl C-O-C symmetrical stretching and 1236 cm^{-1} to glycosidic aryl alkyl C-O-C asymmetrical stretching frequencies (Fig.4.4 B). NMR spectral data confirmed that guaiacol formed C1α-glucoside **21a** and C6-O-arylated **21b** product with **17**. Chemical shift values for C1α

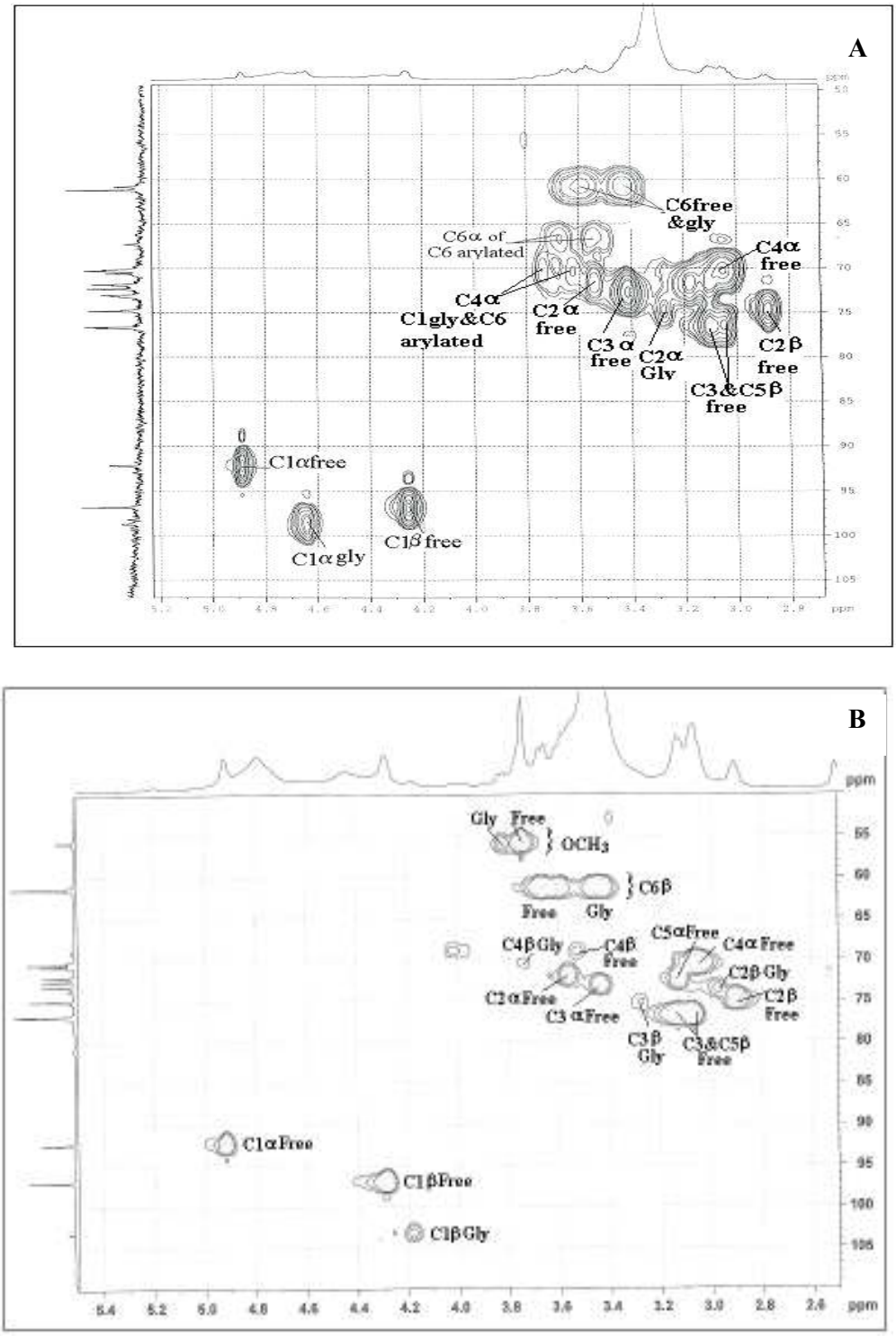

Fig. 4.5 (A) 2D-HSQCT spectrum (C1-C6 region) of guaiacyl-α-D-glucoside **21a** and **b** reaction mixture, using amyloglucosidase. **(B)** 2D-HSQCT spectrum (C1-C6 region) of guaiacyl-β-D-glucoside **22** reaction mixture, using β-glucosidase from sweet almonds. Some of the assignments are interchangeable.

(^{13}C at 98.7 ppm and ^{1}H at 4.65 ppm) and C6' at 113.4 ppm for the glucoside (115.6 ppm for free guaiacol) indicated that the phenolic OH of guaiacol was glucosylated at the C1 carbon of the α-D-glucose anomer (Fig. 4.5A). Chemical shift values of C6-O- at 67.3 ppm (^{1}H at 3.56 and 3.69 ppm) clearly indicated that the C6-O-arylated product was also formed. Mass spectrum for guaiacyl-α−D-glucoside showed *m/z* peak at 286 $[M]^{+}$ supporting the NMR data for the mono glycoside formation.

UV spectrum of guaiacyl-β-D-glucoside **22** showed σ→σ* band at 206 nm and n→π* at 274 nm. The IR spectral band at 1031 cm^{-1} corresponded to the glycosidic aryl alkyl C-O-C symmetrical stretching and at 1250 cm^{-1} for aryl alkyl C-O-C asymmetrical stretching. Two dimensional HSQCT confirmed that the product is guaiacyl-β-D-glucoside **22**. The down field chemical shift for C1β at 103.3 ppm (^{1}H at 4.18 ppm) indicating the formation of only C1β glucoside (Fig. 4.5B).

For guaiacyl-α-D-galactoside, UV spectrum showed σ→σ* band at 201 nm and n→π* band at 282 nm. IR glycosidic aryl alkyl C-O-C symmetrical stretching frequency was observed at 1043 cm^{-1}. Down field chemical shift of C1α signal at 95.2 ppm (^{1}H at 4.97 ppm) indicated that a C1 glycosylated **23a** product was formed with galactose and C6-O- signal at 67.0 ppm (^{1}H at 3.70 ppm) indicated C6-O-arylated product **23b** (Fig. 4.6A). Mass spectrum showed *m/z* peak at 286 $[M]^{+}$ supporting the NMR data for the mono galactoside formation (Fig. 4.6B).

4.3 Eugenyl glycosides

Eugenyl glycosides were synthesized using amyloglucosidase. Eugenyl maltoside synthesis in di-isopropyl ether using amyloglucosidase was optimized in terms of incubation period, pH, buffer concentration and enzyme concentration. The reaction conditions employed were maltose (1.0 mmol), eugenol (10 mmol), 10-80% (w/w

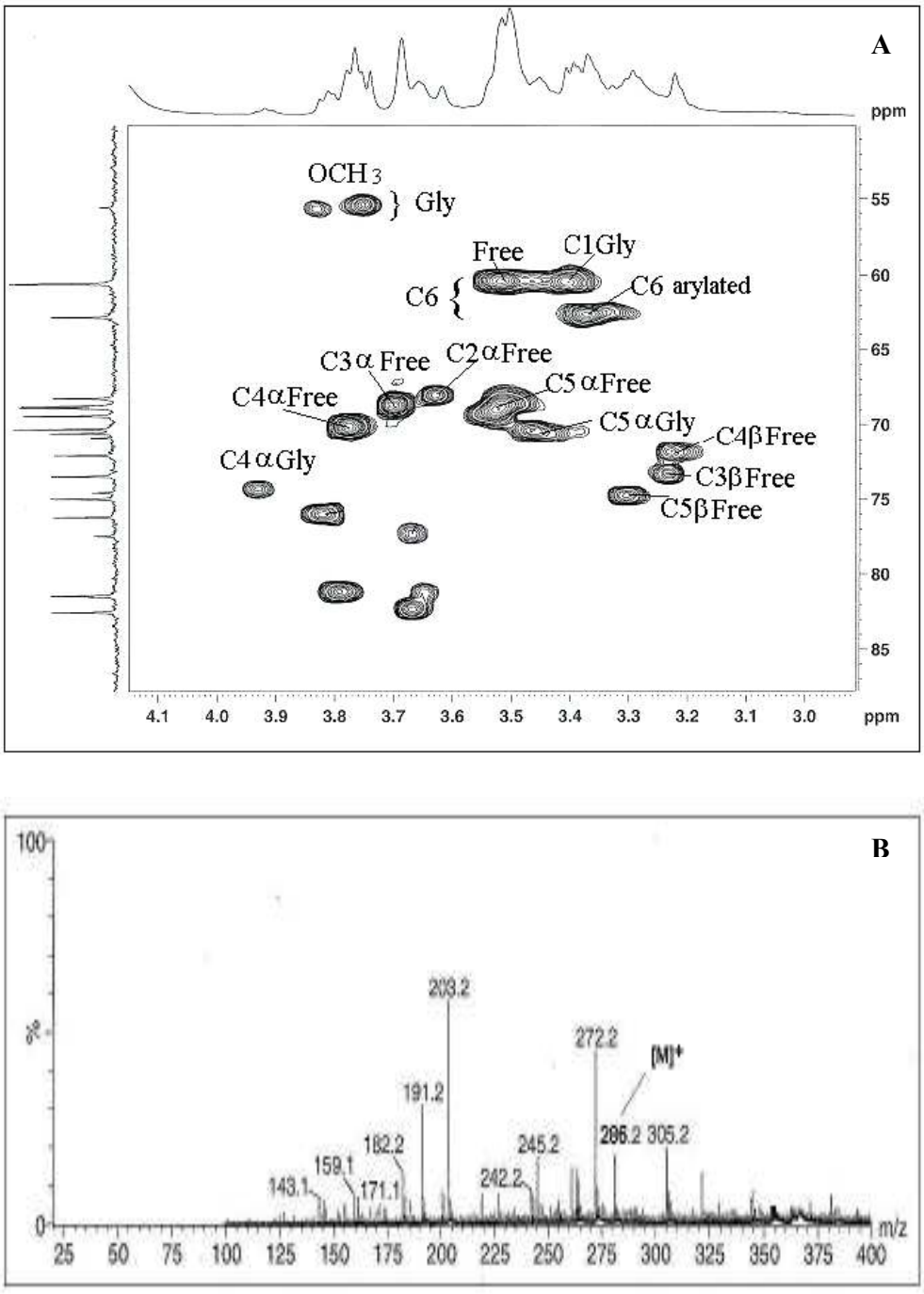

Fig. 4.6 Guaiacyl-α-D-galactoside **23a** and **b (A)** 2D HSQCT spectrum. Some assignments are interchangeable **(B)** Mass spectrum for the same compound.

maltose) amyloglucosidase, 0.04-0.2 mM, pH 4.0-8.0 buffer (0.4-2.0 mL of 0.01 M buffer in 100 mL of reaction mixture), 100 mL di-isopropyl ether solvent and 3 to 96h incubation period **(Scheme 4.2)**. The reaction mixture was monitored by HPLC. Retention times from HPLC are 7.4 min for maltose and 11.3 min for eugenyl maltoside. Conversion yields were determined from the HPLC peak areas of the glycoside and unreacted carbohydrate and expressed as percentage with respect to the free carbohydrate concentration employed. Errors in the HPLC measurements were in the order of ± 5-10%. The product glycosides were isolated by column chromatography by passing through Sephadex G-15 using water as eluent. Although glycosides were separated from the unreacted carbohydrates, individual glycosides could not be separated by this chromatographic procedure due to similar polarity of these molecules. Spectral characterization was carried out by UV, IR, MS and 2-D NMR spectroscopy for the isolated glycosides.

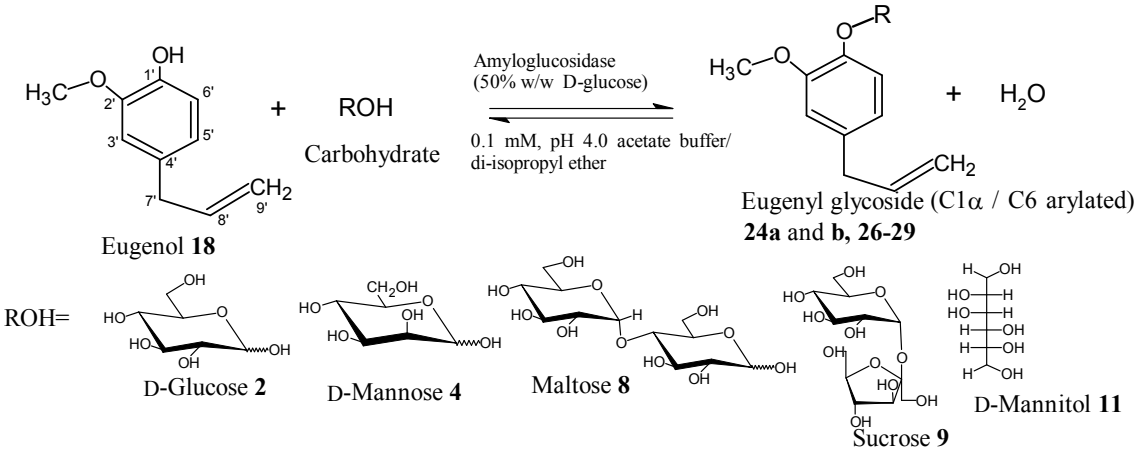

Scheme 4.2 Amyloglucosidase catalyzed synthesis of eugenyl glycosides

4.3.1 Eugenyl maltoside

Amyloglucosidase catalyzed synthesis of eugenyl maltoside was optimized in terms of incubation period, pH, buffer concentration and enzyme concentration as a proto type reaction for detailed investigation.

4.3.2 Effect of incubation period on eugenyl maltoside synthesis

Eugenyl maltoside was synthesized by employing 1:10 equivalents of maltose and eugenol, 40% (w/w maltose) amyloglucosidase and 0.1 mM (1.0 mL), pH 5.0 acetate buffer. Incubation period was varied from 3 h to 96 h (Fig 4.7A). The glycosylation yield increases with the increase in incubation period from 3 h (7% yield) to 72 h (39% yield) and was the highest at 72 h. Conversion yields at other incubation periods are 17% (6 h), 24% (12 h), 28% (24 h) and 33% (48 h). Rate of the reaction from the initial slope was found to be 19.2 μmol/h.

4.3.3 Effect of buffer pH on eugenyl maltoside synthesis

Buffers of different pH ranging from 4.0 to 8.0 and concentration 0.1 mM (1.0 mL of 10 mM buffer added in 100 mL of solvent) were employed (Table 4.4). Maximum glycosylation (39% yield) occurred at pH 5.0 acetate buffer. Between pH 6.0 to 8.0 the glycosylation conversion yields were almost constant (Table 4.4).

Table 4.4 Effect of buffer pH on the synthesis of eugenyl maltoside[a].

pH[b]	Yield %
4.0	32
5.0	39
6.0	23
7.0	25
8.0	25

[a]Conversion yields from HPLC with respect to 1 mmol of maltose. Error in yield measurements ± 5-10%. Maltose - 1.0 mmol, eugenol - 10 mmol, enzyme – 40% (w/w maltose), incubation – 72 h, temperature – 68 °C. [b]0.1 mM (1.0 mL of 10 mM buffer added in 100 mL of reaction mixture).

4.3.4 Effect of buffer concentration on eugenyl maltoside synthesis

At pH 5.0, the range of buffer concentration employed for the study was 0.04 to 0.2 mM (0.4 to 2.0 mL of 10 mM acetate buffer). Conversion yield increased from 14% for 0.04 mM (0.4 mL) to 39% for 0.1 mM (1.0 mL) with the increase in buffer

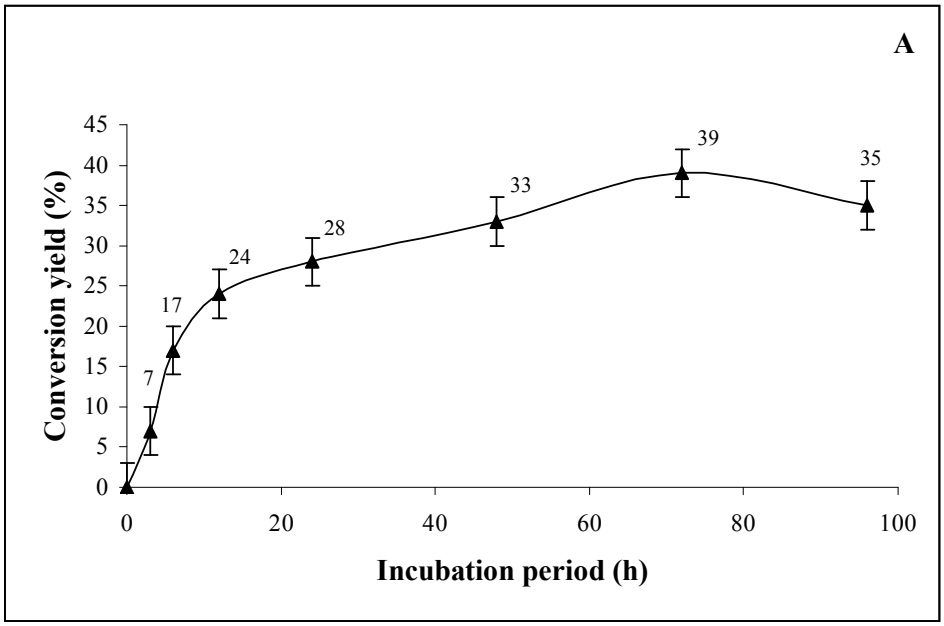

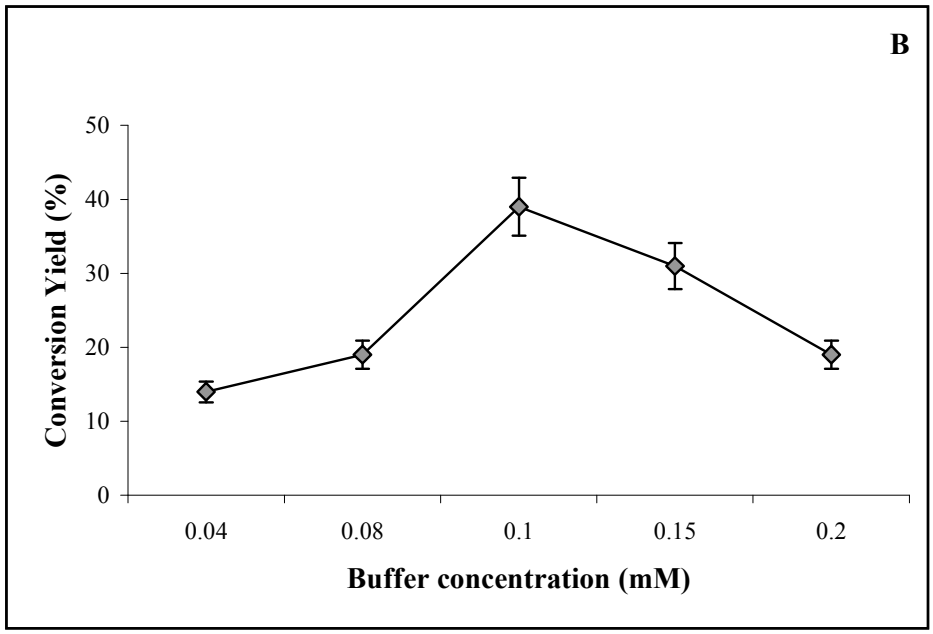

Fig. 4.7 Eugenyl maltoside synthesis. Conversion yields were from HPLC with respect to 1 mmol of maltose. **(A)** Effect of incubation period. Reaction conditions: maltose – 1 mmol, eugenol – 10 mmol, enzyme – 40% (w/w maltose), 0.1 mM (1.0 mL), pH 5.0 acetate buffer. **(B)** Effect of buffer concentration. Reaction conditions: maltose – 1 mmol, eugenol – 10 mmol, enzyme – 40% (w/w maltose), buffer-0.4-2.0 mL of 10 mM, pH 5.0 acetate buffer in 100 mL reaction mixture, solvent-di-isopropyl ether, incubation-72 h.

concentration (Fig 4.7B). Thereafter at above 0.1 mM concentration conversion yield get decreased (Fig 4.7B).

4.3.5 Effect of amyloglucosidase concentration on eugenyl maltoside synthesis

Between 10 to 80% (w/w maltose) of enzyme concentration, 40% enzyme was found to be the best (conversion yield of 39%) and all other enzyme concentrations gave very less conversion yields (less than 19%). Lower conversions were obtained at 10%, 20%, 60% and 80% enzyme concentration (Table 4.5). Only at intermediatory enzyme concentrations the yield was good.

Table 4.5 Effect of amyloglucosidase concentration on the synthesis of eugenyl maltoside[a].

Amyloglucosidase (w/w maltose)	Yield, %
10	17
20	19
40	39
60	15
80	11

[a] Conversion yields from HPLC with respect to 1 mmol of maltose concentration. Error in yield measurements ±5-10%. Maltose - 1.0 mmol, eugenol - 10 mmol, buffer-0.1 mM (1.0 mL of 10 mM buffers added in 100 mL of solvent) of pH 5.0 acetate buffer, incubation period – 72 h, solvent-di-isopropyl ether, temperature – 68 °C.

Thus the optimum conditions for this reaction was found to be maltose and eugenol in 1: 10 equivalent ratio, 40% (w/w maltose) amyloglucosidase, 0.1 mM (1.0 mL), pH 5.0 acetate buffer and 72 h incubation period.

4.3.6 Synthesis of eugenyl glucoside using β-glucosidase

β-Glucosidase isolated from sweet almond employed for the synthesis of eugenol glucoside in di-isopropyl ether solvent gave 19% conversion (from HPLC). The reaction conditions employed were D-glucose-1 mmol, eugenol-10 mmol, 0.1 mM (1.0 mL) pH 5.0 acetate buffer, 40% enzyme (w/w D-glucose) and 72 h incubation period. The glucoside was isolated by column chromatography by using Sephadex G15 as column

material and water as eluent. Spectral characterization (UV, IR, MS and 2D HSQCT) was done for the isolated eugenyl glucoside. Two-dimensional NMR (HSQCT) confirmed formation of eugenyl-β-D-glucoside **25**.

4.3.7 Synthesis of eugenyl glycosides

Eugenyl glycosides of carbohydrates **2-12** were synthesized in di-isopropyl ether solvent. The reaction conditions employed were carbohydrate and eugenol in 1:10 molar ratio, 50% (w/w carbohydrate) amyloglucosidase, 0.1 mM (1.0 mL) pH 4.0 acetate buffer and incubation period 72 h **(Scheme 4.2)**. Extent of glycosylation was analyzed by HPLC and the retention times for the carbohydrates and glycosides are: D-glucose-5.20 min, eugenyl-D-glucoside-7.47 min, D-mannose-4.9 min, eugenyl-D-mannoside-5.87 min, sucrose-6.4 min, eugenyl sucrose-8.02 min, D-mannitol-5.3 min and eugenyl-D-mannitol-7.12 min. From HPLC results it was confirmed that, D-galactose **3**, D-fructose **5**, D-arabinose **6**, D-ribose **7**, lactose **10** and D-sorbitol **12** did not undergo glycosylation with eugenol.

Table 4.6 Eugenyl glycosides with conversion yields and product proportions.

Glycosides and product proportions (%)[a]	**Glycosylation yield[b] %**
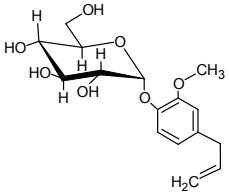 **24a**, eugenyl-α-D-glucoside (53) 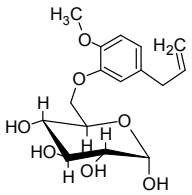 **24b**, C6-O-eugenyl D-glucose (47)	32
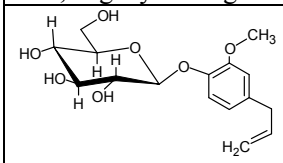 **25**, eugenyl-β-D-glucoside [c]	19

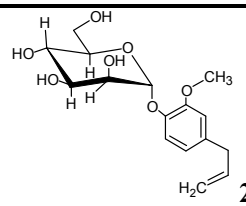 **26**, eugenyl-α-D-mannoside	8
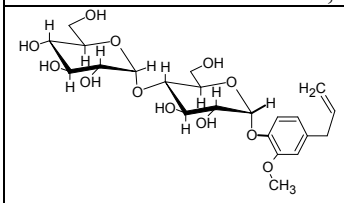 **27a**, eugenyl maltoside (52) 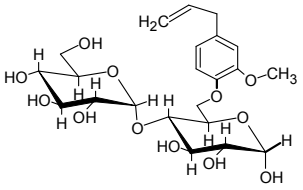 **27b**, C6-O-eugenyl maltose (28) 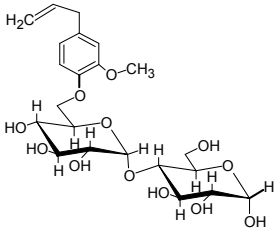 **27c**, C6″-O-eugenyl maltose (20)	17
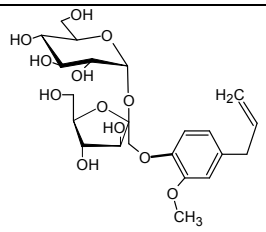 **28a**, C1-O-eugenyl sucrose (35) 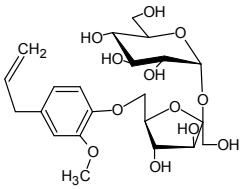 **28b**, C6-O-eugenyl sucrose (45) 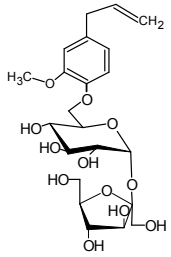 **28c**, C6″-O- eugenyl sucrose (20)	7
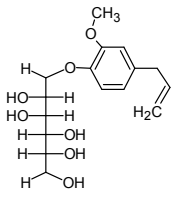 **29**, C1-O-eugenyl mannitol	7

[a] Product proportions determined from 2D-HSQCT NMR C1/C6 cross peak areas are shown in brackets; [b] Conversion yields were from HPLC with errors in yield measurements ± 5-10%. [c] The compound was synthesized by using β-glucosidase from sweet almonds.

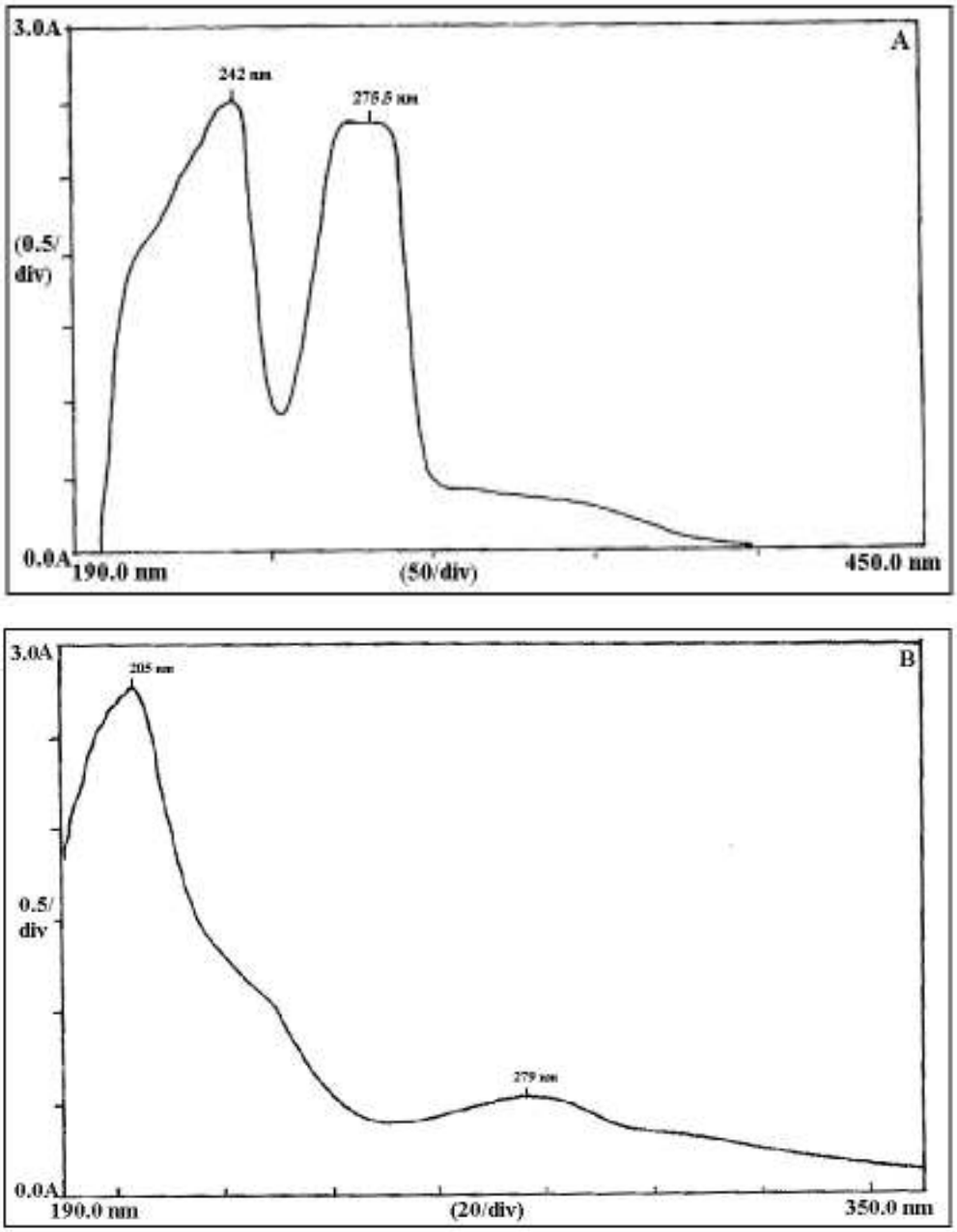

Fig 4.8 Typical UV spectrum: **(A)** Eugenol **18** **(B)** Eugenyl-α-D-glucoside **24a** and **b**.

4.3.8 Spectral characterization

Isolated glycosides were subjected to detailed UV, IR, MS and 2D NMR (HSQCT) spectroscopic investigation. Only resolvable signals are shown. Some assignments are interchangeable. Eugenol signals are primed, non-reducing end glucose signals in maltose and sucrose are double primed. Structures of the glycosides formed, HPLC yield and product proportions are presented in the Table 4.6. Since the synthesized eugenyl glycosides are surfactants, they tend to aggregate in solution giving rise to broad signals. Hence coupling constant values could not be resolved satisfactorily.

Eugenol: Liquid; bp 254°C; UV (DMSO, λ_{max}): 242 nm ($\pi\rightarrow\pi^*$, ε_{242} - 897 M^{-1}), 275.5nm ($n\rightarrow\pi^*$, $\varepsilon_{275.5}$ - 894 M^{-1}) Fig. 4.8A. IR (stretching frequency): 1638 cm^{-1} (allylic C=C), 1612 cm^{-1} (aromatic C=C), 3514 cm^{-1} (OH). ^{13}C NMR δ_{ppm} (125 MHz): 55.8 (OCH_3), 145.5 (C1′), 145.2 (C2′), 112.7 (C3′), 121.3 (C5′), 115.0 (C6′), 39.3 (C7′), 137.3 (C8′), 115.6 (C9′).

4.3.8.1 Eugenyl-α-D-glucoside, 24a and **b:** Solid; UV (H_2O, λ_{max}): 205 nm ($\sigma\rightarrow\sigma^*$, ε_{205} - 1792 M^{-1}), 279 nm ($n\rightarrow\pi^*$, ε_{279} - 396 M^{-1}) Fig. 4.8B; IR (KBr): 1653 cm^{-1} (allylic C=C), 1033 cm^{-1} (glycosidic aryl alkyl C-O-C symmetrical), 1268 cm^{-1}, (glycosidic aryl alkyl C-O-C asymmetrical), 3330 cm^{-1} (OH). $[\alpha]_D^{25}$ = +59.6° (*c* 1, H_2O). MS (*m/z*) - 347 $[M-2+Na]^+$ (Fig. 4.9B). 2D-HSQCT (DMSO-d_6) **eugenyl-α-D-glucoside, 24a:** ^1H NMR δ_{ppm} (500.13 MHz): 4.65 (H-1α), 3.55 (H-2α), 3.28 (H-3α), 3.73 (H-4α), 3.42 (H-6a). 6.86 (1H, s, H-3′), 6.70 (1H, d, H-5′), 6.85 (1H, d, H-6′), 3.28 (H-7′), 5.92 (1H, m, H-8′), 5.10 (H-9′), 3.40 (OCH_3); ^{13}C NMR δ_{ppm} (125 MHz): 97.0 (C1α), 72.5 (C2α), 74.0 (C3α), 69.0 (C4α), 61.0 (C6α), 52.0 (OCH_3),113 (C3′), 120(C5′), 115.3(C6′), 39.0 (C7′), 137.0 (C8′), 116.0 (C9′). **C6-O-eugenyl D-glucose, 24b:** ^1H NMR δ_{ppm}: 3.6 (H-

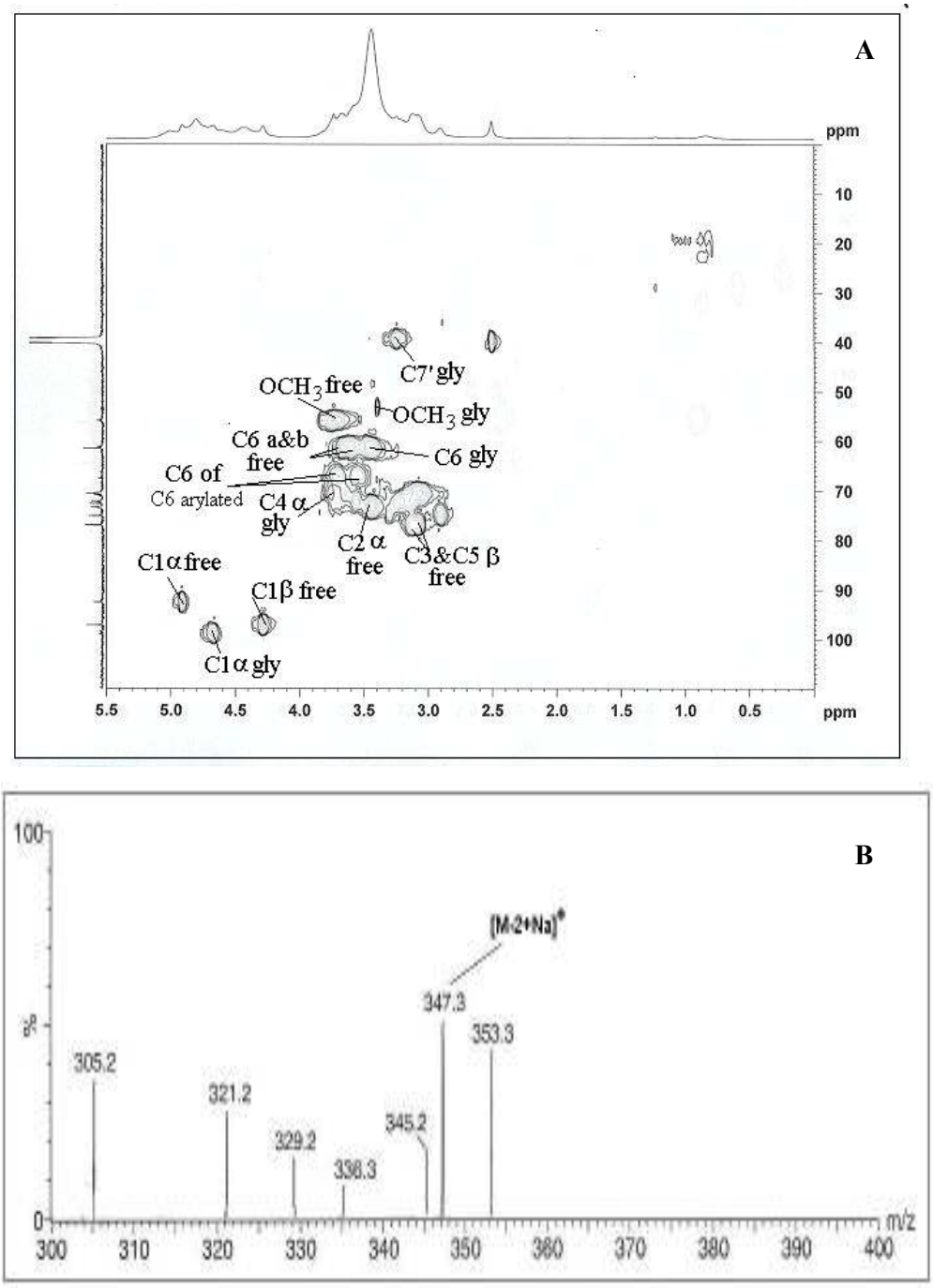

Fig. 4.9 Eugenyl-α-D-glucoside **24a** and **b (A)** 2D HSQCT spectrum (C1-C6 region) of reaction mixture using amyloglucosidase. Some assignments are interchangeable; assignments are based on Sato *at al.* (2003). This applies to subsequent 2D NMR spectra also **(B)** Mass spectrum of **24a** and **b**.

2α), 3.50 and 3.68 (H-6 a & b), 6.90 (1H, s, H-3′), 6.78 (1H, d, H-5′); ^{13}C NMR δ_{ppm}: 69.0 (C2α), 66.0 (C6α), 52.0 (OCH_3), 112 (C3′), 119 (C5′).

4.3.8.2 Eugenyl-β-D-glucoside, 25: Solid; mp 124 °C; UV (H_2O, λ_{max}): 204 nm ($\sigma\rightarrow\sigma^*$, ε_{204} - 1852 M^{-1}), 238 nm ($\pi\rightarrow\pi^*$, ε_{238} - 759 M^{-1}), 280 nm ($n\rightarrow\pi^*$, ε_{280} - 814 M^{-1}); IR (KBr): 1660 cm^{-1} (allylic C=C), 1033 cm^{-1} (glycosidic aryl alkyl C-O-C symmetrical), 1269 cm^{-1}, (glycosidic aryl alkyl C-O-C asymmetrical), 3352 cm^{-1} (OH) (Fig. 4.11A). $[\alpha]_D^{25}$ = -46.9° (*c* 1, H_2O); MS (*m/z*)- 326 $[M]^+$; 2D-HSQCT (DMSO-d_6) ^{1}H NMR δ_{ppm} (500.13 MHz): 4.19 (H-1β), 3.3 (H-2β), 3.10 (H-3β), 3.73 (H-4β), 3.43 (H-6a), 3.43 (OCH_3)6.73 (1H, 6, H-3′), 6.56 (1H, d, H-5′), 6.69 (1H, d, H-6′), 3.23 (H-7′), 5.92 (1H, m, H-8′), 5.10 (H-9′); ^{13}C NMR δ_{ppm} (125 MHz): 103.3 (C1β), 76.2 (C2β), 78.5 (C3β), 70.2 (C4β), 61.5 (C6β), 56.0 (OCH_3), 147.6 (C1′), 112.8 (C3′), 131.0 (C4′), 121.0 (C5′), 116.0 (C6′), 39.0 (C7′), 138.5 (C8′), 115.5 (C9′).

4.3.8.3 Eugenyl-α-D-mannoside, 26: Solid; mp 119°C; UV (H_2O, λ_{max}): 206 nm ($\sigma\rightarrow\sigma^*$, ε_{206} - 1672 M^{-1}), 276 nm ($n\rightarrow\pi^*$, ε_{276} - 440 M^{-1}), 317 nm ($n\rightarrow\pi^*$, ε_{317} -267 M^{-1}). IR (KBr): 1657 cm^{-1} (allylic C=C), 1066 cm^{-1} (glycosidic aryl alkyl C-O-C symmetrical), 1266 cm^{-1}, (glycosidic aryl alkyl C-O-C asymmetrical), 3334 cm^{-1} (OH) (Fig. 4.11B); $[\alpha]^{25}_D$ = -8.9° (*c* 1, H_2O); MS (*m/z*) - 347 $[M-2+Na]^+$; 2D-HSQCT (DMSO-d_6) ^{1}H NMR δ_{ppm} (500.13 MHz): 4.92 (H-1α), 3.50 (H-3α), 3.51 (H-4α), 3.36 (H-5α), 3.62 (H-6a). 6.70 (1H, s, H-3′), 6.58 (1H, d, H-5′), 6.68 (1H, d, H-6′), 3.23 (H-7′), 5.92 (1H, m, H-8′), 5.02 (H-9′), 3.72 (OCH_3); ^{13}C NMR δ_{ppm} (125 MHz): 101.5 (C1α), 72.0 (C2α), 73.0 (C3α), 68.0 (C4α), 73.2 (C5α), 61.5 (C6α), 55.5 (OCH_3), 144.5 (C1′), 151.0 (C2′), 113 (C3′), 130.0 (C4′), 120.2 (C5′), 116.0 (C6′), 39.0 (C7′), 138.0 (C8′), 115.2 (C9′).

4.3.8.4 Eugenyl maltoside, 27a-c: Solid; UV (H_2O, λ_{max}): 199 nm ($\sigma\rightarrow\sigma^*$, ε_{199} - 3337 M^{-1}), 265 nm ($\pi\rightarrow\pi^*$, ε_{265} - 611 M^{-1}). IR (KBr): 1676 cm^{-1} (allylic C=C), 1022 cm^{-1}

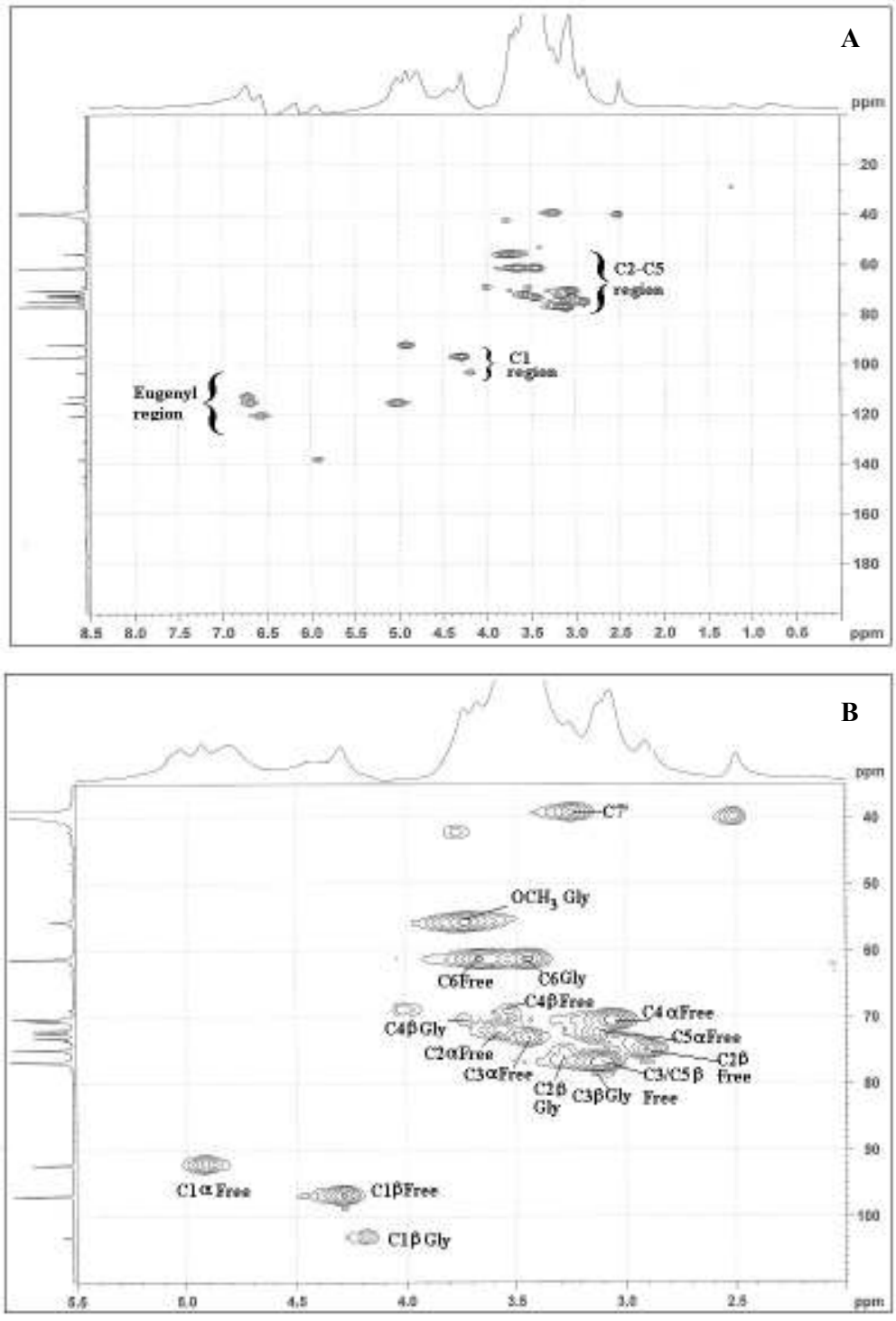

Fig. 4.10 Typical 2D-HSQCT spectrum of eugenyl-β-D-glucoside **25** reaction mixture, using β-glucosidase from sweet almonds. Some of the assignments are interchangeable. NMR assignments are based on Orihara *etal.* (1992) **(A)** Full spectrum **(B)** C1-C6 region.

(glycosidic aryl alkyl C-O-C symmetrical). $[\alpha]^{25}_{D}$ = +55.9^{o} (*c* 1, H_2O); MS (*m/z*)- 510 $[M-1+Na]^{+}$; 2D-HSQCT (DMSO-*d*$_6$) **eugenyl maltoside, 27a:** ^{1}H NMR δ_{ppm} (500.13 MHz) 4.62 (H-1α), 3.28 (H-2α), 3.48 (H-6a). 4.95 (H-1″α), 3.00 (H-2″), 3.12 (H-3″), 3.03 (H-4″), 3.68 (H-6″a), 6.66 (1H, s, H-3′), 6.55 (1H, d, H-5′), 6.68 (1H, d, H-6′), 3.24 (H-7′), 5.90 (1H, m, H-8′), 5.02 (H-9′), 3.74 (OCH_3); ^{13}C NMR δ_{ppm} (125 MHz): 98.5 (C1α), 75.0 (C2α), 61.0 (C6α), 100.2 (C1″α), 73.0 (C2″), 72.0 (C3″), 71.0 (C4″), 61.0 (C6″), 55.2 (OCH_3), 144.3 (C1′), 151.1 (C2′), 113.0 (C3′), 121.0 (C5′), 39.0 (C7′), 138.2 (C8′), 116.0 (C9′). **C6-O-eugenyl maltose, 27b**: ^{1}H NMR δ_{ppm}: 4.90 (H-1α), 3.68 (H-6a). 4.95 (H-1″α), 3.32 (H-4″), 3.67 (H-6″a), 6.66 (1H, s, H-3′), 6.55 (1H, d, H-5′), 6.68 (1H, d, H-6′), 3.24 (H-7′), 5.90 (1H, m, H-8′), 5.02 (H-9′), 3.74 (OCH_3); ^{13}C NMR δ_{ppm}: 91.8 (C1α), 67.0 (C6α), 100.2 (C1″α), 70.2 (C4″), 61.0 (C6″), 55.2 (OCH_3), 144.3 (C1′), 151.1 (C2′), 113.0 (C3′), 121.0 (C5′), 39.0 (C7′), 138.2 (C8′), 116.0 (C9′). **C6″-O-eugenyl maltose, 27c:** ^{1}H NMR δ_{ppm}: 4.90 (H-1α), 3.63 (H-6a). 3.54 (H-6″a), 6.66 (1H, s, H-3′), 6.55 (1H, d, H-5′), 6.68 (1H, d, H-6′), 3.24 (H-7′), 5.90 (1H, m, H-8′), 5.02 (H-9′), 3.74 (OCH_3); ^{13}C NMR δ_{ppm}: 91.8 (C1α), 61.0 (C6α), 67.1 (C6″), 55.2 (OCH_3), 144.3 (C1′), 151.1 (C2′), 113.0 (C3′), 121.0 (C5′), 39.0 (C7′), 138.2 (C8′), 116.0 (C9′).

4.3.8.5 Eugenyl sucrose, 28a-c: UV (H_2O, λ_{max}): Solid; 198 nm ($\sigma\rightarrow\sigma^*$, ε_{198} - 3426 M^{-1}), 268 nm ($\pi\rightarrow\pi^*$,ε_{268} - 685 M^{-1}). IR (KBr): 1596 cm^{-1} (aromatic C=C), 1054 cm^{-1} (glycosidic aryl alkyl C-O-C symmetrical), 1268 cm^{-1} (glycosidic aryl alkyl C-O-C asymmetrical), 3278 cm^{-1} (OH); $[\alpha]^{25}_{D}$ = +3.0^{o} (*c* 1, H_2O); MS (*m/z*) - 511 $[M+Na]^{+}$. 2D-HSQCT (DMSO-*d*$_6$) **C1-O-eugenyl sucrose, 28a:** ^{1}H NMR δ_{ppm} (500.13 MHz) 3.77 (H-1a), 3.74 (H-4), 3.79 (H-5) 3.41 (H-6a). 5.15 (H-1″α), 3.72 (H-2″), 3.11 (H-3″), 3.05 (H-4″), 3.47 (H-5″), 3.63 (H-6″a); 6.71 (1H, s, H-3′), 6.55 (1H, d, H-5′), 6.67 (1H, d, H-6′), 3.26 (H-7′), 5.91 (1H, m, H-8′), 5.0 (H-9′), 3.73 (OCH_3); ^{13}C NMR δ_{ppm} (125 MHz):

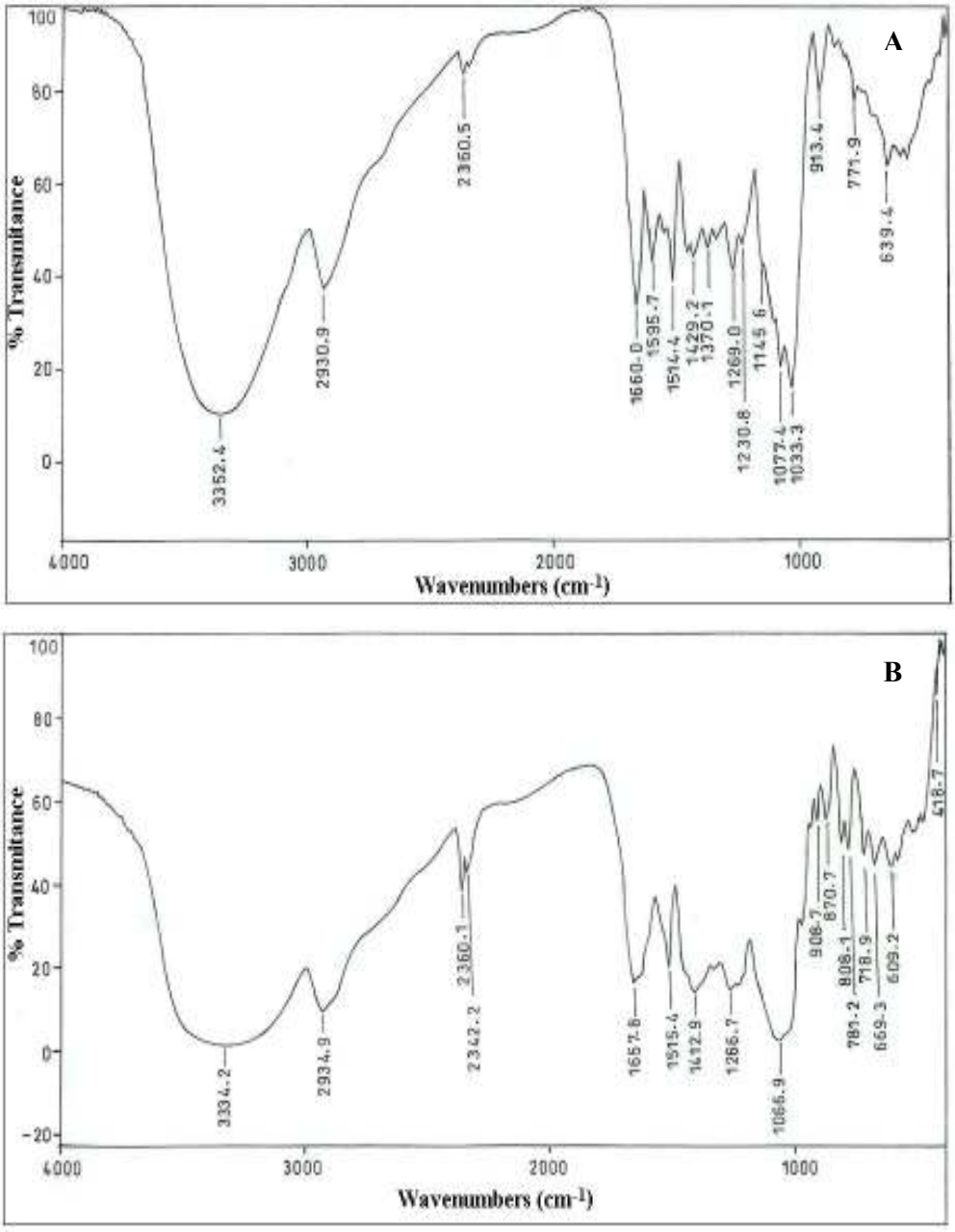

Fig. 4.11 IR spectrum of **(A)** Eugenyl-β-D-glucoside **25 (B)** Eugenyl-α-D-mannoside **26**.

63.5 (C1), 101.9 (C2), 74.0 (C4), 82.5 (C5), 62.0 (C6), 91.8 (C1″α), 75.5 (C2″), 72.2 (C3″), 70.5 (C4″), 61.0 (C6″), 144.9 (C1′), 152.1 (C2′), 113.0 (C3′), 132.5 (C4′), 121.0 (C5′), 115.2 (C6′), 39.0 (C7′), 138.5 (C8′), 116.0 (C9′). 56.0 (OCH_3). **C6-O-eugenyl sucrose, 28b**: ^{1}H NMR δ_{ppm}: 3.54 (H-1a), 3.87 (H-3), 3.71 (H-5), 3.25 (H-6a), 5.15 (H-1″α), 3.19 (H-3″), 3.11 (H-4″), 3.58 (H-6″a), 6.71 (1H, s, H-3′), 6.55 (1H, d, H-5′), 6.67 (1H, d, H-6′), 3.26 (H-7′), 5.91 (1H, m, H-8′), 5.0 (H-9′), 3.73 (OCH_3); ^{13}C NMR δ_{ppm}: 61.8 (C1), 104.0 (C2), 77.0 (C3), 81.0 (C5), 63.0 (C6), 91.8 (C1″α), 72.4 (C3″), 70.0 (C4″), 60.9 (C6″), 144.9 (C1′), 152.1 (C2′), 113.0 (C3′), 132.5 (C4′), 121.0 (C5′), 115.2 (C6′), 39.0 (C7′), 138.5 (C8′), 116.0 (C9′). 56.0 (OCH_3). **C6″-O-eugenyl sucrose, 28c**: ^{1}H NMR δ_{ppm}: 3.54 (H-1a), 3.50 (H-6a), 5.15 (H-1″α), 3.56 (H-4″), 3.54 (H-5″), 3.57 (H-6″a), 6.71 (1H, s, H-3′), 6.55 (1H, d, H-5′), 6.67 (1H, d, H-6′), 3.26 (H-7′), 5.91 (1H, m, H-8′), 5.0 (H-9′), 3.73 (OCH_3); ^{13}C NMR δ_{ppm}: 61.8 (C1), 104.0 (C2), 62.0 (C6), 91.8 (C1″α), 70.0 (C4″), 72.0 (C5″), 67.8 (C6″), 144.9 (C1′), 152.1 (C2′), 113.0 (C3′), 132.5 (C4′), 121.0 (C5′), 115.2 (C6′), 39.0 (C7′), 138.5 (C8′), 116.0 (C9′), 56.0 (OCH_3).

4.3.8.6 Eugenyl-D-mannitol, 29: Solid; mp 157 °C; UV (H_2O, λ_{max}): 199 nm ($\sigma\rightarrow\sigma^*$, ε_{205} - 3015 M^{-1}), 276 nm ($\pi\rightarrow\pi^*$, ε_{276} - 462 M^{-1}), IR (KBr): 1631 cm^{-1} (allylic C=C), 1020 cm^{-1} (glycosidic aryl alkyl C-O-C symmetrical), 1262 cm^{-1}, (glycosidic aryl alkyl C-O-C asymmetrical), 3287 cm^{-1} (OH) (Fig 4.15A); $[\alpha]^{25}_D$ = +17.7^o (*c* 1, H_2O); MS (*m/z*) - 352 $[M+1+Na]^+$; 2D-HSQCT (DMSO-d_6) ^{1}H NMR δ_{ppm} (500.13 MHz) 3.45 (H-1a), 3.47 (H-3), 3.54 (H-4), 3.61 (H-6a), 6.70 (1H, s, H-3′), 6.52 (1H, d, H-5′), 6.68 (1H, d, H-6′), 3.23 (H-7′), 5.92 (1H, m, H-8′), 5.01 (H-9′), 3.70 (OCH_3); ^{13}C NMR δ_{ppm} (125 MHz): 65.0 (C1), 71.0 (C2), 70.0 (C3), 70.0 (C4), 71.0 (C5), 64.0 (C6), 55.5 (OCH_3), 144.3 (C1′), 151.0 (C2′), 112.7 (C3′), 130.1 (C4′), 120.5 (C5′), 115.4 (C6′), 39.2 (C7′), 138.0 (C8′), 115.2 (C9′).

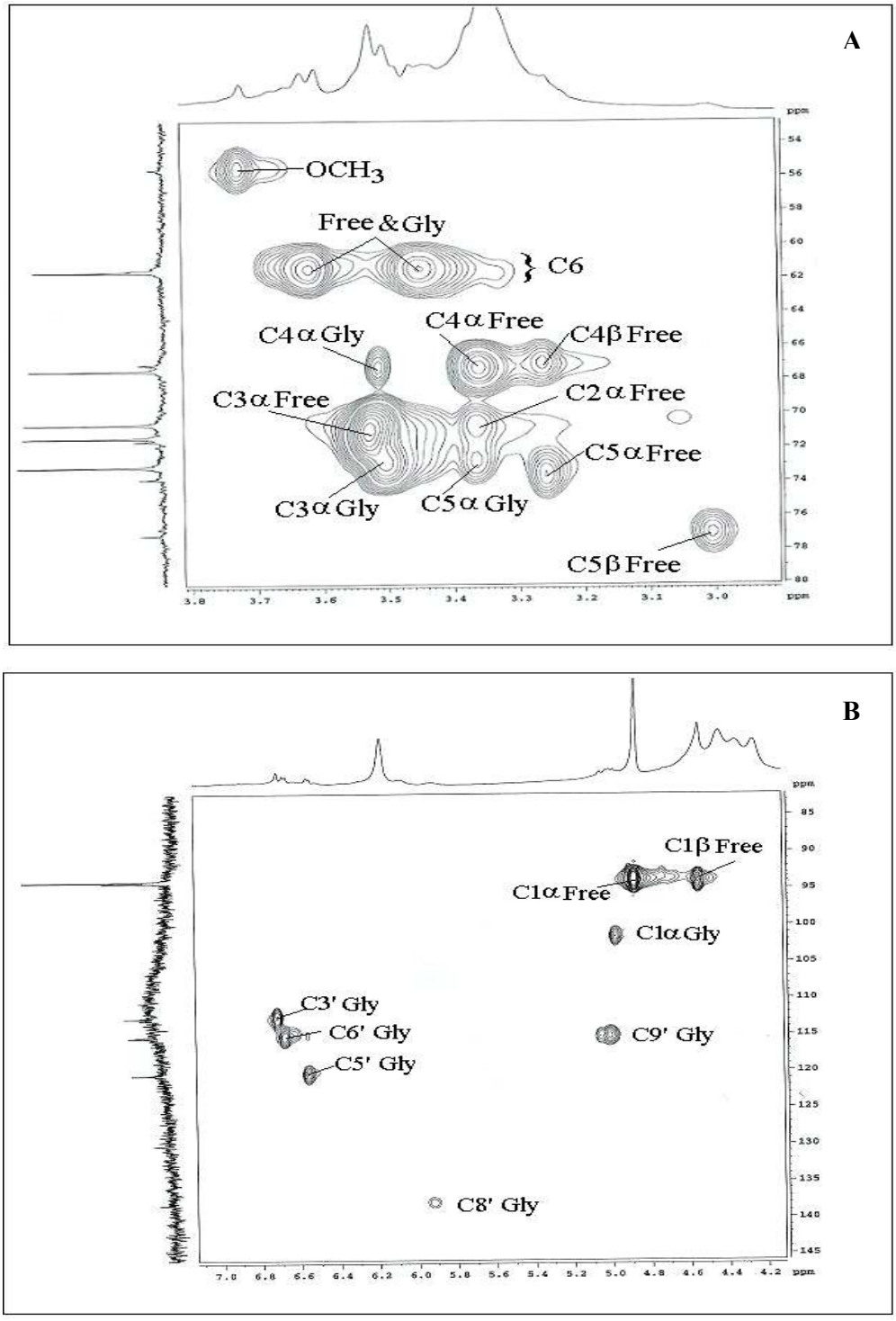

Fig. 4.12 2D-HSQCT spectrum of eugenyl-α-D-mannoside **26 (A)** C2-C6 region **(B)** Anomeric and aromatic region.

UV spectra of the eugenyl glycosides, showed shifts in the wavelength for $\pi \rightarrow \pi^*$ (extended conjugation) band in the range 265 - 279 nm (275.5 nm for free eugenol) confirming product formation. IR C-O-C symmetrical stretching frequencies in the range 1020 - 1066 cm^{-1} and asymmetrical stretching frequencies in the range 1262 - 1268 cm^{-1} indicated that eugenol had undergone glycosylation. Allylic C=C stretching frequency bands for the glycosides were also detected in the range 1631 - 1676 cm^{-1}. In eugenyl-α-D-glucoside 2D HSQCT spectrum showed chemical shift change in the C1α (^{13}C at 97.0 ppm and ^{1}H at 4.65 ppm) when compared to the free **2** (^{13}C at 97.0 ppm and ^{1}H at 4.65 ppm) indicating that the C1 glycoside was formed **24a** (Fig. 4.9A). C6-O-arylated **24b** formation was deduced from the chemical shift value of the C6 cross peak (^{13}C at 66.0 ppm and ^{1}H at 3.50 and 3.68 ppm). D-Mannose **4**, formed only C1α mannoside **26** (Fig. 4.12), as observed from the C1α cross peak (^{13}C at 101.5 ppm and ^{1}H at 3.61 ppm). Maltose formed C1α maltoside **27a**, C6-O-arylated **27b** and C6"-O-arylated **27c** products. The cross peaks C1α (^{13}C at 98.5 ppm and ^{1}H at 4.62 ppm), C6 (^{13}C at 67.0 ppm and ^{1}H at 3.68 ppm) and C6" (^{13}C at 67.1 ppm and ^{1}H at 3.54 ppm) indicated the formation of glycosides **27a, 27b** and **27c** respectively (Fig. 4.13). Sucrose reacted with eugenol and the products **28a, 28b** and **28c** were found to be formed. The cross peaks C1 (^{13}C at 63.5 ppm and ^{1}H at 3.77 ppm), C6 (^{13}C at 63.0 ppm and ^{1}H at 3.25 ppm) and C6" (^{13}C at 67.8 ppm and ^{1}H at 3.57 ppm) indicated the formation of **28a, 28b** and **28c** respectively (Fig. 4.14). D-Mannitol **9**, showed C1-O-arylated product **29** (Fig. 4.15B), as confirmed from the C1 cross peak (^{13}C at 64.0 ppm and ^{1}H at 3.61 ppm). The mass *m/z* peaks (experimental section) further confirmed the formation of above mentioned monoglycosides.

In presence of β-glucosidase D-glucose **2** reacted with eugenol **18** and the only product C1β-glucoside **25** was found to be formed. In the anomeric region the only cross

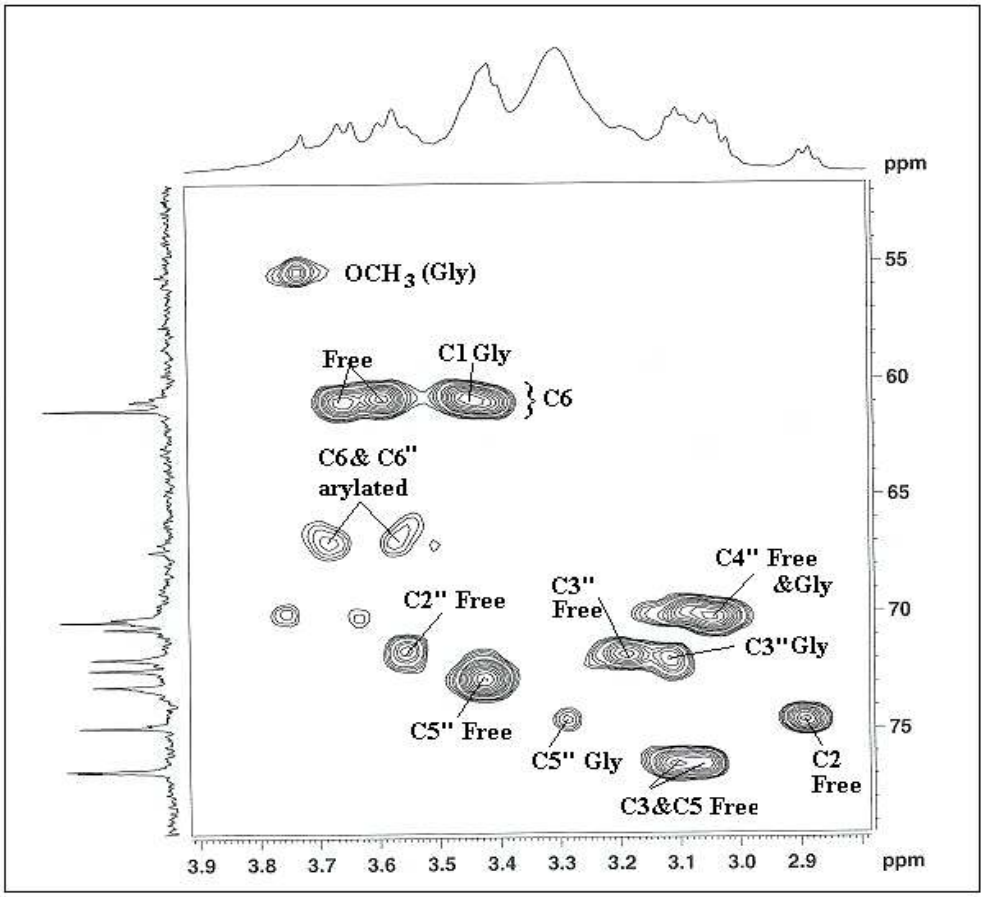

Fig. 4.13 2D HSQCT spectrum of eugenyl maltoside **27a-c**.

peak (^{13}C at 103.3 ppm and ^{1}H at 4.19 ppm) apart from the free C1α and C1β cross peaks indicated the formation of C1β-glucoside **25** (Fig. 4.10).

4.4 Curcuminyl glycosides

Synthesis of Curcuminyl-bis-α-D-glucoside using amyloglucosidase was studied in detail. Curcuminyl-bis-α-D-glucoside synthesis in di-isopropyl ether using amyloglucosidase was optimized in terms of incubation period, pH, buffer concentration, enzyme concentration, curcumin concentration and D-glucose concentration. The reaction conditions employed were 0.09 - 0.54 g D-glucose (0.5-3.0 mmol), 0.07-0.55 g (0.2 – 1.5 mmol) curcumin, 10-75% (w/w D-glucose) amyloglucosidase, 0.01-0.1 mM, pH 4.0-8.0 buffer (0.1-1.0 mL of 0.01 M buffer in 100 mL of reaction mixture), 100 mL di-isopropyl ether solvent and 12 to 72 h incubation **(Scheme 4.3)**. The reaction mixture was monitored by high performance liquid chromatography. HPLC retention times are 5.20 min for D-glucose and 7.52 min for curcuminyl-bis-α-D-glucoside. Conversion yields were determined from the HPLC peak areas of the glycoside and unreacted D-glucose and expressed as percentage with respect to the free D-glucose concentration employed. Errors in the HPLC measurements were in the order of ± 5-10%. The glucoside was isolated by column chromatography by passing through Sephadex G-15 using water as eluent. Here also Sephadex G15 separated only the glycosides from unreacted carbohydrate molecules. The individual glycosides could not be separated because of similar polarity of these glycoside and O-arylated molecules. Spectral characterization was carried out by UV, IR, MS and 2-D NMR spectroscopy for the glucoside and also isolated glycosides.

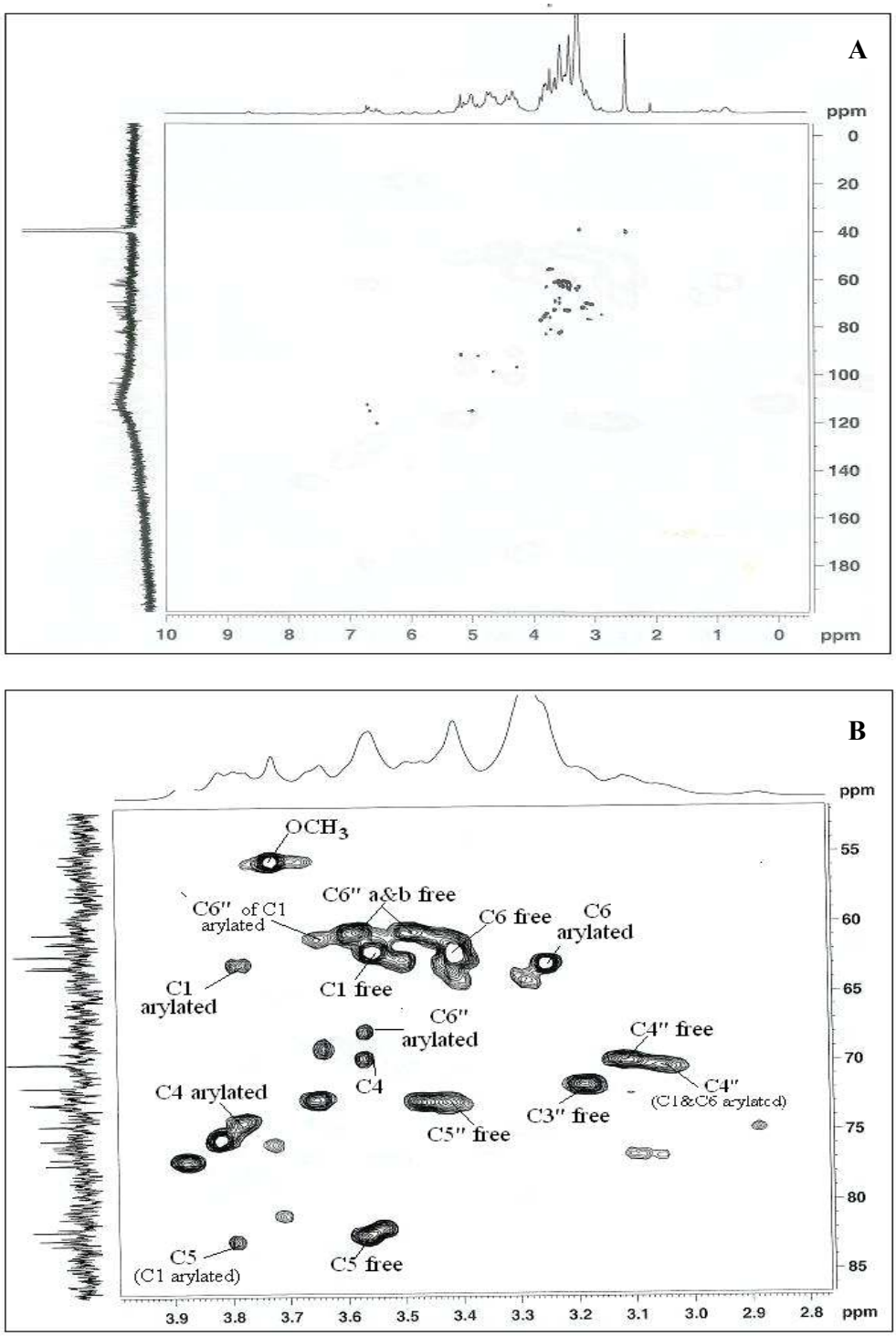

Fig. 4.14 2D HSQCT spectrum of eugenyl sucrose **28a-c (A)** Full spectrum **(B)** Sucrose region in eugenyl sucrose.

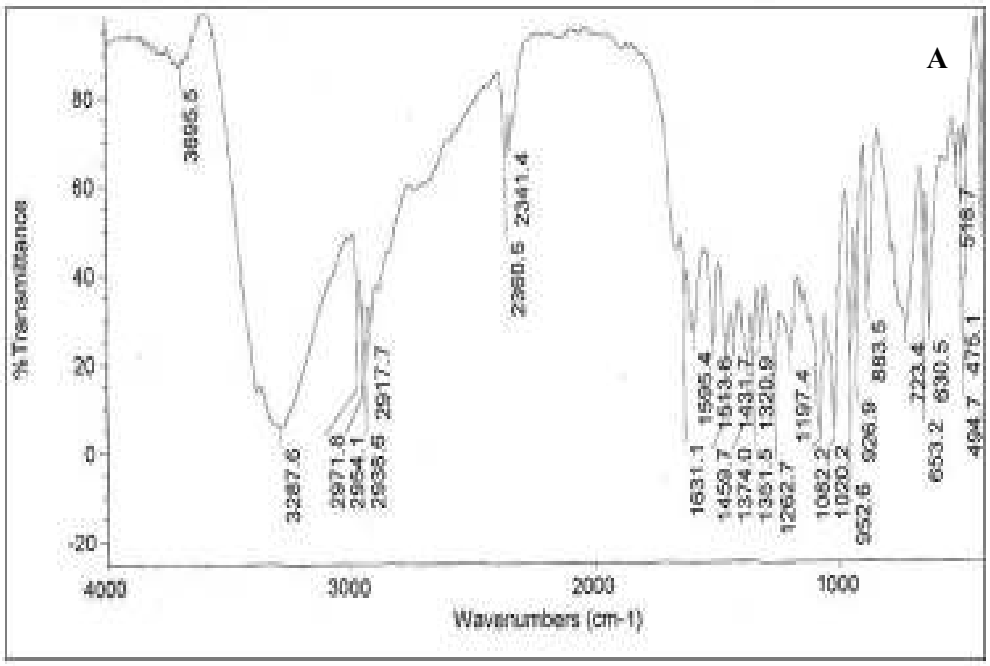

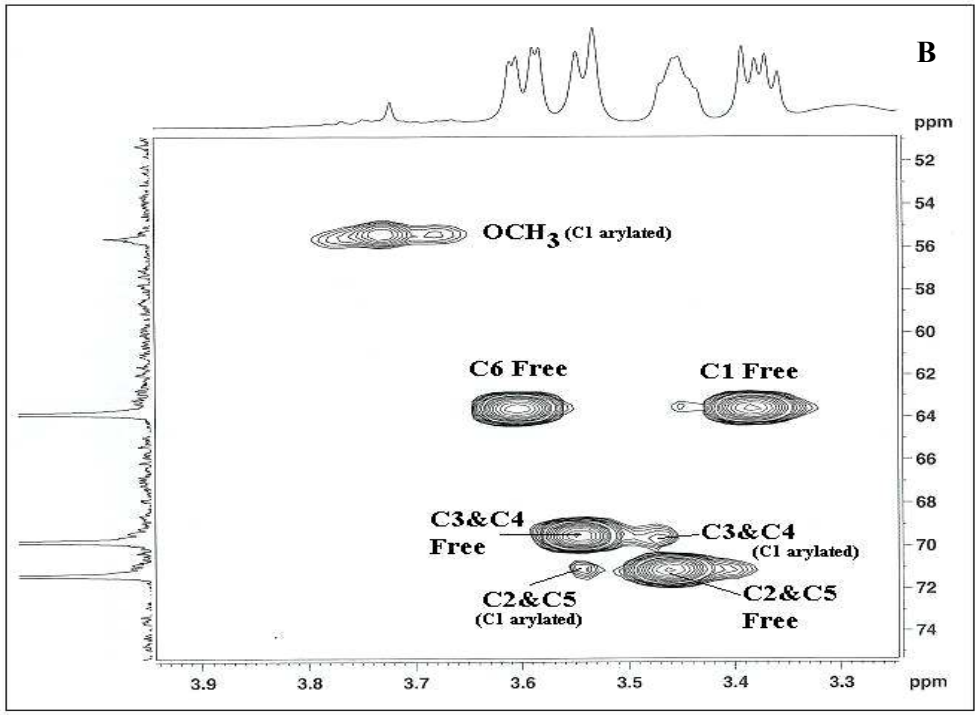

Fig. 4.15 Eugenyl-D-mannitol **29 (A)** IR spectrum **(B)** 2D HSQCT spectrum (C1-C6 region)

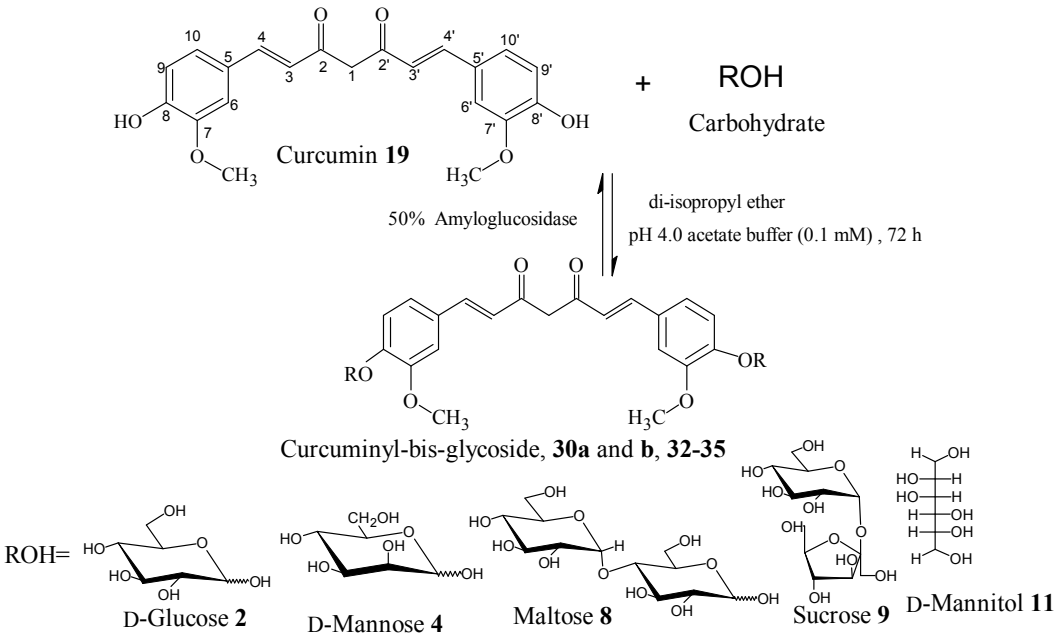

Scheme 4.3 Amyloglucosidase catalyzed synthesis of curcuminyl glycosides

4.4.1 Curcuminyl-bis-α-D-glucoside

4.4.2 Effect of incubation period on curcuminyl-bis-α-D-glucoside synthesis

In presence of 0.06 mM (0.6 mL), pH 6.0 buffer and 50% (w/w D-glucose) amyloglucosidase, a reaction mixture of curcumin and D-glucose (1:2 molar ratio) showed increase in conversion yields: 4% (12 h), 8% (24h), 12% (48 h) and 25% (72 h) with increase in incubation period (Fig. 4.16A). Rate of the reaction from the initial slope was found to be 3.24 μmol/h.

4.4.3 Effect of buffer pH and concentration on curcuminyl-bis-α-D-glucoside synthesis

Buffer pH was varied from pH 4.0 to 8.0 at 0.04 mM (0.4 mL) and its effect on conversion yield studied showed that the highest conversion yield of 29% was obtained at pH 4.0 (Table 4.7). At all other pH values the yields were low. Effect of buffer concentration at pH 4.0, showed that conversion yield increased with increase in buffer concentration from 0.01-0.1 mM (0.1 to 1.0 mL) with the highest yield of 48% at 0.1

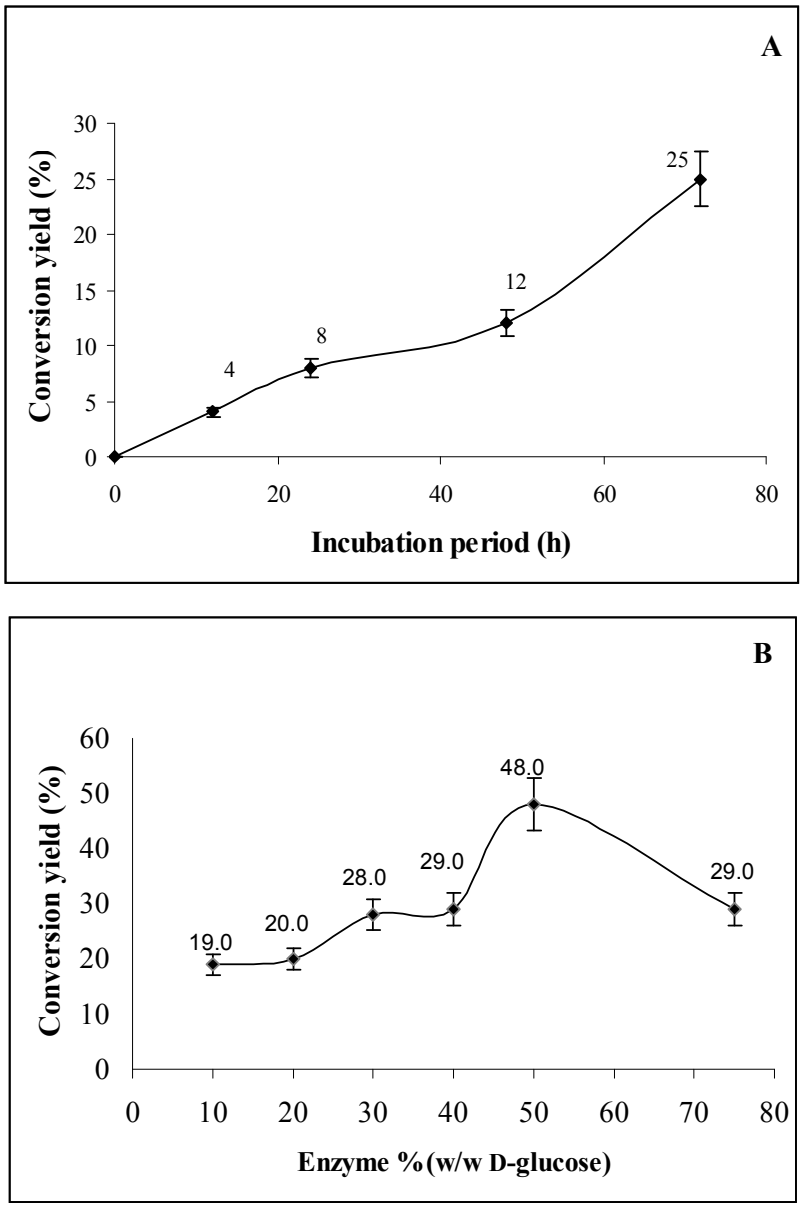

Fig. 4.16 Curcuminyl-bis-α-D-glucoside synthesis. Conversion yields were from HPLC with respect to 1 mmol D-glucose. **(A)** Effect of incubation period. Reaction conditions: D-glucose-1 mmol, curcumin-0.5 mmol, 0.06 mM (0.6 mL), pH 6.0 phosphate buffer. **(B)** Effect of enzyme concentration. Reaction conditions: D-glucose-1 mmol, curcumin-0.5 mmol, incubation period – 72h, 0.1 mM (1.0 mL) of pH 4.0 acetate buffer.

mM (1.0 mL). Increase in water activity at higher buffer concentrations (0.1 mM), could increase the conversion more, besides solublising D-glucose.

Table 4.7 Effect of buffer pH and buffer concentration on the synthesis of curcuminyl-bis-α-D-glucoside[a].

pH[b]	Yield, %	Buffer concentration[c] (mM)	Yield, %
4.0	29	0.01	-
5.0	17	0.02	3
6.0	8	0.04	29
7.0	23	0.06	45
8.0	16	0.08	10
		0.1	48

[a]Conversion yields from HPLC with respect to 1.0 mmol of D-glucose. Error in yield measurements ± 5-10%. Curcumin-0.5 mmol, enzyme - 50% (w/w D-glucose), incubation – 72 h, temperature – 68 °C. [b]0.04 mM (0.4 mL of 10 mM buffers added in 100 mL of solvent). [c]0.1-1.0 mL of pH 4.0 acetate buffer.

4.4.4 Effect of amyloglucosidase concentration on curcuminyl-bis-α-D-glucoside synthesis

Effect of increasing amyloglucosidase concentration from 10 to 75% (w/w D-glucose) showed (Fig. 4.16B) that 50% (w/w D-glucose) enzyme was required to achieve a maximum conversion of 48%. This yield decreased at further higher enzyme concentrations (75% enzyme - 29% yield).

4.4.5 Effect of curcumin concentration on curcuminyl-bis-α-D-glucoside synthesis

Higher curcumin concentrations could be inhibitory to the enzyme as the conversion yield decreased from 37% for 0.2 and 0.4 mmol curcumin to 34% (0.8 mmol), 29% (1.0 mmol), 22% (1.2 mmol) and 9% at 1.5 mmol curcumin.

4.4.6 Effect of D-glucose concentration on curcuminyl-bis-α-D-glucoside synthesis

D-Glucose concentration was varied from 0.5 mmol to 3.0 mmol at 0.5 mmol of curcumin concentration, 90 mg (16.7-100% w/w D-glucose) of amyloglucosidase, 0.1 mM (1.0 mL) of pH 4.0 and 72 h incubation. Maximum glycoside yield of 42 % was

obtained between 1.5 mmol and at 2.0 mmol of D-glucose concentrations. Below 1.5 mmol and above 2.0 mmol of D-glucose, the glycosylation gave lesser conversion yields (Table 4.8).

Table 4.8 Effect of D-glucose concentration on the synthesis of curcuminyl-bis-α-D-glucoside[a].

D-Glucose (mmol)	% Yield
0.5	26
1.0	23
1.5	42
2.0	42
3.0	29

[a]Conversion yields from HPLC with respect to D-glucose concentration employed. Error in yield measurements ±10%. Curcumin-0.5 mmol, enzyme –90 mg (16.7-100% w/w D-glucose), incubation period – 72 h, solvent-di-isopropyl ether, temperature – 68 °C. 0.1 mM (1.0 mL of 10 mM buffer added in 100 mL of solvent) of pH 4.0 acetate buffer.

The optimum conditions for this reaction was found to be curcumin and D-glucose in the 1: 2 molar ratio, 50% (w/w D-glucose) amyloglucosidase, 0.1 mM (1.0 mL), pH 4.0 acetate buffer and 72 h incubation period.

4.4.7 Synthesis of curcuminyl glucoside using β-glucosidase

Curcuminyl glucoside was synthesized using β-glucosidase isolated from sweet almonds under the optimum conditions obtained for amyloglucosidase catalyzed synthesis, which are D-glucose (1.0 mmol), curcumin (0.5 mmol), enzyme 90 mg (50 % w/w D-glucose), 0.1 mM (1.0 mL) pH 4.0 acetate buffer and 72 h of incubation period. The reaction mixture analyzed by HPLC showed 11% conversion yield. The glucoside was isolated by column chromatography by using Sephadex G15 as column material and water as eluent. Spectral characterization (UV, IR, MS and 2D HSQCT) for the isolated glucoside confirmed that the product is curcuminyl-bis-β-D-glucoside **31**.

4.4.8 Antioxidant activity

Antioxidant activity of curcumin and curcuminyl-bis-α-D-glucoside were evaluated by DPPH (2,2-diphenyl-1-picrylhydrazyl) radical scavenging method (Moon and Terao 1998). An antioxidant activity of 80% for curcuminyl-bis-α-D-glucoside was obtained. The antioxidant activity of the glycoside was found to comparable to that of free curcumin (79%). Standard BHA activity was found to be 82%.

4.4.9 Solubility test

Determination of the water solubility of curcuminyl-bis-α-D-glucoside showed that it is soluble to the extent of 14 g/L (section 4.7.3). Hence, curcuminyl-bis-α-D-glucoside was found to exhibit higher solubility than curcumin in water which exhibited negligible solubility.

4.4.10 Total color test

Curcuminyl-bis-α-D-glucoside exhibited a total color of 10.8 in DMSO. The color test was carried out according to the AOAC official methods of analysis (1995). Curcumin was used as the standard (section 4.7.4).

4.4.11 Curcuminyl glycosides of other carbohydrates

Amyloglucosidase catalyzed synthesis of curcuminyl glycosides were synthesized. Carbohydrates, **2-12** were employed for the synthesis under the following conditions carbohydrate - 1 mmol, curcumin-0.33 mmol, 17% (w/w carbohydrate) amyloglucosidase, 0.1 mM (1.0 mL) pH 4.0 acetate buffer and incubation-72 h **(Scheme 4.3)**. The extent of glycosylation was analyzed by HPLC. The retention times are D-glucose-5.20 min, curcuminyl-bis-D-glucoside-7.52 min, D-mannose-4.9 min, curcuminyl-bis-D-mannoside-6.78 min, maltose-7.4 min, curcuminyl-bis-maltoside-10.3 min, sucrose-6.4 min, curcuminyl-bis-sucrose-8.44 min, D-mannitol-5.3 min and curcuminyl-bis-D-mannitol-8.35 min. From HPLC results it was confirmed that, D-

galactose **3**, D-fructose **5**, D-arabinose **6**, D-ribose **7**, lactose **10** and D-sorbitol **12** did not undergo glycosylation with curcumin. The carbohydrates, which underwent glycosylation, are D-glucose **2**, D-mannose **4**, maltose **8**, sucrose **9**, and D-mannitol **11**.

Table 4.9 Curcuminyl glycosides with conversion yields and product proportions

Glycosides and product proportions (%)[a]	**Glycosylation yield**[b] **%**
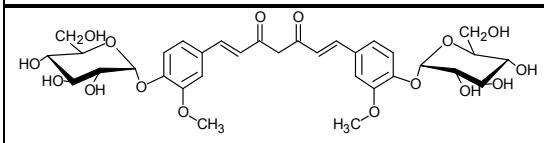 **30a**, curcuminyl-bis-α-D-glucoside (62) 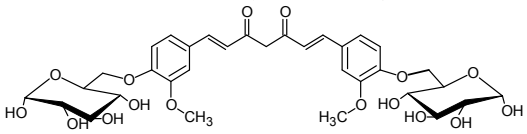 **30b**, C6-O-curcuminyl-bis-D-glucose (38)	48
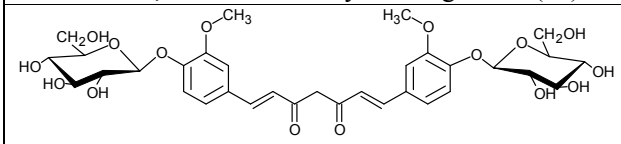 **31**, curcuminyl-bis-β-D-glucoside [c]	11
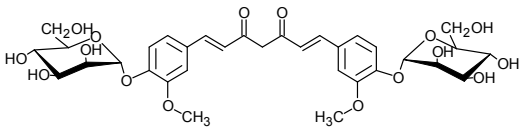 **32**, curcuminyl-bis-α-D-mannoside	9
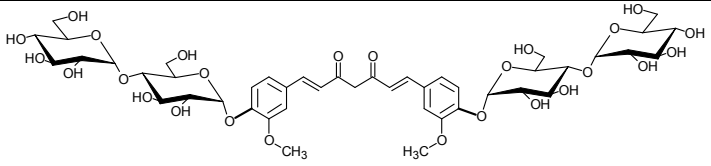 **33a**, curcuminyl-bis-maltoside (37) 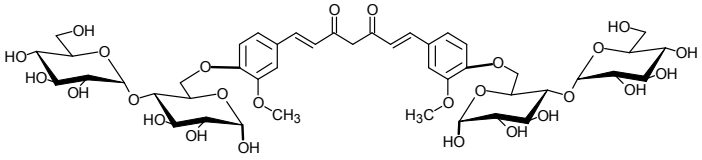 **33b**, C6-O-curcuminyl-bis-maltose (36) 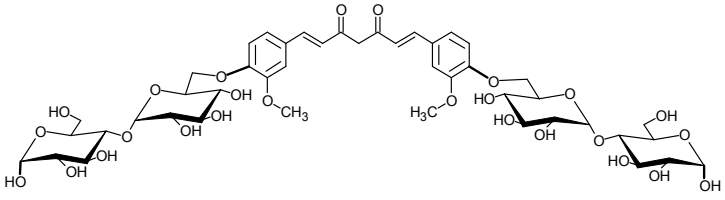 **33c**, C6″-O-curcuminyl-bis-maltose (27)	19

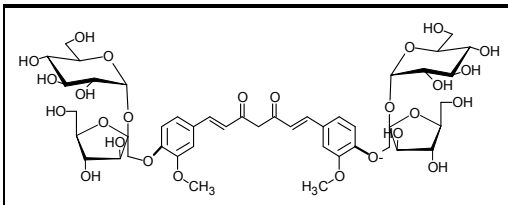 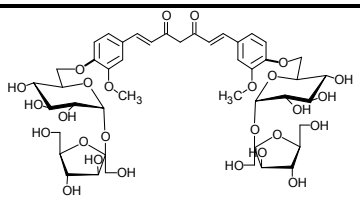 **34a**, C1-O-curcuminyl-bis-sucrose (12) **34b**, C6″-O-curcuminyl-bis-sucrose (18) 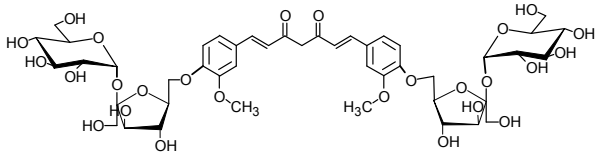 **34c**, curcuminyl-bis-sucrose (70)	19
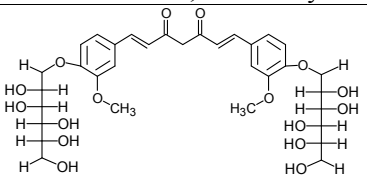 **35**, C1-O-curcuminyl-bis-D-mannitol	14

[a] Product proportions determined from ^{13}C 2D-HSQCT NMR C1/C6 peak areas or their cross peaks are shown in brackets; [b] Conversion yields were from HPLC with errors in yield measurements ± 5-10%.

4.4.12 Spectral characterization

The curcuminyl glycosides were characterized by UV, IR, 2-D NMR (HSQCT) and optical rotation, which provided good information on the nature and proportions of the products formed. The structures of the glycosides formed, HPLC yield and product proportions are presented in the Table 4.9. Only resolvable signals are shown. Some assignments are interchangeable. Curcumin region signals in curcuminyl glycosides are in subscript, non-reducing end glucose signals in maltose and sucrose are double primed. Since these glycosides are surfactants, they tend to aggregate in solution giving rise to broad signals. Hence coupling constant values could not be resolved satisfactorily.

Curcumin, 19: Solid; mp 178 °C; UV (DMSO, λ_{max}): 254 nm ($\pi\rightarrow\pi^*$,ε_{254} – 13087 M^{-1}), 433 nm ($\pi\rightarrow\pi^*$extended conjugation, ε_{430} – 58724 M^{-1}) Fig. 4.17A; IR (KBr): 1628 cm^{-1} (CO), 3340, 3512 cm^{-1} (OH), 1602 cm^{-1} (aromatic C=C); ^1H NMR δ_{ppm} (500.13 MHz) 3.84 (6H, s, 2-OCH_3), 6.05 (1H, s, H_1), 6.76 (2H, d, J=15.8Hz, $H_{3,\ 3'}$), 7.57 (2H, d,

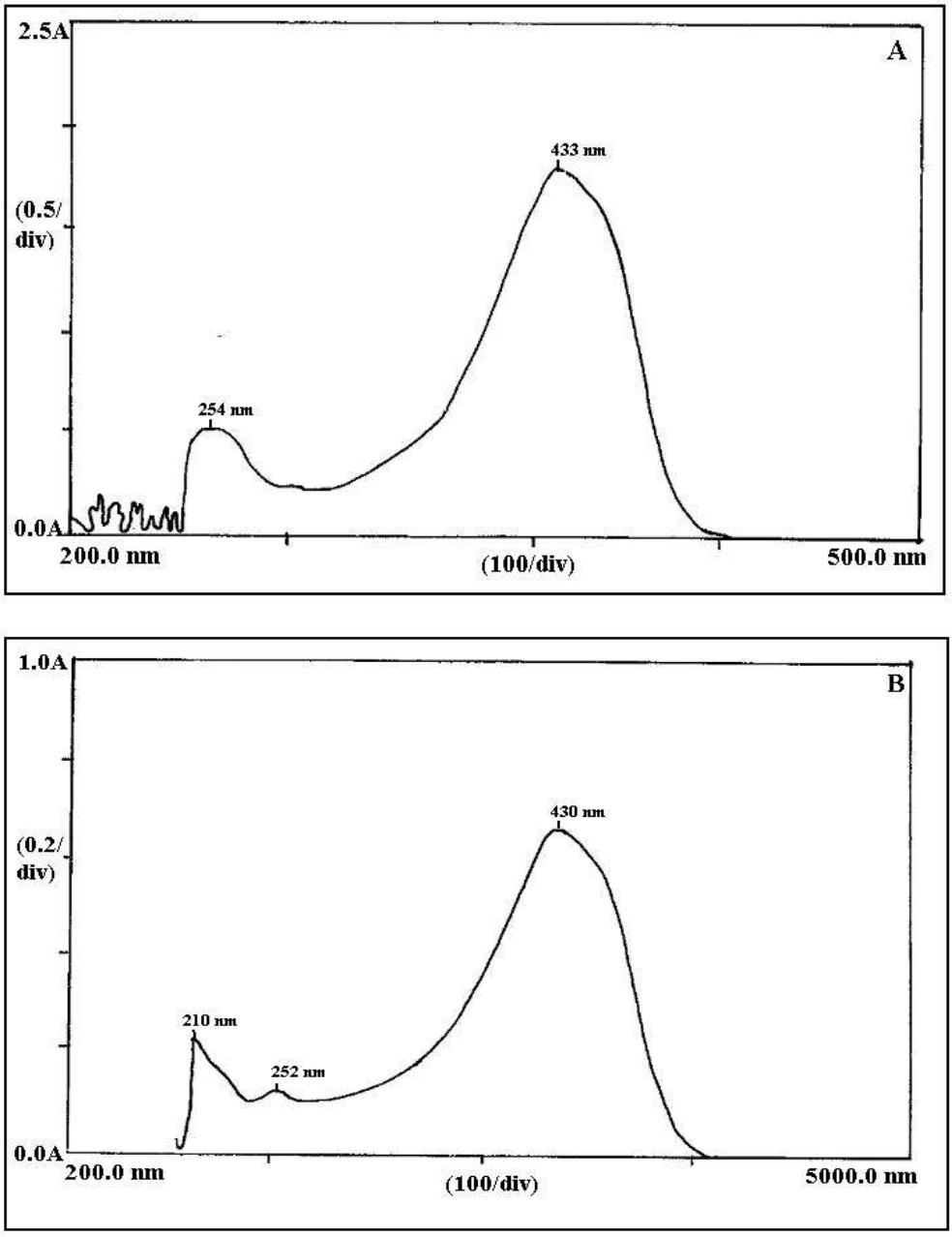

Fig. 4.17. Typical UV spectrum: **(A)** Curcumin **19 (B)** Curcuminyl-bis-α-D-glucoside **30a** and **b**.

J=15.8, $H_{4, 4'}$), 7.32 (2H, s, $H_{6, 6'}$), 6.82 (2H, d, J=8.2Hz, $H_{9, 9'}$), 7.15 (2 H, dd, J=1.45 Hz, $H_{10, 10'}$) (Venkateshwaralu *et al.* 2005).

4.4.12.1 Curcuminyl-bis-α-D-glucoside, 30a and **b:** Solid; UV (H_2O, λ_{max}): 210 nm ($\sigma\rightarrow\sigma^*$, ε_{210} - 1242 M^{-1}), 252 nm ($\pi\rightarrow\pi^*$, ε_{252} – 537 M^{-1}), 430 nm ($\pi\rightarrow\pi^*$extended conjugation, ε_{430} – 42 M^{-1}) Fig. 4.17B; IR (KBr): 1664 cm^{-1} (CO), 1027 cm^{-1} (aryl alkyl C-O-C symmetrical), 1254 cm^{-1} (aryl alkyl C-O-C asymmetrical); $[\alpha]^{25}_D$ = +30.3° (*c* 1, H_2O); MS (*m/z*) - 691 $[M-1]^+$. 2D-HSQCT (DMSO-d_6) **Curcuminyl-bis-α-D-glucoside, 30a:** ^{1}H NMR δ_{ppm} (500.13 MHz): 4.66 (H-1α), 3.15 (H-2α), 3.73 (H-3α), 3.75 (H-4α), 3.53 (H-6a). 3.85 (6H, s, 2-OCH_3), 6.06 (1H, s, H_1), 6.71 (2H, d, J=15.8Hz, $H_{3, 3'}$), 7.51(2H, d, J=15.8, $H_{4, 4'}$), 7.25 (2H, s, $H_{6, 6'}$), 6.81 (2H, d, J=8.2Hz, $H_{9, 9'}$), 7.11 (2 H, dd, J=1.45 Hz, $H_{10, 10'}$); ^{13}C NMR δ_{ppm} (125 MHz): 99.0 (C1α), 72.2 (C2α), 73.6(C3α), 70.6 (C4α), 61.3 (C6α), 56.1 (OCH_3), 101.0 ($C_{1'}$), 183.5 (C_2,$C_{2'}$), 121.5 (C_3,$C_{3'}$), 141.0 (C_4,$C_{4'}$), 126.8 (C_5,$C_{5'}$), 111.6 (C_6,$C_{6'}$), 148.4 (C_7,$C_{7'}$), 150.0 (C_8,$C_{8'}$), 116.1 (C_9,$C_{9'}$), 123.4 (C_{10},$C_{10'}$). **C6-O-curcuminyl-bis-D-glucose, 30b** ^{1}H NMR δ_{ppm}: 3.25 (H-2α), 3.65 (H-4α), 3.52, 3.70 (H-6 a & b), 6.81 ($H_{3, 3'}$), 7.10 ($H_{9, 9'}$); ^{13}C NMR δ_{ppm}: 75.0 (C2α), 70.5 (C4α), 66.5 (C6α), 123.0 (C_3, $C_{3'}$), 116 (C_9,$C_{9'}$).

4.4.12.2 Curcuminyl-bis-β-D-glucoside, 31: Solid; mp 148 °C; UV (H_2O, λ_{max}): 204 nm ($\sigma\rightarrow\sigma^*$, ε_{204} - 1450 M^{-1}), 277 nm ($n\rightarrow\pi^*$,ε_{238} – 759 M^{-1}), 421 nm ($\pi\rightarrow\pi^*$extended conjugation, ε_{421} – 147 M^{-1}); IR (KBr): 1657 cm^{-1} (CO), 1028 cm^{-1} (aryl alkyl C-O-C symmetrical), 1598 cm^{-1} (C=C); 3348 cm^{-1} (OH) Fig. 4.19A; $[\alpha]^{25}_D$ = -13.3° (*c* 1, H_2O); MS (*m/z*) - 691 $[M-1]^+$; 2D-HSQCT (DMSO-d_6) ^{1}H NMR δ_{ppm} (500.13 MHz): 4.16 (H-1β), 3.28 (H-2β), 3.03 (H-3β), 3.75 (H-4β), 3.10 (H-5β), 3.60 (H-6a). 3.82 (6H, s, 2-OCH_3), 6.10 (1H, s, H_1), 6.53 (2H, d, J=15.8Hz, $H_{3, 3'}$), 6.81 (2H, d, J=8.2Hz, $H_{9, 9'}$), ^{13}C NMR δ_{ppm} (125 MHz): 103.2 (C1β), 76.0 (C2β), 79.0 (C3β), 70.5 (C4β), 79.0 (C5β),

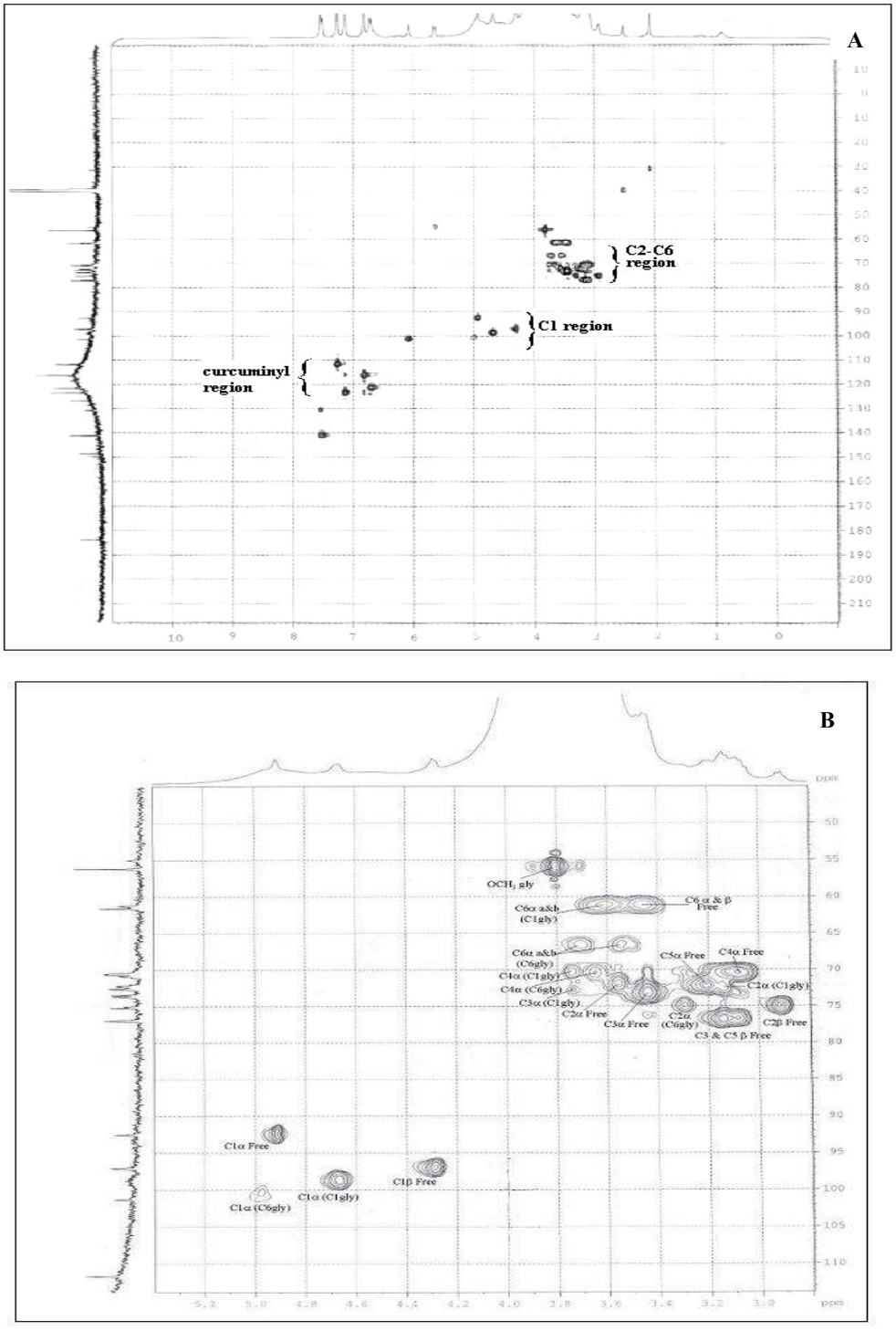

Fig. 4.18 2D-HSQCT spectrum of curcuminyl-bis-α-D-glucoside **30a** and **b (A)** Full spectrum **(B)** C1-C6 region. Some assignments are interchangeable.

62.1 (C6β), 56.0 (OCH_3), 102.0 ($C_{1'}$), 183.0 ($C_{2,\ 2'}$), 121.3 ($C_{3,\ 3'}$), 148.4 ($C_{7,\ 7'}$), 150.0 ($C_{8,\ 8'}$), 116.4 ($C_{9,\ 9'}$).

4.4.12.3 Curcuminyl-bis-α-D-mannoside, 32: Solid; mp 116 °C; UV (H_2O, λ_{max}): 193 nm ($\sigma\rightarrow\sigma^*$, ε_{193}-11167 M^{-1}), 268 nm ($\pi\rightarrow\pi^*$,ε_{268} - 2139M^{-1}), 411 nm ($\pi\rightarrow\pi^*$extended conjugation, ε_{411} – 304 M^{-1}); IR (KBr): 1682 cm^{-1} (CO), 1071 cm^{-1} (glycosidic aryl alkyl C-O-C symmetrical), 1590 (C=C); $[\alpha]^{25}_D$ = +6.38° (*c* 1, H_2O); MS (*m/z*) - 692.4 $[M]^+$; 2D-HSQCT (DMSO-d_6) ^{1}H NMR δ_{ppm} (500.13 MHz): 4.98 (H-1α), 3.38 (H-2α), 4.21 (H-3α), 3.5 (H-4α), 3.92 (H-5α), 3.45 (H-6a), 3.45 (6H, s, 2-OCH_3), 6.10 (1H, s, H-1), 6.71 (2 H, H-3, 3'), 7.25 (2H, s, H-6,6'); ^{13}C NMR δ_{ppm} (125 MHz): 101.0 (C1α), 73.0 (C2α), 73.3 (C3α), 68.0 (C4α), 72.0 (C5α), 62.0 (C6α), 56.1 (OCH_3), 101.0 (C1), 121.4 (C3,C3'), 111.2 (C6,C6').

4.4.12.4 Curcuminyl-bis-maltoside, 33a-c: Solid; UV (H_2O, λ_{max}): 197 nm ($\sigma\rightarrow\sigma^*$, ε_{197} - 4677 M^{-1}), 275 nm ($\pi\rightarrow\pi^*$, ε_{275} – 645 M^{-1}), 410 nm ($\pi\rightarrow\pi^*$ extended conjugation, ε_{410} – 147 M^{-1}); IR (KBr): 1030 cm^{-1} (glycosidic aryl alkyl C-O-C symmetrical), 3418 cm^{-1} (OH); $[\alpha]^{25}_D$ = +82.3° (*c* 1, H_2O); MS (*m/z*) - 1016 $[M]^+$; 2D-HSQCT (DMSO-d_6) **Curcuminyl-bis-maltoside, 33a**: ^{1}H NMR δ_{ppm} (500.13 MHz): 4.65 (H-1α), 3.10 (H-2α), 3.71 (H-3α), 3.75 (H-4α), 3.3 (H-5α), 3.75 (H-6a). 5.0 (H-1″α), 3.75 (H-2″), 3.81 (6H, s, 2-OCH_3), 6.68 (2H, d, J=15.8 Hz, $H_{3,\ 3'}$), 7.45 (2H, d, J=15.8, $H_{4,\ 4'}$), 6.80 (2H, d, J=8.2Hz, $H_{9,\ 9'}$), 7.10 (2 H, dd, J=1.45 Hz, $H_{10,\ 10'}$); ^{13}C NMR δ_{ppm} (125 MHz): 98.5 (C1α), 74.2 (C2α), 72.5 (C3α), 70.2 (C4α), 73.0 (C5α), 61.0 (C6α), 101.0 (C1″α), 75.0 (C2″), 70.0 (C4″), 62.5 (C6″), 56.1 (OCH_3), 121.2 (C_3, $C_{3'}$), 142.0 (C_4, $C_{4'}$), 115.3 (C_9,$C_{9'}$), 124.1 (C_{10},$C_{10'}$). **C6-O-curcuminyl-bis-maltose, 33b**: ^{1}H NMR δ_{ppm}: 4.92 (H-1α), 3.04 (H-2α), 3.32 (H-3α), 3.60 (H-4α), 3.08 (H-5α), 3.68 (H-6 a), 4.95 (H-1″α), 3.66 (H-3″), 3.31 (H-4″), 3.40 (H-6″a), 3.89 (6H, s, 2-OCH_3), 7.45 (2H, d, J=15.8, $H_{4,\ 4'}$),

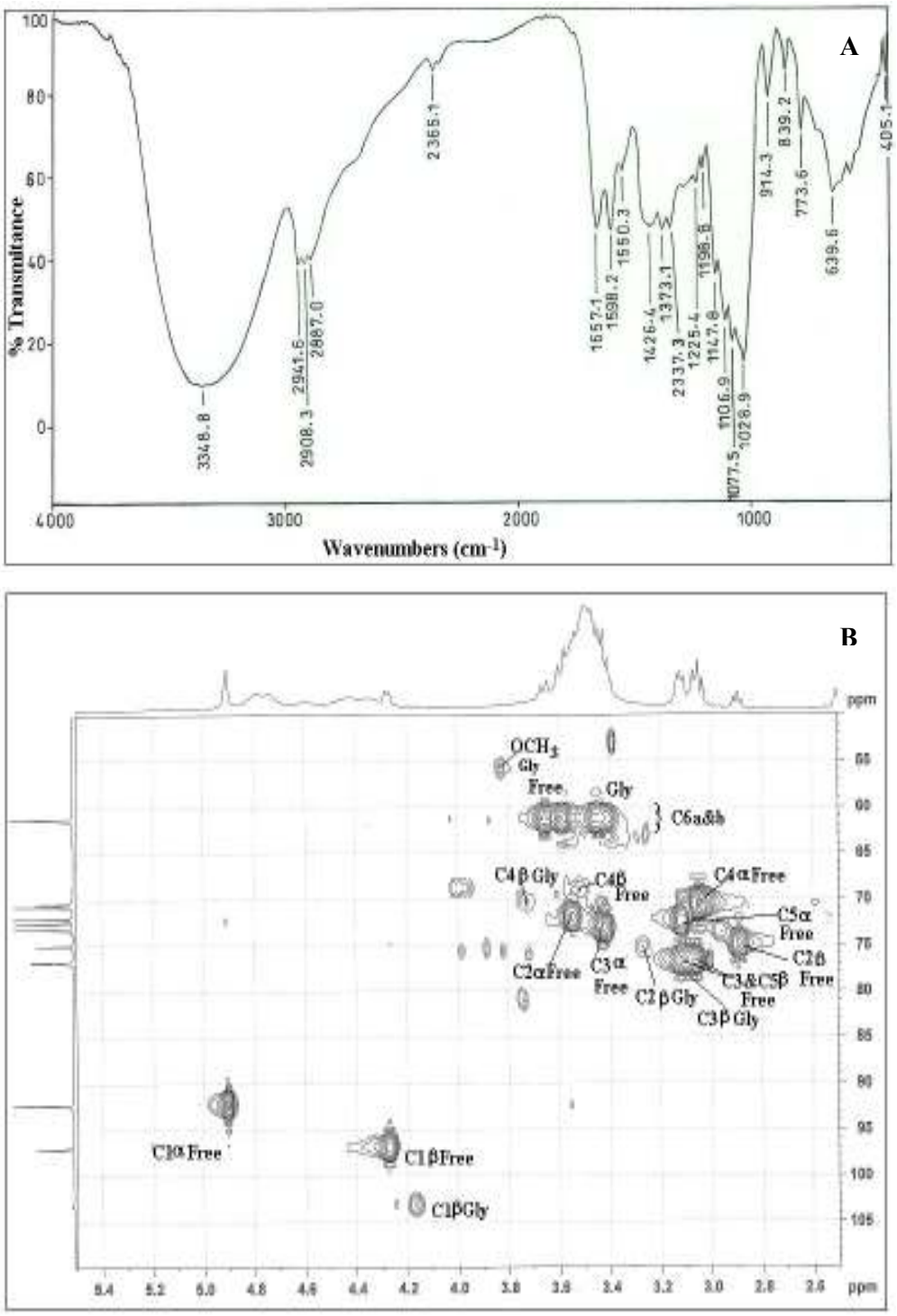

Fig. 4.19 Curcuminyl-bis-β-D-glucoside **31** synthesized by β-glucosidase from sweet almonds **(A)** IR spectrum **(B)** 2D HSQCT (C1-C6 region).

6.80 (2H, d, J=8.2Hz, $H_{9,\ 9'}$), 7.10 (2 H, dd, J=1.45 Hz, $H_{10,\ 10'}$); ^{13}C NMR δ_{ppm}: 92.0 (C1α), 73.2 (C2α), 76.1 (C3α), 70.2 (C4α), 73.0 (C5α), 67.0 (C6α), 100.0 (C1″α), 72.1 (C3″), 70.8 (C4″), 63.0 (C6″), 56.1 (OCH_3), 142.0 (C_4,$C_{4'}$), 115.3 (C_9,$C_{9'}$), 124.1 (C_{10},$C_{10'}$). **C6″-O-curcuminyl-bis-maltose, 33c**: ^{1}H NMR δ_{ppm}: 4.92 (H-1α), 3.42 (H-4α), 3.20 (H-6a), 4.96 (H-1″α), 3.52 (H-6″a), 3.81 (6H, s, 2-OCH_3), 6.68 (2H, d, J=15.8 Hz, $H_{3,\ 3'}$), 7.45 (2H, d, J=15.8, $H_{4,\ 4'}$), 6.80 (2H, d, J=8.2Hz, $H_{9,\ 9'}$), 7.10 (2 H, dd, J=1.45 Hz, $H_{10,10'}$); ^{13}C NMR δ_{ppm}: 92.0 (C1α), 70.0 (C4α), 62.9 (C6α), 101.2 (C1″α), 73.0 (C3″), 67.0 (C6″), 56.1 (OCH_3), 121.2 (C_3,$C_{3'}$), 142.0 (C_4,$C_{4'}$), 115.3 (C_9,$C_{9'}$), 124.1 (C_{10},$C_{10'}$).

4.4.12.5 Curcuminyl-bis-sucrose, 34a-c: Solid; UV (H_2O, λ_{max}): 193 nm (σ→σ*, ε_{193} – 3938 M^{-1}), 288 nm (π→π*,ε_{288} – 531 M^{-1}), 410 nm (π→π*extended conjugation, ε_{410} – 99 M^{-1}); IR (KBr): 1053 cm^{-1} (glycosidic aryl alkyl C-O-C symmetrical), 1260 cm^{-1} (glycosidic aryl alkyl C-O-C asymmetrical), 3271 cm^{-1} (OH); $[\alpha]^{25}_D$ = +8.0^o (*c* 1, H_2O); MS (*m/z*) - 1039 $[M+Na]^+$; 2D-HSQCT (DMSO-d_6) **C1-O-curcuminyl-bis-sucrose, 34a:** ^{1}H NMR δ_{ppm} (500.13 MHz): 3.54 (H-1), 3.39 (H-6). 5.17 (H-1″α), 3.14 (H-3″), 3.10 (H-4″), 3.50 (H-5″), 3.56 (H-6″a); 3.81 (6H, s, 2-OCH_3), 6.30 (2H, s, H_1), 6.72 (2H, d, J=15.8 Hz, $H_{3,\ 3'}$), 7.7 (2H, d, J=15.8, $H_{4,\ 4'}$), 6.81 (2H, d, J=8.2Hz, $H_{9,\ 9'}$), 7.13 (2 H, dd, J=1.45 Hz, $H_{10,\ 10'}$); ^{13}C NMR δ_{ppm} (125 MHz): 65.1 (C1), 107.1 (C2), 62.0 (C6), 92.0 (C1″α), 73.3 (C3″), 70.0 (C4″), 60.8 (C6″), 101.0 ($C_{1'}$), 55.7 (OCH_3), 183.1 (C_2,$C_{2'}$), 121.0 (C_3,$C_{3'}$), 141.0 (C_4,$C_{4'}$), 126.3 (C_5,$C_{5'}$), 112.0 (C_6,$C_{6'}$), 148.0 (C_7,$C_{7'}$), 116.0 (C_9,$C_{9'}$), 123.0 (C_{10},$C_{10'}$). **C6-O-curcuminyl-bis-sucrose, 34b** ^{1}H NMR δ_{ppm}: 3.55 (H-1), 3.77 (H-3), 3.87 (H-4), 3.78 (H-5), 3.25 (H-6), 5.17 (H-1″α), 3.43 (H-2″), 3.10 (H-3″), 3.63 (H-4″), 3.55 (H-5″), 3.63 (H-6″a), 3.81 (6H, s, 2-OCH_3), 6.50 (2H, s, H_1), 6.72 (2H, d, J=15.8 Hz, $H_{3,\ 3'}$), 7.7 (2H, d, J=15.8, $H_{4,\ 4'}$), 6.81 (2H, d, J=8.2Hz, $H_{9,\ 9'}$),

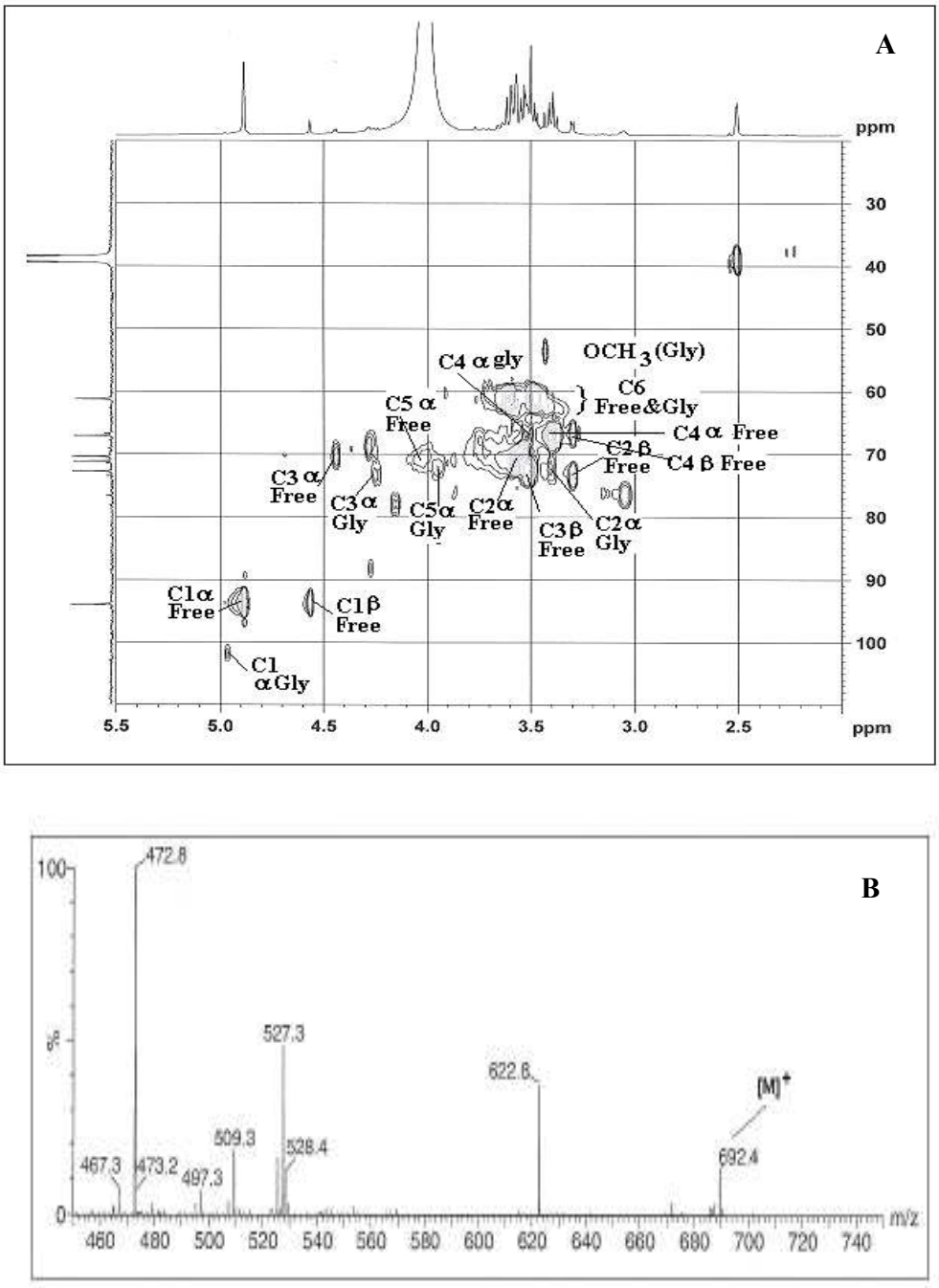

Fig. 4.20 Curcuminyl-bis-α-D-mannoside **32 (A)** 2D HSQCT spectrum (C1-C6 region) **(B)** Mass spectrum.

7.13 (2 H, dd, J=1.45 Hz, $H_{10, 10'}$); ^{13}C NMR δ_{ppm}: 62.0 (C1), 104.0 (C2), 76.8 (C3), 74.8 (C4), 82.2 (C5), 63.2 (C6), 92.0 (C1″α), 72.5 (C2″), 73.0 (C3″), 69.8 (C4″), 74.2 (C5″), 61.0 (C6″), 101.0 ($C_{1'}$), 55.7 (OCH_3), 183.1 (C_2,$C_{2'}$), 121.0 (C_3,$C_{3'}$), 141.0 (C_4,$C_{4'}$), 126.3 (C_5,$C_{5'}$), 112.0 (C_6,$C_{6'}$), 148.0 (C_7,$C_{7'}$), 116.0 (C_9,$C_{9'}$), 123.0 (C_{10},$C_{10'}$). **C6″-O-curcuminyl-bis-sucrose, 34c**: ^{1}H NMR δ_{ppm}: 3.55 (H-1), 3.41 (H-6), 5.17 (H-1″α), 3.56 (H-4″), 3.56 (H-6″a), 3.81 (6H, s, 2-OCH_3), 6.72 (2H, d, J=15.8 Hz, $H_{3, 3'}$), 7.7 (2H, d, J=15.8, $H_{4, 4'}$), 6.81 (2H, d, J=8.2Hz, $H_{9, 9'}$), 7.13 (2 H, dd, J=1.45 Hz, $H_{10, 10'}$); ^{13}C NMR δ_{ppm}: 62.0 (C1), 104.0 (C2), 65.0 (C6), 92.0 (C1″α), 70.0 (C4″α), 60.8 (C6″α), 55.7 (OCH_3), 183.1 (C_2,$C_{2'}$), 121.0 (C_3,$C_{3'}$), 141.0 (C_4,$C_{4'}$), 126.3 (C_5,$C_{5'}$), 112.0 (C_6,$C_{6'}$), 148.0 (C_7,$C_{7'}$), 116.0 (C_9,$C_{9'}$), 123.0 (C_{10},$C_{10'}$).

4.4.12.6 Curcuminyl-bis-D-mannitol, 35: Solid; mp 160 °C UV (H_2O, λ_{max}): 200 nm ($\sigma\rightarrow\sigma^*$, ε_{200} - 7698 M^{-1}), 276 nm ($\pi\rightarrow\pi^*$,ε_{276} - 1085 M^{-1}), 354 nm ($n\rightarrow\pi^*$, ε_{354} – 469 M^{-1}), 412 nm ($\pi\rightarrow\pi^*$ extended conjugation, ε_{412} – 161 M^{-1}); IR (KBr): 1686 cm^{-1} (CO), 1020 cm^{-1} (aryl alkyl C-O-C symmetrical), 1262 cm^{-1} (aryl alkyl C-O-C asymmetrical); $[\alpha]^{25}_D$ = +10.2^o (*c* 1, H_2O); MS (*m/z*) - 719 $[M+Na]^+$; 2D-HSQCT (DMSO-d_6) ^{1}H NMR δ_{ppm} (500.13 MHz): 3.45 (H-1a), 3.58 (H-2), 3.43 (H-3), 3.35 (H-4), 3.45 (H-5), 3.75 (H-6a), 3.80 (6H, s, 2-OCH_3), 5.98 (1H, s, H_1), 6.74 (2H, d, J=15.8Hz, $H_{3, 3'}$), 7.54 (2H, d, J=15.8, $H_{4, 4'}$), 7.28 (2H, s, $H_{6, 6'}$), 6.80 (2H, d, J=8.2Hz, $H_{9, 9'}$), 7.14 (2 H, dd, J=1.45 Hz, $H_{10, 10'}$); ^{13}C NMR δ_{ppm} (125 MHz): 65.0 (C1), 71.0 (C2), 74.0 (C3), 72.0 (C4), 64.0 (C6), 57.0 (OCH_3), 101.0 ($C_{1'}$), 183.5 (C_2,$C_{2'}$), 122.0 (C_3,$C_{3'}$), 140.0 (C_4,$C_{4'}$), 112.0 (C_6,$C_{6'}$), 115.8 (C_9,$C_{9'}$), 122.5 (C_{10},$C_{10'}$).

Curcumin, a higher phenyl propanoid homologue of eugenol also reacted with the same carbohydrate molecules **2, 4, 8, 9** and **11** as eugenol. From the UV spectra, shift in the wavelength for the $\pi\rightarrow\pi^*$ extended conjugation band in the 410 - 430 nm (433 nm

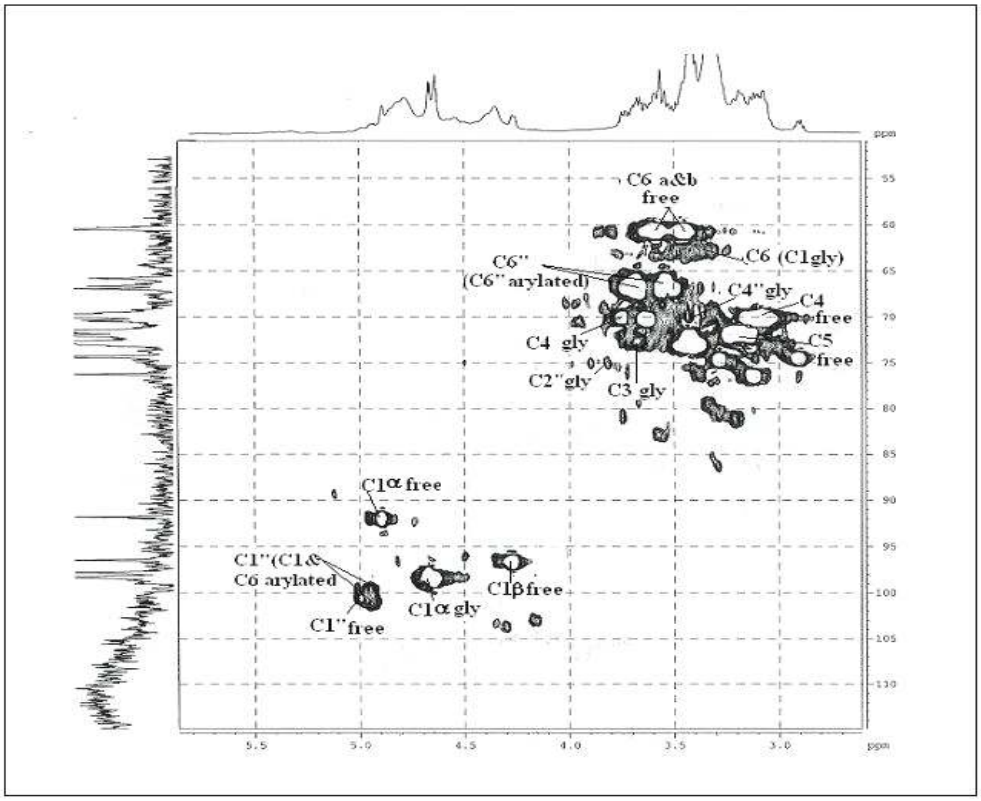

Fig. 4.21 2D-HSQCT spectrum of curcuminyl bis maltoside **33a-c** (maltose region).

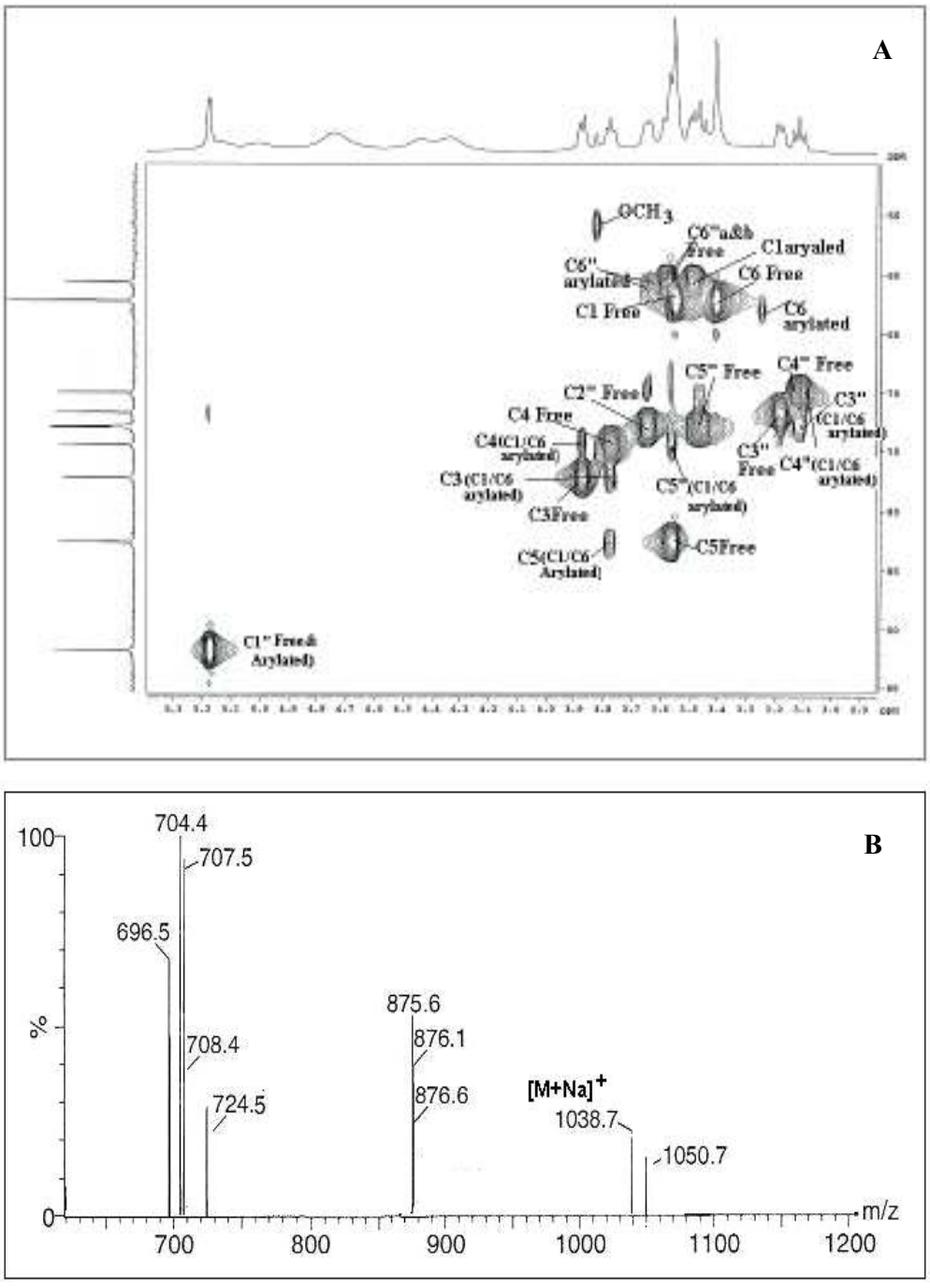

Fig. 4.22 Curcuminyl sucrose **34a-c (A)** 2D-HSQCT spectrum **(B)** Mass spectrum.

for free curcumin) confirmed glycoside formation. IR C-O-C symmetrical stretching frequencies in the range 1020 - 1071 cm^{-1} and asymmetrical stretching frequencies in the range 1254 - 1262 cm^{-1} also indicated that curcumin had undergone glycosylation. The symmetrical chemical shift values in the curcumin region of the product glycosides in the 2D HSQCT spectra indicated that bis glycosylated and bis C6-O-arylated products were formed. Curcumin glycosides did not change color on treatment with dilute alkali indicating that both the phenolic OH groups are glycosylated. Two-dimensional HSQCT NMR spectrum of **30a** showed downfield chemical shift values for C8 and C8' at 150 ppm (149.4 ppm for free **19**) and C1α at 99.0 ppm (^{1}H at 4.66 ppm) respectively confirming that curcumin was glucosylated symmetrically at the C8 and C8' position with the C1 carbon of the α-D-glucose anomer (Fig. 4.18). Chemical shift values of the C6 cross peak (^{13}C at 66.5 ppm and ^{1}H at 3.52 and 3.70 ppm) confirmed C6-O-arylated **30b**, product also being formed. Mass spectrum showed, *m/z* value 691.5 $[M-1]^{+}$ for the bis glycosylated products.

D-Mannose **6**, formed only a bis C1α product **32** (^{13}C at 101 ppm and ^{1}H at 4.99 ppm) Fig. 4.20. Mass spectrum showed *m/z* value at 692.4 $[M]^{+}$ for the bis D-mannoside. Maltose formed C1α maltoside **33a**, C6-O-arylated **33b** and C6"-O-arylated **33c** products. The change in the chemical shift values for C1α (^{13}C at 98.5 ppm and ^{1}H at 4.65 ppm) for **33a**, C6 (^{13}C at 67.0 ppm and ^{1}H at 3.68 ppm) for **33b** and C6" (^{13}C at 67.0 ppm and ^{1}H at 3.52 ppm) for **33c** indicated the formation of the above products (Fig. 4.21). In the mass spectrum, the mass *m/z* peak at 1016 $[M]^{+}$ corresponded to the bis product. A non-reducing sugar, sucrose reacted with **19**, which resulted in the formation of three arylated products, **34a**, **34b** and **34c**. The shift in the peaks for C1-O- (^{13}C at 65.1 ppm and ^{1}H at 3.54 ppm), C6-O- (^{13}C at 63.2 ppm and ^{1}H at 3.25 ppm) and C6"-O- (^{13}C at 65.0 ppm and ^{1}H at 3.41 ppm) indicated formation of **34a, 34b** and **34c**

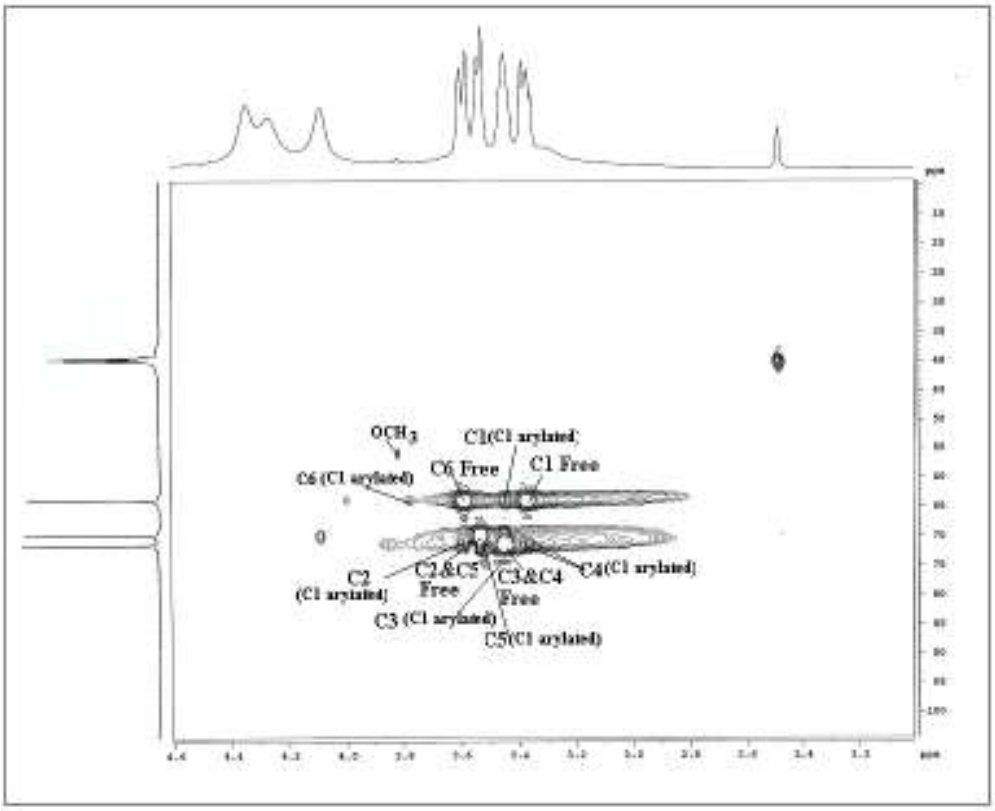

Fig. 4.23 2D-HSQCT spectrum for curcuminyl-bis-D-mannitol **35** (C1-C6 region).

respectively (Fig. 4.22A). Mass spectrum showed the *m/z* peak at 1039 $[M+Na]^+$ confirming the bis arylated product (Fig. 4.22B). D-Mannitol **11**, showed bis C1-O-arylated product (Fig. 23). The C1 cross peak at 65.0 ppm (^1H at 3.45 ppm) indicated the formation of bis C1-O-arylated product **35**, which was also confirmed by the *m/z* peak at 719 $[M+Na]^+$.

Curcuminyl-bis-β-D-glucoside **31** synthesized by using β-glucosidase from sweet almonds was confirmed from the C1 ^{13}C value at 103.2 ppm and the corresponding ^1H value at 4.16 ppm (Fig. 4.19).

4.4.13 Optimization of curcuminyl-bis-α-D-glucoside synthesis using Response Surface Methodology

Response surface methodology is an useful statistical tool to study preparations and processes involving complex and multiple variables (Shieh *et al.* 1995; Huang and Akoh 1996; Ibanoglu and Ibanoglu 2000; Yan *et al.* 2001). Very few reports on optimization relating to enzymatic synthesis of glycosides using response surface methodology (RSM) are currently available (Chahid *et al.* 1994; Ismail *et al.* 1998; Ismail *et al.* 1999). However, RSM studies involving complex aglycons have not been carried out. In this work, amyloglucosidase catalyzed synthesis of curcuminyl-bis-α-D-glucoside by reflux method from curcumin and D-glucose under non-aqueous conditions, optimized using RSM is presented.

A five level (-2, -1, 0, +1, +2), five variable parametric study involving 32 experiments was employed under the Central Composite Rotatable Design. (Montgomery 1991) with amyloglucosidase amount (% w/w of D-glucose), curcumin concentration (mmol), incubation period (h), buffer concentration (mM) and pH as the variables. Extent of glucosylation was the output analyzed. Table 4.10 shows the coded and actual levels of the variables employed in the design matrix. Actual set of experiments undertaken as per CCRD with coded values and the glucosylation yields

obtained are shown in Table 4.11. A second order polynomial equation was developed to study the effects of the variables on the glucoside yields. The general form of Eq (4.1) indicating the effect of variables in terms of linear, quadratic and cross product terms is given below,

$$Y = A_0 + \sum_{i=1}^{N} A_i X_i + \sum_{i=1}^{N} A_{ii} X_i^2 + \sum_{i=1}^{N-1} \sum_{j=i+1}^{N} A_{ij} X_i X_j \qquad (4.1)$$

where Y is the glucosylation yield (%), X_i are the variables, A_o = constant term, A_i are the coefficient of linear terms, A_{ii} are the coefficient of quadratic terms, A_{ij} are the coefficient of cross product terms and N is the number of variables.

Table 4.10 Coded values of the variables and their corresponding actual values used in the design of experiments.

Variables	-2	-1	0	1	2
Amyloglucosidase (%)	10	25	40	55	70
Curcumin (mmol)	0.2	0.4	0.6	0.8	1.0
Incubation period (h)	24	48	72	96	120
Buffer concentration (mM)	0.02	0.04	0.06	0.08	0.1
pH	4.0	5.0	6.0	7.0	8.0

Coefficients of the equation were determined by employing Microsoft Excel software, Version 5.0. Analysis of variance (ANOVA) to test the significance and adequacy of the model for the final predictive equation was also carried out using Microsoft Excel software (Table 4.12). The response surface equation was optimized for maximum yield in the range of the process variables using Microsoft Excel Solver function.

Experimental yields fitted the second order polynomial equation well as indicated by a R^2 value of 0.9 (Table 4.12). ANOVA shows the model to be significant at $P<0.01$. The final predictive equation is given by

$$Y=-61.7385+2.064X_1+28.920X_2+0.264X_3+195.663X_4+4.439X_5-0.014X_1X_1-22.954X_2X_2 -0.0006X_3X_3+1610.79X_4X_4-0.330X_5X_5+0.446X_1X_2-0.003X_1X_3-10.333X_1X_4-0.039X_1X_5- 0.213X_2X_3-381.2\ X_2X_4+5.062\ X_2X_5+4.661X_3X_4-0.022X_3X_5+22.5X_4X_5 \quad (4.2)$$

Where X_1 – amyloglucosidase concentration; X_2 – curcumin concentration; X_3 – incubation period; X_4 – buffer concentration; X_5 – pH.

Table 4.11 Experimental design with experimental and predicted yields of glucosylation based on the response surface equation.

Expt No	Enzyme %	Curcumin (mmol)	Incubation (h)	Buffer concn (mM)	pH	Yield[a] Experimental (%)	Yield Predicted (%)
1	25	0.4	48	0.08	5.0	28.6	29.9
2	25	0.4	48	0.04	7.0	17.4	19.9
3	25	0.4	96	0.04	5.0	20.9	20.7
4	25	0.4	96	0.08	7.0	42.9	44.5
5	25	0.8	48	0.04	5.0	22.1	22.2
6	25	0.8	48	0.08	7.0	35.3	37.1
7	25	0.8	96	0.08	5.0	37.8	37.0
8	25	0.8	96	0.04	7.0	25.6	26.0
9	55	0.4	48	0.04	5.0	28.1	27.2
10	55	0.4	48	0.08	7.0	28.6	29.4
11	55	0.4	96	0.08	5.0	36.8	34.9
12	55	0.4	96	0.04	7.0	24.5	23.9
13	55	0.8	48	0.08	5.0	33.1	31.5
14	55	0.8	48	0.04	7.0	42.1	41.8
15	55	0.8	96	0.04	5.0	35.0	32.0
16	55	0.8	96	0.08	7.0	40.2	38.9
17	10	0.6	72	0.06	6.0	23.6	19.6
18	70	0.6	72	0.06	6.0	21.3	25.2
19	40	0.2	72	0.06	6.0	28.9	27.0
20	40	1.0	72	0.06	6.0	34.4	36.1
21	40	0.6	24	0.06	6.0	33.8	31.4
22	40	0.6	120	0.06	6.0	33.8	36.1
23	40	0.6	72	0.06	4.0	27.7	30.7
24	40	0.6	72	0.06	8.0	40.3	37.2
25	40	0.6	72	0.02	6.0	28.7	29.2
26	40	0.6	72	0.10	6.0	47.1	46.5
27	40	0.6	72	0.06	6.0	38.2	35.3
28	40	0.6	72	0.06	6.0	40.6	35.3
29	40	0.6	72	0.06	6.0	33.3	35.3
30	40	0.6	72	0.06	6.0	35.0	35.3
31	40	0.6	72	0.06	6.0	30.3	35.3
32	40	0.6	72	0.06	6.0	34.9	35.3

[a] Conversion yields were from HPLC with respect to 1 mmol of D-glucose. The experimental yields are an average from two experiments. Error in yield measurements ± 5-10%.

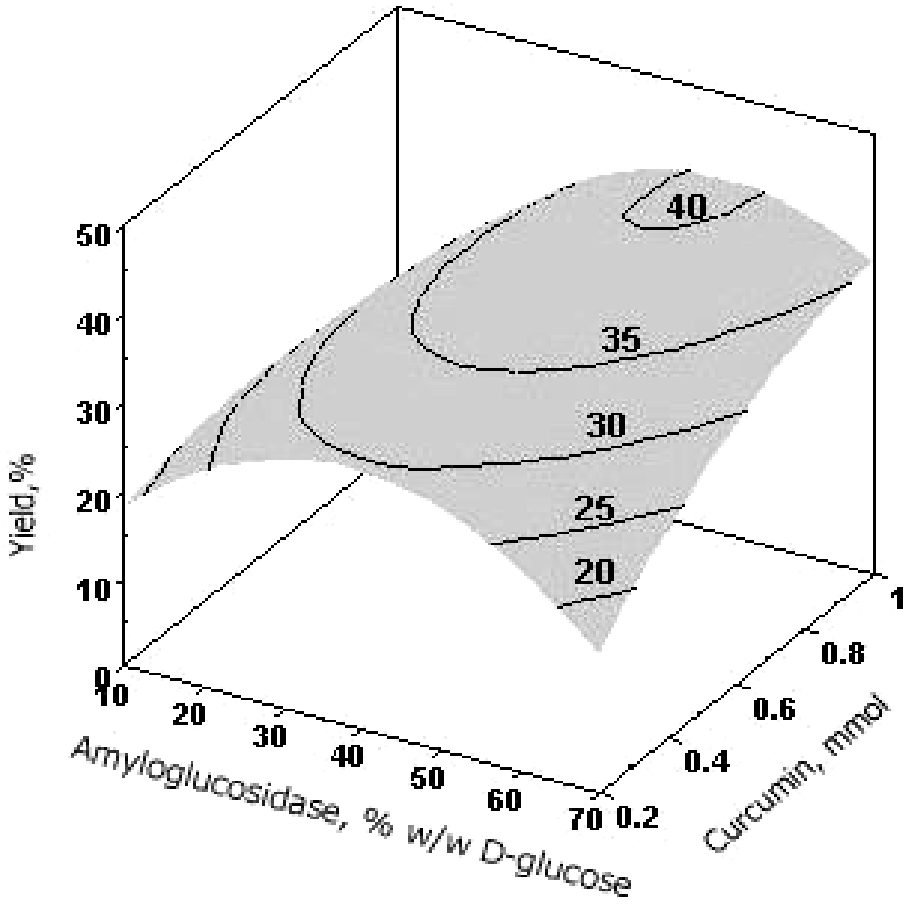

Fig. 4.24 Three dimensional surface and contour plot showing the effect of amyloglucosidase concentration and curcumin concentration on the extent of glucosylation at incubation period – 72 h, buffer concentration – 0.06 mM (0.6 mL of 0.01 M buffer), pH - 6.0.

Average absolute deviation between predicted and experimental yields was found to be 6.0. Amyloglucosidase requires some amount of water to be present for its optimum activity and this is achieved by adding buffer of certain volume, salt concentration and pH (Vic *et al.* 1997; Chahid *et al.* 1992). Salient features of this amyloglucosidase catalyzed reaction are described in the three dimensional surface and contour plots. The plots generated show the effect of two variables with the other three variables maintained at 0 coded levels. In all the experiments, the concentration of D-glucose was maintained at 1.0 mmol.

Effect of various amyloglucosidase and curcumin concentrations on the extent of glucosylation of curcumin is shown in Fig. 4.24. Maximum conversion of 35% was predicted for curcumin concentrations above 0.55 mmol at 35 – 60% (w/w D-glucose) amyloglucosidase concentrations. Iso-glucosylation regions of 15% to 25% yield could be predicted for amyloglucosidase concentrations below 30% and above 60% at all curcumin concentrations in the range 0.2 – 1.0 mmol. While lower amyloglucosidase converted less, higher amyloglucosidase could be inhibitory to curcumin at a constant D-glucose concentration.

Table 4.12 Analysis of variance of the response surface model along with coefficients of the response equation.

Regression Statistics*:*					
Multiple R	0.946				
R Square	0.90				
Standard Error	3.886				
Observations	32				
ANOVA:					
	degrees of freedom	**sum of squares**	**mean sum of squares**	**F ratio**	**Significance F**
Regression	20	1435.6	71.8	4.75	P<0.01**
Residual	11	166.2	15.1		
Total	31	1601.8			

Coefficients	Values of Coefficients	Standard Error	t-Stat
Ao	-61.739	50.06	-1.23
A_1	2.06396	0.576	3.58
A_2	28.9205	43.83	0.66
A_3	0.26375	0.365	0.72
A_4	195.663	438.3	0.45
A_5	4.43902	10.34	0.43
A_{11}	-0.0143	0.003	-4.48
A_{22}	-22.955	17.94	-1.28
A_{33}	-0.0007	0.001	-0.53
A_{44}	1610.8	1794	0.9
A_{55}	-0.3307	0.718	-0.46
A_{12}	0.44583	0.324	1.38
A_{13}	-0.0033	0.003	-1.24
A_{14}	-10.333	3.239	-3.19
A_{15}	-0.0392	0.065	-0.6
A_{23}	-0.2135	0.202	-1.05
A_{24}	-381.25	242.9	-1.57
A_{25}	5.0625	4.858	1.04
A_{34}	4.66146	2.024	2.3
A_{35}	-0.0229	0.04	-0.57
A_{45}	22.5	48.58	0.46

Effect of amyloglucosidase concentration and pH on the extent of glycosylation also exhibited a similar pattern as in Fig. 4.24. A narrow range of amyloglucosidase concentration of 35 – 55% showed maximum glucosylation of 35% at above pH 5.5. Above and below this enzyme concentration range, the conversion yield was lesser in the pH range 4.0 to 8.0. For the hydrolytic activity, the pH optimum for amyloglucosidase is 5.0 and the isoelectric point for the enzyme is 4.2. Above pH 5.5 and towards higher pH 8.0, the ionisable groups especially from acidic amino acid residues (Glu314 and Glu544) in the active site could exist in anionic forms, enabling abstraction of the anomeric hydroxyl proton of glucose to aid in the facile transfer of glucose molecule to curcumin (Frandsen *et al.* 1994; Sierks *et al.* 1990).

Figure 4.25 shows the effect of amyloglucosidase concentration and buffer concentration on the conversion yield of curcuminyl-bis-α-D-glucoside. Buffer

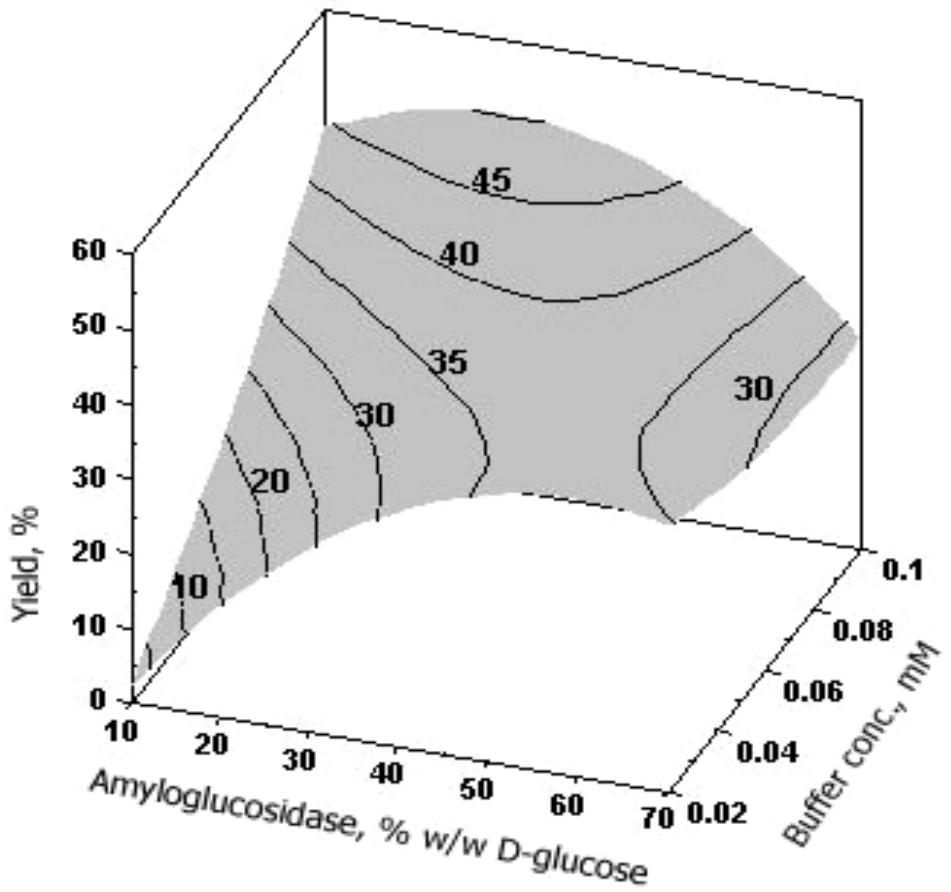

Fig. 4.25 Three dimensional surface and contour plot showing the effect of amyloglucosidase concentration and buffer concentration on the extent of glucosylation at curcumin-0.6 mmol, incubation period-72 h and pH 6.0.

concentration included both the effects of the concentrations of the buffer salts and volume of the buffer. While buffer volume determined the effect of water activity on amyloglucosidase, pH controlled the extent of ionization of the charged amino acid residues of the amyloglucosidase in the active site and on the surface, the latter being also affected by the buffer concentration. Together, both these quantities explain the role of the active conformation of the enzyme, on catalysis at the refluxing temperature of the solvent (at 68 ^{o}C). After 120 h of incubation period, amyloglucosidase was found to lose only 20% of its activity. Between an amyloglucosidase concentration range of 15 to 45%, maximum conversion of 45% could be observed in the buffer concentration range 0.095 to 0.1 mM (0.95 to 1.0 mL of 0.01 M pH 6.0 buffer). The same amyloglucosidase concentration range could not give good conversion yields at buffer concentrations less than 0.08 mM (0.8 mL of 0.01 M pH 6.0 buffer). Besides, amyloglucosidase concentrations above 60%, also showed lesser yields in the buffer concentration range 0.03 to 0.1 mM (0.3 to 1.0 mL of 0.01 M pH 6.0). This feature clearly shows that the extent of glucosylation could be dictated by a critical buffer (0.95 to 1.0 mL of 0.01 M pH 6.0) to enzyme ratio (15 to 45% w/w D-glucose).

Different concentrations of amyloglucosidase at different incubation periods also showed a behavior similar to Fig. 4.24. Here also, maximum conversion yield of 35% was observed in the amyloglucosidase range 30% - 50%. Incubation periods above 60 h showed higher glucosylation.

Effect of curcumin and buffer concentrations on the extent of glucosylation is shown in Fig. 4.26. At a lower buffer concentration of 0.02 mM (0.2 mL of 0.01 M pH 6.0 buffer) conversion yield increased with increase in curcumin concentration and 35% yield was obtained at 1.0 mmol curcumin. Also, at lower curcumin concentrations, extent of glucosylation increased with increase in buffer concentration. A maximum yield of

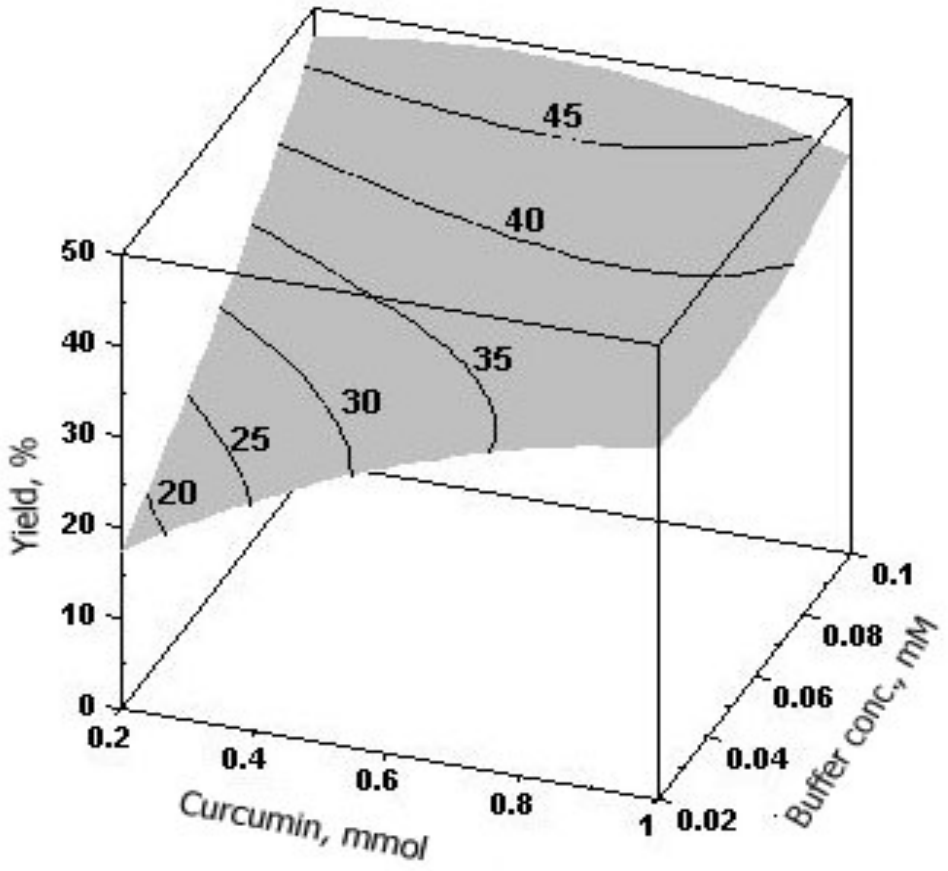

Fig. 4.26 Three dimensional surface and contour plot showing the effect of curcumin concentration and buffer concentration on the extent of glucosylation at amyloglucosidase – 40% (w/w D-glucose), incubation period-72 h and pH – 6.0.

45% was obtained at 0.1 mM (1.0 mL of 0.01 M pH 6.0 buffer) buffer concentration at 0.2 mmol curcumin concentration. However, at higher curcumin concentrations towards 1.0 mmol, increase in glucosylation with increase in buffer concentration was only marginal.

Effect of curcumin concentration and pH on the glucosylation of curcumin is shown in Fig. 4.27. At lower pH (pH 4.0), the extent of glucosylation increased marginally with increase in curcumin concentration and reached a maximum of 30% at 0.6 mmol curcumin concentration which decreased with further increase in curcumin concentration. At higher curcumin concentration of 1.0 mmol, conversion increased with increase in pH from 4.0 to 8.0 reaching a maximum of 45 %.

At all the buffer concentrations (0.2 to 1.0 mL of 0.01M) employed, the effect of pH in the 4.0 to 8.0 pH range on the extent of glucosylation was only marginal. However, with increase in buffer concentration, glucosylation increased in the above specified pH range.

A maximum yield of 65.6% was predicted based on the response model for an amyloglucosidase concentration of 16.9% (w/w D-glucose), 0.33 mmol curcumin concentration, 120 h incubation period and 0.1 mM (1.0 mL of 0.01M pH 6.0 buffer) buffer concentration at pH 7.5. Experiment conducted at the above optimum conditions resulted in an yield of 56.3%. Validation of the response model was also tested by carrying out experiments at selected random conditions. The yields obtained from validation experiments also agreed with the predicted yields with an average absolute deviation of 12.5% (Table 4.13).

Thus, this study showed that this model is very good in predicting the glucosylation of curcumin by the amyloglucosidase enzyme.

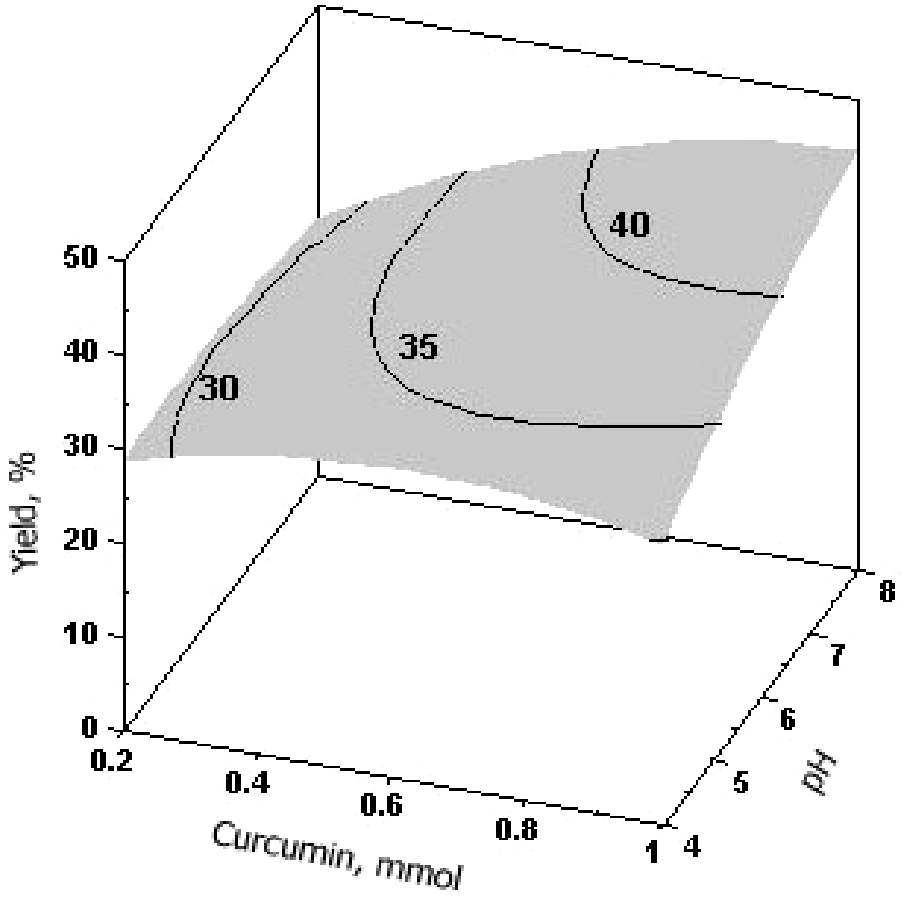

Fig. 4.27 Three dimensional surface and contour plot showing the effect of curcumin concentration and pH on the extent of glucosylation at amyloglucosidase – 40% (w/w D-glucose), incubation period -72 h and buffer concentration – 0.06 mM (0.6 mL of 0.01M buffer).

Table 4.13 Validation of experimental data.

Expt No	Enzyme (%)	Curcumin (mmol)	Incubation period (h)	Buffer conc. (mM)	pH	% Yield Predicted	% Yield[a] Experimental
1	40	0.6	72	0.06	6.0	35.4	39.2
2	40	0.3	72	0.06	5.0	29.5	31.0
3	25	0.6	72	0.07	6.0	34.6	37.1
4	40	0.9	110	0.06	6.0	35.2	28.3
5	40	0.5	20	0.06	6.0	28.5	31.4
6	40	0.6	70	0.06	6.0	35.3	35.7
7	60	0.9	72	0.06	6.0	35.5	36.7
8	20	0.5	72	0.06	6.0	27.3	31.3
9	35	0.6	72	0.06	6.5	35.4	28.0
10	20	0.6	72	0.06	5.5	26.5	32.5
11	40	0.6	65	0.06	6.0	35.0	41.5
12	15	0.6	50	0.06	6.0	20.9	27.5
13	40	0.6	72	0.09	7.0	45.3	46.5
14	40	0.6	72	0.04	5.0	30.1	34.2
15	16.9	0.33	120	0.1	7.5	65.6	56.3

[a] Conversion yields were from HPLC with respect to 1 mmol of D-glucose. The experimental yields are an average from two experiments. Error in yield measurements ± 5-10%.

4.4.14 Kinetic study on the synthesis of curcuminyl-bis-α-D-glucoside using amyloglucosidase

Kinetic studies on few enzymatic hydrolytic reactions involving glucosidases and amyloglucosidase are known (Hiromi *et al.* 1983; Tanaka *et al.* 1983; Ohinishi and Hiromi 1989; Goto *et al.* 1994). However, few kinetic studies on the glycosylation reaction especially those involving a carbohydrate and aglycon molecules have been made. Kinetic studies of synthetic reactions with lipases, show that they follow Ping-Pong Bi-Bi mechanism in several esterification reactions (Marty *et al.* 1992; Janssen *et al.* 1999; Kiran and Divakar 2002; Yadav and Lathi 2004). This mechanism involves binding of acid and alcohol in successive steps releasing water and the product ester

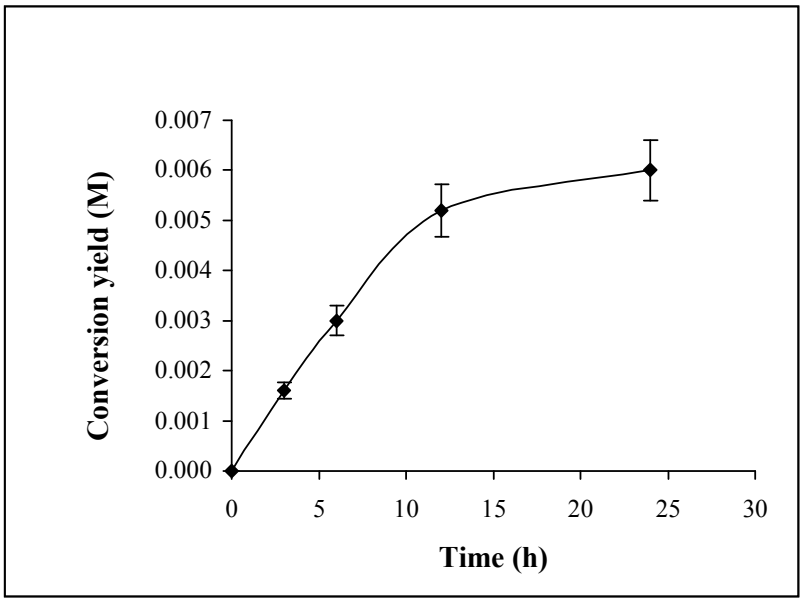

Fig. 4.28 Initial rate (v) plot - conversion yields versus incubation period: Curcuminyl-bis-α-D-glucoside: D-glucose 20 mM, curcumin 5mM, amyloglucosidase 90 mg and 0.6 ml (0.06mM) of 0.01 M, pH 6.0 phosphate buffer.

again in succession. However, no such mechanism has been reported in glycosylation reactions.

Glucoamylases possesses $(\alpha/\alpha)_6$ barrel fold structure which is different from the $(\beta/\alpha)_8$ barrel fold structure of α-amylase, β-amylase and α-glucosidase (Svensson *et al.* 1990; Aleshin *et al.* 1992; Chiba 1997). In the catalytic domain, two glutamic acids Glu314 and Glu544 in *Rhizopus oryzae* (Ashikari *et al.* 1986; Aleshin *et al.* 1992) are reported to be the catalytic amino acid residues directly involved as acid base catalysts in the hydrolytic reaction (Sierks *et al.* 1990; Chiba 1997). It has also been shown that oxo-carbenium ion mechanism is the most suitable for the hydrolytic reaction in both "retaining" and "inverting" enzymes (Chiba 1995). Although, no decisive mechanism has been proposed so far, for the glycosylation reactions, it is generally believed that the oxo-carbenium ion mechanism could be the most probable one.

In the present work, an attempt has been made to carry out a detailed kinetic investigation on the glucosylation reaction involving an amyloglucosidase from *Rhizopus* sp., between D-glucose and curcumin leading to the synthesis of curcuminyl-bis-α-D-glucoside **30a** and **b**. The results from these investigations are described below.

Typical rate plot for the curcumin glucosidic reaction has been shown in Fig. 4.28. Initial velocities (v) were found to be in the range 0.08 to $5.2 \times 10^{-5} Mh^{-1}$.mg protein. At initial periods of incubation, the reaction is relatively fast and slows down at longer incubation periods beyond 24 h which could be due to establishment of equilibrium between substrates and the products. Effect of external mass transfer phenomenon involving internal and external diffusion (Marty *et al.* 1992), if any, were not tested in this present work.

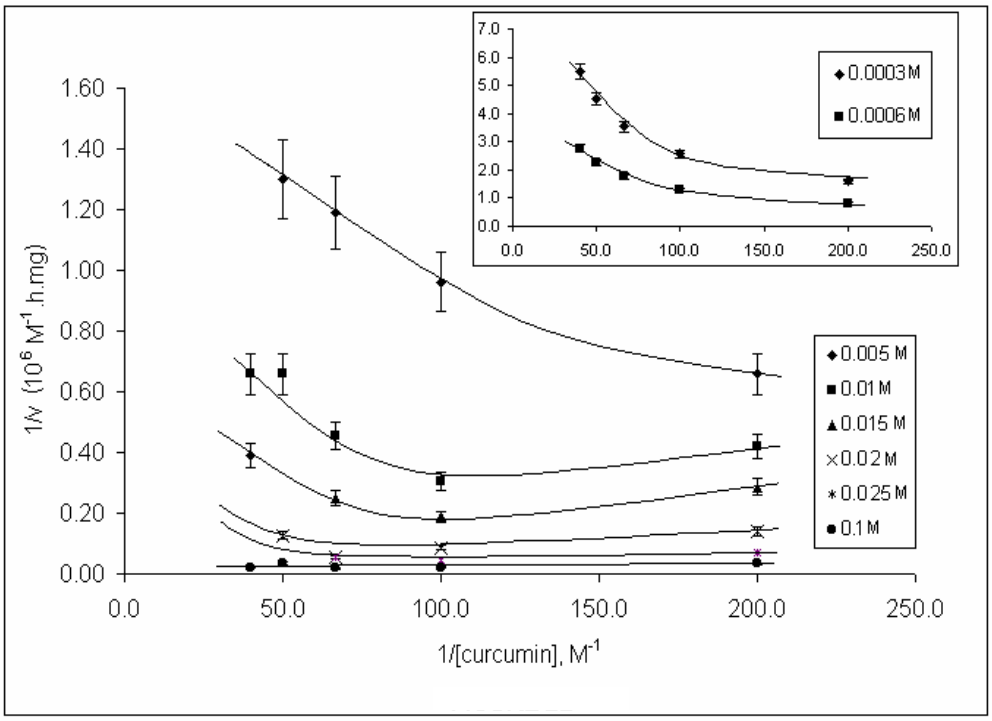

Fig. 4.29 Double reciprocal plot: 1/v versus 1/[curcumin], series of plots from experimentally measured initial rate values showing the effect of varying curcumin concentrations at different fixed concentrations of D-glucose in the range 5 mM to 0.1M. Insets show plots obtained from the computer simulation procedure for 0.3 mM and 0.6 mM concentrations of D-glucose.

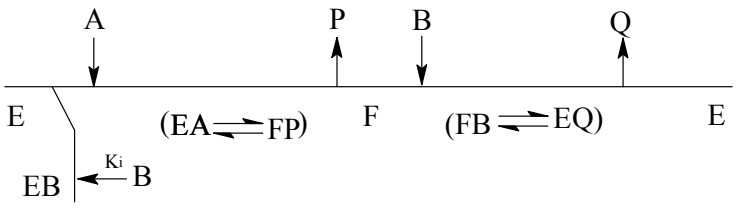

Scheme 4.4 Ping-Pong Bi-Bi model with competitive substrate inhibition

Where, A = D-glucose, P = H_2O, B = curcumin, F = glucosyl-amyloglucosidase complex, E = amyloglucosidase, EA = amyloglucosidase-glucose complex, FP = glucosyl-amyloglucosidase-water complex, EB = amyloglucosidase-curcumin complex, K_i = dissociation constant of amyloglucosidase-inhibitor complex, FB = glucosyl-amyloglucosidase-curcumin complex, EQ = amyloglucosidase-glucoside complex, Q = curcuminyl glucoside

Double reciprocal plots were constructed by plotting 1/v versus 1/[curcumin] and 1/v versus 1/[D-glucose]. The plots are shown in Fig. 4.29 and Fig. 4.30. Figure 4.29 show series of curves obtained for different fixed level concentrations of D-glucose at varying curcumin concentrations, where slight increase in initial rates at lower curcumin concentrations are observed and at higher concentrations of curcumin the rates reduce drastically. Also, increase in D-glucose increases the initial rate at all curcumin concentrations. Figure 4.30 show series of lines obtained for different fixed level concentrations of curcumin at varying D-glucose concentrations, where at fixed lower curcumin concentrations, the lines are parallel and at fixed higher curcumin concentrations, lines with different slopes are observed. The plots in Figures 4.29 and 4.30 showed that the kinetics could be best described by (Segel 1993) Ping-Pong Bi-Bi model **(Scheme 4.4)** with competitive substrate inhibition leading to dead-end inhibition. The rate equation describing the model is shown as:

$$\frac{v}{V_{max}} = \frac{[A]\,[B]}{K_{m\,A}\,[B]\,(1 + [B]/K_i) + K_{m\,B}\,[A] + [A]\,[B]} \qquad (4.3)$$

Where, v = initial rate, V_{max} = maximum velocity, A = D-glucose concentration, B = curcumin concentrations, K_{mA} = Michelis-Menten constant for D-glucose, K_i = dissociation constant of the amyloglucosidase-inhibitor (curcumin) complex, K_{mB} = Michelis-Menten constant for curcumin. Since the initial rates are in Mh^{-1}.mg of the protein, V_{max} is expressed as k_{cat} as $k_{cat} = V_{max}$/enzyme concentration.

Table 4.14 Kinetic parameters for the synthesis of curcuminyl-bis-α-D-glucoside.

Name of the compound		k_{cat} 10^{-5}M/h. mg	K_{mA} mM	K_{mB} mM	K_i mM
Curcuminyl-bis-α-D-glucoside	**a**	**5.0±0.48**	**88.9±8.7**	**25.1±2.3**	**7.0±0.75**
	b	**6.07±0.58**	**10.0±0.9**	**4.6±0.5**	**3.0±0.28**

A = D-glucose, B = curcumin, a = graphical method, b = computer simulated values

The four important kinetic parameters $K_{curcumin}$, $K_{m\ D\text{-}glucose}$, $K_{m\ curcumin}$ and $k_{cat\ curcumin}$ were evaluated graphically. Intercept of the positive slopes of Figure 4.29 on the Y- axis, especially, at the highest concentration of D-glucose (0.1 M) employed, gave 1/ k_{cat} for curcumin (Table 4.14). Figure 4.31 shows the replot of slopes (Fig. 4.30) of 1/[D-glucose] versus [curcumin], from which slope = $K_{m\ D\text{-}glucose}/(k_{cat}\ K_i)$, Y intercept = $K_{m\ D\text{-}glucose}/\ k_{cat}$ and X intercept = $-K_i$, where K_i represents dissociation constant for the amyloglucosidase-curcumin complex. $K_{m\ curcumin}$ was obtained by equation 4.4 generated by rearranging equation 4.3,

$$K_{mB} = \frac{k_{cat}\,[B]}{v} - \frac{K_{mA}\,[B]}{[A]} - \frac{K_{mA}\,[B]^2}{[A]\,K_i} - [B] \qquad (4.4)$$

where, K_{mB} = Michelis-Menten constant for curcumin.

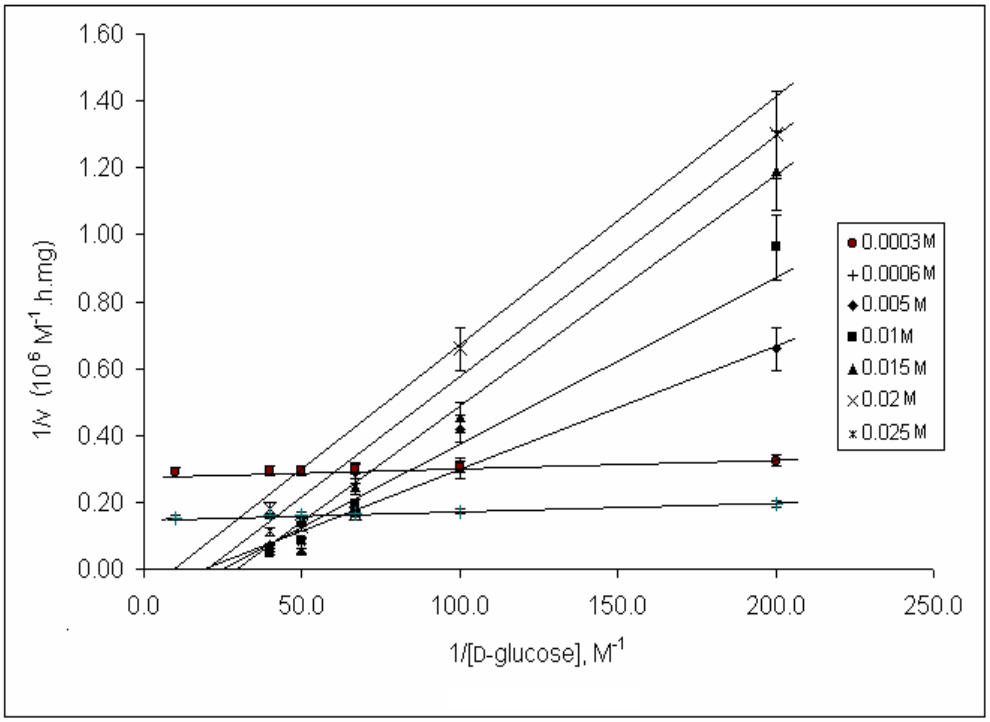

Fig. 4.30 Double reciprocal plot: 1/v versus 1/[D-glucose], series of plots from experimentally measured initial rate values showing the effect of varying D-glucose concentrations at different fixed concentrations of curcumin in the range 5 mM to 0.025 M. The plots shown for 0.3 mM and 0.6 mM concentrations of curcumin are from the computer simulation procedure.

The values of the four important kinetic parameters, $k_{cat,}$ K_i, K_{mA}, and $K_{mB,}$ were also estimated mathematically through computer simulation. The range of values tested for these parameters and the constraints employed for the iteration procedure is as follows: $k_{cat\ curcumin} < 0.01\ Mh^{-1}.mg$, $K_{i\ curcumin} < K_{m\ curcumin,}$ $K_{m\ curcumin} < K_{m\ D\text{-}glucose}$ and $K_{m\ D\text{-}glucose} < 0.1$ M. The iteration procedure involved determination of initial velocities (v_{pred}) by incrementing the above mentioned four kinetic parameters in eq. 4.2 from their lowest approximations (bound by the above mentioned constraints) and subjecting the v_{pred} (obtained for all the concentrations of D-glucose and curcumin) to non-linear optimization, by minimizing the sum of squares of deviations between v_{pred} and v_{exptl}. The set of four kinetic parameters which resulted from minimum sum of squares of deviation between v_{pred} and v_{exptl} were considered to be the best set and they are shown in Table 4.14 which lists graphical as well as the computer simulated values for comparison. Table 4.15 shows the comparison between experimental and predictive initial rate values obtained under different reaction conditions. Computer simulation showed $v_{predicted}$ values with R^2 value of 0.83 emphasizing that this model is reasonably good in explaining the kinetics of this reaction.

With increasing concentrations of D-glucose (Fig. 4.29), the rate increases at lower concentrations of curcumin. At higher concentrations of curcumin corresponding to minimum 1/v, the rate decreases, the plots tend to become closer to 1/v axis. Figure 4.30 also reflect the same behaviour, where at lower concentrations of curcumin, the lines appear parallel probably so for as $K_i > K_{mB}$. However at higher fixed concentrations of curcumin, the slopes vary drastically where $K_i < K_{mB}$. Thus the kinetic data clearly shows the inhibitory nature of curcumin in this reaction. Competition between D-glucose and curcumin for the active site (binding site) of amyloglucosidase could result in

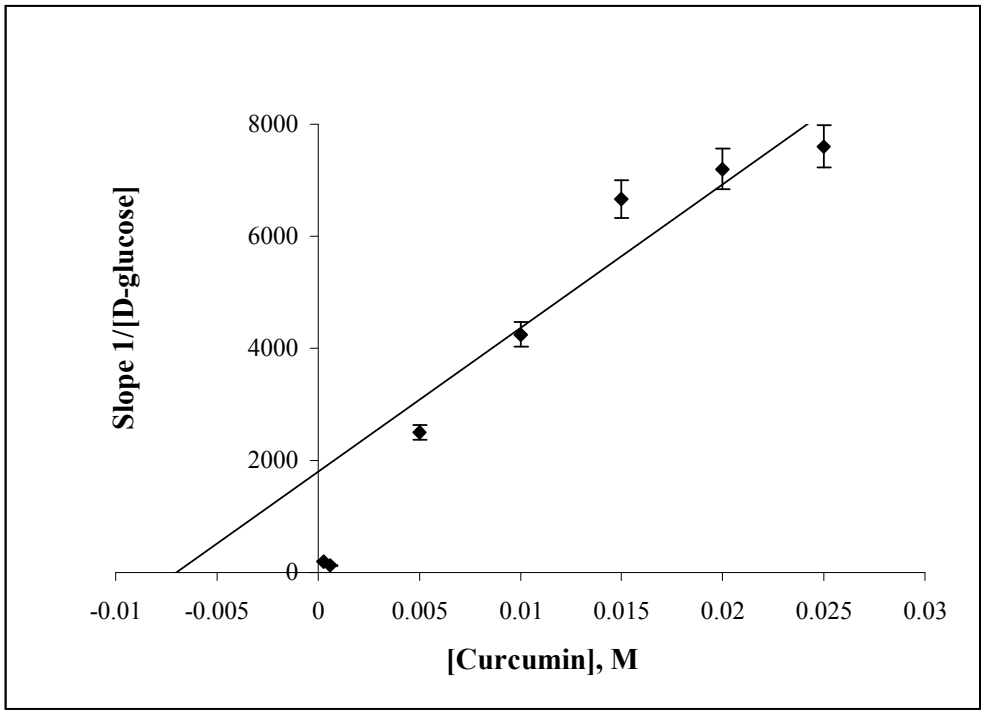

Fig. 4.31 Replot of Slope (from Fig. 4.30) - Slope 1/[D-glucose] versus [curcumin].

predominant curcumin binding at higher concentrations, displacing D-glucose, leading to the formation of the dead-end amyloglucosidase-curcumin complex.

Table 4.15 Experimental and predicted initial rate values for the synthesis of curcuminyl-bis-α-D-glucoside

D-Glucose (M)	Curcumin (M)	$v_{experimental}$ $10^{-5}Mh^{-1}$. mg	$v_{predictive}$ $10^{-5}Mh^{-1}$. mg
0.005	0.005	0.153	0.837
0.005	0.01	0.105	0.600
0.005	0.015	0.084	0.456
0.005	0.02	0.076	0.367
0.005	0.025	0.250	0.306
0.01	0.005	0.238	1.324
0.01	0.01	0.336	1.048
0.01	0.015	0.225	0.831
0.01	0.02	0.153	0.682
0.01	0.025	0.153	0.577
0.015	0.005	0.352	1.643
0.015	0.01	0.543	1.396
0.015	0.015	0.411	1.144
0.015	0.02	0.611	0.957
0.015	0.025	1.204	0.820
0.02	0.005	0.723	1.867
0.02	0.01	1.168	1.674
0.02	0.015	1.835	1.410
0.02	0.02	0.795	1.199
0.02	0.025	1.223	1.038
0.025	0.005	1.456	2.034
0.025	0.01	2.202	1.902
0.025	0.015	1.758	1.638
0.025	0.02	0.568	1.413
0.025	0.025	0.847	1.235
0.1	0.005	3.000	2.779
0.1	0.01	4.580	3.208
0.1	0.015	5.230	3.185
0.1	0.02	2.820	3.041
0.1	0.025	4.580	2.868

In this reaction $K_{m\ D\text{-}glucose}$ (10.0±0.9 mM, Table 4.14) is always higher than K_{mB} (4.6±0.5 mM) which shows that while glucose binding could lead to product formation, curcumin binding to the active site could result in inhibition of the amyloglucosidase activity.

Catalysis occurs mainly between subsites 1 and 2 of glucoamylase and the active site of *Aspergillus niger* glucoamylase is identical to that of *Rhizopus oryzae* (Stoffer *et al.* 1995). Sugar OH groups are held firmly in the active site subsites 1 and 2 of *Rhizopus oryzae* through hydrogen bonds with Arg191, Asp192, Leu312, Trp313, Glu314, Glu315 and Arg443 (Ashikari *et al.* 1986; Aleshin *et al.* 1992). The above mentioned residues can also stabilize planar curcumin bound to the active site through hydrogen bonds. Curcumin could form effective hydrogen bonds between the enolic, phenolic OH and the carbonyl group of curcumin and the Arg191, Asp192, Trp313, Glu315 and Arg443 residues. Hence, higher concentrations of curcumin is capable of displacing the glucose-oxo-carbenium ion from the active site and occupy its position instead, leading thereby to dead end inhibition. This may not happen at lower concentrations of curcumin.

Several lipase catalyzed esterification reactions have been described to follow Ping-Pong Bi-Bi mechanism, which deals with two substrates (acid and alcohol) and two products (water and ester). So far, enzyme mediated glycosylation, especially the one involving a carbohydrate molecule and an aglycon molecule has not been reported to follow Ping-Ping Bi-Bi model. This could be the first report of its kind.

4.5 α-Tocopheryl-α-D-glucoside

Amyloglucosidase catalyzed synthesis of α-tocopheryl-α-D-glucoside was optimized in terms of incubation period, pH, buffer concentration, enzyme concentration and α-tocopherol concentration **(Scheme 4.5)**. The reactions were carried out under nitrogen atmospheric pressure. Di-isopropyl ether solvent was used as reaction media and the temperature maintained was 68 °C. The other reaction conditions employed for the optimization were D-glucose (0.5 mmol), α-tocopherol (0.5 – 2.5 mmol), 10-80% (w/w D-glucose) amyloglucosidase, 0.04-0.4 mM (0.4-4.0 mL in 100 mL of reaction mixture) pH 4.0-8.0 buffer, 100 mL di-isopropyl ether solvent and 3 to 96 h incubation

(Scheme 4.5). The synthetic and work up procedure has been given in detail (Experimental section). The reaction mixture was analyzed by HPLC and the conversion yields were determined from the HPLC peak areas of the unreacted D-glucose and the product glucoside and expressed in percentage. HPLC retention times are 5.20 min for D-glucose and 8.18 min for α-tocopheryl-α-D-glucoside. Error based on the HPLC measurement will be in the order of ± 5-10%. The product glucoside was isolated using Sephadex G-15 (100x1cm) column, eluting with water and subjected to spectroscopic characterization by UV, IR, MS, 2D NMR and by optical rotation. An attempt was made to synthesize the α-tocopheryl glycosides using various other earlier mentioned carbohydrates **2-12** but no other carbohydrates except D-glucose underwent glycosylation with α-tocopherol.

4.5.1 Effect of incubation period on α-tocopheryl-α-D-glucoside synthesis

The effect of incubation period studied from 3 h to 96 h on α-tocopheryl-α-D-glucoside at D-glucose and α-tocopherol (1: 1 molar ratio), 40% w/w (D-glucose) amyloglucosidase and 0.2 mM (2.0 mL), pH 7.0 showed maximum conversion yield at

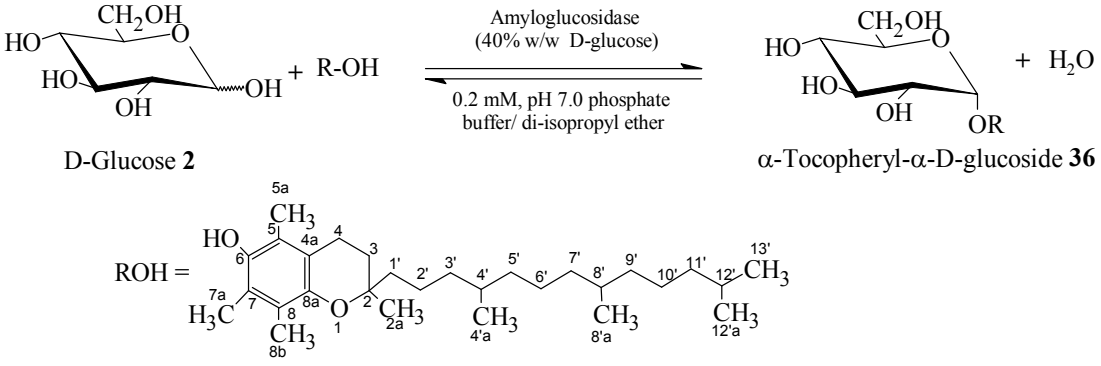

Scheme 4.5 Amyloglucosidase catalyzed synthesis of α-tocopheryl-α-D-glucoside

72 h of incubation period (52% yield). The conversion yield increased with increase in incubation period from 3 h (2% yield) to 72 h (52% yield) and decreased at 96 h of

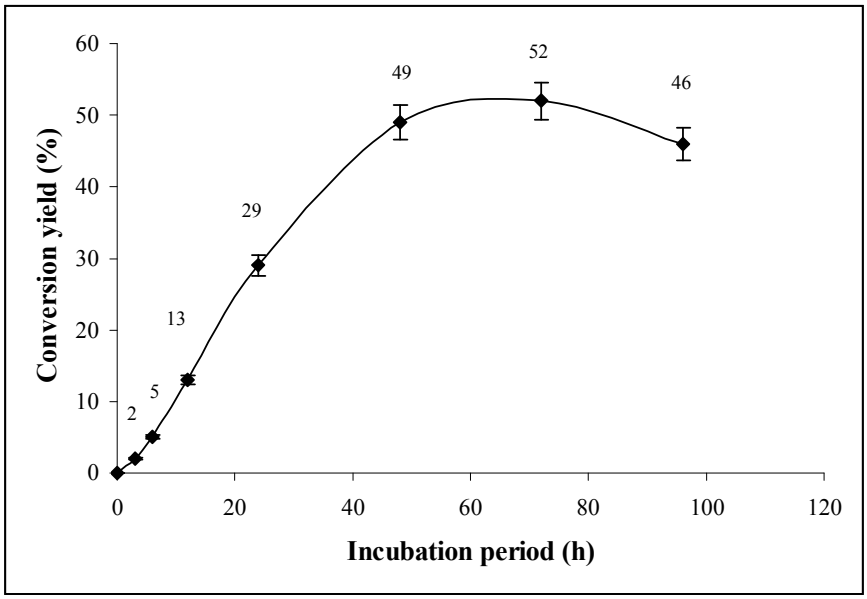

Fig. 4.32 Effect of incubation period on α-tocopheryl-α-D-glucoside synthesis. Conversion yields were from HPLC with respect to 0.5 mmol of maltose. Reaction conditions: D-glucose – 0.5 mmol, α-tocopherol – 0.5 mmol, enzyme – 40% (w/w D-glucose), 0.2 mM (2.0 mL), pH 7.0 phosphate buffer, solvent-di-isopropyl ether, temperature - 68 °C.

incubation period (46% yield). The results are shown in Figure 4.32. From the initial slope the rate of the reaction was found to be 5.7 μmol/h.

4.5.2 Effect of pH on α-tocopheryl-α-D-glucoside synthesis

Buffer pH was varied from pH 4.0 to 8.0. The concentration of the buffer employed was 0.1 mM (1.0 mL of 10 mM buffer added in 100 mL of solvent). The glycosylation yield was the highest at pH 7.0 (42%). A conversion yield of 37% was obtained at pH 6.0. All the other pH gave yields less than 24% (Table 4.16).

Table 4.16 Effect of buffer pH on the synthesis of α-tocopheryl-α-D-glucoside[a].

pH[b]	Conversion yield %
4.0	22
5.0	24
6.0	37
7.0	42
8.0	22

[a]Conversion yields from HPLC with respect to 0.5 mmol of D-glucose. Error in yields measurements ± 5-10%. α-Tocopherol-0.5 mmol, enzyme – 40% (w/w D-glucose), 0.1 mM (1.0 mL) buffer, incubation – 72 h and temperature – 68 °C.

4.5.3 Effect of buffer concentration on α-tocopheryl-α-D-glucoside synthesis

At pH 7.0, buffer concentration was varied from 0.04 mM to 0.4 mM (0.4 mL to 4.0 mL) concentration. The glycosylation yields increased with the increase in buffer concentrations from 0.04 mM (30% yield) to 0.2 mM (52% yield) and thereafter decreased to 9.0% at 0.4 mM (4.0 mL) concentration (Fig. 4.33). Thus the critical buffer concentration was found to be 0.2 mM (2.0 mL).

4.5.4 Effect of amyloglucosidase concentration on α-tocopheryl-α-D-glucoside synthesis

Effect of increase in the enzyme concentration on the synthesis of α-tocopheryl-α-D-glucoside was studied. The enzyme concentration was varied from 10 to 80% (w/w

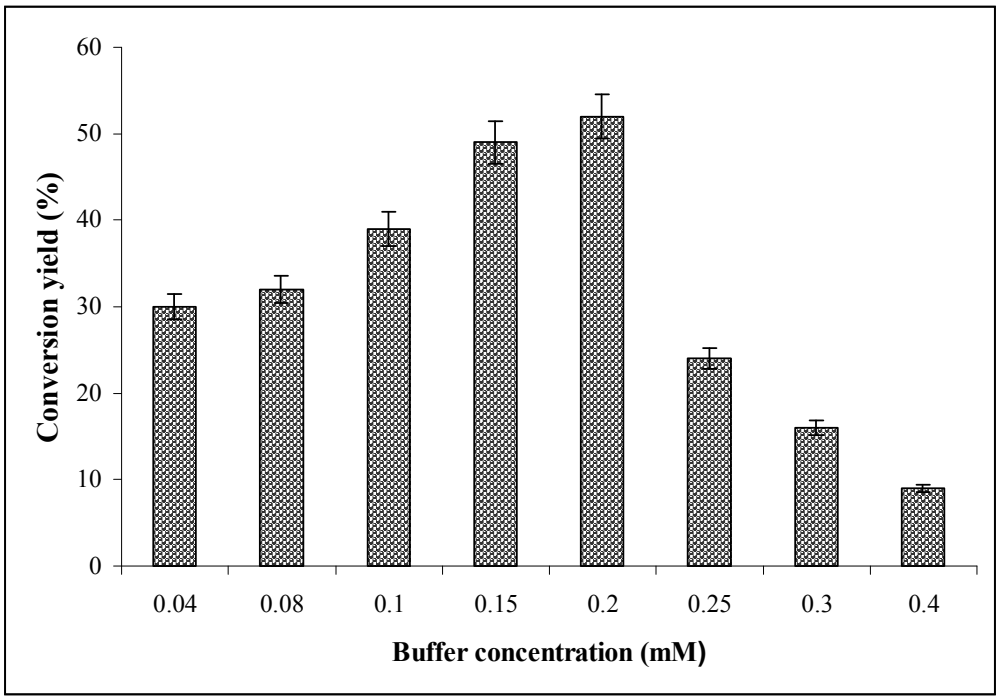

Fig. 4.33 Effect of buffer concentration on α-tocopheryl-α-D-glucoside synthesis. Conversion yields were from HPLC with respect to 0.5 mmol of maltose. Reaction conditions: α-tocopherol – 0.5 mmol, enzyme – 40% (w/w D-glucose), 10 mM, pH 7.0 phosphate buffer, solvent-di-isopropyl ether, incubation-72 h, temperature - 68 °C.

D-glucose) at 1:1 molar ratio of D-glucose and α-tocopherol, 0.2 mM (2.0 mL) pH 7.0 phosphate buffer (2.0 mL) and 72 h of incubation. A 40% enzyme concentration showed the highest glycosylation yield of 52%. At other enzyme concentrations the yields are: 10% enzyme - 25% yield, 20% enzyme - 28% yield, 60% enzyme-34% yield and 80% enzyme-25% yield.

4.5.5 Effect of α-tocopherol concentration on α-tocopheryl-α-D-glucoside synthesis

α-Tocopherol concentration was varied from 0.5 mmol to 2.5 mmol at a fixed D-glucose concentration of 0.5 mmol. The conversion yield was found to decrease with increasing α-tocopherol concentration (Table 4.17). A 1:1 molar ratio of D-glucose and α-tocopherol found to give the best results (yield 52%).

Thus the optimum condition determined for the reaction were found to be D-glucose and α-tocopherol in the 1:1 molar ratio, 40% (w/w D-glucose) amyloglucosidase, 0.2 mM (0.2 mL) pH 7.0 phosphate buffer and 72 h of incubation period.

Table 4.17 Effect of α-tocopherol concentration on the synthesis of α-tocopheryl-α-D-glucoside [a].

α-Tocopherol (mmol)	% Yield
0.5	52
1.0	33
1.5	24
2.0	15
2.5	16

[a]Conversion yields from HPLC with respect to 0.5 mmol D-glucose concentration. Error in yield measurements ± 5-10%. Enzyme – 40% (w/w D-glucose), incubation period – 72 h, solvent-di-isopropyl ether, temperature – 68 °C. 0.2 mM (2.0 mL of 10 mM buffer added in 100 mL of solvent) of pH 7.0 phosphate buffer.

4.5.6 Synthesis of α-tocopheryl glucoside using β-glucosidase

α-Tocopheryl glucoside was also synthesized using β-glucosidase from sweet almonds. The optimum conditions employed were 1:1 D-glucose and α-tocopherol, 0.2

mM (2.0 mL) pH 7.0 phosphate buffer, 40% enzyme and 72 h of incubation period. The reaction mixture analyzed by HPLC showed 24% yield. The glucoside was isolated by column chromatography by using Sephadex G15 as column material and water as eluent. Spectral characterization (UV, IR, MS and 2D HSQCT) for the isolated glucoside confirmed that the formation was α-tocopheryl-bis-β-D-glucoside **37**.

4.5.7 Spectral characterization

α-Tocopheryl glucosides were characterized by UV, IR, 2-D NMR (HSQCT) and optical rotation, which provided information on the product formed. The structures of the glycosides formed, HPLC yield and product proportions are presented in the Table 4.18. Only resolvable signals are shown. Some assignments are interchangeable. D-Glucose signals are double primed. The numbering of carbon atoms in α-tocopherol and its glycosides are according to the nomenclature proposed by the IUPAC (IUPAC-IUB 1982). Since these glycosides are surfactants, they tend to aggregate in solution giving rise to broad signals. Hence coupling constant values could not be resolved satisfactorily.

α-Tocopherol: Viscous liquid; bp 220 °C; UV (DMSO, λ_{max}): 228 nm ($\pi\rightarrow\pi^*$, ε_{228} – 4330 M^{-1}), 292 nm ($n\rightarrow\pi^*$,ε_{292} – 2580 M^{-1}), IR (stretching frequency): 3472 cm^{-1} (OH), 1616 cm^{-1} (aromatic C=C). ^{13}C NMR δ_{ppm} (125 MHz): 74.51 (C2), 31.53 (C3), 20.75 (C4), 117.34 (C4a), 118.45 (C5), 11.27 (C5a), 144.51 (C6), 12.99 (C7), 122.60 (C8), 145.54 (C8a), 12.20 (C7a), 11.77 (C8b), 23.78 (C2a), 39.86 (C1′), 21.05 (C2′), 37.38 (C3′), 32.78 (C4′), 37.38 (C5′), 24.44 (C6′), 37.38 (C7′), 32.78 (C8′), 37.38 (C9′), 24.80 (C10′), 39.37 (C11′), 27.98 (C12′), 22.73 (C12′a), 22.73 (C13), 19.67 (C4′a), 19.67 (C8′a) Witkowski *et al.* (1998).

4.5.7.1 α-Tocopheryl-α-D-glucoside, 36: Solid; mp 110 °C; UV (H_2O, λ_{max}): 198.5 nm ($\sigma\rightarrow\sigma^*$, $\varepsilon_{198.5}$ – 10679 M^{-1}), 223 nm ($\pi\rightarrow\pi^*$, ε_{223} – 4293 M^{-1}), 264.5 nm

($n\rightarrow\pi^*$,$\varepsilon_{264.5}$ – 1818 M^{-1}). IR (KBr) 1031.5 cm^{-1} (C-O-C aryl alkyl symmetrical), 3374 cm^{-1} (OH), 1596 cm^{-1} (aromatic C=C). $[\alpha]^{25}_D$ = +16.16 ^{o} (*c* 1, H_2O); MS (*m/z*) - 615 $[M+Na]^+$. 2D-HSQCT (DMSO-d_6) ^{1}H NMR δ_{ppm} (500.13 MHz): 4.65 (H-1″α), 3.28 (H-2″α), 3.43 (H-3″α), 3.09 (H-4″α), 3.43 (H-6″α). 2.9 (H-4), 1.70 (H-3), 1.25 (H-1′), 1.39 (H-3′), 1.53 (H-4′), 1.22 (H-5′), 1.03 (H-6′), 1.14 (H-8′), 1.15 (H-10′), 1.20 (H-11′), 1.52 (H-12′), 0.86 (H-12′a, H-13′), 0.82 (H-4′a, 8′a), 1.25 (H-2a), 1.85 (H-5a), 2.05 (H-7a), 2.05 (H-8b); ^{13}C NMR δ_{ppm} (125 MHz): 98.5 (C1″α), 72.0 (C2″α), 73.2 (C3″α), 70.2 (C4″α), 60.9 (C6″α), 37.3 (C3), 21.5 (C4), 121.0 (C4a), 122.2 (C5), 14.0 (C5a), 150.5 (C6), 125.5 (C7), 116.2 (C8), 145.5 (C8a), 36.4 (C1′), 37.3 (C3′), 31.8 (C4′), 24.6 (C6′), 32.6 (C8′), 37.4 (C9′), 25.2 (C10′), 39.5 (C11′), 28.9 (C12′), 19.5 (C4′a, C8′a), 11.5 (C7a), 11.5 (C8b).

4.5.7.2 α-Tocopheryl-β-D-glucoside, 37: Semi solid; UV (H_2O, λ_{max}): 195 nm ($\sigma\rightarrow\sigma^*$, ε_{195} – 2542 M^{-1}), 223 nm ($\pi\rightarrow\pi^*$, ε_{223} – 753 M^{-1}), 270.5 nm ($n\rightarrow\pi^*$,$\varepsilon_{270.5}$ – 348 M^{-1}). IR:1028 cm^{-1} (C-O-C aryl alkyl symmetrical), 1259 cm^{-1}(C-O-C aryl alkyl asymmetrical), 3345 cm^{-1} (OH), 1603 cm^{-1} (aromatic C=C). $[\alpha]^{25}_D$ = -5.7 ^{o} (*c* 1, H_2O). MS (*m/z*) - 615 $[M+Na]^+$; 2D-HSQCT (DMSO-d_6) ^{1}H NMR δ_{ppm} 4.18 (H-1″β), 2.98 (H-2″β), 3.28 (H-3″β), 3.72 (H-4″β), 3.43 (H-6″a). 2.5 (H-4), 1.15 (H-1′), 1.32 (H-2′), 1.22 (H-3′), 1.32 (H-4′), 1.05 (H-5′), 1.10 (H-6′), 1.24 (H-7′), 1.23 (H-8′), 0.98 (H-10′), 1.12 (H-11′), 1.50 (H-12′), 0.70 (H-13′), 0.82 (H-12′a, 0.81 (H-8′a), 0.70 (H-4′a), 1.22 (H-2a), 1.92 (H-5a), 1.96 (H-7a), 1.99 (H-8b); ^{13}C NMR δ_{ppm}103.2 (C1″β), 73.0 (C2″β), 76.0 (C3″β), 70.3 (C4″β), 61.2 (C6″β), 20.5 (C4), 120.4 (C4a), 121.0 (C5), 150.0 (C6), 123.0 (C7), 116.8 (C8), 145.2 (C8a), 37.1 (C1′), 20.2 (C2′), 37.0 (C3′), 32.0 (C4′), 39.0 (C5′), 24.0 (C6′), 37.9 (C7′), 32.2 (C8′), 23.0 (C10′), 39.0 (C11′), 27.2 (C12′), 22.5 (C12′a, C13′), 19.4 (C4′a, C8′a), 23.6 (C2a), 14.0 (C5a), 11.5 (C7a), 11.5 (C28b).

UV spectrum showed σ→σ* band at 198.5 nm, π→π* band at 223 nm (228 nm for α-tocopherol) and n→π* band at 264.5 nm (292 nm for α-tocopherol). The IR spectrum of **36** showed 1030.5 cm^{-1} band for glycosidic C-O-C aryl alkyl symmetrical stretching (Fig. 4.34A). α-Tocopheryl-α-D-glucoside was confirmed from 2D HSQCT. The chemical shift value for C1″α (^{13}C at 98.5 ppm and ^{1}H at 4.65 ppm) indicated α-glucoside product formation. The ^{13}C chemical shift change from 145.4 ppm (C6 of free α-tocopherol) to 150.5 ppm (C6 of glucoside) indicated that glucosylation occurred at the phenolic OH group of the α-tocopherol. A MS *m/z* value 615 for $[M+Na]^+$ further confirmed the product formation.

UV spectrum of **37** showed σ→σ* band at 195 nm, π→π* band at 223 nm (228 nm for α-tocopherol) and n→π* band at 270.5 nm (292 nm for α-tocopherol). The IR spectrum of **37** showed 1028 cm^{-1} band for glycosidic C-O-C aryl alkyl symmetrical stretching and 1259 cm^{-1} band for glycosidic C-O-C aryl alkyl asymmetrical stretching frequencies. Two dimensional HSQCT confirmed the product is α-tocopheryl-β-D-glucoside **37**. The chemical shift value for C1″β (^{13}C at 103.2 ppm and the corresponding ^{1}H at 4.18 ppm) confirmed the C1″β glucoside **37** formation (Fig. 34B).

Table 4.18 α-Tocopheryl glucosides with conversion yields and product proportions.

Glycosides and product proportions (%)	Glycosylation yield [a] %
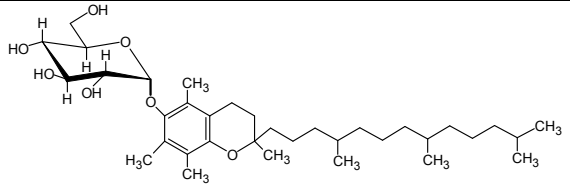 **36, α-tocopheryl-α-D-glucoside**	**52**
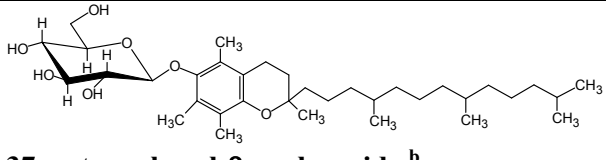 **37, α-tocopheryl-β-D-glucoside** [b]	**24**

[a] Conversion yields were from HPLC with errors in yield measurements ± 5-10%. [b] The compound was synthesized by using β-glucosidase from sweet almonds.

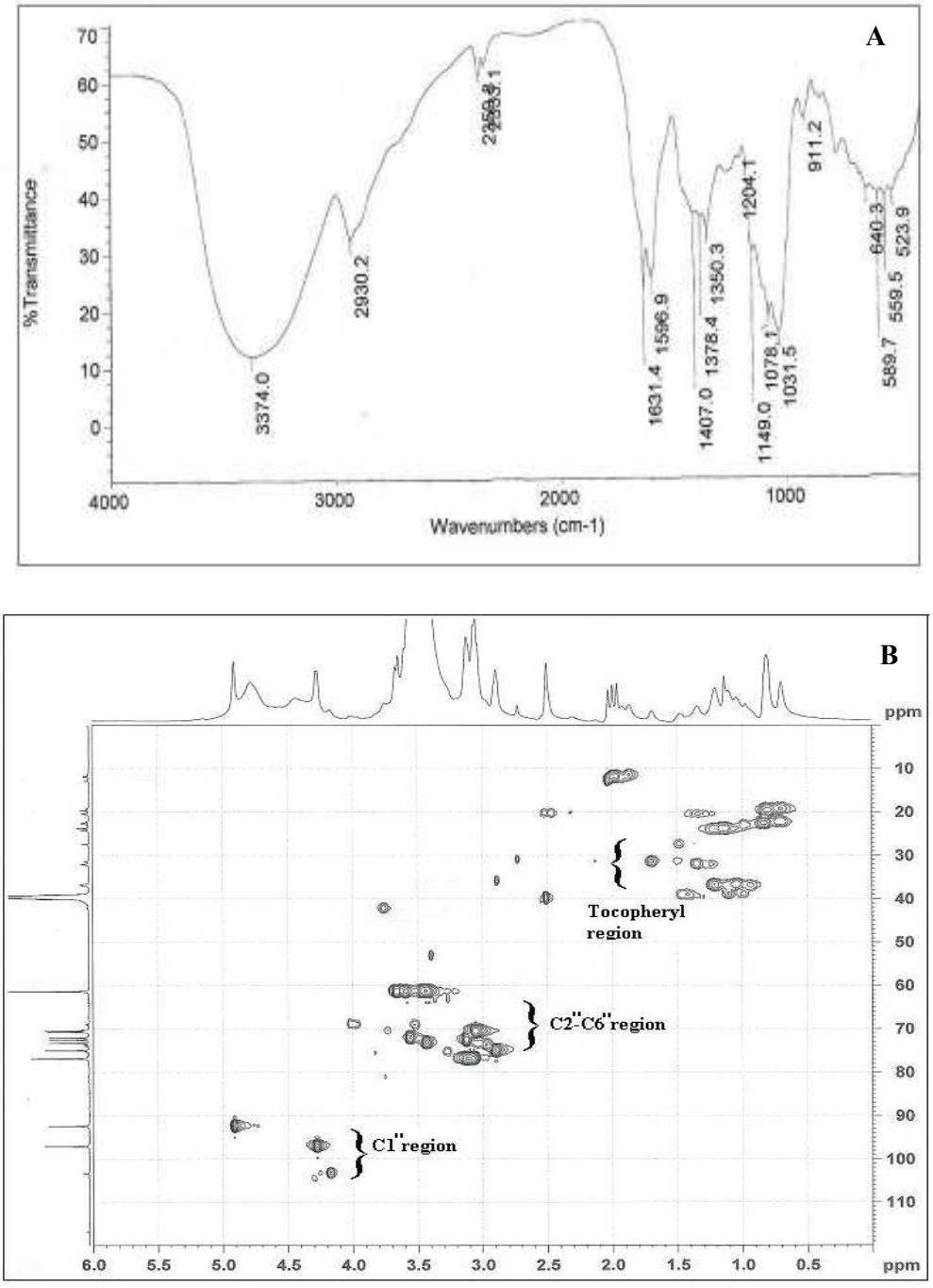

Fig. 4.34 (A) IR spectrum of α- tocopheryl-α-D-glucoside **36**. **(B)** 2D HSQCT spectrum of α- tocopheryl-β-D-glucoside **37**. Assignments were based on Lahman and Thiem (1997).

4.6 Discussion

In an enzyme catalyzed reaction, the equilibrium thermodynamic yield can be determined by the initial substrate concentration, the solubility of substrate and product in the reaction media and the equilibrium constant can be influenced by system properties like pH, temperature and pressure. By optimizing the above parameters, the present work has carried out at the best conditions for maximum conversion for guaiacyl, eugenyl, curcuminyl and α-tocopheryl glycosides.

The optimum conditions determined for this glycosylation reaction by studying the effect of variables like incubation period, enzyme and substrate concentration, pH and buffer concentration clearly explain the behavior of the amyloglucosidase. Most of the effects show that glycosylation increases upto a certain point, and thereafter they remain as such or decrease a little. This complex glycosylation reaction is not controlled by kinetic factors or thermodynamic factors or water activity alone.

Use of lower enzyme concentrations did not result in thermodynamic yields. The thermodynamic binding equilibria regulates the concentrations of the unbound substrates at different enzyme and substrate concentrations and thereby conversion as the reaction proceeds with time. At lesser enzyme concentrations, for a given amount of substrates (enzyme/substrate ratio low), rapid exchange between bound and unbound forms of both the substrates with the enzyme (on a weighted average based on binding constant values of both the substrates) leaves substantial number of unbound substrate molecules at the start of the reaction and they decrease progressively as conversion takes place (Romero *et al.* 2003; Marty *et al.* 1992). This becomes more so, if one of them binds more firmly to the enzyme than the other (higher binding constant value) as the respective enzyme/substrate ratios keep changing (during the course of the reaction) unevenly till the conversion stops due to total predominant binding (inhibition). At intermediatory

enzyme concentrations, such a competitive binding results in favourable proportions of bound and unbound substrates to effect quite a good conversion. At higher enzyme concentrations, most of the substrates would be in the bound form leading to inhibition and lesser conversion (higher enzyme/substrate ratios). Also, the glycosylation reaction requires larger amount of enzyme compared to hydrolysis. While this leads to lesser selectivity, they also give rise to varying bound and unbound substrate concentrations till the conversion ends. For a given amount of enzyme and substrates there is no increase in conversion beyond 72 h to 120 h. Longer incubation periods of especially lesser enzyme concentrations could also result in partial enzyme inactivation. However, not all the enzyme is inactivated before the end of the reaction.

The glycosylation described in the present work (Chapter 3 and 4) did not occur without the use of enzyme. Glycosidase reactions occur only in presence of certain amount of water (Ljunger *et al.* 1994; Vic and Crout 1995), which may be adjusted carefully to get good glycosylation yield. Besides imparting 'pH memory', added water is essential for the integrity of the three-dimentional structure of the enzyme molecule and therefore its activity (Dordick 1989) in a non polar solvent like di-isopropyl ether. Water has been added in the form of 10 mM buffer. When buffer concentration (buffer volume) was varied, the conversion yields were high between 0.04 to 0.1 mM (0.4 to 1.0 mL) concentrations. Both lower and higher buffer concentrations (buffer volume) results in the lesser conversion yields. A lower buffer concentration may not be sufficient to keep the active conformation of the enzyme, and a higher buffer volume could result in hydrolysis of the product.

Zaks and Klibanov (1988) reported that at low water activities, lower the solvent polarity, the higher the enzyme activity. Beyond the critical water concentration, glycosylation decreases because the size of the water layer formed around the enzyme

retards the transfer of the glycosyl donor to the active site of the enzyme (Humeau *et al.* 1998; Camacho *et al.* 2003) and also the water layer surrounding the enzymes makes enzyme to be more flexible by forming multiple H-bonds and interacting with organic solvent causing denaturation (Valiveti *et al.* 1991). Increase in buffer volume affected this glycosylation reaction significantly. It could increase the water activity of the system in the initial stages by increasing the thickness of the microaqueous layer around the enzyme. Higher volumes of the buffer in the microaqueous layer could also cause slight inactivation of the enzyme due to increase in salt concentration beyond a critical point. Patridge *et al.* (2001) reported that when an enzyme is suspended in a low-water organic solvent, the counter ions are in closer contact with the opposite charges on the enzyme because of the lower dielectric constant of the medium. Thus, protonation of the ionizable groups on the enzyme could be controlled by the type and availability of these ions as well as hydrogen ions resulting in a 'pH memory'. The third factor is the increase in ionic strength which could play a favourable role in glycosylation. The effect of pH showed that pH 7.0 for guaiacol and α-tocopherol, pH 5.0 for eugenol and pH 4.0 for curcumin are the best for obtaining maximum conversion. The three dimensional structure of the enzyme upto pH 7.0 may still retain a highly active conformation.

Even the water of reaction formed could also be used to constitute the microaqueous layer around the enzyme. The same could occur even with the addition of added enzyme (with little water content) and buffer volume. The added carbohydrate molecule could also reduce the water content of the reaction mixture. Adachi and Kobayashi (2005) have reported that the hexose, which is more hydrated, decreased the water activity in the system and shifts the equilibrium towards synthesis. All these factors lead to maintenance of an equilibrium concentration of water around the enzyme all the time. Hence, thermodynamic binding equilibria interplayed by inactivation and

inhibition along with maintenance of an optimum water activity could be governing this reaction as reflected by the extent of conversion under different reaction conditions of added buffer, enzyme and substrate concentrations.

Of the glycosides synthesized in the present work, guaiacyl-α-D-glucoside **21a,b**, guaiacyl-α-D-galactoside **23a,b**, eugenyl mannoside **26**, eugenyl maltoside **27a-c**, eugenyl sucrose **28a-c**, eugenyl-D-mannitol **29**, curcuminyl-bis-α-D-mannoside **32**, curcuminyl bis maltoside **33a-c**, curcuminyl bis sucrose **34a-c**, curcuminyl-bis-D-mannitol **35** have not been reported before. Among the carbohydrates employed D-arabinose, D-ribose, D-fructose, lactose and D-sorbitol did not react with any of the phenols studied. Glycosylation reaction occurs through a possible oxo-carbenium ion intermediate (Chiba 1997), which could be difficult with D-fructose, D-arabinose and D-ribose because of the resulting strain on the oxo-carbenium ion of the carbohydrate due to glycosylation. Sorbitol and lactose gave very low conversions. They could function as efficient inhibitors of the amyloglucosidase or could possess very low binding potentiality (low binding constant value) to the enzyme.

Among the carbohydrates employed, only C1 glycosylated and C6-O-arylated products were formed. No other secondary hydroxyl group of the carbohydrates were found to react. Due to inverting nature of the amyloglucosidase, all the phenols formed only C1α glycosides. The β-anomer of the carbohydrates (whereever applicable) did not react at all in these four phenols. Also β-glucosidase gave only β-glucosides (**22**, **25**, **31** and **37**) with all the four phenols studied.

The enzyme, besides effecting glycosylation and arylation reactions, also facilitated the hydrolysis of the disaccharides maltose and sucrose during the course of the reaction and the resultant glucose formed underwent glycosylation giving good yields of the glycosylated product. Lactose did not hydrolyze at all and neither did it react with

these phenols. Among the carbohydrates employed, D-mannose **4** and D-mannitol **11**, gave rise to only a single glycosylated product in case of eugenol and curcumin but the yields were less. Both eugenol and curcumin reacted with the same carbohydrate molecules namely D-glucose **2**, D-mannose **4**, maltose **8**, sucrose **9** and D-mannitol **11**. In case of curcumin all the carbohydrates formed bis-glycosides and bis C6-O-arylated products. Mostly, C1 glycosylated phenols were more. However, the only exception was sucrose where the C6-O-arylated product was more, compared to the C1-O-arylated product. This could be due to the steric hindrance offered by the C2 position of the fructose moiety when it is transferred to such phenolic nucleophiles.

In case of eugenol and curcumin, presence of hydrophobic propanoid group para to the phenolic OH bestows good nucleophilicity in these molecules promoting reaction with quite diverse carbohydrates. In both these phenols, the binding pattern to the enzyme in competition with the carbohydrate molecules could be the same. The loss of regioselectivity could be due to the employment of large amount of the enzyme. This is inevitable, as this reversible reaction requires such large concentrations of enzyme to be employed. A kinetic study showed that, curcumin is a good inhibitor of amyloglucosidase. Both guaiacol and eugenol could also serve as good inhibitors.

Thus this study has shown that phenyl propanoid phenols and other phenols like guaiacol, α-tocopherol can be glycosylated with diverse carbohydrate molecules and this opens up great synthetic possibilities.

4.7 Experimental section

4.7.1 Glycosylation procedures

4.7.1.1 Synthesis of guaiacyl glycosides

For the synthesis of guaiacyl glycosides, 1 mmol carbohydrate, guaiacol (50 M equivalents to carbohydrate) and 50% (w/w carbohydrate) amyloglucosidase were taken

in a 150 mL two-necked flat bottomed flask containing 100 mL di-isopropyl ether. A 0.6 mL of 10 mM pH 7.0 phosphate buffer was added and refluxed for 72 h with stirring at 68 °C. The solvent was then distilled off and the reaction mixture held in a boiling water bath for 5-10 min to denature the enzyme. Unreacted carbohydrate and the glycoside were extracted using 20-30 mL of water and the unreacted and insoluble guaiacol was removed by a separating funnel by extracting with petroleum ether. The aqueous layer was further evaporated to dryness and analyzed by HPLC. The residue was subjected to HPLC analysis using a aminopropyl column (3.9 x 300 mm length) with 80: 20 v/v acetonitrile: water at a flow rate of 1 mL/min and monitoring by RI detector. Conversion yields were determined from the peak areas of the respective glucosides and that of D-glucose in the reaction mixture and expressed as molar concentration of the product glucoside formed. Error in measurement of yields will be in the order ± 5-10%. The product glycosides were isolated from the unreacted carbohydrates and phenols by using Sephadex G15. Although glycosides were separated from unreacted carbohydrates and phenols by column chromatography, further separation of glycosides into individual ones were not possible because of similar polarity of the glycoside molecules.

4.7.1.2 Synthesis of eugenyl glycosides

Carbohydrate (1 mmol), eugenol (10 mmol) and amyloglucosidase (50% w/w carbohydrate) were taken in a 150 mL two-necked flat bottomed flask containing 100 mL di-isopropyl ether. A 0.1 mM (1.0 mL) of pH 4.0 acetate buffer was added and refluxed for 72 h with stirring at 68 °C. The solvent was then distilled off and the reaction mixture held in a boiling water bath for 5-10 min to denature the enzyme. Unreacted carbohydrate and the glycoside were extracted using 20-30 mL of water and the unreacted and insoluble eugenol was removed by a separating funnel by extracting with n-hexane or petroleum ether. The aqueous layer was further evaporated to dryness

and analyzed by HPLC and subjected to column chromatography (as mentioned in section 4.7.1.1).

4.7.1.3 Synthesis of curcuminyl glycosides

A typical synthesis involved reacting carbohydrate (1 mmol), curcumin (0.33 mmol) and amyloglucosidase 17% (w/w carbohydrate) in a 150 mL two necked flat bottomed flask containing 100 mL di-isopropyl ether. Acetate buffer, 0.1 mM (1.0 mL) of pH 4.0 was added and refluxed for 72 h with stirring at 68 °C. The solvent was then distilled off and the reaction mixture held in a boiling water bath for 5-10 min to denature the enzyme. Unreacted carbohydrate and the glycoside were extracted with 20-30 mL of water and further filtered to remove the unreacted curcumin. Filterate was evaporated to dryness and analyzed by HPLC and subjected to column chromatography (as mentioned in section 4.7.1.1).

4.7.1.4 Synthesis of α -tocopheryl glycosides

D-Glucose 0.5 mmol, α–tocopherol 0.5 mmol and amyloglucosidase (40% D-glucose) were taken along with a 0.2 mM (2.0 mL) of pH 7.0 phosphate buffer in a 150 mL of two necked flat bottomed flask containing 100 mL of di-isopropyl ether solvent. Inert atmosphere was maintained throughout the experiment by passing N_2 gas. The reaction mixture was refluxed for 72 h with stirring at 68 °C. The solvent was then distilled off and the reaction mixture held in a boiling water bath for 5-10 min to denature the enzyme. Unreacted carbohydrate and the glycoside were extracted using 20-30 mL of water and the unreacted and insoluble α–tocopherol was removed by a separating funnel by extracting with petroleum ether. The aqueous layer was evaporated to dryness and analyzed by HPLC and subjected to column chromatography (as mentioned in section 4.7.1.1).

4.7.2 Antioxidant activity

Antioxidant activity of guaiacol, guaiacyl-α-D-glucoside, curcumin and curcuminyl-bis-α-D-glucoside by DPPH (2,2-Diphenyl-1-picrylhydrazyl) radical scavenging method (Moon & Terao 1998) was evaluated. Absorbance of a solution in duplicate, containing 0.1 mL of test sample (8.6mM guaiacol and guaiacyl-α-D-glucoside and 5.3 mM curcumin and curcuminyl-bis-α-D-glucoside in DMSO) with 0.9 mL of Tris-HCl buffer (100 mM, pH 7.4) and 1 mL DPPH (500 μM in ethanol) was measured at 517 nm in a UV-Visible spectrophotometer (Shimadzu, UV 1601). Decrease in absorbance with respect to DPPH was a measure of radical scavenging ability of the test samples. Butylated hydroxyanisole (BHA, 5.55 mM) was used as a positive control. Error in the measurements will be $\pm$ 10%.

4.7.3 Solubility test for curcuminyl-bis-α-D-glucoside

Water solubility test for curcuminyl-bis-α-D-glucoside was carried out at room temperature. The solid glycoside compound was dissolved in water with stirring to supersaturation. It was allowed for settling and the absorbance of the supernatant glycoside solution was measured at 254 nm. Concentration of the glycoside solution was detected by the following relation and the solubility was expressed in percentage.

$$C = \frac{A}{\varepsilon \times l}$$

A= absorbance of the glycoside solution at 254 nm.

ε= Molar extension coefficient of the sample at 254 nm (ε_{254}=530 M^{-1}).

l= length of the cell in cm

4.7.4 Color test for curcuminyl-bis-α-D-glucoside

Total color of the synthesized curcuminyl-bis-α-D-glucoside was carried out according to the AOAC official methods of analysis (1995). The procedure followed the

determination of absorbance of the known concentration of the glycoside and that of the standard curcumin in DMSO at 425 nm. By using the following relation total color of the glycoside was determined.

$$\text{Total color} = \frac{A}{\text{Concentration of the glycoside (M)}} \times \frac{\text{Concentration of curcumin(M)}}{A'} \times \%\ \text{Purity of curcumin standard}$$

A= absorbance of curcuminyl-bis-α-D-glucoside at 425 nm

A′= absorbance of curcumin at 425 nm

4.7.5 Response surface methodology - curcuminyl-bis-α-D-glucoside

D-Glucose (1mmol), curcumin (0.2 to 1.0 mmol) and amyloglucosidase (10 to 70% w/w D-glucose) were taken in a 150 mL two necked flat bottomed flask containing 100 mL of di-isopropyl ether solvent. A 0.01 M buffer solution of 0.2 to 1.0 mL (corresponding to 0.02 to 0.1 mM) of appropriate pH (pH 4.0 to 8.0) was added and refluxed with stirring for specified incubation periods (24 to 120 h). Acetate buffer for pH 4.0 and 5.0, phosphate buffer for pH 6.0 and 7.0 and borate buffer for pH 8.0 were employed. After the reaction, solvent was distilled off and the reaction mixture was held in a boiling water bath for 5 – 10 min to denature amyloglucosidase. About 20-30 mL of water was added and stirred to dissolve the unreacted D-glucose and glucoside formed and further filtered to remove the unreacted curcumin. The filtrate was evaporated to dryness and analyzed by HPLC. Conversion yields were determined from HPLC peak areas of the glucoside and free D-glucose with respect to a D-glucose concentration of 1 mmol as described before. Curcumin-bis-α-D-glucoside was separated on a Sephadex G-15 column (100 x 1 cm) using water as eluent and subjected to spectral characterization by UV, IR, MS and 2D HSQCT.

4.7.6 Kinetic experiments

An experimental setup involved 0.005 M to 0.1 M curcumin and D-glucose along with 90 mg amyloglucosidase in 100 mL di-isopropyl ether solvent containing 0.06 mM (0.6 mL) of 0.01 M, pH 6.0 phosphate buffer. Kinetic experiments were carried out at the refluxing temperature of di-isopropyl ether at 68 °C by maintaining one of the substrate constant and varying the other in the concentration range 0.005 M to 0.1M and *vice versa*. Amyloglucosidase exhibits good activity only in the presence of water present as buffer. The water of reaction also contributed to the water activity essential for the enzymatic action. Only curcumin dissolved in di-isopropyl ether and the reaction mixture remained largely heterogenous due to insolubility of the enzyme and D-glucose. Since a constant amount of enzyme was employed for all the reactions, the enzyme/substrate ratio varied with varying substrate concentrations. Product work out and analysis were carried out as described before.

For each concentration of D-glucose and the phenol, individual experiments (30 x 4 for each system) were performed for incubation periods of 3 h, 6 h, 12 h and 24 h. Initial rates (v) were determined from the initial slope values of the plots from amounts of glucoside (M) formed versus incubation periods (h) from experiments performed in duplicate. R^2 values obtained from least square analysis for the initial velocities were found to be around 0.95. The plots shown in the present work were constructed from all the experimentally determined and a few computer generated initial rate values.

4.7.7 Spectral characterization

Ultra Violet-Visible spectra were recorded on a Shimadzu UV-1601 spectrophotometer. Known concentrations of the samples dissolved in the indicated (spectral data) solvents were used for recording the spectra. Infrared spectra were recorded on a Nicolet-FTIR spectrophotometer. Isolated solid glycoside samples (5-8

mg) were prepared as KBr pellets and employed for recording the IR spectra. Phenol standard was employed as such between salt plates to obtain IR spectra. Optical rotations of the isolated glycosides were recorded on Perkin-Elmner 243 Polarimeter. Mass spectra were obtained using a Q-TOF Waters Ultima instrument (Q-Tof GAA 082, Waters corporation, Manchester, UK) fitted with an electron spray ionization (ESI) source.

4.7.8 ^{1}H NMR

^{1}H NMR spectra were recorded on a Brüker DRX 500 MHz NMR spectrometer (500.13MHz). Proton pulse width was 12.25 μs. Sample concentration of about 40 mg of the sample dissolved in DMSO-d_6 was used for recording the spectra at 35 ^{o}C. About 100-200 scans were accumulated to get a good spectrum. The region between 0-10 ppm was recorded for all the samples. Chemical shift values were expressed in ppm relative to internal tetra-methyl silane (TMS) as the standard.

4.7.9 ^{13}C NMR

^{13}C NMR spectra were recorded on a Brüker DRX 500 MHz NMR spectrometer (125MHz). Carbon 90 ° pulse width was 10.5 μs. Sample concentration of about 40 mg dissolved in DMSO-d_6 was used for recording the spectra at 35 ^{o}C. About 500 to 2000 scans were accumulated for each spectrum. A region from 0-200 ppm were scanned. Chemical shift values were expressed in ppm relative to internal tetramethyl silane (TMS) as the standard.

4.7.10 2D-HSQCT

Two-dimensional Heteronuclear Single Quantum Coherence Transfer Spectra (2-D HSQCT) were recorded on a Brüker DRX 500 MHz NMR spectrometer (500.13 MHz for ^{1}H and 125 MHz for ^{13}C). A sample concentration of about 40 mg in DMSO-d_6 was used for recording the spectra.

Chapter 5

Angiotensin Converting Enzyme Inhibition Activity of the Glycosides Synthesized Through Amyloglucosidase Catalysis

5.1 Introduction

Angiotensin I converting enzyme (ACE, peptidyl dipeptidase A, EC 3.4.15.1) is a zinc containing nonspecific dipeptidyl carboxypeptidase widely distributed in mammalian tissues (Li *et al.* 2004), which play an important role in the control of blood pressure and is a part of the renin angiotensin system (Vermeirssen *et al.* 2002). This enzyme catalyzes the conversion of decapeptide angiotensin I into the potent vaso-constricting octapeptide, angiotensin II and increases the blood pressure (Soubrier *et al.* 1988). Angiotensin II brings about several central effects, all leading to a further increase in blood pressure. ACE is a multifunctional enzyme that also catalyses the degradation of bradykinin (blood pressure-lowering nanopeptide) and therefore inhibition of ACE results in an overall antihypertensive effect (Johnston 1992; Li *et al.* 2004).

Searching for ACE inhibitors for use as antihypertensive agents is the keen interest of the researchers after recognizing the role of this enzyme in the regulation of blood pressure. Synthetic drugs available for ACE inhibition exhibit significant side effects. Captopril is a successful synthetic antihypertensive drug and a large number of synthetic molecules like enalapril, perindopril, ceranopril, ramipril, quinapril, and fosinopril, also show ACE inhibitory activities (Hyuncheol *et al.* 2003; Dae-Gill *et al.* 2003; Chong-Qian *et al.* 2004). Some naturally occurring 'biologically active peptides' also act as ACE inhibitors. Deloffre *et al.* (2004) reported that a neuro-peptide from leach brain showed ACE inhibition with an IC_{50} value of 19.8 μM. The N-terminal dipeptide (Tyr-Leu) of β-lactorphin was found to be the most potent inhibitor (Mullally *et al.* 1996). Many peptide inhibitors are derived from different food proteins like Asp-Leu-Pro and Asp-Gly from soy protein hydrolysis (Wu and Ding 2002) and Gly-Pro-Leu and Gly-Pro-Val from bovine skin gelatin hydrolysis (Kim *et al.* 2001). Cooke *et al.*

(2003) prepared 4-substituted phenylalanyl esters of alkyl or benzyl derivatives which exhibited ACE inhibitory activity.

Glycosides from the leaves of *Abeliophyllum distichum* like acteoside, isoacteoside, rutin, and hirsutin moderately inhibited the Angiotensin I converting enzyme activity (Hyuncheol *et al.* 2003). Glycosides like 3-*O*-methyl crenatoside from *Microtoena prainiana* also showed more than 30% ACE inhibitory activity (Chong-Qian *et al.* 2004). Phenyl propanoid glycosides from *Clerodendron trichotomum* such as acteoside, leucosceptoside A, martynoside, aceteoside isomer and isomartynoside also showed ACE inhibitory effect (Dae-Gill *et al.* 2003).

Certain glycosides are used widely in food and pharmaceutical applications as sweeteners, surfactants, antibiotics, nutraceuticals and antitumor agents (Shibata *et al.* 1991; Balzar 1991; Kren and Martinkova 2001). Literature survey showed that certain glycosides showed ACE inhibitory activity and this stimulated an interest to test the enzymatically synthesized glycosides for ACE inhibition as described in the present work.

5.2 Present work

Totally 16 glycosides were tested for the ACE inhibitory activities. ACE was isolated from pig lung. The enzymatic reactions were carried out under optimized conditions worked out for these reactions. The enzymatic procedure employed unprotected and unactivated alcohols, phenols and carbohydrates. n-Octyl glycosides (n-octyl-D-glucoside **13a-c**, n-octyl maltoside **15** and n-octyl sucrose **16a** and **b**), guaiacyl glycosides (guaiacyl-α-D-glucoside **21a** and **b** and guaiacyl-α-D-galactoside **23a** and **b**), eugenyl glycosides (eugenyl-α-D-glucoside **24a** and **b**, eugenyl-α-D-mannoside **26**, eugenyl maltoside **27a-c**, eugenyl sucrose **28a-c** and eugenyl-D-mannitol **29**) and curcuminyl glycosides (curcuminyl-bis-α-D-glucoside **30a** and **b**, curcuminyl-bis-α-D-

mannoside **32**, curcuminyl bis maltoside **33a-c**, curcuminyl bis sucrose **34a-c** and curcuminyl-D-mannitol **35**) and α-tocopheryl-α-D-glucoside **36** were tested for ACE inhibition.

ACE inhibition activity of the above mentioned glycosides of carbohydrates were determined by the Cushman and Cheung method (1971). Since hippuryl-L-histidyl-L-leucine (HHL) mimics the carboxyl dipeptide of angiotensin I, it has been used as the substrate for screening ACE inhibitors.

Underivatised alcohols, phenols and carbohydrates were also tested for ACE inhibition as such as controls and they did not show any ACE inhibitory activities. Only glycosides showed activities. Isolated ACE inhibitor tested for lipase and protease activity (Table 5.1) showed a small extent of protease activity (13.3%) compared to ACE activity but no lipase activity. In presence of glycosides prepared, the isolated ACE showed 8.2% protease activity (Table 5.1) compared to the ACE activity. This confirmed that the ACE inhibition observed in the presence of glycosides prepared is more due to ACE inhibition rather than protease inhibition.

Table 5.1 Inhibition of protease in ACE by eugenyl-α-D-glucoside [a]

System	**Protease activity Unit $min^{-1}mg^{-1}$ enzyme protein** [b]	**Percentage of protease activity with respect to ACE activity** [c]
Control: ACE- 0.5 mL + 0.5 ml of 0.6% hemoglobin + 0.5 mL Buffer	0.0436	13.3
Eugenyl-α-D-glucoside: 0.5 mL glycoside + ACE - 0.5 mL + 0.5 mL of 0.6% hemoglobin	0.0292	8.2

[a] Conditions: ACE – 0.5 mL (0.5mg), All the solutions were prepared in 0.1 M pH 7.5 Tris-HCl, incubation period – 30 min, temperature – 37 ^{o}C, 0.5 mL of 10% trichloro acetic acid added to arrest the reaction; Blank performed without enzyme and glycoside; Absorbance measured at 440 nm; Eugenyl-α-D-glucoside – 0.5 mL of 0.8 mM; [b] Average absorbance values from three individual experiments; [c] Percentage protease activity with respect to an ACE activity of 0.327 μmol/min.mg protein.

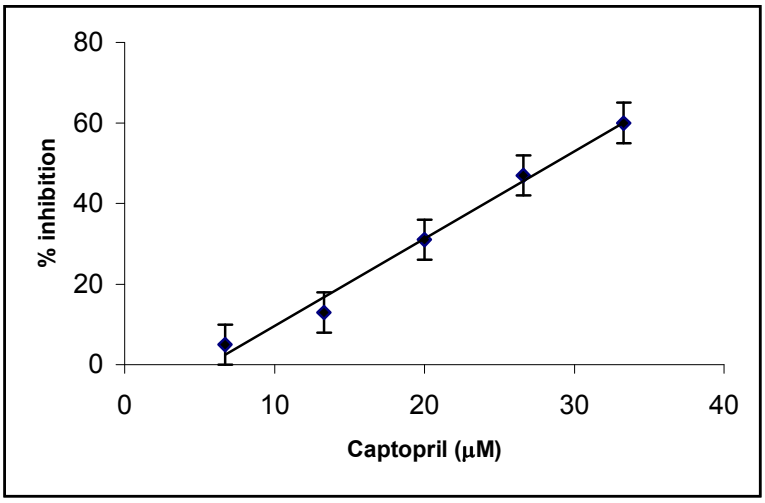

Fig. 5.1 A typical ACE inhibition plot for captopril, concentrations range 6.7 – 33.3 μM. Substrate – 0.1 mL hippuryl-histidyl-leucine (5 mM), buffer – 100 mM phosphate buffer pH 8.3 containing 300 mM NaCl, incubation period – 30 min, temperature – 37 °C. IC_{50} value – 0.060 ± 0.006 mM.

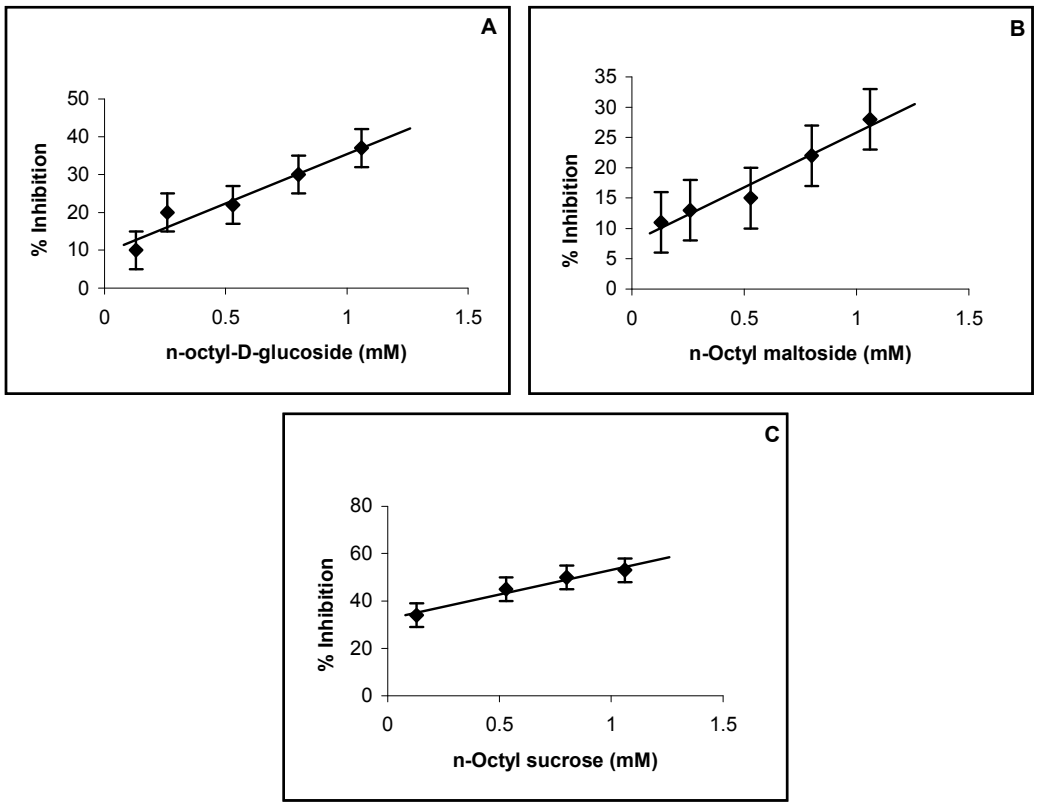

Fig. 5.2 ACE inhibition plots for n-octyl glycosides, **(A)** n-octyl-D-glucoside **13a-c**, **(B)** n-octyl maltoside **15**, **(C)** n-octyl sucrose **16a** and **b**. Concentration range – 0.13 – 1.06 mM, substrate – 0.1 mL hippuryl-histidyl-leucine (5 mM), buffer – 100 mM phosphate buffer pH 8.3 containing 300 mM NaCl, incubation period – 30 min, temperature-37 °C.

Table 5.2 IC_{50} values for ACE inhibition by glycosides[a]

Glycoside	Yield[b] (%)	Products formed (% Proportions)[c]	IC_{50} value (mM)[d]
n-octyl-D-glucoside, **13a-c**	46	C1α-glucoside (63), C1β-glucoside (25), C6-alkylated (12)	1.0±0.09
n-octyl maltoside, **15**	22	C1α-maltoside	1.5±0.13
n-octyl sucrose, **16a** and **b**	13	C1-O-alkylated (44), C6-O-alkylated (56)	1.7±0.15
Guaiacyl-α-D-glucoside, **21a** and **b**	52	C1α glucoside (52), C6-O-arylated (48)	3.7±0.36
Guaiacyl-α-D-galactoside, **23a** and **b**	17	C1α-galactoside (95), C6-O-arylated (5)	2.3±0.22
Eugenyl-α-D-glucoside, **24a** and **b**	32	C1α glucoside (53), C6-O-arylated (47)	0.5±0.04
Eugenyl-α-D-mannoside, **26**	8	C1α-mannoside	5.3±0.51
Eugenyl maltoside, **27a-c**	17	C1α-maltoside (52), 6-O-arylated (28), C6″-O-arylated (20)	0.7±0.06
Eugenyl sucrose, **28a-c**	7	C1-O-arylated (45), C6-O-arylated (35), C6″-O-arylated (20)	1.7±0.15
Eugenyl-D-mannitol, **29**	7	C1-O-arylated	2.1±0.21
Curcuminyl-bis-α-D-glucoside, **30a** and **b**	48	C1α-glucoside (62), C6-O-arylated (38)	1.5±0.13
Curcuminyl-bis-α-D-mannoside, **32**	9	C1α-mannoside	1.0±0.09
Curcuminyl-bis-maltoside, **33a-c**	19	C1α-maltoside (37), C6-O-arylated (36), C6″-O-arylated (27)	1.2±0.11
Curcuminyl-bis-sucrose, **34a-c**	19	C1-O-arylated (12), C6-O-arylated (70), C6″-O-arylated (18)	1.8±0.17
Curcuminyl-bis-D-mannitol, **35**	14	C1-O-arylated	1.8±0.17
α-Tocopheryl-α-D-glucoside, **36**	52	C1α-glucoside	1.2±0.11

[a] Respective alcohols, phenols and carbohydrates as controls did not show any ACE inhibition activities; non reducing sugar unit carbons of disaccharide are double primed; [b] Conversion yields were from HPLC; [c] Product proportions determined from 2D-HSQCT NMR C1/C6 cross peak areas; [d] IC_{50} values compared to that of captopril 0.060 ± 0.005 mM determined by Cushman and Cheung method.

Typical ACE inhibition plot for captopril, which showed an IC_{50} value of 0.060± 0.006 mM is shown in Fig. 5.1. Typical ACE inhibition plots for all the tested glycosides such as n-octyl glycosides (Fig. 5.2), guaiacyl glycosides (Fig. 5.3), eugenyl glycosides (Fig. 5.4), curcuminyl and α-tocopheryl glycosides (Fig. 5.5) are shown. Table 5.2 shows

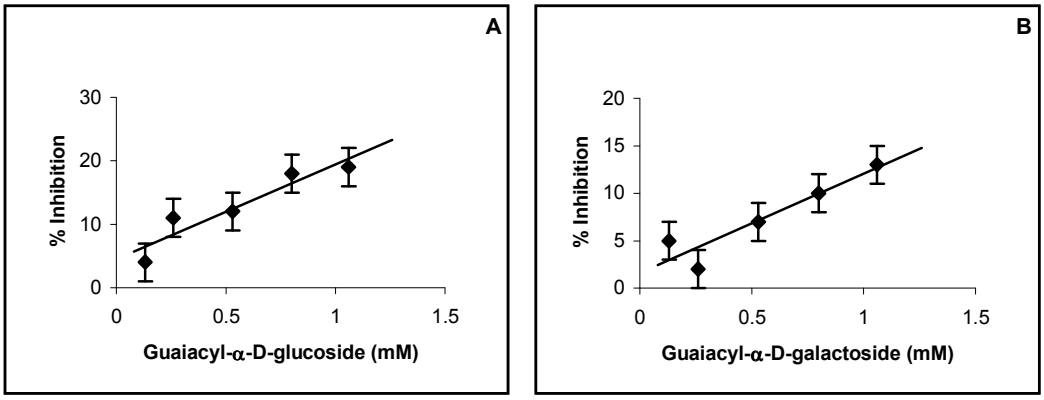

Fig. 5.3 ACE inhibition plots for guaiacyl glycosides, **(A)** guaiacyl-α-D-glucoside **21a** and **b**, **(B)** guaiacyl-α-D-galactoside **23a** and **b**. Concentration range – 0.13 – 1.06 mM, substrate – 0.1 mL hippuryl-histidyl-leucine (5 mM), buffer – 100 mM phosphate buffer pH 8.3 containing 300 mM NaCl, incubation period – 30 min, temperature – 37 °C.

the glycosides tested, their conversion yields from the respective enzymatic reactions, proportions of the products formed and ACE inhibitory activities for these compounds.

The compounds were characterised by two-dimensional Heteronuclear Single Quantum Coherence Transfer (2D-HSQCT) NMR spectra (Chapter 3 and Chapter 4). In case of glycoside syntheses, the major product was the glycosylated product and relatively lesser amounts of C6-O-alkylated or C6-O-arylated products were also detected. The reaction was between the alcohol or phenolic OH groups and the anomeric and/or primary C6-OH groups of the carbohydrates.

It was not possible to separate the individual glycosides from the mixtures in spite of separating the glycosides from the unreacted carbohydrates through column chromatography using Sephadex G15. Thus the activities described are for the mixtures of these compounds.

5.3 Discussion

The present work for the first time has shown the ACE inhibitory potency of the above mentioned glycosides prepared enzymatically. Among the glycosides tested, eugenyl-α-D-glucoside **24a** and **b** (0.5±0.04 mM), eugenyl maltoside **27a-c** (0.7±0.06 mM), octyl-D-glucoside **13a-c** (1.0±0.09 mM) and curcuminyl-bis-α-D-mannoside **32** (1.0±0.09 mM) exhibited the best ACE inhibitory activities ($IC_{50} \leq 1.0$ mM; Table 1). Among the carbohydrates employed, both glucosides and maltosides showed the best ACE inhibitory activities. Alkyl glycosides showed better inhibitory activities than the phenolic glycosides.

Captopril is N-[(S)-3-mercapto-2-methylpropionyl]-L-proline containing prolyl unit as essential for ACE inhibition (Michaud *et al.* 1997). The glycosides tested in the present work overall, clearly possess groups like alkyl side chains and phenolic groups which can be accommodated in the hydrophobic S1 and S2 subsites of angiotensin I

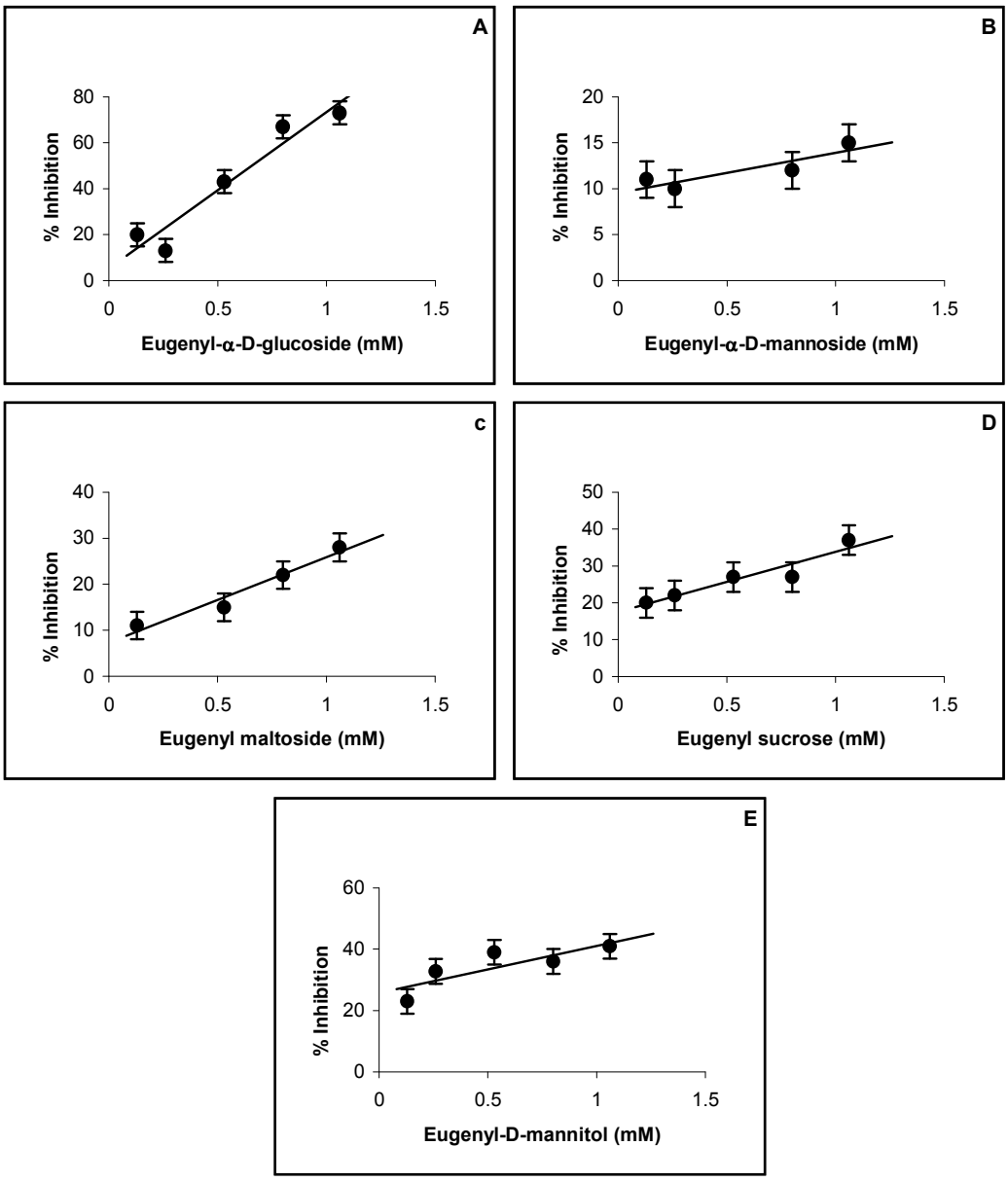

Fig. 5.4 ACE inhibition plots for eugenyl glycosides, **(A)** eugenyl-α-D-glucoside **24a** and **b**, **(B)** eugenyl-α-D-mannoside **26**, **(C)** eugenyl maltoside **27a-c**, **(D)** eugenyl sucrose **28a-c**, **(E)** eugenyl-D-mannitol **29**. Concentration range – 0.13 – 1.06 mM, substrate – 0.1 mL hippuryl-histidyl-leucine (5 mM), buffer – 100 mM phosphate buffer pH 8.3 containing 300 mM NaCl, incubation period – 30 min, temperature – 37 °C.

converting enzyme (Michaud *et al.* 1997; De Lima 1999). Carbohydrates in glycosides could also bind to the hydrophobic and/or hydrophilic subsites of angiotensin I converting enzyme, as they possess both hydrophobic and/or hydrophilic groups in their structure. Although the ACE preparation of the present work from pig lung is ACE I (Sanchez *et al.* 2003), it showed a low protease inhibitory activity but no lipase activity indicating that the glycosides inhibit ACE rather than the protease activity as protease inhibition activity can be construed to be ACE inhibition. The results indicate that the glycosides bind to these enzymes and hence hold promise as potential inhibitors for the ACE.

5.4 Experimental section

5.4.1 Extraction of ACE from pig lung

ACE was extracted from pig lung using the method described by Sanchez *et al.* (2003). A 100 g of pig lung was minced and homogenized using a blender with 10 mM HEPES buffer pH 7.0 containing 0.4 M NaCl at a volume ratio of 5:1 (v/w of pig lung) at 4 ^{o}C. The homogenate was centrifuged at 9000 g for 60 min. The supernatant was discarded and the precipitate was washed twice with 200 mL of 10 mM HEPES buffer pH 7.0 containing 0.4 M NaCl. The final precipitate was resuspended in 200 mL of 10 mM HEPES buffer pH 7.0 containing, 0.4 M NaCl, 10 μM $ZnCl_2$, 0.5% (w/v) Triton X100 and stirred over night at 4 ^{o}C. The solution was centrifuged to remove the pellets. The supernatant was dialyzed against water and later lyophilized. The protein content of ACE determined by Lowry's method was found to be 8.3%.

5.4.2 Glycosylation procedure

A typical procedure for the preparation of various glycosides involved refluxing carbohydrates **2-12** and alcohol/phenols (n-octanol **1**, guaiacol **17**, eugenol **18**, curcumin **19** and α-tocopherol **20**) in the molar ratio of 1: 50 in case of n-octanol/alkanol and

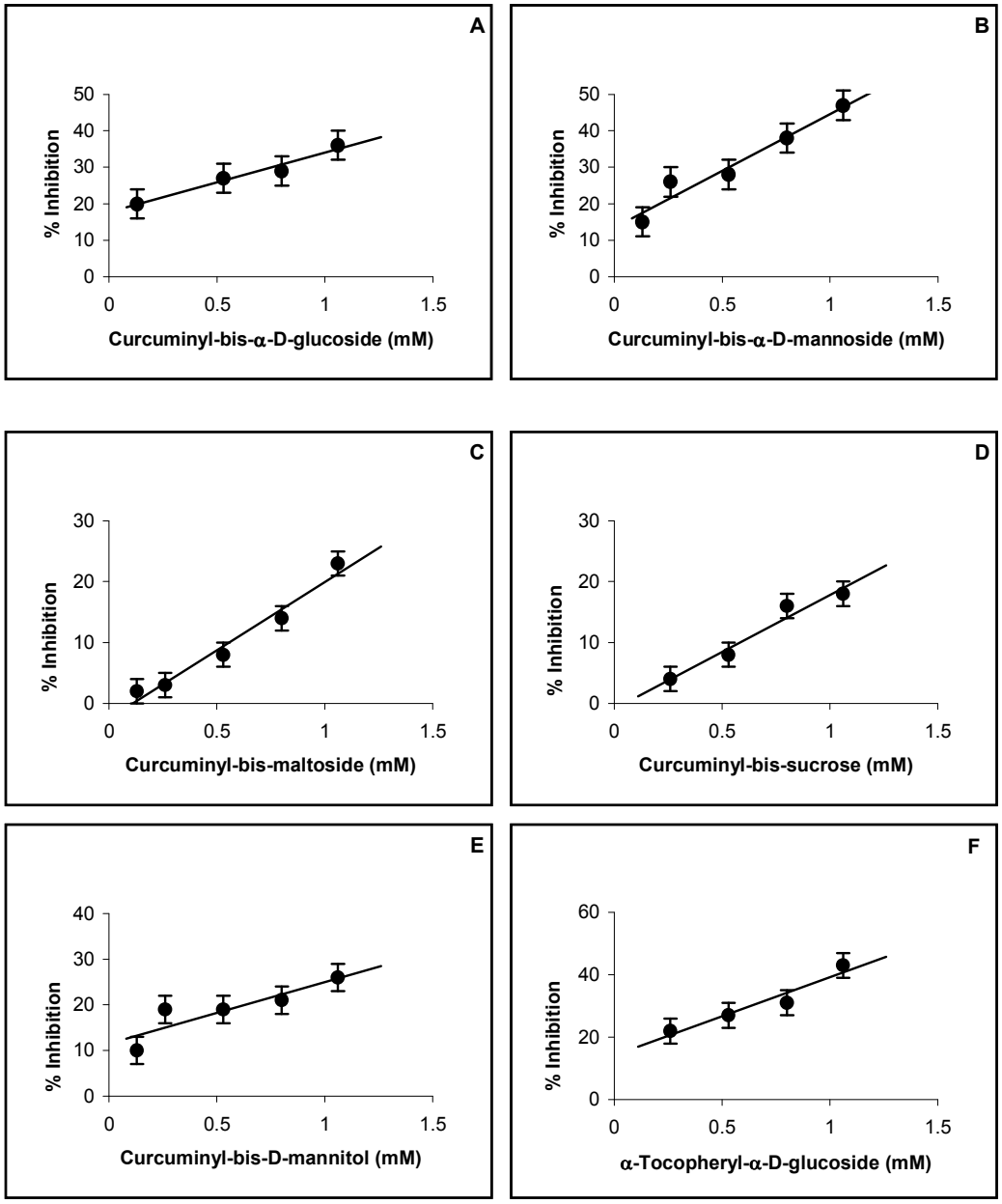

Fig. 5.5 ACE inhibition plots for curcuminyl and α-tocopheryl glycosides, (A) curcuminyl-bis-α-D-glucoside **30a** and **b**, (B) curcuminyl-bis-α-D-mannoside **32**, (C) curcuminyl-bis-maltoside **33a-c**, (D) curcuminyl-bis-sucrose **34a-c**, (E) curcuminyl-bis-D-mannitol **35**, (F) α-tocopheryl-α-D-glucoside **36**. Concentration range – 0.13 – 1.06 mM, substrate – 0.1 mL hippuryl-histidyl-leucine (5 mM), buffer – 100 mM phosphate buffer pH 8.3 containing 300 mM NaCl, incubation period – 30 min, temperature-37 °C.

guaiacol, 1:10 for eugenol, 1:0.3 for curcumin and 1:1 for α-tocopherol in 100 mL di-isopropyl ether solvent in the presence of amyloglucosidase (30 to 50% w/w carbohydrate) and 0.01-0.2 mM (0.1-2.0 mL of 10 mM buffer in 100 mL reaction mixture) pH 4.0 - 7.5 for a 72 h incubation time. The solvent was distilled off and the reaction mixture was held on a boiling water bath for 5-10 min to denature the enzyme. The unreacted carbohydrate and the product glycosides were extracted with 20-30 mL water. The unreacted alcohol/phenol (n-octanol, guaiacol, eugenol, and α-tocopherol) was isolated from the reaction mixture by extracting with petroleum ether or n-hexane. In case of curcumin glycosides, unreacted curcumin was separated through filtration. The aqueous layer was evaporated to dryness to get the unreacted carbohydrate and the product glycoside. The reaction mixtures were analyzed by HPLC using an amino-propyl column (3. 9 x 300 mm length) and acetonitrile: water in 80:20 ratio (v/v) as the mobile phase at a flow rate of 1mL/min with refractive index detector. Conversion yields were determined from HPLC peak areas of glycoside and free carbohydrate with respect to the free carbohydrate employed. Error in HPLC measurements will be ± 5-10%. The glycosides formed were separated through size exclusion chromatography using Sephadex G-15 and eluting with water. The product glycosides separated were subjected to spectral characterization by UV, IR, Mass, optical rotation and 2D-NMR.

5.4.3 Angiotensin Converting Enzyme (ACE) inhibition assay

ACE inhibition assay for the glycosides prepared were performed by the Cushman and Cheung method (1971). Aliquots of glycoside solutions in the concentration range 0.13 to 1.06 mM (0.1 mL to 0.8 mL of 2.0 mM stock solution) were taken and to this 0.1 mL of ACE solution (0.1% in 0.1 M phosphate buffer, pH 8.3 containing 300 mM NaCl) was added. To this solution, 0.1 mL of 5.0 mM hippuryl-L-histidyl-L-leucine (HHL) was also added and the total volume made upto 1.25 mL by

adding phosphate buffer (0.95 mL to 0.25 mL of 0.1 M pH 8.3 containing 300 mM NaCl). The solution was incubated on a Heto-Holten shaking water bath for 30 min at 37 ^{o}C. Blanks were performed without the enzyme by taking only the glycoside solution (0.1 to 0.8 mL) along with 0.1 mL of 5.0 mM HHL. The total volume was made upto to 1.25 mL by adding same buffer (1.05 mL to 0.35 mL). The reaction was terminated by adding 0.25 mL of 1 M HCl. Hippuric acid formed in the reaction was extracted with 1.5 mL of ethyl acetate. One mL of the ethyl acetate layer was evaporated to dryness and treated with equal amount of distilled water and absorbance was measured at 228 nm for hippuric acid. The hippuric acid formed in 1.5 mL of ethyl acetate was determined from a calibration plot prepared by using a standard hippuric acid in 1 mL of distilled water in the concentration range 0-400 nmol and measuring its absorbance at 228 nm. Specific activity was expressed as mM of hippuric acid formed per min per mg of enzyme protein.

$$\text{Specific activity} = \frac{A_{ts} - A_{blank}}{T \times S \times E}$$

A_{ts} = absorbance of test solution, A_{blank} = absorbance of blank solution, T = incubation period in min, S = slope value of the calibration plot (1.006×10^{-2} Abs units/nmol of hippuric acid), E = amount of the enzyme in mg protein.

Percentage inhibition was expressed as the ratio of the specific activity of ACE in the presence of the inhibitor to that in the absence of the inhibitor, the latter being considered as 100%. IC_{50} value was expressed as the concentration of the inhibitor required for 50% reduction in ACE specific activity. Molecular weights of the glycosides employed in the calculations are weighted averages of molecular weights of glycosides detected by NMR spectroscopy and MS spectroscopy.

A Shimadzu UV-1601 spectrophotometer was employed for the measurement of absorbance readings at 228 nm.

5.4.4 Protease and lipase assay

Protease activity for the ACE inhibitor was determined by the method described by Dubey and Jagannadham (2003) and lipase activity by the tributyrin method (Vorderwulbecke *et al.* 1992) in presence of eugenyl-D-glucoside (0.8 mM in 0.1M, pH 7.5, Tris-HCl buffer). Specific protease activity was expressed as the increase in absorbance at 440 nm per min per mg of the protein employed. Similarly specific lipase activity was determined as μmol of butyric acid formed per min per mg of the protein employed.

Conclusions

The important findings of the present investigation are:

1. Glycosylation potentialities of amyloglucosidase from *Rhizopus* sp. was explored in detail in the synthesis of alkyl (alcohols of carbon chain length C1-C18), guaiacyl, eugenyl, curcuminyl and tocopheryl glycosides of aldohexoses (D-glucose **2**, D-galactose **3** and D-mannose **4**), ketohexose (D-fructose **5**), pentoses (D-arabinose **6** and D-ribose **7**), disaccharides (maltose **8**, sucrose **9** and lactose **10**) and carbohydrate alcohols (D-mannitol **11** and D-sorbitol **12**). n-Octanol **1** reacted with D-glucose **2**, maltose **8** and sucrose **9**, guaiacol **17** reacted with D-glucose **2** and D-galactose **3,** eugenol **18** and curcumin **19** reacted with D-glucose **2**, D-mannose **4**, maltose **8**, sucrose **9** and D-mannitol **11** and α-tocopherol **20** reacted with only D-glucose **2**.
2. Synthetic potentiality of the β-glucosidase isolated from sweet almonds was also tested for the glucosylation of n-octanol, guaiacol, eugenol, curcumin and α-tocopherol.
3. An experimental setup was developed for even large-scale synthesis of glycosides using lesser enzymes and larger concentrations of substrates to give higher yields than there obtained from shake flask experiments. This set up involved refluxing the reaction mixture containing the alcohol/phenol, the carbohydrate, appropriate concentrations of the enzyme in the presence of specified pH and concentrations of the buffer solutions in 100 mL of di-isopropyl ether solvent at 68 °C.
4. Amyloglucosidase catalyzed synthesis of n-octyl-α-D-glucoside **13a-c**, guaiacyl-α-D-glucoside **21a** and **b**, eugenyl maltoside **27a-c**, curcuminyl-bis-α-D-glucoside **30a** and **b** and tocopheryl-α-D-glucoside **36** were optimized in terms of

incubation period, buffer pH, buffer concentration, enzyme concentration and substrate concentrations.

5. Two-dimensional HSQCT NMR studies confirmed that C1 glycosylation was the major reaction in the amyloglucosidase catalyzed glycosylation reaction yielding larger amounts of C1 glycosides. In the amyloglucosidase catalyzed reactions only α-anomers of D-glucose, D-galactose, D-mannose and maltose reacted with alcohols and phenols with the exception of n-octyl-β-D-glucoside where the β-anomer reacted was also obtained. However, only C1 glucosylation occurred in β-glucosidase catalyzed reaction resulting in β-glucosides.
6. Both 2D-HSQCT and MS studies confirmed that mono glycosylated and/or mono C6-O-alkylated in case of glycosylation of n-octanol, mono glycosylated and/or mono C6-O-arylated products in case of glycosylation of guaiacol, eugenol and α-tocopherol and bis glycosylated and/or bis C6-O-arylated products in case of curcumin were found to be formed. No other secondary hydroxyl groups of the carbohydrates were found to undergo alkylation or arylation.
7. Amyloglucosidase, besides effecting glycosylation also facilitated the hydrolysis of maltose and sucrose. Lactose did not hydrolyze at all and neither did it react with n-octanol and the phenols employed. Eugenol and curcumin reacted with the same carbohydrate molecules: D-glucose **2**, D-mannose **4**, maltose **8**, sucrose **9** and D-mannitol **11**. D-Fructose **5**, D-arabinose **6**, D-ribose **7**, lactose **10** and D-sorbitol **12** did not react with any of the alcohol and phenols.
8. Out of all the synthesized C1 glycosides and C6-O-alkylated/arylated of the carbohydrates **2-12**, the new compounds reported in the present work are n-octyl-sucrose **16a** and **b**, guaiacyl-α-D-glucoside **21a** and **b**, guaiacyl-β-D-glucoside **22**, guaiacyl-α-D-galactoside **23a** and **b**, eugenyl-α-D-mannoside **26**, eugenyl

maltoside **27a-c**, eugenyl sucrose **28a-c**, eugenyl-D-mannitol **29**, curcuminyl-bis-α-D-mannoside **32**, curcuminyl bis maltoside **33a-c**, curcuminyl bis sucrose **34a-c** and curcuminyl-bis-D-mannitol **35**.

9. Water solubility of the curcumin-bis-α-D-glucoside prepared was found to be 14g/L whereas curcumin itself is practically insoluble in water (Section 4.4.9). Curcuminyl-bis-α-D-glucoside exhibited a total color of 10.8 in DMSO (Section 4.4.10).
10. Lack of stereo and regio specificity could be due to employment of larger amounts of the enzymes. This is inevitable, as this reversible reaction required such large concentrations of the enzymes to effect glycosylation.
11. Response surface methodological studies, useful for scaling up were carried out for the optimization of n-octyl-α-D-glucoside **13a-c** synthesis by shake flask method and curcuminyl-α-D-glucoside **30a** and **b** synthesis by reflux method. A Central Composite Rotatable Design (CCRD) involving n-octanol concentration, amyloglucosidase concentration, curcumin concentration, pH, buffer concentration (buffer volume), temperature and incubation period as variables at five levels were employed to get optimized conditions in both these reactions. Predictive equations were worked out in both these reactions to predict the yields of glycosides from the reaction conditions employed. The reactions carried out at both optimized and random level conditions gave yields in good correspondence with predicted yields.
12. Kinetic studies of glucosylation between D-glucose and curcumin catalyzed by amyloglucosidase showed that kinetics followed Ping-Pong Bi-Bi mechanism with competitive substrate inhibition by curcumin at higher concentrations leading to dead end amyloglucosidase-inhibitor (curcumin) complex formation.

13. Biological activities of the synthesized glycosides were explored in the present work. Guaiacyl-α-D-glucoside **21a** and **b** and curcuminyl-bis-α-D-glucoside **30a** and **b** showed antioxidant activities. Synthesized glycosides n-octyl-D-glucoside **13a-c**, n-octyl maltoside **15**, n-octyl sucrose **16a** and **b**, guaiacyl-α-D-glucoside **21a** and **b**, guaiacyl-α-D-galactoside **23a** and **b**, eugenyl-α-D-glucoside **24a** and **b**, eugenyl-α-D-mannoside **26**, eugenyl maltoside **27a-c**, eugenyl sucrose **28a-c**, eugenyl-D-mannitol **29**, curcuminyl-bis-α-D-glucoside **30a** and **b**, curcuminyl-bis-α-D-mannoside **32**, curcuminyl bis maltoside **33a-c**, curcuminyl bis sucrose **34a-c**, curcuminyl-bis-D-mannitol **35** and tocopheryl-α-D-glucoside **36** showed ACE inhibition activities. Eugenyl-α-D-glucoside **24a** and **b** exhibited best ACE inhibition activity (IC_{50} value 0.5±0.04 mM).

Thus the present work has shown that alcohols and phenols can be glycosylated with diverse carbohydrate molecules using amyloglucosidase from *Rhizopus* sp. and β-glucosidase from sweet almonds.

Summary

Synthesis of glycosides involving regio and stereo selectivity is an important and difficult area in synthetic organic chemistry, which is of prime concern to researchers working in this area. Glycosides are used as surfactants (Busch *et al.* 1994), colorants and flavoring agents (Sakata *et al.* 1998), sweeteners (Shibata *et al.* 1991), antioxidants, anti-inflammatory (Gomes *et al.* 2002), antibiotics (Ikeda and Umezawa 1999; Kren and Martinkova 2001), antifungal (Tapavicza *et al.* 2000), antimicrobial (Zhou 2000) and cardiac related drugs (Ooi *et al.* 1985). Alkyl and phenolic glycosides are even useful as detergents, cosmetics and food additives. For the past decade or two a variety of glycosidases or transglycosidases have been employed for the glycosylation of mono and disaccharides with a variety of acceptor molecules (Katusumi *et al.* 2004; Vic and Crout 1995; Sato *et al.* 2003). However, reports involving amyloglucosidase for the synthesis of alkyl/phenolic glycosides are practically nil. Amyloglucosidase from *Rhizopus* sp. and β-glucosidase isolated from sweet almonds were found to catalyze the synthesis of alkyl, guaiacol, eugenol, curcumin and α-tocopherol glycosides and the results from this investigation is presented in this work in detail.

Chapter **ONE** deals with literature reports on enzymatic transformations, glycosidases and their sources, structural features of glucoamylase and β-glucosidase, glycosylation and their methods, glycosylation mechanism and applications of various enzymatically synthesized glycosides. A detailed report on investigations on some important factors that influence the glycosidase catalyzed reactions in organic solvents like nature of substrate, nature of solvent, thermal stability, role of water, kinetic studies of glycosidase catalyzed reactions and immobilization are presented. Besides, the advantages of carrying out glycosylation using reverse micelles, super critical carbon di-oxide, microwave assisted glycosylation reactions and response surface methodology

(RSM) in glycosylation have been discussed. This chapter ends with a brief scope of the present investigation.

Chapter **TWO** describes materials and methods involved in the present work. Enzyme and chemicals employed and their sources are shown. Glycosylation procedure by shake flask and reflux methods and the related analytical and assay procedures are described in detail.

Chapter **THREE** describes synthesis of n-alkyl glucosides of alcohols of carbon chain length C1-C18 using amyloglucosidase by both shake flask and reflux methods besides investigating the synthesis of n-octyl-D-glucoside **13a-c** in detail. Effects of incubation period, pH, buffer concentration and enzyme concentration were studied by both shake flask and reflux methods in the synthesis of n-octyl-D-glucoside. The highest conversion yield of 28% (w/w D-glucose) by shake flask method and 46% (w/w D-glucose) by reflux method were obtained. Optimum reaction conditions for the shake flask experiments were found to be D-glucose and n-octanol in 1: 50 equivalent ratio, 30% (w/w D-glucose) amyloglucosidase concentration and 0.8 mM (0.4 mL of 10 mM buffer), pH 6.0 phosphate buffer for an incubation period of 72 h. For the reflux method D-glucose and n-octanol in 1: 50 equivalent ratio, 30% (w/w D-glucose) amyloglucosidase concentration and 0.04 mM (0.4 mL of 10 mM buffer in 100 mL solvent), pH 6.0 phosphate buffer for an incubation period of 72 h was found to be the optimum. The specific alcohols, employed for the preparation of n-alkyl glucosides are: methyl alcohol, ethyl alcohol, n-propyl alcohol, n-butyl alcohol, n-amyl alcohol, n-hexyl alcohol, n-heptyl alcohol, n-octyl alcohol, n-nonyl alcohol, n-decyl alcohol, lauryl alcohol, cetyl alcohol and stearyl alcohol. The reaction mixtures were analyzed by HPLC. Glucoside yields obtained from the reflux method (5-44%) were better than those from the shake flask method (3-28%). While the shake flask method favored

glucosylation of medium chain length alcohols, the reflux method at pH 5.0, favored glucosylation of all the chain lengths.

n-Octanol **1**, glycosylation with carbohydrates (D-glucose **2**, D-galactose **3**, D-mannose **4**, D-fructose **5**, D-arabinose **6**, D-ribose **7**, maltose **8**, sucrose **9**, lactose **10**, D-mannitol **11** and D-sorbitol **12**) using amyloglucosidase was attempted. Only n-octyl maltoside **14** (conversion yield 15%) and n-octyl sucrose **16a** and **b** (conversion yield 13%) were the glycosides formed besides n-octyl-D-glucoside **13a-c**. However, HPLC indicated glycosylation of D-galactose **3**, D-mannose **4** and D-mannitol **11** with conversion yields less than 5%. n-Octyl-β-D-glucoside **14** synthesized by the reflux method using β-glucosidase isolated from sweet almonds showed an extent of glycosylation of 23%. Spectral characterization of the isolated glycosides by UV, IR, 2D NMR, optical rotation and MS studies confirmed that mono glycosylated and/or mono C6-O-alkylated products were formed.

Amyloglucosidase catalyzed synthesis of n-octyl-D-glucoside **13a-c** by shake flask level was optimized using RSM. A Central Composite Rotatable Design (CCRD) involving 32 experiments of five variables at five levels was employed to study the glucosylation reaction. The variables employed were n-octanol (15-75 molar equivalents to D-glucose), enzyme (20 –100 mg, 20 to 100% w/w D-glucose), pH (4.0-8.0), 0.3-4.3 mM (0.2-1.0 mL) of 10 mM buffer and temperature (30-70 °C). Amyloglucosidase concentration, pH and temperature were found to be significant. Experimental data fitted the second-order polynomial equation well, as indicated by R^2 value of 0.89. Validation experiments carried out under predicted conditions showed good correspondence between experimental and predicted yields. Various surface plots were generated to describe the relationship between operating variables and the conversion yields. The

highest yield of 53.5% predicted at optimum conditions of 75 equivalents n-octanol, 20 mg (20% w/w D-glucose) amyloglucosidase, 0.3 mM (0.2 mL), pH 7.8 buffer at 50 °C showed good correspondence to the experimental yield of 53.8% under these conditions.

Chapter **FOUR** describes amyloglucosidase catalyzed synthesis of phenolic glycosides: guaiacyl-α-D-glucoside **21a** and **b**, eugenyl maltoside **27a-c**, curcuminyl-bis-α-D-glucoside **30a** and **b** and α-tocopheryl-α-D-glucoside **36** by reflux method in di-isopropyl ether solvent at 68 °C. The parameters optimized were incubation period, enzyme concentration, pH and buffer concentration and substrate concentration. Maximum conversion yields obtained were guaiacyl-α-D-glucoside 52% for **21a** and **b**, 39% for eugenyl maltoside **27a-c**, 48% for curcuminyl-bis-α-D-glucoside **30a** and **b** and 52% for α-tocopheryl-α-D-glucoside **36**. Optimum conditions for guaiacyl-α-D-glucoside **21a** and **b** synthesis were: D-glucose **2** and guaiacol **17** in 1: 50 equivalent ratio, 50% (w/w D-glucose) amyloglucosidase, 0.06 mM (0.6 mL in 100 mL solvent) pH 7.0 phosphate buffer and 72 h incubation period. Those for eugenyl maltoside **27a-c** were 1: 10 equivalent ratio of maltose **8** and eugenol **18**, 40% (w/w maltose) amyloglucosidase, 0.1 mM (1.0 mL), pH 5.0 acetate buffer and 72 h incubation period. For curcuminyl-bis-α-D-glucoside **30a** and **b** the conditions were: curcumin **19** and D-glucose **2** in 2:1 molar ratio, 50% (w/w D-glucose) amyloglucosidase, 0.1 mM (1.0 mL), pH 4.0 acetate buffer and 72 h incubation period. For α-tocopheryl-α-D-glucoside **36** optimized conditions were D-glucose **2** and α-tocopherol **20** in 1:1 molar ratio, 40% (w/w D-glucose) amyloglucosidase, 0.2 mM (2.0 mL) pH 7.0 phosphate buffer and 72 h incubation period.

Under the optimized conditions, glycosides of guaiacol **17**, eugenol **18**, curcumin **19** and α-tocopherol **20** synthesis with various carbohydrates **2-12** were attempted. The conversion yields in the range 17-52% for guaiacyl glycosides, 7-32% for eugenyl

glycosides, 9-48% for curcuminyl glycosides and 52% for α-tocopheryl glucoside were obtained. Guaiacol **17** reacted with D-glucose **2** and D-galactose **3,** eugenol **18** and curcumin **19** reacted with D-glucose **2**, D-mannose **4**, maltose **8**, sucrose **9** and D-mannitol **11** and α-tocopherol **20** reacted only with D-glucose **2**. The glucosylation yields obtained using β-glucosidase from sweet almonds were 22% for guaiacyl-β-D-glucoside **22**, 19% for eugenyl-β-D-glucoside **25**, 11% for curcuminyl-β-D-glucoside **31** and 24% for α-tocopheryl-β-D-glucoside **37**. Of the 33 glycosides synthesized, the following glycosides are reported for the first time from this work: n-octyl-sucrose **16a** and **b**, guaiacyl-α-D-glucoside **21a** and **b**, guaiacyl-β-D-glucoside **22**, guaiacyl-α-D-galactoside **23a** and **b**, eugenyl-α-D-mannoside **26**, eugenyl maltoside **27a-c**, eugenyl sucrose **28a-c**, eugenyl-D-mannitol **29**, curcuminyl-bis-α-D-mannoside **32**, curcuminyl bis maltoside **33a-c**, curcuminyl bis sucrose **34a-c** and curcuminyl-bis-D-mannitol **35**. Both 2D-HSQCT and MS studies confirmed formation of the mono glycosylated and/or mono C6-O-arylated products for guaiacol **17**, eugenol **18** and α-tocopherol **20** and bis glycosylated and/or bis C6-O-arylated products in case of curcumin **19**. No other secondary hydroxyl groups of the carbohydrates were found to undergo arylation.

Curcuminyl-bis-α-D-glucoside **30a** and **b** exhibited water solubility at 14 g/L and a total colour of 10.8 in DMSO. Antioxidant activities of guaiacol **17** and curcumin **19** and their glucosides, guaiacyl-α-D-glucoside **21a** and **b** and curcuminyl-bis-α-D-glucoside **30a** and **b** showed 62% activity for guaiacyl-α-D-glucoside **21a** and **b** (89% for free guaiacol) and 80% activity for curcuminyl-bis-α-D-glucoside **30a** and **b** (79% for free curcumin).

Response surface methodology (RSM) was employed to optimize amyloglucosidase-catalyzed synthesis of curcuminyl-bis-α-D-glucoside **30a** and **b** by

reflux method. A CCRD was employed involving five variables (enzyme concentration, curcumin concentration, incubation period, buffer concentration and pH) at five levels. A second-order polynomial equation with a R^2 value 0.9 showed good correspondence between experimental and predicted yields. Three-dimensional surface and contour plots generated described the catalytic efficiency of amyloglucosidase under the reaction conditions employed. Experiments under optimum predicted conditions of 16.9% (w/w D-glucose) amyloglucosidase, 0.33 mmol curcumin, 120 h incubation period, 0.1 mM (1.0 mL of 0.01 M buffer in 100 mL reaction mixture) buffer concentration at pH 7.5 gave a conversion yield of 56%. Validation experiments carried out under selected random conditions also showed good correspondence between experimental and predicted yields.

Kinetic studies of the glucosylation reaction catalyzed by amyloglucosidase from *Rhizopus* sp. leading to the synthesis of curcuminyl-bis-α-D-glucoside **30a** and **b** from D-glucose **2** and curcumin **19** was investigated in detail. Initial reaction rates (v) were determined from kinetic runs involving different concentrations of D-glucose and curcumin (0.005 to 0.1 M). Graphical double reciprocal plots showed that the kinetics of the amyloglucosidase catalyzed reaction followed Ping-Pong Bi-Bi mechanism where competitive substrate inhibition by curcumin led to dead end amyloglucosidase-curcumin complex at higher concentrations of curcumin. An attempt to obtain the best fit of this kinetic model through computer simulation yielded in good approximation, the values of four important kinetic parameters, k_{cat} = 6.07±0.58 10^{-5} Mh^{-1}.mg, K_i = 3.0±0.28 mM, $K_{m\ D\text{-glucose}}$ = 10.0±0.9 mM and $K_{m\ curcumin}$ = 4.6±0.5 mM.

Chapter **FIVE** describes the Angiotensin Converting Enzyme (ACE) inhibition activity of the synthesized glycosides. Out of all the synthesized glycosides n-octyl-D-glucoside **13a-c**, n-octyl maltoside **15**, n-octyl sucrose**16a** and **b**, guaiacyl-α-D-glucoside

21a and **b**, guaiacyl-α-D-galactoside **23a** and **b**, eugenyl-α-D-glucoside **24a** and **b**, eugenyl-α-D-mannoside **26**, eugenyl maltoside **27a-c**, eugenyl sucrose **28a-c**, eugenyl-D-mannitol **29**, curcuminyl-bis-α-D-glucoside **30a** and **b**, curcuminyl-bis-α-D-mannoside **32**, curcuminyl bis maltoside **33a-c**, curcuminyl bis sucrose **34a-c**, curcuminyl-bis-D-mannitol **35** and tocopheryl-α-D-glucoside **36** were found to be ACE inhibitors. ACE inhibition activity (IC_{50} values) in the range 0.5±0.04 to 5.3±0.51 were obtained for the glycosides tested. Of these eugenyl-α-D-glucoside **24a** and **b** exhibited the best ACE inhibition activity (IC_{50} value 0.5±0.04 mM).

Thus the present investigation has brought out clearly the glycosylation potentialities of amyloglucosidase from *Rhizopus* sp. and β-glucosidase from sweet almonds of n-alkanols and phenols like guaiacol, eugenol, curcumin and α-tocopherol, explored with diverse carbohydrate molecules.

References

Adachi, S., Kobayashi, T., 2005. Synthesis of esters by immobilized lipase catalyzed condensation reaction of sugar and fatty acids in water-miscible organic solvent. **J. Biosci. Bioeng.** 99, 87-94.

Aga, H., Yoneyama, M., Sakai, S., Yamamoto, I., 1990. Synthesis of 2-O-α-D-glucopyranosyl L-ascorbic acid by cyclomaltodextrin glucotransferase from *Bacillus stearothermophilus*. **Agric. Biol. Chem.** 55, 1751-1756.

Akao, T., Yoshino, T., Kobashi, K., Hatlori, M., 2002. Evaluation of salicin as an antipyretic prodrug that does not cause gastric injury. **Planta Med.** 68, 714-718.

Aleshin, A.E, Golubev, A., Firsov, L.M., Honzatko, R.B., 1992. Crystal structure of glucoamylase from *Aspergillus awamori* var X100 to 2.2-Å resolution. **J. Biol. Chem.** 267, 19291-19298.

Aleshin, A.E., Firsov, L.M., Honzatko, R.B., 1994. Refined structure for the complex of acarbose with glucoamylases from *Aspergillus awamori* var. X100 to 2.4 A° resolution. **J. Biol. Chem.** 269, 15631-15639.

Ali, S., Hossain, Z., 1991. Characteristics of glucoamylase from *Aspergillus terreus*. **J. Appl. Bacteriol.** 71, 144 -146.

Allen, M.J., Fang, T.Y., Li, Y., Liu, H.L., Chen, H.M., Coutinho, P., Honzatko, R., Ford C., 2003. Engineering *Aspergillus awmori* glucoamylase variants for improved thermostability reduced isomaltase formation and increased pH optimum. **US 6537792 B1** (CA 138:250712).

Andersson, M., Adlercreutz, P., 2001. A kinetic study of almond-β-glucosidase catalyzed synthesis of hexyl-glycosides in low aqueous media Influence of glycosyl donor and water activity. **J. Mol. Catal. B: Enzym.** 14, 69-76.

Antonini, E., Carrea, G., Cremonesi, P., 1981. Enzyme catalyzed reactions in water-organic solvent two phase systems. **Enzyme Microb. Technol.** 3, 291-296.

AOAC official methods of analysis. 1995. 16th Edn, Vol II, Chapter 46, pp 12.

Ashikari, T., Nakamura, N., Tanaka, Y., Kiuchi, N., Shibano, Y., Tanaka, T., Amachi, T. and Yoshizumi, H., 1986. *Rhizopus* raw-starch-degrading glucoamylase: Its cloning and expression in yeast, **Agric. Biol. Chem.** 50, 957-964.

Auge, C., Fernandez, R.F., Gautheron, C.M., 1990. The use of immobilized glycosyltransferases in the synthesis of sialyl oligosaccharides. **Carbohydr. Res.** 200, 257-268.

Balzar, D., 1991. Alkylglucosides, their physico-chemical properties and their uses. **Tenside Surf. Det.** 28, 419-427.

Barolini, M., Cavrini, V., Andrisano, V., 2004. Monolithic micro-immobilized enzyme reactor with human recombinant acetylcholinesterase for on line inhibition studies. **J. Chromatogr.** 1031, 27-34.

Bender, H., 1981. A bacterial glucoamylase degrading cyclodextrins. **Eur. J. Biochem.** 115, 287-291.

Berfoldo, C., Anthranikian, G., 2001. Amylolytic enzymes from hyperthermophiles. **Methods Enzymol.** 330, 269-289.

Book, K., Pedersen, C., 1983. In: Carbon 13 NMR spectroscopy of monosaccharides. **Adv. Carbohydr. Chem. Biochem.** 41, 27-66.

Book, K., Pedersen, C., Pedersen, H., 1983. Stuart-Tipson and Horton (ed) In: Carbon 13 NMR data for oilgosaccharides. **Adv. Carbohydr. Chem. Biochem.** 42, 27-66.

Braun, H., Cogoli, A., Semenza, G., 1977. Carboxyl groups at the two active centers of sucrose-isomaltoase from rabit small intestine **Eur. J. Biochem.** 73, 437-442.

Brink, L.E.S., Tramper, J., 1985. Optimization of organic solvent in multiple biocatalysis. **Biotechnol. Bioeng.** 27, 1259-1269.

Brown, J.R., Guther, M.L.S., Field, R.A., Ferguson, M.A.J., 1997. Hydrophobic mannosides act as acceptors for trypanosome α-mannosyltransferases. **Glycobiology** 7, 549-558.

Buchholz, K., Kasche, V., Bornscheuer, U.T., 2005. **Biocatalysts and enzyme technology.** Willey-VCH, Weinheim.

Busch, P., Hensen, H., Khare, J., Tesmann, H., 1994. Alkylpolyglycosides-a new cosmetic concept for milderness. **Agro-Food-Ind. Hi-Tech** 5, 20-28.

Butler, L.G., 1979. Enzymes in non-aqueous solvets. **Enzyme Microb. Technol.** 1, 253-259.

Cai, H-C., Fang, Y., Xia, Y-M., Cai, K., 2003. New catalytic technique: microwave irradiation-enzyme coupling catalysis. **Youji Huaxue** 23, 298-304 (Chinese).

Camacho, P.B., Robles, M.A., Camacho, R.F., Gonzalez, M.P., Molina, G.E., 2003. Modeling the effect of free water on enzyme activity in immobilized lipase-catalyzed reactions in organic solvents. **Enzyme Microb. Technol.** 33, 845-853.

Chaga, G., Porath, J., Illeni, T., 1993. Isolation and purification of amyloglucosidase from *Halobacterium sodomenase.* **Biomed. Chromatogr.** 7, 256-261.

Chahid, Z., Montet, D., Pina, M., Bonnot, F., Graille, J., 1994. Biocatalyzed octylglycoside synthesis from a disaccharide. **Biotechnol. Lett.** 16, 795-800.

Chahid, Z., Montet, D., Pina, M., Graille, J., 1992. Effect of water activity on enzymic synthesis of alkyl glycosides. **Biotechnol. Lett.** 14, 281-284.

Chang, M-Y., Juang, R-S., 2005. Activities, stabilities and reaction kinetics of three free and chitosan-clay composite immobilized enzymes. **Enzyme Microb. Technol.** 36, 75-82.

Chen, C.W., Ou-Yang, C-C., Yeh, C-W., 2003. Synthesis of galactooligosaccharides and transgalactosylation modeling in reverse micelles. **Enzyme Microb. Technol.** 33, 497-507.

Chen, H.C., Chang, C.C., Chen, C.X., 1997. Optimization of arachidonic acid production by *Mortierella alpina* Wuji-H4 isolate. **J. Am. Oil Chem. Soc.** 74, 569-578.

Chen, S-X., Wei, D-Z., Hu, Z-H., 2001. Synthesis of galacto-oligosaccharides in AOT/isooctane reverse micelles by β-galactosidase. **J. Mol. Catal. B: Enzym.** 16, 109-114.

Chiba, S., 1995. Enzyme chemistry and molecular biology of amylase and related enzymes, edited by the amylase research society of Japan, CRC press, Boca raton, Ann arbor, London, Tokyo. pp 68-82.

Chiba, S., 1997. Molecular mechanism in α-glucosidase and glucoamylase. **Biosci. Biotech. Biochem.** 61, 1233-1239.

Chojecki, A., Blaschek, H.P., 1986. Effect of carbohydrate source on alpha-amylase and glucoamylase formation by *Clostrodium acetobutylicum* SA-1. **Ind. Microbiol.** 1, 63-67.

Chong-Qian, L., Bo-Gang, L., Hua-Yi, Q., Qi-Lin, L., Feng-Peng, W., Guo-Lin, Z., 2004. Three cyclooctapeptides and one glycoside from *Microtoena prainiana* **J. Nat. Prod.** 67, 978-982.

Clarks, A, J., Svensson, B., 1984. Identification of an essential tryptophanyl residue in the primary structure of glucoamylase G2 from *Aspergillus niger*. **Carlesberg. Res. Commun.** 49, 559-566.

Colowick, S.P., Kaplan, N.O., 1976. Immobilized enzymes. Ed. By Mosbach, K. **Methods Enzymol.** 44, 101.

Cooke, J.W.B., Hayes, D., Henson, R.A., Hermitage, S.A., Ward, R.A., Whitehead, A.J., 2003. Process for the preparation of 4-substituted phenylalanyl ester derivatives, PCT Int. Appl. **WO 2003068725 A2** (CA 138:180345).

Crout, D.H.G., Vic, G., 1998. Glycosidases and glycosyl transferases in glycoside and oligosaccharides synthesis. **Biocatal. Biotransform.** 2, 98-111.

Cushman, D.W., Cheung, H.S., 1971. Spectrophotometric assay and properties of the Angiotensin-Converting Enzyme of rabbit lung. **Chem. Pharmacol.** 20, 1637-1638.

Czjzek, M., Cicek, M., Zamboni, V., Burmeister, W.P., Beven, R.B., Henrissat, B., Essen, A., 2001. Crystal structure of a monocotyledon (maize ZmGlu1) β-glucosidase and a model of its complex with p-nitrophenyl β-D-thioglucoside. **Biochem. J.** 354, 37-46.

Dae-Gill, K., Yong-Sup, L., Hyoung-Ja, K., Yun-Mi, L., Ho-Sub, L., 2003. Angiotensin converting enzyme inhibitory phenylpropanoid glycosides from *Clerodendron trichotomum*. **J. Etanopharmacol.** 89, 151-154.

Davies, G., Henrissat, B., 1995. Structures and mechanisms of glycosyl hydrolases. **Structure** 3, 853-859.

Davis, B.G., Boyer, V., 2001. Biocatalysis and enzymes in organic synthesis. **Nat. Prod. Rep.** 18, 618-640.

De Lima, D.P., 1999. Synthesis of angiotensin converting enzyme (ACE) inhibitors: an important class of anti-hypertensive drugs, **Quim Nova** 22, 375-381.

De Oliveira, R.N., De Freitas, F.J.R., Srivastava, R.M., 2002. Microwave-induced synthesis of 2,3-unsaturated O-glycosides under solvent-free conditions. **Tetrahedron Lett.** 43, 2141-2143.

Deloffre, L., Sautiere, P.E., Huybrechts, R., Hens, K., Vieau, D., Salzet, M., 2004. Angiotensin-converting enzyme inhibition studies by natural leech inhibitors by capillary electrophoresis and competition assay. **Eur. J. Biochem.** 271, 2101-2106.

Dixon, M., Webb, E. C., (Eds). 1958. Enzyme specificity: In Enzymes, Longmans Green and Co Ltd. London. pp 242-295.

Donho, M., Kimura, T., Hara, H., 1996. Methods of producing geranyl β-D-galactopyranoside as flavoring material by enzymatic galactosylation of citronellol. **Jpn. Kokai Tokkyo Konho JP 8188589-8188591** (CA 125:222344).

Dordick, J.S., 1989. Enzymatic catalysis in monophasic organic solvents. **Enzyme Microb. Technol.** 11, 194-211.

Drauz, K., Waldmann, H., (Eds), 2002. Enzyme catalysis in organic synthesis, 2nd edition, Vols 1-3, Willey-VCH, Weinheim.

Dubey, V.K. Jagannadham, M.B., 2003. Procerain, a stable cysteine protease from the latex of *Calotropis procera*. **Phytochemistry** 62, 1057-1071.

Ducret, A., Troni, M., Larotie, R., 2002. Screening of various glycosides for the synthesis of octyl glucoside. **Biotechnol. Bioeng.** 77, 752-757.

Eriksson, S., Nylen, U., Rojas, S., Boutonnes, M., 2004. Preparation of catalysis from microemulsions and their applications in heterogeneous catalysis. **Appl. Catalysis. A: General** 265, 207-219.

Ermer, J., Rose, K., Huber, G., Schhellenenberger, A., 1993. Subsite affinities of *Aspergilus niger* glucoamylase II determined with *p*-nitophenylmaltooligosaccharides. **Biol. Chem. Hoppe-Seyler** 374, 123-128.

Ernst, B., Hart, G.W., Sinay, P., 2000. In Carbohydrates in chemistry and biology. Willey-VCH, Weinheim. Vol 1 pp 177-193.

Eveleigh, D.E., Perlin, A.S., 1969. A proton magnetic resonance study of the anomeric species produced by D-glucosidases. **Carbohydr. Res.** 10, 87-95.

Faber, K., 2004. Biotransformations in organic chemistry, 5th edition, Springer, Berlin.

Fadnavis, N.W., Deshpande, A., 2002. Synthetic applications of enzymes entrapped in reverse micelles and organo gels. **Cur. Org. Chem.** 6, 393-410.

Fagerstrom, R., 1991. Subsite mapping of *Hormoconis resinae* glucoamylase and their inhibition by gluconolactone. **J. Gen. Microbiol.** 137, 1001-1008.

Fischer, E., 1894. Einfluss der konfiguration auf die wirkung der enzyme. **Ber. Chem. Ges.** 27, 2985-2993.

Fogarty, W.M., (ed.) 1983. Microbial amylases. In Microbial Enzymes and Biotechnology. Appl. Science Publishers, London. pp 1-92.

Fourage, L., Dion, M., Color, B., 2000. Kinetic study of a thermostable β-glucosidase of *thermos thermophilus*. Effects of temperature and glucose on hydrolysis and transglycosylation reactions. **Glycoconj. J.** 17, 377-383.

Frandsen, T.P., Dupont, C., Lehmbeck, J., Stoffer, B., Sierks, M.R., Honzatko, R.B., Svensson, B., 1994. Site-directed mutagenesis of the catalytic base Glutamic acid 400 in glucoamylase from *Aspergillus niger* and of Tyrosine 48 and Glutamine 401, both hydrogen bonded to the gamma-carboxylate group of Glutamic acid 400. **Biochemistry** 33, 13808-13816.

Fujimoto, H., Isomura, M., Ajisaka, K., 1997. Syntheses of alkyl β-D-mannopyranosides and β-1,4-linked oligosaccharides using β-mannosidase from *Rhizopus niveus*. **Biosci. Biotechnol. Biochem.** 61, 164-165.

Gargouri, M., Smaali, I., Maugardb, T., Dominique, L.M., Marzouki, N., 2004. Fungus β-glycosidases: immobilization and use in alkyl-β-glycoside synthesis. **J. Mol. Catal. B: Enzym.** 29, 89-94.

Gellissen, G., Janowicz, Z.A., Merckelbach, A., Piontek, M., Keup, P., Weydemann, U., Hollenberg, C.P., Srasser, A.W.M., 1991. Heterologus gene expression in *Hansenula polymorpha*: Efficient secretion of glucoamylase. **Biotechnol.** 9, 291-295.

Gelo-Pujic, M., Guibe-Jampel, E., Loupy, A., Tricone, A., 1997. Enzymic glycosidation in dry media under microwave irradiation. **J. Chem. Soc. Perkin Trans.** 1, 1001-1002.

Ghosh, A., Chatterjee, B.S., Das, A., 1990. Characterization of glucoamylase from *Aspergillus terreus* 4. **FEMS Microbial. Lett.** 66, 345-349.

Gill, R.K., Kaur, J., 2004. A thermostable glucoamylase from a thermophilic *Bacillus* sp. characterization and thermal stability. **J. Industrial Microbiol. Biotechnol.** 31, 540-543.

Glew, R.H., Gopalan, V., Forsyth, G.W., VanderJagt, D.J., 1993. In β-glucosidases: Biochemistry and molecular biology, Americal Chemical Society, Washington, D. C. pp 83-112.

Golik, J., Clardy, J., Dubay, G., Groenewold, G., Kawaguchi, H., Konishi, M., Krishnan, B., Ohkuma, H., Saitoh, K., Dobye, T.W., 1987. Esperamicins, a novel class of potent antitumor antibiotics. 3. Structures of esperamicins A1, A2 and A1b. **J. Am. Chem. Soc.** 109, 3461-3464.

Gomes, D.C.F., Alegrio, L.V., Leon, L.L., de Lima, M.E.F., 2002. Total synthesis and anti-leishmanial activity of some curcumin analogues. **Arzneim-Forsch.** 52, 695-698.

Goto, M., Tanigava, K., Kanlayakrit, W., Hayashida, S., 1994. The molecular mechanism of binding of glucoamylases I from A*spergillus awamori* var. kawachi to cyclodextrin and raw starch, **Biosci. Biotech. Biochem.** 58, 49-54.

Gunata, Z., Vallier, M.J., Sapis, J.C., Baumes, R., Bayonove, C., 1994. Enzymic synthesis of monoterpeny β-D-glucosides by various β-glucosidases. **Enzyme Microb. Technol.** 16, 1055-1058.

Gunther, S., Heymann, H., 1998. Di and oligosaccharide substrate specificities and subsite binding energies of pig intestinal glucoamylase-maltase. **Arch. Biochem. Biophys.** 354, 111-116.

Gygax, D., Spies, P., Winkler, T., Pfaar, U., 1991. Enzymatic synthesis of β-D-glucuronides with *in situ* regeneration of uridine 5'-diphosphoglucuronic acid. **Tetrahedron** 47, 5119-5122.

Haasum, I., Ericksen, S.H., Jensen, B., Olsen, J., 1991. Growth and glucoamylase production by the thermophilic fungus *Thermophilus lanuginose* in a synthetic medium. **Appl. Microbiol. Biotechnol.** 34, 656-660.

Halling, P.J., 1992. Salt hydrates for water activity control with biocatalysts in organic media. **Biotechnol. Lett.** 6, 271-276.

Hamada, H., Ohiwa, S., Nishida, T., Katssuragi, H., Takeda, T., Hamada, H., Nakajima, N., Ishihara, K., 2003. One step glucosylation of capsaicinoids by cultured cells of *Phytolacca americana.* **Plant Biotechnol.** 20, 253-255.

Hamada, K., Ikamoto, T., 2001. Effects of clove bud oil related eugenyl glucoside on hair growth. **Fragrance J.** 29, 47-52 (Japanese).

Harris, E.M.S., Aleshin, A.E., Firsov, L.M., Honzatko, R.B., 1993. Refined structure of the complex of 1-deoxynojirimycin with glucoamylase from *Aspergillus awamori* var X100. **Biochemistry** 32, 1618-1626.

Hays, W.S., Jeniso, S.A., Yamada, T., Pastuszyn, A.P., Glew, R.H., 1996. Primary structure of the cytosolic β-glucosidase of guinea pig liver. **Biochem. J.** 319, 829-837.

Hays, W.S., Vander Jagt, D.J., Bose, B., Serianni, A.S., Glew, R.H., 1998. Catalytic mechanism and specificity for hydrolysis and transglycosylation reactions of cytosolic β-glucosidase from guinea pig liver. **J. Biol. Chem.** 273, 34941-34948.

He, S., Withers, S.G., 1997. Assignment of sweet almond β-glucosidase as a family 1 glycosidase and identification of its active site nucleophile. **J. Biol. Chem.** 272, 24864-24867.

Helferich, B., Kleinschmidt, T., 1965. Data on sweet emulsion, **Z. Physiol. Chem.** 340, 31.

Hergenhahn, M., Bertram, B., Wiessler, M., Sorg, B.L., 2002. Saccharide containing curcumin derivatives with improved water solubility for pharmaceuticals German Patent application. **WO 2001-DE 2337** (CA 136:90984).

Hestrin, S., Feingold, D.S., Schramm, M., 1955. β-Glucosidase from sweet almond emulsin. Colowick, S.P., Kaplan, N.O (Eds), **Methods Enzymol.** 1, 234-240.

Hiromi, K., 1970. Interpretation of dependency of rate parameters on the degree of polymerization of substrate in enzyme-catalyzed reactions. Evaluation of subsite affinities of exoenzyme. **Biochem. Biophys. Res. Comm.** 40, 1-6.

Hiromi, K., Kawai, M., Ono, S., 1966a. Kinetic studies on glucoamylase IV. Hydrolysis of isomaltose. **J. Biochem.** 59, 476-480.

Hiromi, K., Nitta, Y., Numata, C., Ono, S., 1973. Subsite affinities if glucoamylase examination of the validity of the subsite theory. **Biochem. Biophys. Acta.** 302, 362-375.

Hiromi, K., Ohnishi, M., Tanaka, A., 1983. Subsite structure and ligand binding mechanism of glucoamylase, **Mol. Cell. Biochem.** 51, 79-95.

Hiromi, K., Takahashi, K., Hamazu, Z., Ono, S., 1966b. Kinetic studies on glucoamylase III. The influence of pH on the rates of hydrolysis of maltose and panose. **J. Biochem.** 59, 469-475.

Hofmann, R.W., Swinny, E.E., Bloor, S.J., Markham, K.R., Ryan, K.G., Campbell, B.D., Jordan, B.R., Fountain, D.W., 2000. Responses of nine *Trifolium repens L.* populations to ultraviolet-B radiation. Differential flavonol glycoside accumilation and biomass production. **Ann. Bot.** 86, 527-537.

Huang, K.H., Akoh, C.C., 1996. Optimization and scale up of enzymatic synthesis of structured lipids using RSM. **J. Food Sci.** 61,137-141.

Humeau, M., Girardin, B., Rovel, A.M., 1998. Effect of the thermodynamic water activity and the reaction medium hydrophobicity on the enzymatic synthesis of ascorbyl palmitate. **J. Biotechnol.** 63, 1-8.

Huo, Y., Li, Y., Yuan, Z., Huang, J., 2004. Immobilization of glucoamylase onto novel porous polymer supports of vinylene carbonate and 2-hydroxy ethyl methacrylate. **Appl. Biochem. Biotechnol.** 119, 121-131.

Hyun, H.H., Zeikus, J.G., 1985. General biochemical characterization of thermostable pullulanase and glucoamylase from *Clostridium thermohydrosulfuricum.* **Appl. Environ. Microbiol.** 49, 1168-1173.

Hyuncheol, O., Dae-Gill, K., C., Hun-Taeg, L., Ho-Sub, L., 2003. Four glycosides from the leaves of *Abeliophyllum distichum* with inhibitory effects on angiotensin converting enzyme. **Phytotheraphy Res.** 17, 811-813.

Ibanoglu, E., Ibanoglu, S., 2000. Foaming behavior of liquorice (*Glycyrrhiza glabra*) extract. **Food chem.** 70, 333-336.

Ichikawa, Y., Look, G.C., Wong, C.H., 1992. Enzyme-catalysed oligosaccharide synthesis. **Anal. Biochem.** 202, 215-238.

Igarashi, K., 1977. The Koenigs-Knorr reaction. **Adv. Carbohydr. Chem. Biochem.** 34, 243-283.

Ikeda, D., Umezawa, S., 1999. In naturally occurring glycosides: Ikan, R., Ed., Jhon Willey & Sons, Ltd., New York. pp 1-42.

Ismail, A., Ghoul, M., 1996. Enzymatic synthesis of butyl glycosides by glycosidases. **Biotechnol. Lett.** 18, 1199-1204.

Ismail, A., Linder, M., Ghoul, M., 1999. Optimization of butylgalactoside synthesis by β-galactosidase from *Aspergillus oryzae.* **Enzyme Microb. Technol.** 25, 208-213.

Ismail, A., Soultani, S., Ghoul, M., 1998. Optimization of the enzymatic synthesis of butyl glucoside using response surface methodology. **Biotechnol. Prog.** 14, 874-878.

Itoh, T., Sakata, Y., Akada, R., Nimi, O., Yamshita, I., 1989. Construction and characterization of mutant glucoamylases from the yeast *Sacharomycopsis fibuligera.* **Agric. Biol. Chem.** 53, 3159-3168.

IUBM 1992. International Union of Biochemistry and Molecular biology Nomenclature Committee Enzyme Nomenclature Committee of the International Union of Biochemistry and Molecular biology (IUBM) on the nomenclature and classification of enzymes. Academic press, New York.

IUPAC-IUB Joint Commission on Biochemical Nomenclature (JCBN). 1982. Nomenclature of tocopherols and related compounds. Recommendations 1981. **Eur. J. Biochem.** 123, 473-475.

Jacobson, R.H., Kuroki, R., Weaver, L.H., Zhang, X.-J., Matthews, B.W., 1995. In Enzymatic degradation of insoluble carbohydrates, Saddler, J.N., Penner, M.H. (eds.), **ACS Symposium series,** Washington, 618, 38-50.

Jacobson, R.H., Zhang, X-J., DuBose, R.F., Matthews, B.W., 1994. Three dimensional structure of β-galactosidase from *E. Coli.* **Nature** 369, 761-766.

James, J.A., Lee, B.H., 1995. Cultural conditions for production of glucoamylase from *Lactobacillus amylovorus* ATCC 33621. **J. Appl. Bacteriol.** 79, 499-505.

Janssen, A.E.M., Sjursnes, B.J., Vakurov, A.V., Halling, P.J., 1999. Kinetics of lipase-catalysed esterification in organic media: correct model and solvent effects on parameters, **Enzyme Microb. Technol.** 24, 463-470.

Jianping, Z., Weizhong, G., Jianqian, W., Hui, Y., 2003. Immobilization of glucoamylase on polyvinyl alcohol complex gel. **Weishengwuxue Tongbao** 30, 10-13 (Chinese).

Johnston, I., 1992. Renin-angiotensin system: a dual tissue and hormonal system for cardiovascular control. **J. Hypertens.** 10, 13-26.

Kaljuzhin, O.V., Shkalev, M.V., 2000. Immunomodulator and pharmacuitical compositions with antitumor properties, and a food additive. Patent **EP1038532** (CA 129:335732).

Kaminaga, Y., Nagatsu, A., Akiyama, T., Sugimoto, N., Yamazaki, T., Maitani, T., Mizukami, H., 2003. Production of unnatural glucosides of curcumin with drastically enhanced water solubility by cell suspension cultures of *Catharanthus roseus*. **FEBS Lett.** 555, 311-316.

Kaper, T., Lebbink, J.H.G., Pouwels, J., Kopp, J., Schulz, G.E., Oost, J.V., Vos, W.M., 2000. Coparitive structural analysis and substrate specificity engineering of the hyperthermostable β-glucosidase CelB from *Pyrococcus furious*. **Biochemistry** 39, 4963-4970.

Katusumi, K., Mikio, F., Yoshiteru, I., Hiroyuki, A., 2004. Simple synthesis of β-D-glycopyranosides using β-glycosidase from almonds. **Chem. Pharm. Bull.** 52, 270-275.

Ken, V., Cvak, L., 1999. Ergot genus *Claviceps*, medicinal and aromatic plants-industrial profiles, Harwood Publ. Ltd. Amsterdam, London.

Kengen, S.W.M., Luesink, E.J., Stams, A.J.M., Zehnder, A.J.B., 1993. Purification and characterization of an extremely thermostable β-glucosidase from the hyperthermophilic archaeon *Pyrococcucus furious*. **Eur. J. Biochem.** 213, 305-312.

Kim, S.K., Byun, H.G., Park, P.J., Shahidi, F., 2001. Angiotensin I converting enzyme inhibitory peptides purified from bovine skin gelatin hydrolysate. **J. Agric. Food Chem.** 49, 2992-2997.

Kim, W.D., Kaneko, S., Park, G.G., Tanaka, H., Kusakabe, I., Kobayashi, H., 2003. Purification and characterization of α-galactosidase from sunflower seeds. **Biotechnol. Lett.** 25, 353-358.

Kiran, K.R., Divakar, S., 2002. Enzyme inhibition by *p*-cresol and lactic acid in lipase-mediated synthesis of *p*-cresyl acetate and steroyl lactic acid: a kinetic study. **World J. Microb.Biotechnol.** 18, 707-712.

Kiran, K.R., Karanth, N.G., Divakar, S., 1999. Preparation of stearyl lactic acid catalyzed by immobilized lipases from *Rhizomucor miehei* and pancreas. Optimization using response surface methodology. **Appl. Microbiol. Technol.** 52, 579-584.

Kiran, K.R., Manohar, B., Karanth, N.G., Divakar, S., 2000. Response surface methodological study of esterification of lactic acid with palmitic acid catalyzed by immobilized lipases from *mucor miehei* and porcine pancreas. **Z. Lebm. Unt. Fors.** 211, 130-135.

Kleinman, M.J., Wilkinson, A.E., Wright, I.P., Evans, I.H., Bevan, E.A., 1988. Purification and properties of an extracellular glucoamylase from a diastatic strain of *Saccharomyces cerevisiae.* **Biochem. J.** 249, 163-170.

Klibanov, A.M., 1986. Enzymes that work in organic solvents, **Chemtech.** 16, 354-359.

Kohda, H., Kasai, R., Yamasaki, K., Tanaka, O., 1976. New sweet diterpene glucosides from *Stevia rebaudiana*. **Phytochemistry** 15, 981-983.

Kojima M., Maruo, S., Ohgi, T., Ezure, Y., 1996. Enzymatic synthesis of 4-O-β-D-glactopyranosylmoranoline and 3-O-β-D-galactopyranosylmoranoline by using β-galactosidase from *Bacillus circullans*. **Biosci. Biotech. Biochem.** 60, 694-696.

Kometani, T., Tanimoto, H., Nishimura, T., Kanbara, I., Okada, S., 1993a. Glucosylation of capsaicin by cell suspenion cultures of *Coffea arabica.* **Biosci. Biotech. Biochem.** 57, 2192-2193.

Kometani, T., Tanimoto, H., Nishimura, T., Okada, S., 1993b. Glucosylation of vanillin by cultured plant cells. **Biosci. Biotech. Biochem.** 57, 1290-1293.

Konstantinovic, S., Predojevic, J., Gojkovic, S., Ratkovic, Z., Mojsilovic, B., Pavlovic, V., 2001. Synthesis of C7-C16 alkyl 2,3 dideoxy glucosides from glucose and fatty acids. **Ind. J. Chem. 40B** 1242-1244.

Kosary, J., Stefanovits-Banyai, E., Boross, L., 1998. Reverse hydrolytic process for O-alkylation of glucose catalyzed by immobilized α- and β-glucosidases. **J. Biotechnol.** 66, 83-86.

Kouptsova, O.S., Klyachko, N.L., Levashov, A.V., 2001. Synthesis of alkyl glycosides catalyzed by β-glycosidases in a system of reverse micelles. **Russian J. Bioorg. Chem.** 27, 380-384.

Krause, D.R., Wood, C.J., Mac Lean, D.J., 1991. Glucoamylase (exo-1,4-α-D-gluanohydrolase, E.C. 3.2.1.3) is the major starch-degrading enzyme secreted by the phytopathogenic fungus *Colletotrichm gloeosporiodes*. **J. Gen. Microbiol.** 137, 2463-2468.

Kren, V., Chemical biology and biomedicine of glycosylated natural compounds. 2001. In Glycoscience Chemistry and Chemical Biology, Eds. Fraser-Reid, B., Tatsuta, K., Thiem, J., Springer Berlin, 3, 2471-2529.

Kren, V., Martinkova, L., 2001. Glycosides in medicine: The role of glycosidic residue in biological activity. **Curr. Med. Chem.** 8, 1313-1338.

Kurashima, K., Fujii, M., Ida, Y., Akita, H., 2004. Simple synthesis of β-glycopyranosides using β-glycosidase from almonds. **Chem. Pharm. Bull.** 52, 270-275.

La Cara, F., Scarfi, M.R., D'Auria, S., Massa, R., D'Ambrosio, G., Franceschetti, G., Rossi, M., De Rosa, M., 1999. Different effects of microwave energy and conventional heat on the activity of a thermophilic β-galactosidase from *Bacillus acidocaldarius.* **Bioelectromagnetics,** 20, 172-176.

Laane, C., Boeren, S., Vos, K., Veeger, C., 1987. Rules for optimization of biocatalysis in organic solvents. **Biotechnol. Bioeng.** 30, 81-87.

Lahmann, M., Thiem, J., 1997. Synthesis of α-tocopheryl oligosaccharides. **Carbohydr. Res.** 299, 23-31.

Lamelli, U.K., 1970. Cleavage of structural protein during the assembly of the head of bacteriophageT4. **Nature** 227, 680-685.

Laroute, V., Willemot, R.M., 1992a. Glucoside synthesis by glucoamylase or β-glucosidase in organic solvents. **Biotechnol. Lett.** 14, 169-174.

Laroute, V., Willemot, R.M., 1992b. Effect of organic solvents on stability of two glycosidases and on glucoamylase-catalyzed oligosaccharides synthesis. **Enzyme Microb. Technol.** 14, 528-534.

Lee, H-J., Larue, J. N., Wilson, I. B., 1971. Angiotensin converting enzyme from guinea pig and hog lung. **Biochem. Biophys. Acta** 250, 549-557.

Lee, M.D., Dunne, T.S., Chang, C.C., Ellestad, G.A., Siegel, M.M., Morton, G.O., McGahren, W.J., Borders, D.B., 1987. Calichemicines, a novel family of antitumor antibiotics 2. Chemistry and structure of calichemicin, γ^{I}, **J. Am. Chem. Soc.** 109, 3466-3468.

Lehinger, A.L., 1975. Sugars, Storage polysaccharides and cell walls. Biochemistry. Worth publishers Inc. New York, pp 249-276.

Li, G.H., Le, G.W., Yong-Hui, S., Shrestha, S., 2004. Angiotensin I–converting enzyme inhibitory peptides derived from food proteins and their physiological and pharmacological effects. **Nutrition Res.** 24, 469-486.

Limousin, C., Cleophax, J., Petit, A., Loupy, A., Lukacs, G., 1997. Solvent-free synthesis of decyl D-glycopyranosides under focused microwave irradiation. **J. Carbohydr. Chem.** 16, 327-342.

Linder, M., Fanni, J., Parmentier, M., Sergent, M., Phan-Tan-Luu, R., 1995. Protein recovery from veal bones by enzymatic hydrolysis. **J. Food Sci.** 60, 949-952.

Liu, H.L., Wang, W.C., 2003. Protein engineering to improve the thermostability of glucoamylase from *Aspergillus awmori* based on molecular dynamics simulations. **Protein Eng.** 16, 19-25.

Liu, H-S., Cheng, Y-C., 2000. Stability enhancement of α-amylase by supercritical carbon dioxide pretreatment. **Prog. Biotechnol.** 16, 149-154.

Ljunger, G., Adlercreutz, P., Mattiasson, B., 1994. Enzymatic synthesis of octyl-β-glucoside in octanol at controlled water activity. **Enzyme Microb. Technol.** 16, 751-755.

Long, B.H., Golik, J., Forenza, S., Ward, B., Rehfuss, R., Onbeowiak, J.C., Catino, J.J., Musial, S.T., Brookshire, K.W., Doyle, T., 1989. Esperamicins, a class of potent antitumor antibiotics: mechanism of action. **Proc. Natl. Acad. Sci.** USA. 86, 2-6.

Lowry, O.H., Rosenbrough, N.J., Farr, A.L., Randal, R.J., 1951. Protein measurement with Folin Phenol reagent. **J. Biol. Chem.** 193, 265–275.

Luisi, P.L., Gimini, M., Pileni, M.P., Robinson, B.H., 1998. Reverse micelles as hosts for proteins and small molecules. **Biochem. Biophys. Acta** 947, 209-246.

Madsen, T., Petersen, G., Seiero, C., Torslov, J., 1996. Biodegradability and aquatic toxicity of glycoside surfactants and a nonionic alcohol etherate. **J. Am. Oil Chem. Soc.** 73, 929-933.

Malek, S.A.S., Hossain, Z., 1994. Purification and characterization of a thermostable glucoamylase from *Myrothecium* isolate. **J. Appl. Bacteriol.** 76, 210-215.

Manohar, B., Divakar, S., 2002. Application of Central Composite Rotatable Design to lipase catalyzed synthesis of *m*-cresyl acetate. **World. J. Microbiol. Biotechnol.** 18, 745-751.

Marana, S.R., Andrade, E.H., Ferreira, C., Terra, W.R., 2004. Investigation of the substrate specificity of a β-glycosidase from *Spodoptera frugiperda* using site-directed mutagenesis and bioenergetics analysis. **Eur. J. Biochem.** 271, 4169-4177.

Marana, S.R., Jacobs-Lorena, M., Terra, W.R., Ferreira, C., 2001. Amino acid residues involved in substrate binding and catalysis in an insect digestive β-glycosidase. **Biochem. Biophys. Acta.** 1545, 41-52.

Margolin, A.L., Tai, D.F., Klibanov, A.M., 1987. Incorporation of D-amino acids into peptides via enzymatic condensation of organic solvents. **J. Am. Chem. Soc.** 109, 7885-7887.

Mariano, G-G., Agustin, L-M., Eduardo., 2000. Alcoholysis and reverse hydrolysis reactions in organic one-phase system with a hyperthermophilic β-glycosidase. **Biotechnol. Bioeng.** 69, 627-632.

Marty, A., Chulalaksananukul, W., Willemot R.M., Condoret, J.S., 1992. Kinetics of lipase-catalysed esterification in supercritical CO_2. **Biotechnol. Bioeng.** 39, 273-280.

Masumura, Y., Kasunoki, M., Harada, W., Kakudo, M., 1984. Structure and possible catalytic residues of taka amylase A. **J. Biochem.** 95, 697-702.

Matsuda, T., Harada, T., Nakamura, K., 2002. Biotransformations in supercritical carbon dioxide. **Fain Kemikaru** 31, 40-49 (Japanese).

Matsumura, S., Imai, K., Yoshikawa, S., Kawada, K., Uchibori, T., 1990. Surface activities, biodegradability and antimicrobial properties of n-alkyl glucosides, manosides and galactosides. **J. Am. Oil. Chem. Soc.** 67, 996-1001.

Matsumura, S., Nakamura, T., Yao, E., Toshima, K., 1999. Biocatalytic one-step synthesis of n-Octyl β-D-xylotrioside and xylobioside from xylan and n-octanol in supercritical carbon dioxide. **Chem. Lett.** 7, 581-582.

Maugard, T., Gaunt, D., Legoy, M.D., Besson, T., 2003. Microwave-assisted synthesis of galacto-oligosaccharides from lactose with immobilized β-galactosidase from *Kluyveromyces lactis*. **Biotechnol. Lett.** 25, 623-629.

Mc Carter, J., Withers, S.G., 1994. Mechanisms of enzymatic glycoside hydrolysis. **Cur. Opin. Struct. Biol.** 4, 885-892.

Miao, W., Yao, S., 1999. Study of β-1,4-glucosidase in water/PC/heptane-butanol reverse micelles. **Wuli Huaxue Xuebao** 15, 930-937(Chinese).

Michaud, A., Williams, T.A., Chauvet, M.T., Corvol, P., 1997. Substrate dependence of angiotensin I converting enzyme inhibition: Captopril displays a selectivity for

inhibition of N-acetyl-seryl-aspartyl-lysyl-proline hydrolysis compares with that of angiotensin I. **Mol. Pharmacol.** 51, 1070-1076.

Mitsuo, N., Takeichi, H., Satoh, J., 1984. Synthesis of β-alkyl glucosides by enzymatic transglycosylation. **Chem. Pharm. Bull.** 32, 1183-1187.

Mohri, K., Watanable, Y., Yoshida, Y., Satoh, M., Isobe K., Sugimoto, N., Tsuda, Y., 2003. Synthesis of glycosylcurcuminoids. **Chem. Pharm. Bull.** 51, 1268-1272.

Monsan, P.F., Paul, F., Pelenc, P., Bouler, E., 1996. Enzymatic production of α-butyl glucoside and its fatty acid esters. **Ann. New York Acad. Sci.** 799, 633-641.

Montgomery, D.C., 1991. Design and analysis of experiments. John Wiley and Sons, New York. pp 542-547.

Moon, J.H., Terao, J., 1998. Antioxidant activity of caffeic acid and dihydrocaffeic acid in Lard and human low-density lipoprotein. **J. Agri. Food chem.** 46, 5062-5065.

Mori, T., Okahata, Y., 1998. Effective biocatalytic transgalactosylation in a supercritical fluid using a lipid-coated enzyme. **Chem. Commun.** 20, 2215-2216.

Mori, T., Okahata, Y., 2000. Enzyme-catalyzed reactions in supercritical fluids. **Chorinkai Saishin Gijutsu** 4, 36-40 (Japanese).

Mori, T., Okahata, Y., 2002. Enzyme catalytic reactions in supercritical fluids. Chorinkai Ryutai no Subete. Edited by: Arai, Y., Tekuno, S., Tokyo, Japan. pp 543-547.

Mori, T., Okahata, Y., 2003. Control of enzymatic reactions by supercritical fluids. **Kagaku Kogyo** 54, 93-97 (Japanese).

Mullally, M.M., Meisel, H., FitzGerald, R.J., 1996. Synthetic peptides corresponding to a lactalbumin and β-lactoglobulin sequences with angiotensin-I-converting enzyme inhibitory activity. **Biol. Chem.** 377, 259-260.

Mutua, L.N., Akoh, C.C., 1993. Synthesis of alkyl glucoside fatty acid esters in non aqueous media by *Candida* sp. lipase **J. Am. Oil Chem. Soc.** 70, 43-46.

Nakamura, T., Komori, C., Lee, Y,-Y., Hashimoto, F., Yohara, S., Nohara, T., Ejima, A., 1996. Cytotoxic activities of solanum steroidal glycosides. **Biol. Pharm. Bull.** 19, 546-566.

Nakamura, T., Toshima, K., Matsumura, S., 2000. One-step synthesis of n-octyl β-D-xylotrioside, xylobioside and xyloside from xylan and n-octanol using acetone powder of *Aureobasidium pullulans* in supercritical fluids. **Biotechnol. Lett.** 22, 1183-1189.

Natarajan, S.K., Sierks, M.R., 1997. Minimizing nanoproductive substrate binding: A new look at glucoamylase substrate affinities. **Biochemistry** 36, 14946-14955.

Nielsen, B.R., Lehmbeck, J., Frandsen, T.P., 2002. Cloning heterologous expression and enzymatic characterization of a thermostable glucoamylase from *Talaromyces emersonii.* **Protein expres. purif.** 26, 1-8.

Nilsson, K.G.I., 1987. A simple strategy for changing the regio selectivity of glycosidase catalyzed formation of disaccharides. **Carbohydr. Res.** 167, 95-103.

Nuchter, M., Ondruschka, B., Lautenschlager, W., 2001. Microwave-assisted synthesis of alkyl glycosides. **Synthetic Commun.** 31, 1277-1283.

Oakes, R.S., Clifford, A.A., Rayner, C.M., 2001. The use of supercritical fluids in synthetic organic chemistry. **J. Chem. Soc. Perkins Trans 1** 9, 917-941.

Ohinishi, H., Sakai, H., Ohta, T., 1991. Purification and some properties of a glucoamylasse from *Clostridium sp. G0005.* **Agric. Biol. Chem.** 55, 1901-1902.

Ohinishi, M., 1990. Subsite structure of *Rhizopus niveus* glucoamylase, estimated with the binding parameters for maltooligosaccharides. **Starch/Starke** 42, 311-313.

Ohnishi, M., Hiromi, K., 1989. Binding of maltose to *Rhizopus niveus* glucoamylases in the pH range where the catalytic carboxyl groups are ionized. **Carbohydr. Res.** 195, 138-144.

Okada, G., Unno, T., 1989. A glucodextranase accompanied by glucoamylase activity from *Arthrobacter globiformis I* 42. **Agric. Biol. Chem.** 53, 223-228.

Ooi, Y., Hashimoto, T., Mitsuo, N., Satoh, T., 1985. Enzymatic formation of β-galactosidase from *Aspergillus oryzae* and its application to the synthesis of chemically unstable cardiac glycosides. **Chem. Pharm. Bull.** 33, 1808-1814.

Oosterom, M.W., Rantwijk, F., Sheldon, R.A., 1996. Regioselective acylation of disaccharides in tert-butyl alcoholcatalyzed by *Candida antarctica* lipase. **Biotechnol. Bioeng.** 49, 328-333.

Orihara, Y., Furuya, T., Hashimoto, N., Deguchi, Y., Tokoro, K., Kanisawa, T., 1992. Biotransformation of isoeugenol and eugenol by cultured cells of *Eucalyptus perriniana.* **Phytochemistry** 31, 827-831.

Orlich, B., Schomacker, R., 2002. Enzyme catalysis in reverse micelles. **Adv. Biochem. Eng./Biotechnol.** 75, 185-208.

Palma, M., Taylor, L.T., Zoecklein, B.W., Douglas, L.S., 2000. Supercritical Fluid Extraction of Grape Glycosides. **J. Agric. Food Chem.** 48, 775-779.

Panintrarux, C., Adachi, S., Araki, Y., Kimura, Y., Matsuno, R., 1995. Equilibrium yield of n-alkyl-β-D-glucoside through condensation of glucose and n-octanol by β-galactosidase in a biphasic system. **Enzyme Microb. Technol.** 17, 32-40.

Papanikolaou, S., 2001. Enzyme-catalyzed synthesis of alkyl-β-glucosides in a water-alcohol two-phase system. **Bioresource Technol.** 77, 157-161.

Partridge, J., Harper, N., Moore, B., Halling, P.J., 2001. Enzymes in nonaqueous solvents methods and protocols In Series: **Methods Biotechnol.** 227-234.

Pazur, J.H., Knull, H.R., Cepure, A., 1971. Glucoenzymes: Structure and properties of the two forms of glucoamylase from *Aspergillus niger*. **Carbohydr. Res.** 20, 83-96.

Pornpong, S., Saovanee, D., Sitliwat, L., 2005. Effect of glycation on stability and kinetic parameters of thermostable glucoamylase from *Aspergillus niger.* **Proc. Biochem.** 40, 2821-2826.

Post, C.B., Karplus, M., 1986. Does lusozyme follow the lusozyme pathway? An alternative based on dynamic structural and stereoelectronic considerations. **J. Am. Chem. Soc.** 108, 1317-1319.

Pouchert, C.J., 1983. The Aldrich library of NMR spectra. 2nd Edn, Vol. 1 pp102D.

Pretorius, I.S., Lambrechts, M.G., Marmur, J., 1991. The glucoamylase multigene family in *Saccharomyces cerevisiae var. diastaticus*: an overview. **CRC Crit. Rev. in Biochem. Mol. Biol.** 26, 53-76.

Pugh, T.A., Shah, J.C., Magee, P.T., Clancy, M.J., 1989. Characterization and localization of the sporulation glucoamylase from *Saccharomyces cerevisiae.* **Biochem. Biophys. Acta.** 994, 200-209.

Ramasesh, N., Srekantiah, K.R., Murthy, V.S., 1982. Studies on the two forms of amyloglucosidase from *Aspergillus niger van Tieghem.* **Starch/Starke,** 34, 346-351.

Rantwijk, F.V., Oosterom, M.W., Shedon, R.A., 1999. Glycosidase-catalyzed synthesis of alkyl glyosides. **J. Mol. Catal. B: Enzym.** 6, 511-532.

Rao, V.B., Sastri, N.V.S., Rao, P.V.S., 1981. Purification and characterization of a thermostable glucoamylase from the thermophilic fungus *Thermomyces lanuginose*. **Biochem. J.** 193, 379-385.

Rhode, O., Witt, S., Hardacker, I., 1999. Method for preparation of alkyl-glycosides using microwave irradiation. German patent **DE 19730836 A1** (CA 130: 110555).

Robyt, J.F., 1998. Essentials of carbohydrate chemistry. Springer, New York. pp 64-68.

Roig, M.G., Slade, A., Kennedy, J.F., Taylor, D.W., Garaita, M.G., 1995. Investigations of stabilities, pH, and temperature profiles and kinetic parameters of glucoamylase immobilized on plastic supports. **Appl. Biochem. Biotechnol.** 50, 11-33.

Roitsch, T., Lehle, L., 1989. Structural requirements for protein N-glycosylation. Influence of acceptor peptides on cotranslational glycosylation of yeast influence and site-directed mutagenesis around a sequon sequence. **Eur. J. Biochem.** 181, 525-529.

Romero, M.D., Calvo, L., Alba, C., Daneshfar, A., Ghaziaskar, H.S. 2003. Enzymatic synthesis of isoamyl acetate with immobilized *Candida antarctica* lipase in *n*-hexane. **Enzyme Microb. Technol.** 37, 42-48.

Rosenthal, K.S., Koussale, F., 1983.Critical micelle concentration determination of non-ionic detergent with comassive brilliant blue-G250. **Anal. Chem.** 55, 1115-1117.

Rubio, E., Fernandez M.A., Klibanov, A.M., 1991. Effect of the solvent on enzyme regio-selectivity. **J. Am. Chem. Soc.** 113, 695-696.

Saha, B.C., Zeikus, J.G., 1989. Microbial glucoamylases: biochemical and biotechnological features. **Starch/Starke,** 41, 57-64.

Sakata, I., Maruyama, I., Kobayashi, A., Yamamoto, I., 1998. Production of phenethyl alcohol glycoside. **Jpn. Kokai Tokkyo Konho**, Japan Patent **JP 10052297** (CA 128:229438).

Sakurai, T., Margolin, A.L., Russell, A.J., Klibanov, A.M., 1988. Control of enzyme enantioselectivity by the reaction medium. **J. Am. Chem. Soc.** 110, 7236-7237.

San-Aparicio, J., Hermoso, J.A., Martinz-Ripoll, M., Laquerica, J.L., Polaina, J., 1998. Crystal structure of β-glucosidase A from *Bacillus polymyxa*: in sights into the catalytic activity in family1 glycosyl hydrolases. **J. Mol. Biol.** 275, 491-502.

Sanchez, M.A., Artigar, A.C., Perez, V.J., 2003. Purification of angiotensin I converting enzyme from pig lung using concanavalin-A sepharose chromatography. **J Chromatogr.** B, 783, 247-252.

Sato, T., Takeuchi, H., Takahashi, K., Kurosu, J., Yoshida, K., Tsugane, T., Shimura, S., Kino, K., Kirimura, K., 2003. Selective α-glucosylation of eugenol by α-glucosyl transfer enzyme of *Xanthomonas campestris* WU-9701. **J. Biosci. Bioeng.** 96, 199-202.

Schmid, B., Kotter, I., Heide, L., 2001. Pharmacokinetics of salicin after oral administration of a standard willow bark extract. **Eur. J. Clinic. Pharmacol.** 57, 387-391.

Schulze, B., Wubbolts, M.G., 1999. Biocatalysis for industrial production of fine chemicals. **Curr. Opin. Biotechnol.** 10, 609-615.

Segel, I.H., 1993. Enzyme Kinetics-Behavior and analysis of rapid equilibrium and steady - state enzyme systems. A Wiley-interscience publication. pp 826-829.

Shah, C., Sellappan, S., Madamwar, D., 2000. Entrapment of enzyme in water-restricted microenvironment -amyloglucosidase in reverse micelles. **Process Biochem.** 35, 971-975.

Shibata, H., Sonoke, S., Ochiai, H., Nishihashi, H., Yamada, M., 1991. Glucosylation of steviol and steviol glucosides in extracts from *Stevia rebaudiana Bertoni*. **Plant Physiol.** 95, 152-156.

Shieh, C.J., Akoh, C.C., Koehler, P.E., 1995. Four-factor response surface optimization of the enzymatic modification of triolin to structured lipids. **J. Am. Oil Chem. Soc.** 72, 619-623.

Shin, H.K., Kong, J.Y., Lee, J.D., Lee, T.H., 2000. Synthesis of hydroxy benzyl-α-glucosides by amyloglucosidase-catalysed transglycosylation. **Biotechnol. Lett.** 22, 321-325.

Shinoyama, H., Kamiyama, Y, Yasui, T., 1988. Enzymatic synthesis of alkyl β-xylosides from xylobiose by application of the transxylosyl reaction of *Aspergillus niger* β-xylosidase. **Agri. Biol. Chem.** 52, 2197-2202.

Sierks, M.R., Ford, C., Reilly, P.J., Svensson, B., 1990. Catalytic mechanism of fungal glucoamylases as defined by mutagenesis of Asp 176, Glu179, and Glu180 in the enzyme from *Aspergillus awamori,* **Protein Eng.** 3, 193-198.

Sills, A.M., Saunder, M.E., Stewart, G.G., 1984. Isolation and characterization of the amylolytic system of *Schwanniomyces castellii.* **J. Inst. Brew.** 90, 311-316.

Sinnot, M.L., 1990. Catalytic mechanism of glycosyl transfer. **Chem. Rev.** 90, 1171-1202.

Soni, B.K., Kapp, C., Goma, G., Soucaille, P., 1992. Solvent production from starch: effect of pH on α-amylase and glucoamylase localization and synthesis in synthetic medium. **Appl. Microbiol. Biotechnol.** 37, 539-543.

Soubrier, F., Alhenc-Gelas, F., Hubert, C., Allegrini, J., John, M., Tregear, G., Corvol, P., 1988. Two putative active centers in human Angiotensin-I converting enzyme revealed by molecular cloning. **Proc. Natl. Acad. Sci.** USA. 85, 9386-9390.

Specka, U., Mayer, F., Antranikian, G., 1991. Purification and properties of thermoactive glucoamylase from *Clostridium thermosaccharolyticum.* **Appl. Environ. Microbiol.** 57, 2317-2323.

Srivastava, A., Strasser, R.J., 2001. Biomolecules in reverse micelles. Biophysical Processes in Living Systems, Eds. Saradhi, P. Pardha. Science Publishers, Inc. Enfield, N. H. pp 1-23.

Srivastava, R.A.K., 1984. Studies on extracellular and intracellular purified amylases from a thermophilic *Bacillus stearothermophilus*. **Enzyme. Microb. Technol.** 6, 422-426.

Stevenson, D.E., Furneaux, R.H., 1996. High yield synthesis of ethyl and 2-fluroethyl β-D-galactopyranosides using *Streptococcus thermophilus* β-galactosidase. **Enzyme Microb. Technol.** 18, 513-518.

Stevenson, D.E., Stanley, R.A., Furneaux, R.H., 1993. Optimization of alkyl β-D-galactopyronoside synthesis from lactose using commercially available β-galactosidase. **Biotechnol. Bioeng.** 42, 657-666.

Stevenson, D.E., Stanley, R.A., Furneaux, R.H., 1996. Oligosccharide and alkyl β-galactopyranoside synthesis from lactose with C*aldocellum saccharolyticum* β-glycosidase. **Enzyme Microb. Technol.** 18, 544-549.

Stoffer, B., Aleshin, A.E., Firsov, L.M., Svensson, B., Honzatko, R.B., 1995. Refined structure for the complex of D-gluco-dihydroacarbose with glucoamylases from *Aspergillus awamori* var. X100 to 2.2 Å resolution: dual conformation for extended inhibitors bound to the active site of glucoamylases, **FEBS Lett.** 358, 57-61.

Stoffer, B., Frandsen., T., Busk, P., Schneider, P., Svendsen, I., Svensson, B., 1993. Production, purification and characterization of the catalytic domain of glucoamylase from *Aspergillus niger*. **Biochem. J.** 292, 197-202.

Sumner, J.B., Sisler, E.B., 1944. A simple method for blood sugar, **Arch. Biochem.** 4, 333-336.

Suzuki, Y., Suzuki, K., 1991. Enzymatic formation of 4G-α-D-glucopyranosyl rutin. **Agri. Biol. Chem.** 55, 181-187.

Suzuki, Y., Uchida, K., 1994. Enzymatic formation of a new derivative of thiamin, β-galactosylthiamin. **Biosci. Biotech. Biochem.** 58, 1273-1276.

Svendsen, A., 2003. Glucoamylase variants exhibiting improved specific activity and thermal stability for useful industrial applications. PCT Int. Appl. **WO 2003029449 A2** (CA 138:267698).

Svensson, B., Clarke, A.J., Svendsen, I., Moller, H., 1990. Identification of carboxylic acid residues in glucoamylase G2 from *Aspergillus niger* that participate in the catalysis and substrate binding. **Eur. J. Biochem.** 18, 29-38.

Svensson, B., Larsen, K., Svendsen, I., Boel, E., 1983. The complete aminoacid sequence of the glycoprotein glucoamylase G1 from *Aspergillus niger*. **Carlsberg. Res. Commun.** 48, 529-544.

Takahashi, T., Kato, K., Ikegami, Y., Irie, M., 1985. Different behavior towards raw starch of three forms of glucoamylase from a *Rhizopus* sp. **J. Biochem.** 98, 663-671.

Taki, T., Ishikawa, D., Hamasaki, H., Handa, S., 1997. Preparation of peptides which mimic glycoshingolipids by using phage peptide library and their modulation on β-galactosidase activity. **FEBS Lett.** 418, 219-223.

Tanaka, A., Yamashita, T., Ohnishi, M., Hiromi, K., 1983. Steady-state and transient kinetic studies on the binding of maltooligosaccharides to glucoamylases, **J. Biochem.** 93, 1037-1043.

Tanaka, Y., Ashikari, T., Nakamura, N., Kiuchi, N., Shibano, Y., Amachi, T., Yoshizumi, H., 1986. Comparision of aminoacid sequences of three glucoamylases and their structure-function relationships. **Agric. Biol. Chem.** 50, 965-969.

Tapavicza, S.V., Bell, D., Kopp-Holtwiesche, B., 2000. Plant growth enhancement against phytopathogenic fungi and /or soil borne pests. Patent **WO 0002451** (CA 132:60488).

Taylor, P.M., Napier, E.J., Fleming, I.D., 1978. Some properties of a glucoamylase produced by the thermophilic fungus *Humicola lanuginose.* **Carbohydr. Res.** 16, 301-308.

Thiem, J., 1995. Applications of enzymes in synthetic carbohydrate chemistry. **FEMS. Microbiol. Rev.** 16, 193-211.

Torres, R., Pessela, B.C., Mateo, C., Ortiz, C., Fuentes, M., Guisan, J.M., Fernandez-Lafuente, R., 2004. Reversible immobilization of glucoamylase by ionic adsorption on sepabeads coated with polyethyleneimine. **Biotechnol Prog.** 20, 1297-300.

Trincone, A., Pagnotta, E., Giordano, A., Perugino, G., Rossi, M., Moracci M., 2003. Enzymatic synthesis of 2-deoxyglycosides using the β-glycosidase of the archaeon *Sulfolobus solfataricus*. **Biocatal. Biotransform.** 21, 17-24.

Uchida, K., Suzuki, Y., 1998. Enzymatic synthesis of a new derivative of thaiamin, O-α-glucosylation. **Biosci. Biotechnol. Biochem.** 62, 221-224.

Valivety, R.H., Johnston, G.A., Suckling, C.J., Halling, P.J., 1991. Solvent effect on Biocatalysis in organic systems: equilibrium position and rates of lipase catalysed esterification. **Biotechnol. Bioeng.** 38, 1137-1143.

Valivety, R.H., Halling, P.J., Macrae A.R., 1992. *Rhizomucor miehei* lipase remains highly active at water activity below 0.001. **FEBS Lett.** 301, 258-260.

Venkateshwaralu, S., Ramachandra, M.S., Subbaraju, G.V., 2005. Synthesis and biological evolution of polyhydroxy curcuminoids. **Bioorg. Med. Chem.** 13, 6374-6380.

Verdoucq, L., Czjzek, M., Moriniere, J., Beven, D.R., Esen, A., 2003. Mutational and structural analysis of aglycone specificity in maize and sorghum β-glucosidase. **J. Biol. Chem.** 278, 25055-25062.

Vermeirssen, V., Van-Camp, J., Verstraete, W., 2002. Optimization and validation of an angiotensin-converting enzyme inhibition assay for the screening of bioactive peptides. **J. Biochem. Biophy. Methods,** 51, 75-87.

Vic G., Hastings, J.J., Crout, D.H.G., 1996. Glycosidase catalyzed synthesis of glycosides by an improved procedure for reverse hydrolysis. Application to the chemoenzymatic synthesis of galactopyranosyl-(1→4)-O-α-galactopyranoside derivatives. **Tetrahedron Asymmetry,** 7, 1973-1984.

Vic, G., Biton, J., Beller, D.L., Michel, J.M., Thomas, D., 1995. Enzymatic glycosylation of hydrolytic alcohols in organic medium by the reverse hydrolysis reaction using almond β-D-glucosidase. **Biotechnol. Bioeng.** 46, 109-116.

Vic, G., Crout, D.H.G., 1994. Synthesis of glucosidic derivatives with a spaces arm by reverse hydrolysis using almond β-D-glucosidase. **Tetrahedron Asymmetry** 5, 2513-2516.

Vic, G., Crout, D.H.G., 1995. Synthesis of allyl and benzyl β-D-glucopyranosides and allyl β-D-galactopyranoside from D-glucose or D-galactose and the corresponding alcohol using almond β-D-glucosidase. **Carbohydr. Res.** 279, 315-319.

Vic, G., Thomas, D., 1992. Enzyme-catalyzed synthesis of alkyl-β-D-glucosides in organic media. **Tetrahedron Lett.** 33, 4567-4570.

Vic, G., Thomas, D., Crout, D.H.G., 1997. Solvent effect on enzyme-catalyzed synthesis of β-D-glucosides using the reverse hydrolysis method: application to the preparative-scale synthesis of 2-hydroxybenzyl and octyl β-D-glucopyronosides. **Enzyme Microb. Technol.** 20, 597-603.

Voorhorst, W.G.B., Eggen, R.I.K., Luesink, E.J., De Vos, W.M., 1995. Characterization of the Cel B gene coding for β-glucosidase from the hyperthermophilic archean *Pyroccus furiosus* and its expression and site directed mutation in *Escherichia coli.* **J. Bacteriol.** 177, 7105-7111.

Vorderwulbecke, T., Kieslich, K., Erdmann, H., 1992. Comparison of lipases by different assays. **Enzyme Microb. Technol.** 14, 631-639.

Vulfson, E.N., Patel, R., Beecher, J.E., Andrews, A.T., Law, B.A., 1990. Glycosidases in organic solvents: I. Alkyl-β-glucoside synthesis in a water-organic two-phase system. **Enzyme Microb. Technol.** 12, 950-954.

Ward, O.P., Singh, A., 2000. Enzymatic asymmetric synthesis by decarboxylases. **Curr. Opin. Biotechnol.** 11, 520-526.

Wasserman, B.P., Burke, D., Jacobson, B.S., 1982. Immobilization of glucoamylase from *Aspergillus niger* on poly(ethylenimine)-coated non-porous glass beads. **Enzyme Microb. Technol.** 4, 107-109.

Weast, R.C., 1983. Handbook of Chemistry and Physics, 64th ed. (Weast, R.C., Astle, M.J., Beyer, W.H., eds.) CRC Press, Boca Raton. C-696.

Wiesmann, C., Hengstenberg, W., Schulz, G.E., 1997. Crystal structures and mechanism of 6-phospho-β-galactosidase from *Lactococcus lactis.* **J. Mol. Biol. Chem.** 269, 851-860.

Williamson, G., Belshaw, N.J., Williamson, M.P., 1992. O-Glycosylation in *Aspergillus* glucoamylase. Confirmation and role in binding. **Biochem. J.** 282, 423-428.

Withers, G.G., Warren, R.A.J., Street, I.P., Rupitz, K., Kempton, J.B., Abersold, R., 1990. Unequivocal demonstration of the involvement in the mechanism of a retaining glycosidase. **J. Am. Chem. Soc.** 112, 5887-5889.

Withers, S.G., Street, I.P., 1988. Identification of a covalent α-D-glucopyranosyl enzyme intermediate formed on a β-glucosidase. **J. Am. Chem. Soc.** 110, 8551-8553.

Witkowski, S., Walejko, P., Wawer, I., 1998. ^{13}C CP MAS NMR study of 6-O-(β-D-glucopyranosyl)-and 6-O-(β-D-mannopyranosyl)-d-α-tocopherols. **Solid State Nuclear Magnetic Resonance,** 10, 123-128.

Woudenberg-van O.M., van Belle, H.J.A., van Rantwijk, F., Sheldon, R.A., 1998. Immobilized β-galactosidases and their use in galactoside synthesis. **J. Mol. Catal. A: Chem.** 134, 267-274.

Wu, J., Ding, X., 2002. Characterization of inhibition and stability of soy-protein derived angiotensin I converting enzyme inhibitory peptides. **Food Res. Int.** 35, 367-375.

Yadav, G.D., Lathi, P.S., 2004. Synthesis of citronellol laurate in organic media catalyzed by immobilized lipases: kinetic studies, **J. Mol. Catal. B: Enzym.** 27, 113–119.

Yan, Y., Bornscheuer, U.T., Stadler, G., Wahl, S.L., Reuss, R., Schmid, R.D., 2001. Production of sugarfatty acid esters by enzymatic esterification in a stirred-tank membrane reactor. Optimization of parameters by response surface methodology. **J. Am. Oil Chem. Soc.** 78, 147-152.

Yankov, D., Beschkov, V., Rouleau, D., 1997. Kinetics and modeling of the enzyme hydrolysis of maltose with free and immobilized glucoamylase. **Starch/Starke,** 49, 288-293.

Yoon, S-H., Fulton, D.B., Robyt, J.F., 2004. Enzymatic synthesis of two salicin analogues by reaction of salicyl alcohol with *Bacillus macerans* cyclomaltodexrin glucanyltransferase and *Leuconostoc mesenteroides* B-742CB dexransucrase. **Carbohydr. Res.** 339, 1517-1529.

Yu, R.C., Hang, Y.D., 1991. Purification and characterization of a glucoamylase from *Rhizopus oryzae*. **Food chem.** 40, 301-308.

Zaks, A., Klibanov, A.M., 1984. The effect of water on enzyme reaction in organic media. **J. Biol. Chem.** 263, 8017-8021.

Zaks, A., Klibanov, A.M., 1986. Substrate specificity of enzymes in organic solvents vs. water is reversed. **J. Am. Chem. Soc.** 108, 2767-2768.

Zaks, A., Klibanov, A.M., 1988. Enzyme catalysis in monophasic organic solvents. **J. Biol. Chem.** 263, 3194-3201.

Zechel, D.L., Withers S.G., 2001. Dissection of nucleophilic and acid–base catalysis in glycosidases. **Curr. Opin. Chem. Biol.** 5, 643-649.

Zeng, Q., Huang, S., 2000. Supercritical CO_2 extraction from the leaves of *Ginkgo biloba.* **Guangdong Yaoxueyuan Xuebao** 16, 304-306 (Chinese).

Zhang, S., Liu, S., Zhang, L., 1998. Kinetics of saccharification of potato starch with glucoamylase. **Zhongguo Liangyou Xuebao** 13, 21-25 (Chinese).

Zhou, J.H., 2000. Herbal sweetening and preservative composition comprising licorice extract and mogrosides obtained from plants belonging to cucurbitaceae and/or momordica. Patent **US 6103240** (CA 133:168393).